Towards Better Performance in the Face of Input Uncertainty while Maintaining Interpretability in AI

This thesis is submitted for the degree of
Doctor of Philosophy

Direnc Pekaslan

4276123

Supervised by

Christian Wagner

Jonathan M. Garibaldi

School of Computer Science

University of Nottingham

Submitted March 2021

Abstract

Uncertainty is a pervasive element of many real-world applications and very often existing sources of uncertainty (e.g. atmospheric conditions, economic parameters or precision of measurement devices) have a detrimental impact on the input and ultimately results of decision-support systems. Thus, the ability to handle input uncertainty is a valuable component of real-world decision-support systems. There is a vast amount of literature on handling of uncertainty through decision-support systems. While they handle uncertainty and deliver a good performance, providing an insight into the decision process (e.g. why or how results are produced) is another important asset in terms of having trust in or providing a 'debugging' process in given decisions.

Fuzzy set theory provides the basis for Fuzzy Logic Systems which are often associated with the ability for handling uncertainty and possessing mechanisms for providing a degree of interpretability. Specifically, Non-Singleton Fuzzy Logic Systems are essential in dealing with uncertainty that affects input which is one of the main sources of uncertainty in real-world systems. Therefore, in this thesis, we comprehensively explore enhancing non-singleton fuzzy logic systems capabilities considering both capturing-handling uncertainty and also maintaining interpretability. To that end the following three key aspects are investigated; (i) to faithfully map input uncertainty to outputs of systems, (ii) to propose a new framework to provide the ability for dynamically adapting system on-the-fly in changing real-world environments. (iii) to maintain level of interpretability while leveraging performance of systems.

The first aspect is to leverage mapping uncertainty from input to outputs of systems through the interaction between input and antecedent fuzzy sets i.e. firing strengths. In the context of Non-Singleton Fuzzy Logic Systems, recent studies have shown that the standard technique for determining firing strengths risks information loss in terms of the interaction of the input uncertainty and antecedent fuzzy sets. This thesis explores and puts forward novel approaches to generating firing strengths which faithfully map the uncertainty affecting system inputs to outputs. Time-series forecasting experiments are used to evaluate the proposed alternative firing strength generating technique under different levels of input uncertainty. The analysis of the results shows that the proposed approach can also be a suitable method to generate appropriate firing levels which provide the ability to map different uncertainty levels from input to output of FLS that are likely to occur in real-world circumstances.

The second aspect is to provide dynamic adaptive behaviours to systems at run-time in changing conditions which are common in real-world environments. Traditionally, in the fuzzification step of Non-Singleton Fuzzy Logic Systems, approaches are generally limited to the selection of a single type of input fuzzy sets to capture the input uncertainty, whereas input uncertainty levels tend to be inherently varying over time in the real-world at run-time. Thus, in this thesis, input uncertainty is modelled -where it specifically arises- in an online manner which can provide an adaptive behaviour to capture varying input uncertainty levels. The framework is presented to generate Type-1 or Interval Type-2 input fuzzy sets, called ADaptive Online Non-singleton fuzzy logic System (ADONiS). In the proposed framework, an uncertainty estimation technique is utilised on a sequence of observations to continuously update the input fuzzy sets of non-singleton fuzzy logic systems. Both the type-1 and interval type-2 versions of the ADONiS frameworks remove the limitation of the selection of a specific type of input fuzzy sets. Also this framework enables input fuzzy sets to be adapted to unknown uncertainty levels which is not perceived at the design stage of the model. Time-series forecasting experiments are implemented and results show that our proposed framework provides performance advantages over traditional counterpart approaches, particularly in environments that include high variation in noise levels, which are common in real-world applications. In addition, the real-world medical application study is designed to test the deployability of the ADONiS framework and to provide initial insight in respect to its viability in replacing traditional approaches.

The third aspect is to maintain levels of interpretability, while increasing performance of systems. When a decision-support model delivers a good performance, providing an insight of the decision process is also an important asset in terms of trustworthiness, safety and ethical aspects etc. Fuzzy logic systems are considered to possess mechanisms which can provide a degree of interpretability. Traditionally, while optimisation procedures provide performance benefits in fuzzy logic systems, they often cause alterations in components (e.g. rule set, parameters, or fuzzy partitioning structures) which can lead to higher accuracy but commonly do not consider the interpretability of the resulting model. In this thesis, the state of the art in fuzzy logic systems interpretability is advanced by capturing input uncertainty in the fuzzification -where it arises- and by handling it the inference engine step. In doing so, while the performance increase is achieved, the proposed methods limit any optimisation impact to the fuzzification and inference engine steps which protects key components of FLSs (e.g. fuzzy sets, rule parameters etc.) and provide the ability to maintain the given level of interpretability.

Declaration

The work in this thesis is based on research carried out at the Intelligent Modelling and Analysis Research Group (IMA) and the Lab for Uncertainty in Data and Decision Making (LUCID), in the School of Computer Science, the University of Nottingham, United Kingdom. I hereby declare that this thesis was composed by myself, that the work contained herein is my own except where explicitly stated otherwise in the text, and that this work has not been submitted for any other degree or processional qualification except as specified.

Direnc Pekaslan

4276123

August 2021

Acknowledgements

First and foremost, I would like to express my sincere gratitude to my supervisors, Prof. Christian Wagner and Prof. Jonathan M. Garibaldi for their invaluable advice, continuous support, and patience during my PhD journey. I am thankful to them for not only being academic supervisors but also mentoring personally throughout my PhD journey in Nottingham.

I would like to extend my sincere thanks to friends/the members of IMA and LUCID groups, specifically Utkarsh, Javier, Zixiao, Zack, Chao and more. Their insightful comments, suggestions and encouragements significantly enriched this thesis. Also, their valuable friendships made my time in Nottingham so fulfilling.

I would also like to mention my 'away from PhD' friends, Fatih, Ayse Giz, Tugba and Necip, for the wonderful times we shared (i.e. went through hard times and also celebrated accomplishments together)

My appreciation also goes to my parents and my aunt for their continuous love, support and inspiration throughout my life. I am also grateful to my elder sister Nehir and my cousins Hursia, Nursia and Direncan for always being there for me.

Finally, my special thanks to my beloved girlfriend Damla. I am thankful for her unconditional love, encouragement and making my life more cheerful.

Contents

List of Tables

List of Figures

List of Algorithms

List of Abbreviations

AARS : Approximate Analogical Reasoning Schema

ADONiS : ADaptive ONline Non-Singleton fuzzy logic system

AI : Artificial Intelligence

ANFIS : Adaptive Network-based Fuzzy Inference System

cen-NS: Centroid-based firing strength determining approach

COG : Center Of Gravity

COVID-19 : Coronavirus disease

CRI : Compositional Rule of Inference

dB : decibel

ECG : electrocardiogram

EKM : Enhanced Karnikand Mendel

ENG : Electroneurographic

FLS : Fuzzy Logic System

FOU : Footprint Of Uncertainty

FS : Fuzzy Set

GT2 : General Type-2

HR: Heart Rate

IT2 : Interval Type-2

MF : Membership Function

MG : Mackey-Glass time series

MISO : Multi Input Single Output

MSE : Mean Square Error

NSFLSs : Non-Singleton Fuzzy Logic Systems

O_2: Oxygen

QMC : Queen's Medical Centre

RMSE : Root Mean Square Error

SD : Standard Deviation

SFLS : Singleton Fuzzy Logic System

sim-NS: Similarity- based firing strength determining approach

SISO : Single Input Single Output

sMAPE : Symmetric Mean Absolute Percent Error

SNR : Signal-to-Noise Ratio

SpO_2: Saturated Oxygen

sta-NS: Standard firing strength determining approach

sub-NS: Subsethood-based firing strength determining approach

T1 : Type-1

T2 : Type-2

TSK : Takagi Sugeno Kang

UAV : Unmanned Aerial Vehicle

UMBRAE : Unscaled Mean Bounded Relative Absolute Error

WMA : Weighted Moving Average

Chapter 1

Introduction

Fuzzy set (FS) theory, introduced by Zadeh [189] as an extension of the classical set theory which is formed by crisp sets. FSs provide a way to represent uncertainty and are generally designed in respect to linguistic labels. When FSs are interconnected by linguistic rules, they establish the basis for Fuzzy Logic Systems (FLSs). Thus, while FLSs are considered as systems to cope with uncertainty, they are also frequently referred to as 'interpretable' systems for applications.

As will be elaborated in the next sections, input uncertainty is a pervasive element in real-world decision-support applications. In this thesis, in order to further develop handling input uncertainty capacity of systems, three key aspects are explored:

(i) Interaction of non-singleton input and antecedent FSs to faithfully map input uncertainty to outputs of systems by generating firing strengths with respect to different input uncertainty levels.

(ii) Proposal of a new framework to dynamically capture different levels of input uncertainty at run-time, which provides the ability to adapt input FS in changing real-world environments.

(iii) Maintaining the given level of interpretability in systems while leveraging the capacity of input uncertainty handling and increasing the performance of systems.

The structure of this chapter is as follows. Section 1.1 presents a brief history of logic.

Section 1.2 describes a historical overview of the uncertainty concept in science. Section 1.3 explains what uncertainty is. Section 1.4 provides the background and motivation for the research in this thesis. Section 1.5 then presents the aims and objectives of this thesis, followed by the thesis structure in Section 1.6.

1.1 Historical Overview of Logic

In 450 BC, Protagoras claimed that *True* is a subjective matter and he exemplified this idea stating, *"while the wind is cold to a person, it might be warm to another person"*, leading to the idea that there is no absolute *True* for all [6].

Later, Plato discussed this opinion in the dialogue named *Theaetetus* as below:

SOCRATES: *Do you call thinking what I call thinking?*

THEAETETUS: *What is that?*

SOCRATES: *The talk which the soul holds with herself on what she sees. It appears to me that, when she thinks, she is doing nothing else than conversing, asking questions and giving answers, affirming and denying. When she reaches a decision and is not in doubt, we can that opinion. So what I call forming an opinion is talking and opinion is speech that is held not with someone else or aloud but in silence with oneself.*

Here the identification of thoughts or opinion with talk suggests the transference of predicates, *true* and *false*. Overall, Plato investigated the question of *What is it that can properly be called true or false?* [6, 77]

Later, Aristotle laid a foundation for Aristotelian logic which often led him to be regarded as the father of logic [6]. During the rise of modern formal logic following Frege and Peirce, adherents of traditional logic (seen as the descendant of Aristotelian Logic) and the new mathematical logic tended to see one another as rivals, with incompatible notions of logic [159].

Over the years, logic has been extensively studied by considering different concepts. In 1662, Port-Royal Logic was published by Antoine Arnauld and Pierre Nicole and it was one of the influential works on logic after Aristotle until the nineteenth century [18]. Then, Boolean algebra was introduced by George Boole in his first book The Mathematical Analysis of Logic in 1847 [14].

1.2 Historical Overview of Uncertainty

In Boolean logic, a statement can be true (1) or false (0) —and nothing in between. According to this logic, for instance, an element can either belong to a set or not. For instance, assume a person is regarded as *young* at the age of 25. According to boolean logic, a person at the age of 24 or 26 may not be regarded as *young*. This way of *certainty* eventually indicates that the structures and parameters of a model are definitely known and there are no doubts about their values or their occurrence [196]. However, uncertainty has a prominent role in ordinary human life and also decision-making systems, in all their varieties, require an understanding of this uncertainty concept [76]. With regards to the *certainty* existence in life, the philosopher Bernard Russell has made the following statement [143]:

> "All traditional logic habitually assumes that precise symbols are being employed. It is, therefore, not applicable to this terrestrial life but only to an imagined celestial existence."

Even though the fact that uncertainty is often an inseparable component in most measurements at the empirical level, the concept of uncertainty was neglected in the emergence of developments until the nineteenth century. The general attitude was that 'scientific knowledge should be expressed in precise numerical terms; imprecision and other types of uncertainty do not belong to science' [76].

Despite the general attitude, Ludwig Boltzmann generalised Maxwell's approach for the kinetic theory of dilute gases to non-equilibrium processes. His particle distribution function gives

the statistical average number of molecules, rather than specific manifestations of microscopic entities [50, 76]. This was to pave the way for a new field of physics which later developed as *statistical mechanics*.

Thus, in comparison to the previously used mechanics, this new approach (using statistics) provided advantages for complex systems. Following the development of statistical mechanics, this statistical method was applied in many different fields such as telephone networks, marketing, insurance, investment etc. The studies showed that the larger the system and the higher the randomness, the better these methods perform [76]. As the beginning of the emergence of large systems, in 1973, Zadeh has made the following statement regarding systems complexity:

> "As the complexity of a system increases, our ability to make precise and yet significant statements about its behaviour diminishes until a threshold is reached beyond which precision and significance (or relevance) become almost mutually exclusive characteristics" [190].

Prior to statistical usage, analytical methods were utilised in *simple systems* where the system contained a very small number of components related to each other in a predictable way. On the other hand, statistical methods are applied to *complex systems* that contain a very large number of components and a very high degree of randomness [76]. In 1948, Weaver [180] referred to these two systems as complementary *organised simplicity* and *disorganised complexity* - in two extreme complexity and randomness scales - and claimed that the area between these two systems' fields was subject to further research.

Albeit, in the second half of the twentieth century, the development of computer technology relatively helped in terms of the computational power requirement, it was soon revealed that it was not adequate to make substantial progress in the scientific development between the concepts of *organised simplicity* and *disorganised complexity*, so a new broader view unfolded to take into consideration developing mathematical theories formalising their various facets. Thereby, the broader uncertainty theory was born from the probabilistic approaches [76, 196].

1.3 What is Uncertainty

According to the Cambridge Dictionary [1], the word *uncertainty* is defined as "a situation in which something is not known, or something that is not known or certain". From the scientific perspective, there is no consistent definition of uncertainty and it depends mostly on the context of the discussion. Yet, in a broad sense, "uncertainty implies that in a certain situation an observer does not dispose about information which quantitatively and qualitatively is appropriate to describe, prescribe or predict deterministically and numerically a system, its behavior or other characteristica" [195]. As uncertainty is involved in many real phenomena, it can stem from various sources, for instance, the information may be incomplete, imprecise, fragmentary, unreliable, vague, or contradictory. Traditionally, these effects define the type of associated uncertainty [76]. In decision-making systems, generally, the associated uncertainty types can be viewed under two clusters: *model uncertainty* and *data uncertainty*.

Model uncertainty can be related to a given model's components or structure. By implementing further studies, (e.g. using various training techniques or alternative training data), model uncertainty can be reduced in decision-making models. Therefore, the model uncertainty can also be regarded as *reducible uncertainty*.

On the other hand, data uncertainty relates to inputs of a system may result from data measurement errors, inconsistencies between measured values, limited sample sizes during data collection and those used by the model (e.g. in their level of aggregation/averaging). Thus, it is often an inseparable companion at the empirical level [76]. For instance, a sensor measurement can be affected by non-ideal situations, such as measurement conditions, the measuring instrument, adopted measurement methods, the model with which the measurand is described etc. Therefore, since the early beginning of scientific experimental activity, this measurement process has only been capable of providing an approximation of the crisp *perfect* value [48]. Considering the heterogeneity and diversity in real-world conditions, data uncertainty can also be regarded as *irreducible uncertainty.*

In this thesis, the *irreducible uncertainty* is focused, as it is one of the principal uncertainty

in real-world conditions. Rather than attempting to reduce it and processing inputs as discrete *perfect* values, we aim to model system inputs as distributions and process these distributions in a faithful manner to map input uncertainty to outputs of systems.

1.4 Background and Motivation

As mentioned in Section 1.3, real-world environments are subject to uncertainty. Thus, uncertainty handling becomes a vital factor in many decision-support systems, such as time-series forecasting, robotics, signal processing, bioinformatics etc. While one of the key aspects of decision-support systems is to establish an accurate decision, understanding and validating these decision processes (e.g. why or how the results are produced) is another important asset of these systems, since the interpretability capacity can potentially establish safety, trustworthiness, fairness and allow debugging process etc. in given decisions.

In 1965, Zadeh [189] introduced FS theory which provides the basis for FLSs. While FLSs are considered as robust systems for uncertainty handling, they are also frequently referred to as 'interpretable' systems. The main rationale for the latter is that FSs are generally designed in respect to linguistic labels and are interconnected by linguistic rules in FLSs, which can provide both the ability of handling of uncertainty and insight of why or how results are produced [54, 137]. One of the initial decision-making systems was developed to control a steam engine with fuzzy rule-base systems in 1975 [88]. Since then, FLSs have been successfully applied in a broad variety of decision-making systems, such as control [9, 178], robotics [145, 175], medical application [163], business [13], group decision-making [15] etc.

As real-world applications are generally subject to changing conditions, a system's inputs are often influenced by these conditions which may cause a broad range of uncertainty. In order to capture input uncertainty, in 1994, NSFLSs were formalised to utilise non-singleton FSs in the fuzzification step of FLSs [105]. Since then, NSFLSs have been utilised in a range of applications including non-linear time series forecasting, classifications and robotics [12, 17, 52, 53, 66, 131, 146, 188, 192].

Although NSFLSs show performance benefits in applications, in order to leverage uncertainty mapping from input to outputs of systems, specifically, the following three key aspects are focused on in this thesis: (I) faithfully mapping input uncertainty to outputs, (II) proposing a new framework to adapt input FSs to different uncertainty levels on-the-fly, (III) maintaining the given level of interpretability in systems (e.g. not altering rules, antecedents, consequents etc.), while delivering performance benefits.

The *first* aspect is to faithfully map different input uncertainty to outputs of systems by systematically generating firing strengths in the interaction between antecedent and input FSs. Traditionally, in the inferencing step of FLSs, inputs are processed with respect to the system rules through interaction between the input and antecedent FSs, resulting in rule firing strengths which have a significant role driving the mapping of antecedents to consequents. In NSFLSs, the most common firing strength generation technique is to adopt the maximum membership degree grade of the intersection between the input and antecedent FSs. However, recent studies show that the adopting the maximum point of the intersection to determine the firing strength can be imperceptive to different uncertainty levels in input FSs. For instance, two different input FSs (i.e. $Input_1$ and $Input_2$ in Fig. 1.1) may intersect an antecedent at the same membership grade, resulting in the same firing level. Despite the fact that these input FSs are clearly different and contain different levels of uncertainty (widths), the same firing strengths are generated for different input FSs. In other words, the system is 'blind' to the change in input uncertainty. Recent firing strength generation studies have demonstrated advantages over the standard approach [131, 176].

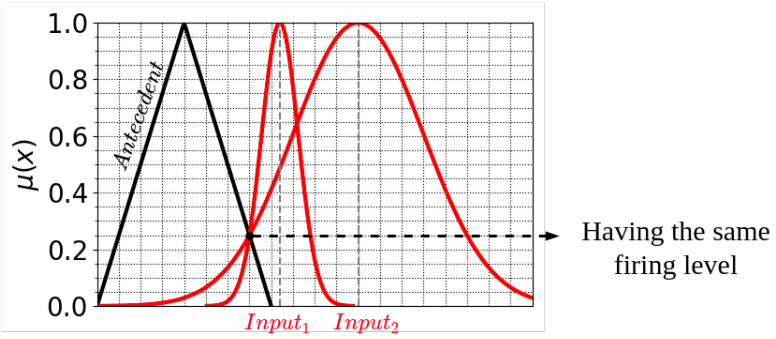

Figure 1.1: An illustration of two distinct input FSs (with different uncertainty levels [widths]) having the same firing level with the antecedent FSs.

In this thesis, as presented in our studies [120, 122], we will analyse the current firing strength determining approaches and explore behaviours of these approaches under different levels of input uncertainty. Later, building on the critical analysis, a novel approach is put forward to systematically generate firing strengths which faithfully map the uncertainty affecting system inputs (as explained in Chapter 3).

The *second* aspect of this thesis is to provide dynamic adaptive behaviours to NSFLS on-the-fly under different input uncertainty levels. This adaptive behaviour can cope with the real-world environment which contains different sources of uncertainty, causing different settings in different time periods. When input data contains uncertainty, NSFLSs are useful to model it and generally have the potential to deliver better performance compared to Singleton Fuzzy Logic System (SFLSs) [19, 32, 94]. In NSFLS design, traditionally, input FSs are built through a priori knowledge about the uncertainty level or implementing an optimisation technique to define parameters of systems [106]. While efficient, these approaches are invariably dependent on the availability of a priori knowledge or the availability of a training dataset which accurately reflects all potential real-world operating conditions. Furthermore, these approaches generally lead to a limited selection of one type of input FS models which prevents NSFLSs from being able to adapt to the breadth of changing uncertainty levels inherent to real-world applications.

In this thesis, as presented in our studies [121, 124], a complete ADaptive ONline Non-Singleton (ADONiS) framework is proposed to dynamically configure input FSs at run-time, in an online manner, which provides the ability to adapt into real-world circumstances without requiring a priori knowledge or training procedures and also without limiting the system to the selection of one type of input FS (as explained in Chapter 4).

Moreover, real-world environments are subject to different sources of uncertainty which may vary in magnitude over time. In other words, different sources of uncertainty may affect input values at different levels at different times which inevitably cause a variation in input uncertainty levels over time. Type-2 (T2) input FSs provide the ability to also capture variation in uncertainty levels by means of extra degrees of freedom. Thus, as presented in our study [123], the proposed ADONiS is later extended to a new type of noise-robust, adaptive interval type-

2 (IT2) input NSFLS which enables on-the-fly adaptation of the input FS to capture both the current uncertainty and the variation in uncertainty levels over time (as explained in Chapter 5).

The *third* aspect of this thesis is to maintain a given level of interpretability of fuzzy models. In recent years, an increasing number of studies have focused on fundamental questions such as what *interpretability* is in general, and in particular in respect to FLSs and how an interpretable FLS can be achieved etc. [3, 4, 71, 82]. These studies show that the interpretability of FLSs depends on their various components e.g. the number of rules, the structure of the rule set and the actual interpretability of each rule - which in turn depends on how meaningful the actual FSs are, how well they reflect the model which the interpreting stakeholder has in mind when considering the given linguistic label [54, 57, 137].

Assessing the interpretability degree of FLSs is a challenging task and it is related to multiple components in multiple contexts. When the aim is to increase the accuracy of FLSs, traditionally, some parametric equations and/or statistical optimisation techniques are used to tune/alter key components (e.g. MFs, rule parameters) based on data-driven approaches. Although changing parameters can provide an increase in accuracy, it usually causes a poorer interpretability as the key parameters are altered in a data-centric manner. Therefore, as the third aspects of this thesis -as presented in our study [119]-, while we increase performances of FLSs, in conjunction with the first two aspect of this thesis, we also focus on not changing key interpretability parameters and maintaining a given interpretability level of FLSs (as explained in Chapter 6).

Throughout the thesis, handling of input uncertainty approaches are proposed and evaluated in the context of time-series prediction experiments. Chapter 7 moves beyond time series prediction towards a real-world case study which was in part motivated by the international COVID-19 crisis in 2019: the automated control of breathing (oxygenation) support for neonatal babies. The case study was designed to test the deployability of ADONiS in a real-world setting and to provide initial insight in respect to its viability in replacing traditional approaches, in particular standard, singleton fuzzy logic control systems. In this application, the system rules and MFs parameters are defined by a medical expert and sensory inputs are processed as inputs to provide the oxygen level suggestions as output. The particularly interesting aspect of the

application is that there is an expectation from the medical professionals to be able to understand the decision making underpinning the oxygen flow, thus ideally the model parameters and rules should be preserved – unless the medical experts themselves decide to change them. This provides the challenge of how best to deal with input (sensor) uncertainty affecting the control system and thus an ideal case study for ADONiS.

In the next section, we present the aim and objectives to further develop input uncertainty capturing-handling capacity of NSFLSs.

1.5 Aims and Objectives

The aim of this thesis is to further develop input uncertainty capturing and handling capacity while also maintaining the 'interpretability' of NSFLSs. To achieve this aim, the following objectives were identified:

1. To conduct a critical analysis of the specific behaviour of different firing strength determining approaches in mapping input uncertainty to outputs of NSFLSs, and to put forward a novel approach to generating firing strengths which faithfully handles the uncertainty affecting system inputs.

2. To develop a framework that enables capturing different levels of input uncertainty - as one of the principal sources of uncertainty - and to model the input uncertainty dynamically, on-the-fly, where it arises.

3. To extend the proposed framework with an extra mechanism of adaptation to the magnitude of uncertainty change over time, achieving a compromise between reactivity and smoothness. Thus, to capture both the uncertainty in the last observed value(s) and uncertainty levels variation over time by means of the extra degree of freedom.

4. To maintain the given level of interpretability in the FLSs through the preservation of the key parameters for interpretability, while also providing an increase in performance of FLSs.

5. To test the deployability of the proposed framework to provide initial insight in respect to its viability in real-world applications.

1.6 Thesis Structure and Key Contributions

Chapter 2 outlines an overview of background material including FS theory, FS operations and FLSs. Also, a review of the current NSFLS studies is presented with a focus on inference engine and fuzzification steps which are traditionally associated with input uncertainty handling and capturing, respectively. The chapter then highlights the current challenges that are faced by current NSFLS literature in further developing the input uncertainty capacity of NSFLSs. Later, to link the NSFLS to the interpretability concept of FLSs, a brief overview of interpretability is provided. Lastly, since time-series forecasting is the application employed to evaluate the proposed technique and frameworks in this thesis, the time-series generation and noise adding procedures are presented along with the evaluation methods.

Chapter 3 puts forward novel approaches to systematically generate firing strengths which is to leverage mapping the uncertainty affecting system inputs to outputs. To highlight the strength and key challenges of current firing strength determining approaches, a critical analysis study is undertaken. Building upon this analysis, an alternative approach is proposed which provides a mapping of different levels of uncertainty information from inputs to outputs of NSFLSs, addressing objective 1. Chapter 3's contribution is pinpointed in the inferencing step of Fig. 1.2.

Chapter 4 proposes an end-to-end framework to adaptively configure non-singleton input FSs to the changing uncertainty levels. Considering the fact that a broad range of uncertainty sources can vary greatly in magnitude over time, the adaptation of NSFLSs to the varying environments can provide an efficient and effective solution for input uncertainty mapping to outputs of NSFLSs, by addressing objective 2. In this chapter, to highlight the strength of the proposed framework, extensive time-series forecasting experiments are implemented and comparisons results are reported. Chapter 4's contribution is located in the fuzzification step of Fig. 1.2.

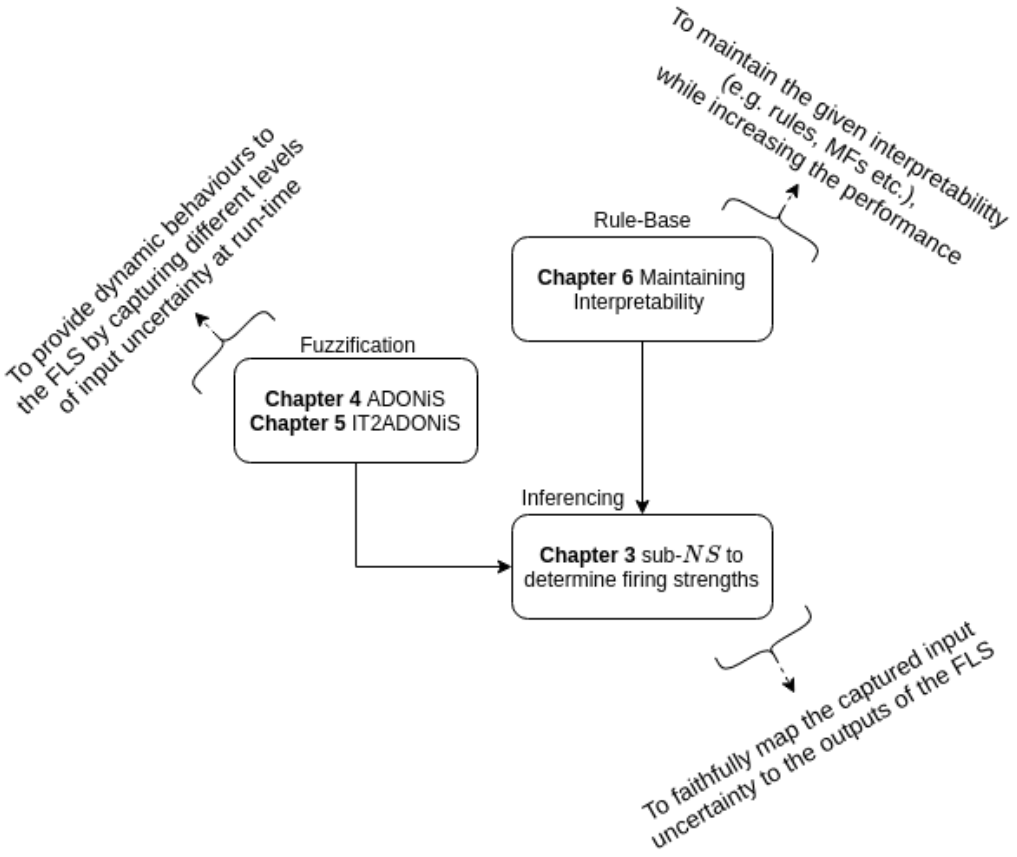

Figure 1.2: The representation of the overall contribution of each Chapters 3 - 6 of the thesis.

Chapter 5 puts forward the extension of the proposed framework from Chapter 4 by capturing both the uncertainty and its magnitude change over time, achieving a compromise between reactivity and smoothness. While capturing the last observed input uncertainty adaptively in the principal T1 input FS, the extra degree of freedom (i.e. footprint of uncertainty [FOUs]) of IT2 input FSs are used to capture/model the variation in uncertainty levels in an adaptive manner. This provides the dynamic structure of having different widths and FOU values on generated input FSs which can enable models to be prepared for drastic changes in environments, by addressing objective 3. This extension of our proposed framework is also tested on time-series forecasting experiments to provide a comparative study under different level of noise and noise variations over time. Chapter 5 is illustrated in Fig. 1.2.

The focus of Chapter 6 is expanded to encompass interpretability, considering specifically whether the mechanisms developed in Chapters 3 - 5 can be usefully applied to maintain a given level of interpretability of models. This chapter first presents an overview of the literature

on the concept of interpretability for FLSs to present the main parameters for an interpretable FLS. Then the proposed framework is examined in terms of maintaining interpretability of systems while it provides increased performance. Through a detailed set of time-series prediction experiments, the potential of the proposed framework is explored in comparison to a traditional optimised approach, by addressing objective 4. The behaviour and performance of both approaches are analysed with a view to informing future research aimed at developing FLSs with both high performance and high interpretability. Chapter 6's focus is pointed in the rule-base step of Fig. 1.2.

In Chapter 7, the neonatal baby O_2 support suggestion application is undertaken to test the deployability of ADONiS in a real-world setting and to provide initial insight in respect to its viability in replacing traditional approaches, in particular standard, singleton fuzzy logic control systems. First, an overall neonatal baby study overview is presented with related literature. Then, the system design and methodology are presented. Later, the application results are presented with medical expert opinions.

Chapter 8 summarises and concludes the work presented in this thesis, highlighting the main contributions, limitations, future works and articles produced with forthcoming papers.

1.7 Publications Arising from the Thesis

[122] **PEKASLAN, D.**, KABIR, S., GARIBALDI, J. M., AND WAGNER, C. Determining firing strengths through a novel similarity measure to enhance uncertainty handling in non-singleton fuzzy logic systems. *In Proceedings of the 9th International Joint Conference on Computational Intelligence - Volume 1: IJCCI, (2017)*, INSTICC, SciTePress, pp. 83–90. (Contribution to Chapter 3)

[120] **PEKASLAN, D.**, GARIBALDI, J. M., AND WAGNER, C. Exploring subsethood to determine firing strength in non-singleton fuzzy logic systems. *In Fuzzy Systems (FUZZ-IEEE), IEEE International Conference on (2018),* IEEE.(Contribution to Chapter 3)

[121] **PEKASLAN, D.**, GARIBALDI, J. M., AND WAGNER, C. Noise parameter estimation for non-singleton fuzzy logic systems. In *2018 IEEE International Conference on Systems, Man, and Cybernetics (SMC) (2018)*, pp. 2960–2965. (Contribution to Chapter 4 and Chapter 5)

[124] **PEKASLAN, D.**, WAGNER, C., AND GARIBALDI, J. M. Adonis—adaptive online non-singleton fuzzy logic systems. *IEEE Transactions on Fuzzy Systems 28, 10 (2020)*, 2302–2312. (Contribution to Chapter 4)

[123] **PEKASLAN, D.**, WAGNER, C., AND GARIBALDI, J. M. Leveraging IT2 Input Fuzzy Sets in Non-Singleton Fuzzy Logic Systems to Dynamically Adapt to Varying Uncertainty Levels. *IEEE International Conference on Fuzzy Systems 2019-June (2019*). (Contribution to Chapter 5)

[119] **PEKASLAN, D.**, CHEN, C., WAGNER, C., AND GARIBALDI, J. M. Performance and interpretability in fuzzy logic systems – can we have both? *In Information Processing and Management of Uncertainty in Knowledge-Based Systems (Cham, 2020)*, M.-J. Lesot, S. Vieira, M. Z. Reformat, J. P. Carvalho, A. Wilbik, B. Bouchon-Meunier, and R. R. Yager, Eds., Springer International Publishing, pp. 571–584. (Contribution to Chapter 6)

[125] **PEKASLAN, D.**, WAGNER, C., GARIBALDI, J. M., MARIN, L. G.,AND SÁEZ, D. Uncertainty-aware forecasting of renewable energy sources. *In 2020 IEEE InternationalConference on Big Data and Smart Computing (BigComp)(2020)*, IEEE, pp. 240–246

Chapter 2

Background

Uncertainty is a pervasive element of many real-world applications, and very often, its have a detrimental effect on inputs of decision-support systems. Since inputs are generally affected by different levels of uncertainty, the ability to faithfully map these uncertainty levels (from input to output) becomes an essential aspect for decision-support systems. Furthermore, while carrying out the decision process, providing an insight of these processes is also another important asset which allows us to understand and validate the functioning of a the given decisions or systems.

As mentioned in the previous chapter, FLSs are considered as robust systems for handling uncertainty and are also frequently referred to as 'interpretable' systems. Taken together, this thesis aims to further develop input uncertainty handling capacity of FLSs in an adaptive manner, as well as maintain the given interpretability level of FLSs. Hence, while different uncertainty levels can be handled on run-time, an insight of why or how results are produced can be provided in the decision-support process of FLSs. The structure of this chapter is as follows.

FSs and FSs operations are mainly the foundation of FLSs. Thus, Section 2.1 introduces the theoretical background of Type-1 and Type-2 FSs and Section 2.2 outlines FS operations.

As one of the commonly used models, Mamdani [88] fuzzy systems are not only good at handling uncertainty but also offer a comprehensible way of characterising system behaviours [194], which provides interpretability for the model. Thus, Mamdani fuzzy systems are chosen to be employed throughout the thesis and Section 2.3 provides details of three different Mamdani

FLSs (singleton, non-singleton, Type-2 non-singleton) which generally comprise three essential steps: fuzzification, inferencing and defuzzification.

Section 2.4 and 2.5 provides the literature survey of NSFLSs as they are specifically designed to cope with input uncertainty. A literature survey which focuses on the inference step of (NS)FLSs and fuzzification step of NSFLSs are provided, respectively.

Section 2.6 presents an overview of the concept of interpretability in FLSs. Also maintaining given level of interpretability is presented.

Since time-series forecasting provides an ideal test-bed for systematic evaluation -such as offering the potential to accurately control the levels of uncertainty-, time series forecasting case studies are provided throughout the thesis. Therefore, Section 2.7 introduces chaotic nonlinear time-series generations, noise injection procedures and performance evaluations.

Lastly, Section 2.8 gives summary of this chapter. Also, to assist the reader, the list of used abbreviations can be found at the beginning of this thesis.

2.1 Fuzzy Sets

Human thinking is described by using language and linguistic terms which are, by nature, imprecise. Zadeh [189] introduced FS theory with the aim to capture uncertain information characterised by MFs. FSs are generally designed with respect to linguistic labels and are the basis for FLSs. In the following subsections, the concepts and definitions related to FSs are introduced.

2.1.1 Type-1 Fuzzy Sets

In classical set theory, a subset F of a set X can be defined by its characteristic function (also called discrimination function or indicator function) $\mu_F(x)$ as a mapping from the elements of X to the elements of the set {0,1} [94]

$$F \Rightarrow \mu_F(x) = \begin{cases} 1 & if\ x \in F \\ 0 & if\ x \notin F\ . \end{cases} \tag{2.1}$$

Thus F can be defined as conditions $F = \{x \mid x \text{ meets some condition(s)}\}$ and mathematically knowing the $\mu_F(x)$ is the same as knowing F itself.

A Type-1 Fuzzy Sets (T1 FSs) A is a generalisation of the crisp set, and it is defined on a universe of discourse X. FSs are characterised by MF $\mu_A(x)$ that takes value in the interval $[0, 1]$. An FS A in X can be represented as a set of ordered pairs of a generic element x and its grade of MF is shown as follows:

$$A = \{(x, \mu_A(x)) \mid x \in X\} \tag{2.2}$$

If membership grades are constrained to be either 0 or 1, then a crisp set is obtained. Otherwise, membership grades $\mu_A(x)$ takes the value in the interval of $[0, 1]$ for each element $x \in X$ [94].

When X is continuous, MF A is commonly written as:

$$A = \int_X \mu_A(x)/x, \tag{2.3}$$

where $\int$ denotes the collection of all points $x \in X$ with associated $(/)$ MF $\mu_A(x)$. When X is discrete, A is commonly written as:

$$A = \sum_X \mu_A(x)/x, \tag{2.4}$$

where the $\sum$ denotes the denotes the collection of all points $x \in X$ with associated $(/)$ MF $\mu_A(x)$.

While different pre-defined shapes can be used for MFs, it can also be non-parametric (e.g.

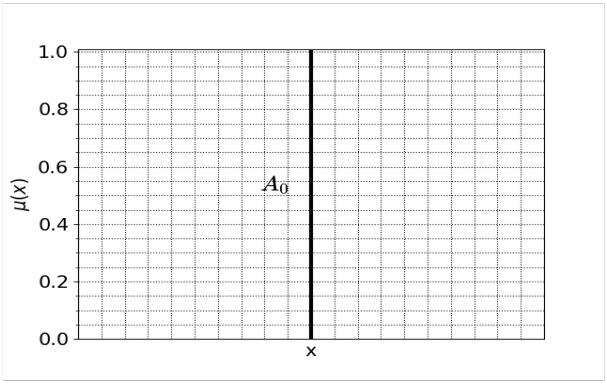

(a) A Singleton MF

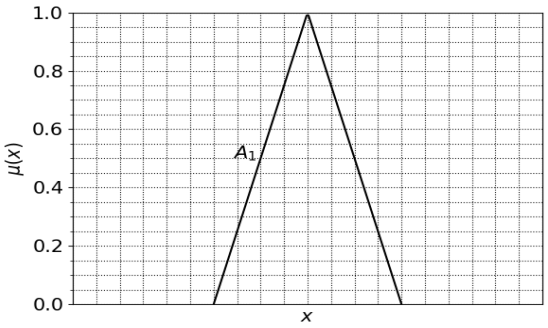

(b) A Triangular shaped MF

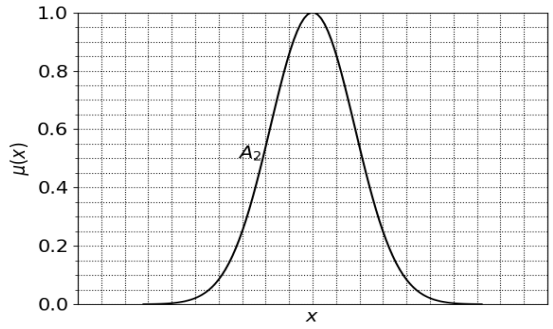

(c) A Gaussian shaped MF

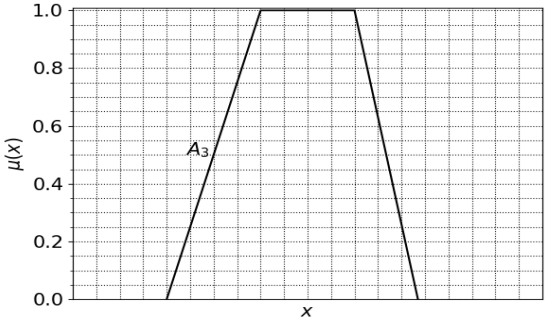

(d) A Trapezoid shaped MF

Figure 2.1: Four different MF samples

not defined shaped). Four samples of pre-defined shaped MFs are shown in Fig. 2.1.

2.1.2 Type-2 Fuzzy Sets

In the previous section, the difference between crisp sets and FSs is presented. When the membership function cannot represent only either 0 or 1, T1 FSs are utilised to get membership grades between the interval of $[0, 1]$. Similarly, when the circumstances are more uncertain, the membership grade itself may not be represented as a crisp number. To capture these more fuzzy circumstances, Type-2 Fuzzy sets (T2 FSs) introduced by Zadeh in 1975 [191].

2.1.2.1 General Type-2 Fuzzy Sets

A T2 FS is characterised by a fuzzy MF that has a membership grade for each element of the set as a fuzzy set in [0,1]. A General Type-2 FS (GT2 FS) [191] is constructed using a T2

membership function formulated as $0 \leq \mu_{\widetilde{A}}(x,u) \leq 1$ where $x \in X$ and $u \in J_x \subseteq [0,1]$ as follows:

$$\widetilde{A} = \{(x, \mu_A(x,u)) \mid x \in X, u \in J_x \subseteq [0,1]\} \tag{2.5}$$

where x is the primary and u is the secondary variable, while J_x refers to the primary membership, $\mu_A(x,u)$ is referred to the secondary membership of x.

$$\widetilde{A} = \int_{x \in X} \int_{u \in J_x} \mu_{\tilde{A}}(x,u)/(x,u) \quad J_x \subseteq [0,1] \, . \tag{2.6}$$

where $\int$ denotes the collection of all points $x \in X$ with associated $(/)$ MF $\mu_A(x)$. When X is discrete, A is commonly written as:

$$\widetilde{A} = \sum_{x \in X} \sum_{u \in J_x} \mu_{\tilde{A}}(x,u)/(x,u) \quad J_x \subseteq [0,1] \, . \tag{2.7}$$

Regardless of the extra degree of freedom capacity, GT2 FSs have limited usage in applications, due to high computational cost. In the literature, several approaches have been developed to reduce this computational burden. For instance, [55, 110] focus on GT2 FS type-reduction and defuzzification steps. Another study [175] introduced a framework, which is referred to as *zSlices* based GT2 FS in fuzzy systems. The proposed approaches lead to a reduction in both the complexity and the computational requirements for GT" FSs applications, and it has been implemented, for example, two-wheeled mobile robot which operates in a real-world outdoor environment.

2.1.2.2 Interval Type-2 Fuzzy Sets

Even though the GT2 FSs are successfully applied in many applications, as mentioned, it has been perceived to be computationally expensive techniques for uncertainty management in real-world applications. Hence, Interval Type-2 Fuzzy Sets (IT2) FSs introduced, which simplifies

the secondary membership grades to be 0 or 1 [94]. So that the (2.6) can be re-expressed by considering all $\mu_{\tilde{A}}(x,u)$=1 as:

$$\widetilde{A} = \int_{x\in X} \int_{u\in J_x} 1/(x,u) \quad J_x \subseteq [0,1] \; . \tag{2.8}$$

where $\int$ denotes the collection of all points $x \in X$ with associated ($/$) MF $\mu_A(x)$. When X is discrete, A is commonly written as:

$$\widetilde{A} = \sum_{x\in X} \sum_{u\in J_x} 1/(x,u) \quad J_x \subseteq [0,1] \; . \tag{2.9}$$

2.1.2.3 Footprint of Uncertainty

Overall, the region bounded by the primary membership function is called the footprint of uncertainty (FOU) [95] and it is the union of all primary memberships as shown below.

$$FOU(\widetilde{A}) = \bigcup_{\forall x\in X} J_x \tag{2.10}$$

The FOU concept is utilised to focus attention on the uncertainty in a primary membership function. Therefore FOU provides a convenient verbal and graphical representation.

Depending on applications and design choices, many different FOU assembly can be implemented. In this thesis, we will be using the *uncertain standard deviation* technique to generate FOU on the primary membership [95]. While the FS shape is defined as Gaussian (See Fig. 2.2a), the uncertainty on the primary membership function is applied by adding and subtracting a given uncertainty level (n) from the standard deviation (σ) of the FS A ($\sigma \pm n$=$[\sigma_1, \sigma_2]$), shown in Fig. 2.2b.

$$\mu_A(x) = \exp\left[-\frac{1}{2}\left(\frac{x-c}{\sigma}\right)^2\right] \quad \sigma \in [\sigma_1, \sigma_2], \tag{2.11}$$

where c and σ are the centre and the variance of the MF, respectively.

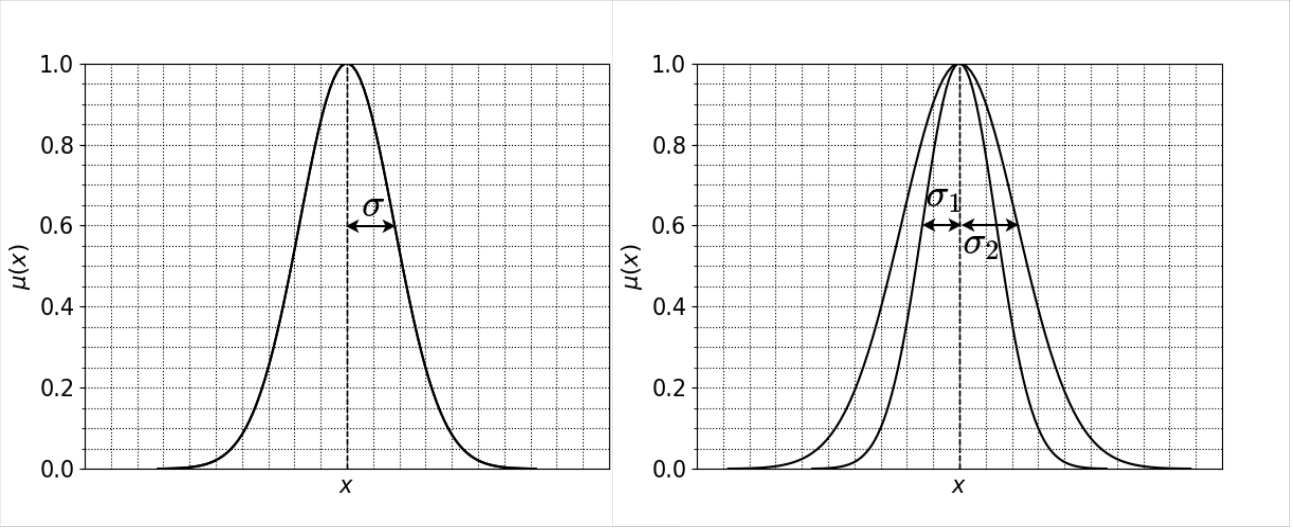

(a) Gaussian MF. (b) IT2 FS.

Figure 2.2: FOU for Gaussian MF with uncertain standard deviation $\sigma \pm n$=$[\sigma_1, \sigma_2]$

Since IT2 FSs are defined based on the FOU (lower $\underline{\mu}_{\tilde{A}}(x)$ and upper $\bar{\mu}_{\tilde{A}}(x)$ membership functions 2.2b), the computational cost is reduced significantly.

$$\underline{\mu}_{\widetilde{A}}(x) = \exp\left[-\frac{1}{2}\left(\frac{x-c}{\sigma_1}\right)^2\right] , \tag{2.12}$$

$$\bar{\mu}_{\widetilde{A}}(x) = \exp\left[-\frac{1}{2}\left(\frac{x-c}{\sigma_2}\right)^2\right] , \tag{2.13}$$

where c is the centre, σ_1 is calculated by $\sigma - n$ and σ_2 is calculated by $\sigma + n$ where n is the given uncertainty level on the principal MF.

For instance, on a restaurant rating scale from $0 - 10$, the rating 5 may represent the word *average* in the crisp sense, as shown in Fig. 2.3a. Accordingly, any rating which is less than 5 (e.g. 4.99) or more (e.g 5.01) can be considered as *not average*. Yet, by nature, that decision can include some uncertainty and the value 5 may not exactly define the only decision of *average* for the restaurant. In that case, the rating can be represented as a FS by taking into account the uncertainty (e.g. it can be represented as Gaussian MF, shown in Fig. 2.3b. Furthermore, if the membership grades of this representation can not be determined as exact degrees, T2 FSs are designed to allow the uncertainty to be represented in the membership grade as well (Fig. 2.3c).

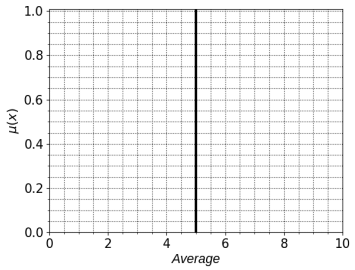

(a) Rating *average* 5 with exact value.

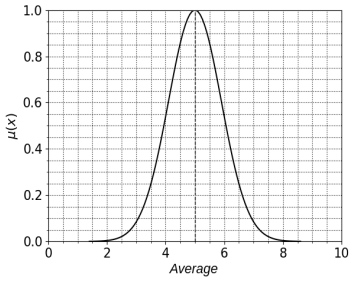

(b) Rating *average* 5 with uncertainty.

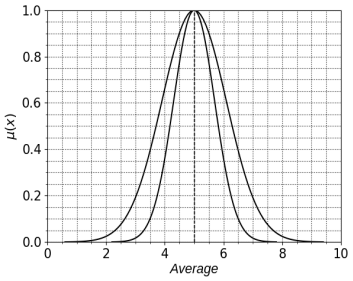

(c) Rating *average* 5 with higher uncertainty.

Figure 2.3: Three different MF samples to represent the work *average*

Even though this type of extensions can be elaborated more and the secondary degree can be represented by FS and so on, for practical reasons, commonly, T1 and IT2 FSs are used in many applications.

After having a detailed T1 and T2 FSs background, we will now proceed with the FS operations.

2.2 Fuzzy Set Operations

As mentioned in the previous section, FSs are a generalisation of the crisp sets, and as it is practised in the crisp set theory, intersection, union and complement operations are applied to FSs [189].

Let T1 FSs A and I be described by their MFs $\mu_A(x)$ and $\mu_I(x)$ on X. A fuzzy union operation can be described as follows[189]. :

$$A \cup I \Leftrightarrow \mu_{A \cup I}(x) = max[\mu_A(x), \mu_I(x)] = \mu_A(x) \vee \mu_I(x), \ \forall x \in X, \tag{2.14}$$

where $\vee$ denotes the maximum operator, as shown in Fig 2.4c.

Fuzzy intersection definition can lead to the MF:

$$A \cap I \Leftrightarrow \mu_{A \cap I}(x) = min[\mu_A(x), \mu_I(x)] = \mu_A(x) \wedge \mu_I(x), \ \forall x \in X, \tag{2.15}$$

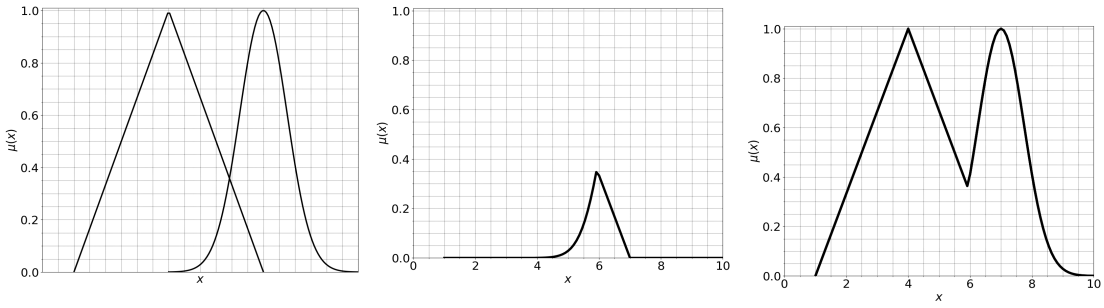

(a) Sample of two (Triangular and Gaussian) fuzzy sets.

(b) Intersection of the two fuzzy sets.

(c) Union of the two fuzzy sets.

Figure 2.4: Example of fuzzy operations (b) intersection (min as t-norm) and (c) union (max as t-conorm).

where $\wedge$ denotes the minimum operator, as shown in Fig. 2.4b.

The general name for these operations are t-norm ($\star$) for intersection and t-conorm operator for the union, and in the literature, different methods are proposed for these operations. For instance, algebraic sum, bounded sum or drastic sum as t-conorm and algebraic product, bounded product or drastic product for t-norm operator [39, 41, 75, 94, 184, 189].

Throughout this thesis, as the most common operator, we will be using *minimum* for t-norm and *maximum* for t-conorm operator between FSs. Regarding the use of these FSs in decision-support models, we will now introduce the Fuzzy rule-based systems step-by-step.

2.3 Fuzzy Rule-Based Systems

In the field of artificial intelligence (machine intelligence), there are various ways to represent knowledge [139]. One of the convenient and intuitive approach to represent human knowledge is to form it into natural language expressions such as:

IF premise (antecedent), THEN conclusion (consequent).

In the literature, different models utilise this type of rules in different ways. For instance, traditionally, Takagi-Sugeno (TS) [162] or Adaptive-Network-based Fuzzy Inference System (ANFIS) [70] utilise FSs in the premise part of the rules, and some parametric equations or

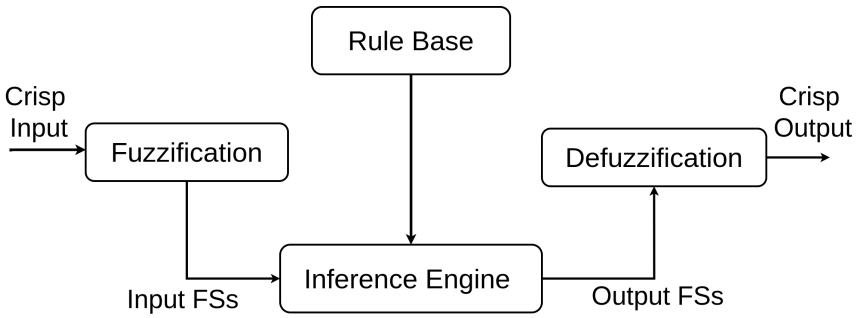

Figure 2.5: A block diagram of fuzzy Mamdani model.

FSs are used in the conclusion part of the rules. Generally, tuning procedures are applied to update/define the parameters of different models. In Mamdani [88] fuzzy rule-based systems, traditionally, FSs are utilised in both premise and consequents part of the system rules.

Since FSs are linguistically labelled, FLSs mechanisms can be understood by humans and insight of questions why or how results are produced? can be provided. Yet, as tuning procedures are applied (e.g. ANFIS), the model parameters are altered in a data-driven way which usually causes reducing the model interpretability –even though the accuracy of models can be increased [21, 23, 63, 111].

Since Mamdani models' rule premises and conclusions are established by FSs, it provides a more interpretable decision-making process than other models, e.g. TSK or ANFIS. Thus, Mamdani fuzzy models are preferred to be used in many applications [4, 194].

In this thesis, while the core part of our investigations focuses on increasing models' performance -by mapping input uncertainty to output-, the other focus is to maintain the given level of interpretability of the model. Therefore, throughout the investigation, the Mamdani model is chosen to be used which traditionally compound from four different components; fuzzification, rule-base, inference engine and defuzzification (See Fig. 2.5). Depending upon the used FSs, different versions of models as Singleton, Non-Singleton and Type-2 Non-Singleton Mamdani fuzzy models are employed, and for the sake of simplicity, the details of each model are presented on a sample of single-input single-output (SISO) model with a single representative rule. Later, a brief explanation with multi-input and single-output (MISO) is also provided after each SISO example.

2.3.1 Singleton Fuzzy Logic System

In this model, inputs are assumed to be exact/correct value and the operations are employed as detailed below.

2.3.1.1 Fuzzification - Singleton

In the fuzzification step of singleton FLSs, a given crisp input is transformed into a singleton input FS (See Fig. 2.6). Assume that I is a fuzzy set in the universe of discourse X where an FS $\mu_I(x)$ takes values in the interval [0,1], formulated as:

$$I = \{x, \mu_I(x) \mid \forall x \in X\} \ . \tag{2.16}$$

Singleton fuzzy sets are characterised by a single value x with a membership of 1 as follows:

$$\mu_I(x) = \begin{cases} 1 & if\ x \in I \\ 0 & if\ x \notin I \ . \end{cases} \tag{2.17}$$

In the case of multiple inputs are given (**x**=$(x_1, \ldots, x_n)^T \in U_1, ..., U_n$), each x_i is fuzzified into MFs ($I_i \quad i = 1, \ldots, n$).

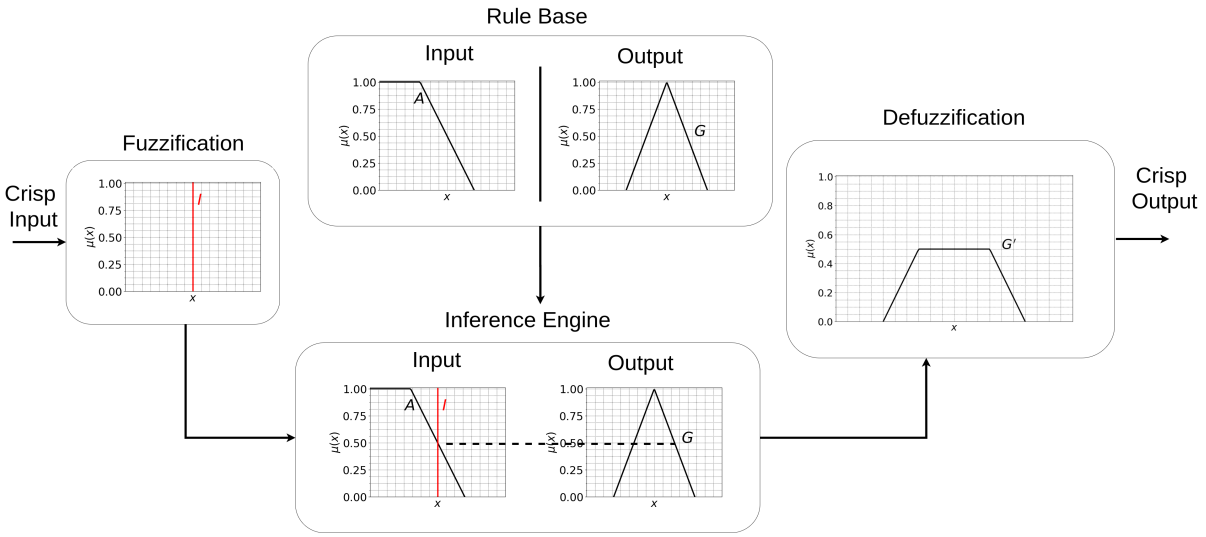

Figure 2.6: Singleton Fuzzy Logic System

2.3.1.2 Rule Base

Fuzzy rules can be generated from expert knowledge and/or by using data-driven techniques. In FLSs, rules consist of two main parts: IF-$THEN$ and in the Mamdani model, both IF and the consequents ($THEN$) parts consist of FSs. A sample of a rule can be seen in (2.18) and visualised in Fig. 2.6.

2.3.1.3 Inference Engine - Singleton

The inference engine in the Mamdani model provides a mapping of singleton input FSs to output FSs. During this process, firing strength levels are calculated in each interaction of singleton input FS and the corresponding antecedent FSs in rules. After each rule is evaluated separately, a decision is made for each individual rule by using operators logical operators.

$$Rule = \text{IF}\, x\, is\, A\ \text{THEN}\, y\, is\, G \tag{2.18}$$

As shown in Fig. 2.7, the input is designed in singleton FS and the firing strength between this interaction ($\mu_I(x) \star \mu_A(x)$) is only a function of input x which provides a scalar value. The firing strength between input FS (I) and antecedent FS (A) is reflected in the output FS (G), as shown as the representative sample of this inferencing procedure in Fig. 2.6.

In the case of multi-input single output (MISO) model, the rule is formed as follows:

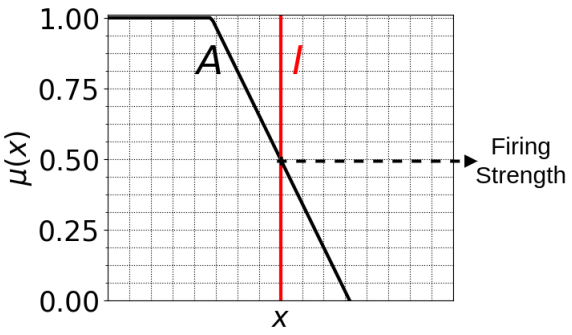

Figure 2.7: Firing Strength of singleton input FS (I) and antecedent FS (A).

$$Rule^1 = \text{IF } x_1 \, is \, A_1 \text{ and } \ldots \text{ and } IF \, x_n \, is \, A_n \text{ THEN } y \, is \, G \tag{2.19}$$

where $x_1 \in U_1, ..., x_n \in U_n$ and the output $y \in V$ which represented by fuzzy relation between input space in $U_1 \times \cdots \times U_n$ and the output space Y and denoted as follows:

$$R^1 = A_1 \times \cdots \times A_n \rightarrow G \tag{2.20}$$

The MF of this mapping is denoted by $\mu_{A_1 \times \cdots \times A_n \rightarrow G}(\mathbf{x}, y)$ where input $\mathbf{x} = (x_1, ..., x_n)^T$. This MF can be re-expressed as follows:

$$\begin{aligned} \mu_{A_1 \times \cdots \times A_n \rightarrow G}(\mathbf{x}, y) &= \mu_{A_1 \times \cdots \times A_n \rightarrow G}(\mathbf{x}) \star \mu_G(y) \\ &= \mu_{A_1}(x_1) \star \cdots \star \mu_{A_n}(x_n) \star \mu_G(y) \\ &= \Big[T_i^n \mu_{A_i}(x_i)\Big] \star \mu_G(y) \end{aligned} \tag{2.21}$$

where multiple antecedents are connected by t-norm operator and T refers to t-norm.

When inputs $\mu_I(\mathbf{x})$ are delivered to the model, they are processed over the rule as follows:

$$\begin{aligned} \mu_{G^1}(y) &= \sup_{x \in U}[\mu_I(\mathbf{x}) \star \mu_{A_1 \times \cdots \times A_n \rightarrow G}(\mathbf{x}, y)] \\ &= \sup_{x \in U}\Big[T_i^n \mu_I(x_i) \star \Big[T_i^n \mu_{A_i}(x_i)\Big] \star \mu_G(y)\Big] \\ &= \sup_{x \in U}\Big\{\Big[T_i^n \mu_I(x_i) \star \mu_{A_i}(x_i)\Big] \star \mu_G(y)\Big\} \\ &= \mu_G(y) \star \Big\{\Big[sup_{x_1 \in U_1} \mu_I(x_1) \star \mu_{A_1}(x_1)\Big] \star \\ &\qquad \cdots \star \Big[sup_{x_n \in U_n} \mu_I(x_n) \star \mu_{A_n}(x_n)\Big]\Big\}, y \in V \end{aligned} \tag{2.22}$$

In 2.22 a single Rule (R^1) inferencing is shown which provides B'. If we assume there are M rules (where $R^l \quad l = 1, \ldots, M$), then the final fuzzy set B is determined by combining for all B's from each rule as follows:

$$G' = G^1 \oplus \cdots \oplus G^M. \tag{2.23}$$

where $\oplus$ is t-conorm operator.

2.3.1.4 Defuzzification

After obtaining the output FS (G'), the defuzzifier convert this set into a crisp value (See Fig. 2.6). In the literature, there are different defuzzifier have been proposed [94]. In this thesis, the centroid defuzzification method (COG) is used over the obtained output FSs in all experiments.

2.3.2 Non-Singleton Fuzzy Logic System

As real-world settings often include uncertainty sources which affect system inputs at different levels. NSFLSs are designed to capture input uncertainty and handle it in the inference engine steps. Apart from the fuzzification and inference engine steps, the same procedures as singleton models are followed in the rule base and defuzzification steps.

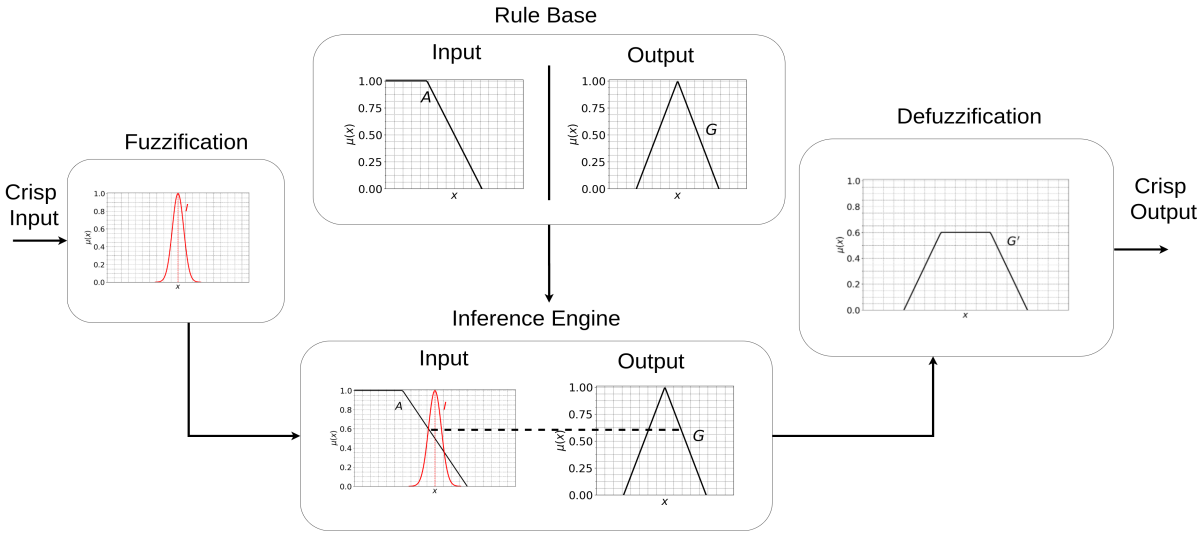

Figure 2.8: Non-Singleton Fuzzy Logic System

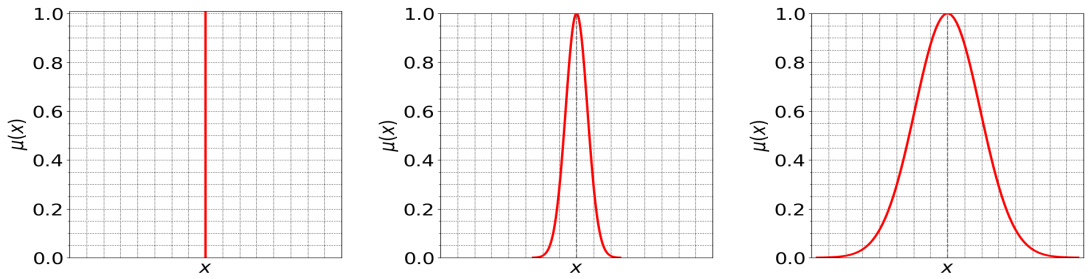

(a) Singleton input FS with no uncertainty (b) Non-Singleton input FS with lower uncertainty (c) Non-Singleton input FS with higher uncertainty

Figure 2.9: Singleton and Non-Singleton Gaussian FSs

2.3.2.1 Fuzzification - Non-Singleton

When input data has uncertainty (e.g. measurement imprecision, noise by external factors etc.), coping with this uncertainty becomes critical in decision-making systems. In non-singleton fuzzification step, capturing uncertainty is done by associating input data (x) with non-singleton FSs (See Fig. 2.8). Conceptually, it is assumed that the input x is the value which is likely to be correct, but because of existing uncertainty, neighbouring values of x's have also potential to be the correct value. As we go away from the input x value, the possibility of being the correct value is decreasing [104]. Therefore, the width of the non-singleton FS is associated with the uncertainty level in the given input. For instance, while high uncertainty can result in wider non-singleton FSs, low uncertainty leads to narrower or even singleton (noise-free) input FSs. As shown in Fig. 2.9, different uncertainty levels are captured with different width of FSs. Non-singleton FSs can thus capture input uncertainty in an efficient manner, without requiring changes to other (unrelated) parts of the FLSs, such as antecedents or consequents. While the different design of non-singleton FSs can be characterised, such as convex shapes or non-convex etc., in this thesis (in Chapters 3-6), we use the most common choice; Gaussian input FSs, and standard deviation (σ) is used to define the uncertainty level as it defined the width of the FS:

$$\mu_I(x) = \exp\left[-\frac{1}{2}\left(\frac{x - x'}{\sigma}\right)^2\right], \tag{2.24}$$

where σ is the input uncertainty level, x' are the neighbouring values of the mean, which is located at x.

In the case of multiple inputs are given (**x=**$(x_1, \ldots, x_n)^T \in U_1, ..., U_n$) and inputs are contain some levels of uncertainty, in order to capture this uncertainty, given inputs are mapped into non-singleton MFs ($I_i \quad i = 1, \ldots, n$)

After capturing the input uncertainty in non-singleton input FSs, it proceeds to the inference engine to interact with the given rules.

2.3.2.2 Rule Base

The rule-base of NSFLSs is the same as the singleton fuzzy logic systems which is mentioned in the previous section. So that the same rules -with the same parameters in antecedent and output FSs- can be employed in both singleton or non-singleton fuzzy systems. See Fig. 2.8

2.3.2.3 Inference Engine - Non-Singleton

In the inference engine step, the constructed non-singleton input FSs interact with the corresponding antecedent FSs in the given rules, as shown in Fig. 2.8. The captured input uncertainty from the fuzzification is handled in this step and this uncertainty is reflected as firing strength between the interaction of input and antecedent FSs. Therefore, it can be sad that firing strength has a significant role in terms of mapping input uncertainty to outputs of FLSs.

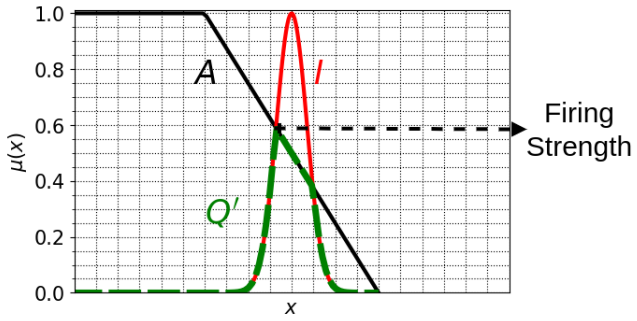

Figure 2.10: Firing Strength of non-singleton input FS (I) and antecedent FS (A) over the intersection (Q').

Traditionally, as shown in Fig. 2.10, another FS (Q') emerges from the interaction between the input and antecedent FSs.

$$\mu_{Q'}(x) = \mu_I(x) \star \mu_{A_i}(x) \tag{2.25}$$

where $\star$ is the t-norm operator.

Later, the maximum membership degree of the Q' FS is defined as the firing strength level of that interaction, as shown in Fig. 2.10. Throughout the thesis, we use the acronym *sta*-NS for this standard approach in firing strength definition.

After evaluating each individual rule, output FS is obtained by using the defined operator.

2.3.2.4 Defuzzification

As it is practised in singleton systems, structurally the same output FSs (G') are obtained in the defuzzification step, as shown in Fig 2.8. Thus, the same defuzzifier approaches can be employed in this step to obtain the crisp output of the system.

As can be seen in NSFLS design in Fig. 2.8, input uncertainty changes the fuzzification and inference engine firing strength definitions, and the remaining procedures are employed the same as the singleton models.

2.3.3 Interval Type-2 Non-Singleton Fuzzy Logic System

As mentioned in Section 2.1.2, T2 FSs are useful when the circumstances more fuzzy and the membership grade itself of T1 FS may not be able to reflect the uncertainty level as a crisp number. In this case, membership grade is defined as interval, and because of the computational simplicity, IT2 FSs are usually preferred models in applications.

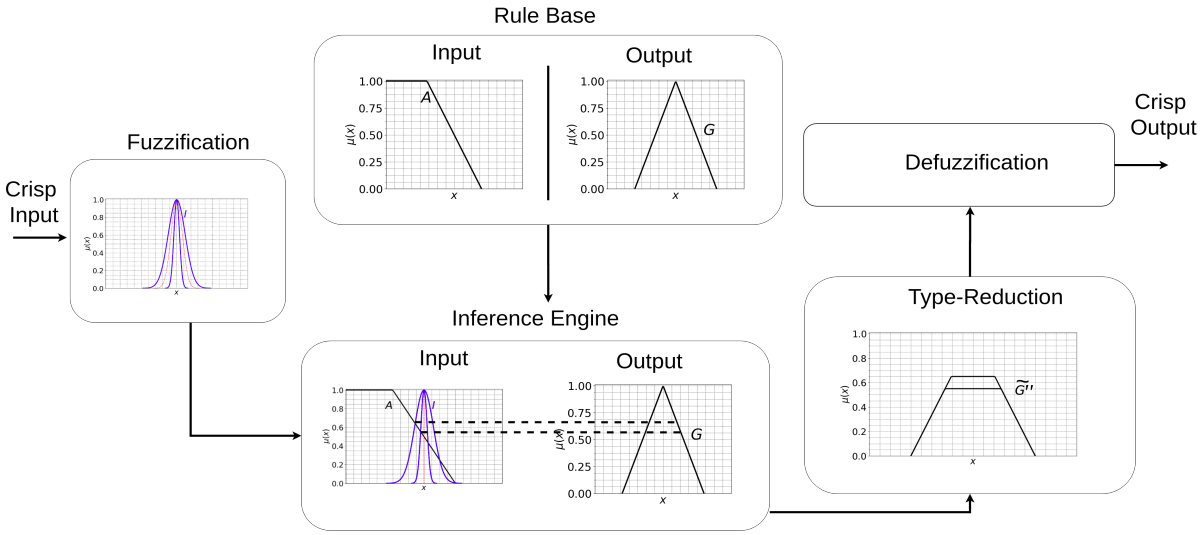

Figure 2.11: IT2 input FSs Non-Singleton Fuzzy Logic System

2.3.3.1 Fuzzification - Interval Type-2 Non-Singleton

In IT2 NFLSs, the given input (x) are defined as IT2 FS, as shown in Fig. 2.11. Based on the design choice, the extra degree of freedom of IT2 input FSs can be utilised to capture different uncertainty types. In this thesis, in Chapter 5, while the core T1 input FSs are used to capture the input uncertainty, the FOU of IT2 input FSs is used to capture the variation in uncertainty over a period of time. The widths of the primary FS is associated with the uncertainty level and the width of secondary MF (FOU) is associated with the variation in uncertainty levels over time. Thus, constant unstable environmental conditions (varying uncertainty levels) are captured in the extra degree of freedom of IT2 input FSs.

The lower and upper input FSs can be defined as follows with a given input x and uncertainty level (σ) while the variation in uncertainty level is n:

$$\underline{\mu}_{\widetilde{I}}(x) = \exp\left[-\frac{1}{2}\left(\frac{x-x'}{\sigma-n}\right)^2\right], \tag{2.26}$$

$$\bar{\mu}_{\widetilde{I}}(x) = \exp\left[-\frac{1}{2}\left(\frac{x-x'}{\sigma+n}\right)^2\right], \tag{2.27}$$

While different defined shape or without pre-defined shapes can be used in IT2 input FSs,

we use Gaussian shape with uncertain standard deviation technique to construct IT2 input FSs which are proceed to the inference engine step.

2.3.3.2 Rule Base

As it is employed in singleton and Type1 NSFLSs, the same rule base are used in IT2 NSFLSs as well (Fig. 2.11).

2.3.3.3 Inference Engine - Interval Type-2 Non-Singleton

Practically, the same firing strength definition method from T1 NSFLS is used in IT2 NSFLSs. However, as there are two (upper and lower) FSs in the IT2 input FSs, each FS is processed separately on T1 antecedent FSs, and an interval firing strength is obtained for each individual rule, as shown in Fig. 2.11. This interval firing strength is reflected in the consequent of each rule and output FS ($\widetilde{G''}$) is obtained.

2.3.3.4 Type Reduction

Unlike the NSFLSs, IT2 output FSs are generated in IT2 NSFLSs. Therefore, type-reduction procedure is applied to the obtained output set ($\widetilde{G''}$), as shown in Fig. 2.11. In literature different, type reduction procedures are proposed, and in this thesis, the common Enhanced Karnik and Mendel (EKM) [181] is employed on the obtained output FS to find the left and right points.

2.3.3.5 Defuzzification

In the defuzzification of IT2 NSFLSs, the calculated left and right values from EKM algorithm are simply averaged to calculate the crisp output of IT2 NSFLSs. (Fig. 2.11)

So far, three different fuzzy Mamdani rule base have been detailed in each step. We now proceed with the literature reviews regarding determining firing strengths and the fuzzification step of NSFLSs.

2.4 A Review in Regards to Firing Strengths

As mentioned in the previous sections, firing strengths have a significant role in driving the mapping of antecedents to consequents, being based on the interaction of the input and antecedent FSs. In this section, first, we present the literature with respect to early firing strength related studies. Later, a literature survey of firing strength determining studies in optimised and Mamdani FLSs will be provided, respectively.

Over the years, a large body of work has explored the use of other approaches to establishing what is effectively the compatibility between FSs through various measures in reasoning [16, 34, 36, 44, 59, 86, 142]. Even though Zadeh's Compositional Rule of Inference (CRI) provided successful results in various systems, some drawbacks have been highlighted [167, 168] and different similarity-based fuzzy reasoning methods have been proposed over the years.

2.4.1 Approximate Reasoning Studies

Early studies have shown that the notion of a similarity measure between two fuzzy sets may be successfully applied in fuzzy reasoning. The Approximate Analogical Reasoning Schema (AARS) has been proposed which mainly built on a distance measure and a pre-defined threshold (τ) value to avoid going through the conceptually complicated CRI [167, 168]. AARS method has been applied on linguistic variables by calculating the distance measure between A' and A which is denoted as $D(A', A)$ in (2.28). The distance measure calculation can be implemented among several mentioned distances (i.e., Disconsistency measure, Hausdorff measure, Kaufman and Gupta measure, Gupta measure). After calculating the $D(A', A)$ by a chosen measure, it is used to obtain similarity measure (S_{AARS}) as:

$$S_{AARS} = \frac{D(A', A)}{(1 + D(A', A))}; \quad S_{AARS} \in [0, 1] \tag{2.28}$$

A simple rule with the defined threshold value and a given fact is given below.

Rule: if X is A, then Y is B (threshold $\boldsymbol{\tau}$)

Fact: X is A' (such that S_{AARS} exceeds $\boldsymbol{\tau}$)

Conclusion: Y is B'

If the calculated similarity measure S_{AARS} is greater than the defined τ, then the rule is fired, otherwise not fired. Lastly, the B' is deducted by using modification techniques *Expansion* or *Reduction* form methods [165, 166, 167, 168].

In addition to the AARS method, another two similar approaches for medical diagnostic problems have been proposed [28]. In that method, patients' symptoms are represented by A, which is linked to fuzzy quantifier. Then a user provides features which are represented by A' and are also linked to the fuzzy quantifiers. The cosine similarity between these two vectors A' and A is calculated as follows:

$$S_{cos}(A', A) = \frac{|A'||A|cos\theta}{max(|A'||A|, |A'||A'|)} \tag{2.29}$$

where, |A'| and |A| the length of the vectors and $cos\theta$ is the cosine of the angle between vectors and S_cos is the similarity measure.

After the S_{cos} is calculated, the rule firing decision is made based on a pre-defined threshold τ as well. If the $S_{cos} \geq \tau$, the rule is fired. Later, this study has been extended by including weight parameters in the similarity measure and the same threshold controlling mechanism is applied [29]. In other studies, a subsethood measure between the A' and A has been used and this study has been extended later in [185, 186, 187] by using different similarity measures or including weights parameters in the used similarity measures. Then, as it is practised in the previous studies, the gathered similarity measure is compared with a pre-defined threshold and the rule is only fired, if the calculated measure is greater than the threshold, otherwise not fired.

A new similarity measure has been recently proposed and extended the work AARS [168] in the first scheme of the work [112, 133, 134] . Also, in the second scheme, a new similarity measure (between A' and A) has been proposed and used to modify the fuzzy relation (between

A and B). In the application scheme (i.e. Mamdani model), they also have utilised a defined threshold (ϵ), and the rules are fired based on this threshold check mechanism as well.

Firing strength has an essential role in terms of mapping input uncertainty to outputs of systems. Thus, determining firing strength systematically is an essential task for FLSs. The inference schemes listed above have a similar mechanism to eliminate the computational cost of fuzzy relation calculation. However, they rely on pre-defined thresholds, and the measures are used to make a decision on whether a rule can be fired or not, rather than directly being associated with firing level itself.

2.4.2 Inference Step of NSFLSs

Fuzzy reasoning had extensive attention, and over the years, many researches have been carried out which are mostly on theoretical bases. This section will investigate the practical application of different reasoning or inferencing approaches in the context of *optimised* NSFLSs.

In one of the initial work [115], to capture input uncertainty, the fuzzy neural system inputs have been mapped into fuzzy numbers. Firing levels between input and system weight MFs are defined by using the mutual subsethood measure (ξ) and the fuzzy inner product is used between each node to define the firing level of the corresponding rule. (2.30).

$$\xi(s, w) = \frac{C(s \cap w)}{C(s) + C(w) - C(s \cap w)} \in [0, 1], \tag{2.30}$$

where s is a fuzzified input value, w is the system weight, $c()$ is the cardinality and ξ is the calculated mutual subsethood measure.

In the training procedure, antecedents, consequents and input spread parameters (uncertainty levels) are updated in a data-driven manner. The proposed inference approach has been employed in several applications [58, 102, 108, 114, 116, 117, 127, 154] as well as evolving extensions [155, 157], T-S models [118], fuzzy cognitive maps for classification and prediction [160] and also implementation of asymmetry input fuzzy numbers [30, 170]. Even though the promising results have been obtained over different applications, the mutual subsethood

measure is degree to which input FSs equal to weight FSs which can be seen a special case of Jaccard index, where the union operator is replaced by the probabilistic sum. For instance, a firing strength between high uncertainty input (a 'wide' width in input FS) and low uncertainty antecedent (a 'narrow' width in antecedent FS) can produce the same firing level with the case of low uncertainty input and high uncertainty antecedent. In a traditional sense, this firing strength may be expected to be different because of the distinct circumstances in uncertainty levels. Thus, using the mutual subsethood measure may not produce faithful firing levels under certain circumstances. The details of this aspect will be elaborated in Chapter 3. In addition, traditionally, FLSs are frequently being referred to as 'interpretable' systems. When the optimisation procedures are applied, the ANFIS model parameters are often altered in a data-central manner. Although this can provide high accuracy, but commonly do not consider whether the resulting model is interpretable. Thus, it can also be said that the protecting interpretability of the system was not mainly considered either in the aforementioned studies. Furthermore, offline training procedures leads to a single parameter input FS spread which may not be able to capture varying input uncertainty levels in real-world circumstances. Thus, having a single width parameter for input FSs may prevent NSFLSs to adapt different uncertainty levels of real-world environments.

Another study on fuzzy neural network has been conducted by using the AARS approach related to firing rules, and in this study, different similarity measures have been investigated to compare with the defined threshold [132]. However, as it was practised in the initial AARS work [168], rather than determining firing level, the firing rule is decided based on the threshold value which is also defined through a supervised training procedure. As mentioned before, firing levels are one of the way of mapping input uncertainties to outputs of systems. Therefore, determining firing levels systematically is an important asset, whereas the study is conducted whether a rule should be fired or not based on calculated measures between input and weight MFs.

As mentioned in Section 2.3.2, the traditional way to define firing strengths in NSFLSs is to adopt maximum membership degree grade of the intersection between the input and antecedent FSs [94]. Throughout this thesis, we will use the term *sta*-NS to refer to this traditional approach

in determining firing strength.

Even though *sta*-NS has provided promising results, it may not systematically map different uncertainty levels in inputs to output of systems in different firing strength levels. Because different input FSs which have different uncertainty levels may intersect the antecedent at the same membership grade, resulting in the same firing level, despite the fact that these input FSs are clearly different. (A detailed critical analyses will be given in Chapter 3). In order to determine more systematic firing levels, a new approach has been proposed to utilise the centroid of intersection between input FSs (I) and antecedent FSs (A) [130, 131]. In this approach, first, the centroid of the intersection between I and A has been calculated. Then, the corresponding membership degree of the centroid position of the intersection has been defined to be the firing strengths. This centroid-based approach has been used in time series predictions and UAV studies successfully [131, 51]. More recently, Wagner et al., (2016) have proposed to use similarity measures to define firing strength between the input and antecedent FSs [176]. In their work, the Jaccard similarity measure [68] between input FS (I) and antecedent FS (A) has been used to define firing level, and this study has also shown advantages in time series prediction and robotics applications [52, 53, 188]. Throughout this thesis, the centroid based and similarity-based approaches will be referred as *cen*-NS and *sim*-NS, respectively. Different aspects of these approaches will be elaborated and critically analysed in Chapter 3. Furthermore, a novel approach will be put forward to generating firing strengths which faithfully map the uncertainty affecting system inputs to outputs.

While firing strength plays a crucial role in terms of input uncertainty handling, capturing uncertainty is also another important asset for NSFLSs. Especially, as the input uncertainty levels tend to vary in the real-world, capturing it adaptively can provide advantages and even maybe essential under certain situations. Therefore, in the next subsection, we will provide a literature survey which focuses on input uncertainty capturing in the fuzzification step of NSFLSs.

2.5 A Review in Regards to the Fuzzification Step of NSFLSs

This section will review the NSFLSs literature by focusing on how input FSs parameters are defined in various study and applications.

Initial works have introduced the idea of expressing systems' input data as FSs; Hayashi, Buvklet and Czogala (1992) have used the system inputs as vectors of fuzzy sets during processing in fuzzy neural network [65]. Later, this method has also been used in [10] fuzzy neural network with the control of an metal-cutting process application.

2.5.1 Fuzzification of NSFLSs

Later on, NSFLSs formulation has been presented [104] and forecasting of a chaotic noisy time series [107] and financial markets application has been implemented [105]. Overall, non-singleton input FSs show better performance in compare to counterpart singleton fuzzy models. Considering the dynamic behaviours of applications, the first implementation of dynamic NSFLSs has been carried out [106]. In this work, the fuzzy neural network has been trained to achieve a desired mapping defined by a set of input–output pairs of a target system. During this optimisation, different parameters (i.e. width of antecedent and input FSs) have been altered in a data-driven manner. As a result, the dynamic NSFLSs have provided performance benefits. However, the offline training procedures rely upon the training dataset. Also, defining a single width parameter tends to prevent NSFLSs from being able to adapt to the breadth of changing uncertainty levels inherent to real-world applications. Furthermore, altering key parameters based on the data-driven method may not comply with the initial interpretability settings of models (e.g. changing key parameters may cause poorer interpretability).

NSFLSs have also been employed in signal processing simulation by training parameters over various noise levels [126] and this study results have shown that non-singleton input FSs have performance advantages in terms of handling noisy signals. In another study [25], TSK fuzzy models have been used in controlled neuroprostheses based on the processing of sensory electroneurographic (ENG) signals. In their approach, genetic algorithms was utilised to define system parameters (e.g standard deviation of input FSs) and the comparable results were presented. NSFLSs have also been employed in the classification of cardiac arrhythmia by using ECG signals [32]. In their classification model, the TSK model has been used, and in training, the genetic algorithm has also been utilised to define model parameters. Results have indicated that NSFLSs outperform its corresponding SFLSs by using features that contain uncertainty. Even though genetic algorithms may often show advantages to find *globally* optimal solutions [25], parameters changing procedure has been implemented based upon the training dataset and on the real-world application phase, single constant parameters for input FSs (e.g. the same width value for all inputs) may not fully capture different uncertainty levels in inputs. Also, modifying rule sets or antecedent parameters in a data-centric manner may affect the interpretability of models –if rules and sets were designed by experts or understood well initially.

Type-1 and Type-2 neuro-fuzzy NSFLSs have also been used to make one step ahead prediction of the daily exchange rate between Mexican Peso and US Dollar [98]. In the parameters determination, the recursive least-squared-back-propagation hybrid learning method has been utilised and the advantage of a comparative study of different NSFLSs have been reported. IT2 input FSs in the TS model are also used in two experiments as Mackey-Glass time series forecasting and robotic hand identification [164]. In their approach, as it is a general practice, parameter tuning has been applied to the defined IT2 input FSs as well as other elements of the model. Results have showed that the IT2 Fuzzy modelling is a tool that allows dealing with a high level of uncertainty problems. Although IT2 input FSs have been applied successfully to capture uncertainty, after the tuning procedures, single parameter (widths) has been utilised for input FSs. However, using a single parameter for input FSs may not efficiently capture different real-world uncertainty levels.

Another study has been carried out for removing Mixed Gaussian and Impulse Noise from images by using non-singleton T1 input FSs with IT2 antecedents in neuro-fuzzy FLSs [192]. In this study, Quantum-behaved Particle Swarm Optimisation algorithm has been utilised to define parameters. During the training, 30% of additive Gaussian white noise and 50% impulse noise have been injected into the clean images and parameters tuning procedure has been employed over this contaminated image dataset. The proposed method has been compared to different filter techniques (i.e. median filter, Wiener filter, Gaussian filter, ROAD, IPAMF+BM) and counterpart SFLSs on benchmark datasets. Although successful image filtering results have been obtained overall, offline parameters tuning may prevent the model from adapting to different noise levels over time. Because, traditionally, input FS width parameters should be corresponding to image noise levels. As different noise level naturally occur in images, that input FS parameter may not capture it efficiently.

A recent two-wheeled self-balancing robot study has used different TSK fuzzy logic controller (singleton, non-singleton T1, IT2 and GT2) and compared the robot's performance balancing under noise-free and noisy conditions [193]. Study results have shown that non-singleton T1 FLS outperform singleton counterparts under noisy conditions. Also, GT2 FLSs have led the robot to adjust faster than IT2 FLSs under different conditions. Fuzzy neural networks have been used with ellipsoidal non-singleton Type-2 MFs [72] in an H-∞ based synchronisation of the fractional order chaotic systems [103]. In the proposed method, firstly, a clustering method has been utilised to optimise T2 MFs parameters. Later, Invasive Weed optimisation has been applied to shape rules of the system. The proposed method has been compared to singleton and various counterpart methods (e.g. self-organising fuzzy modified least-squares network, simple evolving Takagi–Sugeno fuzzy model etc.). Results have indicated that the proposed method provides better performances under the variance of added white noise 0.1. Although the aforementioned evolving mechanisms can provide advantages, optimising parameters based on a training dataset in an offline manner may not provide overall flexibility in adapting to different noise levels in the real-world. Also, the interpretability of the model relies on only the used data, as all the key parameters are determined/altered based on data-driven algorithms. Thus, it can deliver improved performance at the cost of poorer interpretability.

Moreover, different applications of standard NSFLSs have been utilised, such as control of motors [2, 135], pattern classification [17], state-space identification of UAV [150]. In addition that, as the tuning parameters require extra computational cost, different methodologies has also been proposed to expedite the *converge* time [99, 138, 38] and a structural and capability classification of different variants of FLSs is also reported [169].

Overall, real-world applications are often subject to varying conditions which are associated with uncertainty sources affecting systems' inputs at run-time. Even though the aforementioned studies provide promising results, it can be said that training aspects are dependent on offline optimisation which leads to single parameters for input FSs. This having a single parameter for input FSs prevents NSFLSs from being able to adapt to the changing uncertainty levels that are inherent to real-world applications. As stated in objectives 2, dynamically capturing different levels of input uncertainty and modelling it where it arises can provide advantages for being able to adapt different uncertainty conditions of real-world. These concepts will be discussed in details in Chapters 4 and 5.

Furthermore, traditionally, the aforementioned models use generally statistical optimisation techniques to tune parameters based on data-driven approaches. While these optimisation procedures provide performance benefits, they often cause building more complex fuzzy rule sets, rule parameters, MFs or fuzzy partitioning structures with high accuracy but commonly do not consider whether the resulting model is interpretable or not [3, 4, 22, 153]. Regarding the rule structure, Mamdani model rules [88] -where conclusions are FSs- are widely admitted as the more interpretable rules [4] which can provide the overall ability to be interpretable to the model. The details of the maintaining interpretability concept will be explored in Chapter 6 along with a comparison between an optimised model and the proposed framework from Chapter 4.

Mamdani NSFLS has been used to classify battlefield ground vehicles, and the steepest descent optimisation procedure has been applied to determine system parameters (e.g. width of input FSs) [183]. This method of design has been played a part of three different architectures (nonhierarchical, hierarchical in parallel and hierarchical in series) classifier and conducted a

comparison compared to Bayesian classifier results. Results have indicated that fuzzy systems outperforms Bayesian classifier. Even though the Mamdani model can provide advantages in terms of interpretability capacity, optimising parameters in a data-driven manner may distort the meaning of parameters. Also, when input widths are defined based on the training dataset, different settings may require different widths to capture different levels of uncertainty which may not be achieved with a single determined width parameter (e.g. MFs).

In an inverse scattering image procedure, Mamdani NSFLSs have been used as part of the proposed method to limit the noise's effects on the retrieval procedure and fully exploit the information content [12]. Regarding input width determining step in fuzzification, a heuristic calibration has been carried out, and different widths for input FSs have been varied in a range to define the *optimum* width parameter which constructs Type-1 input FSs. The experiment results have shown that the proposed method is effective, providing both acceptable reconstruction accuracy and robustness to the noise. However, traditionally, the width of input FS is associated with the noise level and having a single *optimum* value in input FSs may not accurately capture different noise levels during the inverse scattering.

In another study, Type-1 and Type-2 Mamdani NSFLSs have been explored to deal with the uncertainty in urban water management systems [87]. The study results have indicated that using fuzzy numbers instead of crisp data points for input can effectively address high data uncertainty problems. In the fuzzification of non-singleton input FSs, a range of different width values have been employed and the results are compared. This approach may also not be well suited to input FS widths corresponding to the data's actual uncertainty level.

Apart from those, as mentioned in the previous section, other studies have utilised non-singleton Type-1 fuzzifications in the Mamdani model in a different context, such as time-series prediction and robotics applications which generally shows that non-singleton systems outperform singleton counterparts models [51, 52, 53, 130, 131, 176, 188]. In those studies, either a priori knowledge or different trials have been utilised to define the input FSs parameters. Even though a priori knowledge of the uncertainty level can be efficient to define input width parameters, this approach is invariably dependent on the availability of this knowledge and does not

allow the modelling of levels of uncertainty which vary over time.

Adaptive Mamdani NSFLSs models, which *update* input FS parameters on the run-time, have been proposed to put forward IT2 input FSs generation [146, 147, 148, 149] and later these studies have been extended [140, 141]. In these studies, on robotic sensors, some trials have been carried out by generating noise (i.e. changing temperature, sound noise, and wind while recording measurements at a fixed distance) and the collection of 10000 sensor measures have been used to generate a non-specified convex shape piece-wise linear T1 input FSs. Then, different noise effects -with various levels- have been performed and different T1 sets have been generated which later utilised to construct IT2 input FSs in trails. After defining the IT2 through the different experiment settings in the pre-trials, on the run-time of the actual experiment, 5 consecutive crisp measurements from the sensor at the given instance have been collected, and the average of these 5 measurements has been interpolated with the previously constructed type-2 fuzzy sets at the right and left of the incoming measurement to generate an interpolated type-2 fuzzy input. These studies have shown that non-singleton input FSs usage and update it at run-time provides performance benefits in the used robotic applications. Even though the adaptive manner is very plausible and endorsed by experiments, it is still limited to the pre-trial conditions which was employed on the sensor with changing temperature, sound noise, and wind while recording measurements in advance. For instance, if conditions of pre-trials are changed (e.g. generation higher noise), a different IT2 may have been obtained. Consequently, during the testing phase, input FSs would be interpolated with the gathered IT2 from pre-trials. This may lead to a wider width, despite the testing may be performed in noise-free conditions. Thus, it can be said that, although updating input FS parameters is a very plausible approach, non-singleton input FSs may not sensitively be implemented based on the actual noise level of the testing-phase.

More recently, using of a weighted moving average (WMA) has been suggested to update the input value in time-series forecasting experiments [129] which has shown the advantages of non-singleton input FSs usage under different levels of noise. In this study, after WMA has altered input values, input FSs have been constructed over this new input. However, it has been assumed that the synthetic and stable noise levels had been known a priori, and the width of

input FSs have been kept constant. Although efficient performance increase has been achieved, this study focused only on update input values rather than widths of input FSs which suppose to capture noise in input value. While updating input values can be efficient, this approach is invariably dependent on the availability of this a priori knowledge in term of input noise levels and does not allow the modelling of different levels of uncertainty which vary over time.

Overall, real-world settings contain different uncertainty sources (e.g. environmental conditions) which usually affect input values at different levels at different times. Thus, an effective uncertainty mapping -from input to outputs- becomes an essential characterisation for NSFLSs. In this thesis, we build this input uncertainty mapping by adaptively capturing input uncertainty where it arises at run-time (Chapters 4 and 5) and systematically handling this uncertainty over rules of models (Chapter 3). While we capture-handle input uncertainty and provide performance benefits, synchronously, we also aim to maintain the interpretability of FLSs (Chapter 6). Thus, in the next section, we will present an overview of FLSs interpretability.

2.6 Interpretability

A key aspect of the vision of interpretable artificial intelligence (AI) is to have decision-making models which can be understood by humans. Thus, while an AI application may deliver a good performance, providing an insight of the decision process is also an important asset in terms of trust, fairness, privacy, reliability or robustness of models [40]. Traditionally, the accuracy and interpretability aspects yield a trade-off which attracts growing interest in the research community and it is assumed that this trade-off plays an essential role in the current literature panorama of computational intelligence [3]. Even though the interpretability-accuracy of AI is widely acknowledged to be a critical issue, it still remains a challenging task [74].

Historically, it has been acknowledged that FLSs are considered as interpretable systems in terms of having linguistic rules and FSs etc. As mentioned in the previous sections, in Mamdani models [88], FSs are used in both parts of rules (premises and consequents) which offer a more comprehensible way of characterising system behaviours that can provide an interpretable

structure in decision-making [194].

In the literature, there is no formal consensus on the definition of interpretability. However, informally an *interpretable* model can be characterised as on which a human can understand why or how results are produced in a given model. The readability of these models can be regarded as the first step to achieve an interpretable model [4].

Overall, a growing body of literature has examined to assess interpretability of FLSs [4, 54, 93] and different taxonomies have been proposed to cover different component of systems in the context of interpretability. Traditionally, it can be said that there are multiple aspects to consider interpretability of FLSs, such as, *FS-based* interpretability (e.g. labels, distinguishability, a moderate number of FSs etc) or *rule-based* interpretability (e.g. readability of a single rule or parsimony of rule-set etc.).

FS-based interpretability covers semantic constraint criteria in fuzzy modelling. During the construction of a FLS, if expert knowledge is available to build up the overall system, experts can *inherently* follow the interpretable FS designs and the semantics can be understandable, based on that expert knowledge. If expert knowledge is not available, data-driven approaches can be utilised to define FSs of FLSs. In this type of model construction, common properties can be followed to provide interpretability to FSs of system.

Rule-based interpretability focuses on fuzzy rules to generate a compact and consistent rule base. Experts can also create system rules which reflect experts' knowledge and the interpretability is provided naturally. If expert knowledge is not available, various taxonomies [54, 194] can be followed to provide an interpretable rule-set, such as rule-set simplicity, completeness, consistency etc. Also, hybrid approaches exist to construct interpretable FLSs in terms of both FS-based and rule-based aspects.

As the literature shows, interpretability of a FLS can be related to multiple aspects in multiple views which makes the interpretability concept a complex field. While this thesis particularly focuses on further developing input uncertainty capturing-handling capacity in an adaptive manner at run-time, it is assumed that a degree of interpretability is given in models. While the performance of FLS is increased through coping with input uncertainty, the aim is also to main-

tain the given degree of interpretability of FLSs by not changing key parameters which will be elaborated in the next subsection.

2.6.1 Maintaining Interpretability

One view of why FLSs are interpretable is that it allows us to use sets of interpretable FSs and/or rules which can be defined by experts in order to generate a desired behaviour. In this sense, it can be said that if a fuzzy system is constructed with understandable rules (e.g. simpler rules, parsimony in rule-sets) and parameters (e.g. labels, MFs), these components play a crucial role in the interpretability of systems which is beneficial to preserve throughout the implementation.

Although an interpretability degree is provided in a FLS by experts or in a data-driven way, real-world inputs can vary, and these varying circumstances may not fully correspond to the initial design of fuzzy systems which result in low performances in models. Therefore, in practice, very often those systems that have such rule bases and FSs that are further optimised in order to cope with changes, such as operating conditions, variations uncertainty, and noise levels in real-world environments. In order to increase the accuracy of these fuzzy systems, some fuzzy models (e.g. ANFIS) rely on data-driven design techniques, and due to their accuracy-oriented nature, this often leads to less interpretable FLSs by altering the key parameters (e.g. MFs, rules etc.) [3]. Even though a final model structure can provide high accuracy, the interpretability of the fuzzy system usually deteriorates [92, 194], although the interpretability had achieved during the designing stage of the system initially.

Therefore, while achieving an improved accuracy in the face of different real-world uncertainty conditions, the minimising altering the given FLS parameters can help maintain the initially given interpretability of FLSs. In this thesis, we focus on interpretability in the sense of minimising the changes that affect the key interpretability components. While coping with input uncertainty capacity is enhanced, the given interpretability can be maintained. In Chapter 6, we will investigate whether the proposed approaches in this thesis can be usefully applied to maintain interpretability by addressing objective 4.

Throughout this thesis, in each chapter (in Chapters 3-6), case studies are employed in time-series forecasting experiments to assess the characteristic of each proposed approach/framework. Thus, in the next section, time-series generation and noise injection procedures are detailed as well as the performance evaluation metrics.

2.7 Datasets and Evaluation

Because of offering the potential to control the levels of uncertainty accurately, time series forecasting provides an ideal test-bed for the systematic evaluation of decision-support models. In the literature many different studies have been successfully employed and tested in time series forecasting [24, 45, 69, 94, 116, 130, 129].

Due to the uncertainty controlling advantages and the usability, in this thesis, we conduct time-series predictions case studies on two of the most commonly used chaotic nonlinear time-series Mackey-Glass (MG) [85] and Lorenz time series [84].

2.7.1 Mackey-Glass Time series

The Mackey-Glass equation is the nonlinear time delay differential equation which is formulated as:

$$\frac{dx(t)}{dx} = \frac{ax(t-\tau)}{1+x^{10}(t-\tau)} - bx(t) \tag{2.31}$$

where a, b and n are constant real numbers, t is the current time, and τ is the delay time.

2.7.2 Lorenz Time series

The Lorenz Time series was derived from a model of the earth's atmospheric convection flow heated from below and cooled from above, and it is described using nonlinear differential equa-

tions as follows [84]:

$$\dot{x} = \sigma(y - x) \qquad \dot{y} = x(p - z) - y \qquad \dot{z} = xy - bz \tag{2.32}$$

where the dots denote the next values to the three variables x, y, z in the time series.

The defined parameters values for both MG and Lorenz time-series will be provided in each experiment.

2.7.3 Adding Noise to Time Series

In the literature, noise is generally measured by the signal-to-noise ratio (SNR) which is often expressed in decibels (dB). While lower noise levels are represented by higher SNR values, higher levels of noise are represented by lower SNR values. SNR is calculated as follows:

$$SNR = 10 * log\Big(\frac{\sigma_{nf}^2}{\sigma_n^2}\Big) \ , \tag{2.33}$$

where σ_{nf} is the standard deviation of the noise-free dataset and σ_n is the noise level.

Often, it is assumed that the values SNR and σ_{nf} are known a priori. Thus, when the σ_n is sought, (2.33) is re-arranged as follows:

$$\sigma_n = \frac{\sigma_{nf}}{10^{(\frac{SNR}{20})}}. \tag{2.34}$$

Gaussian noise represents a generally appropriate approximation of noise in real-world scenarios and it is thus one of the common variants for noise adding procedures [83]. Here, the mean value is set to zero and the noise level (σ_n) is used to drive the standard deviation of the Gaussian distribution. Then a random noise value is picked from the created distribution and is added to the noise-free set (x_t) as follows:

$$x_t' = x_t + \mathcal{N}(0,\, \sigma_n^2) \qquad t = 1, 2, 3, ..., N \ , \tag{2.35}$$

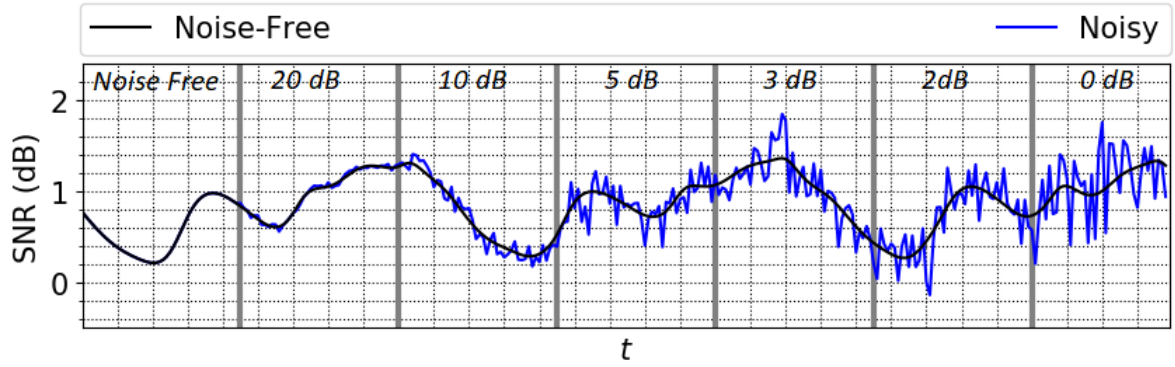

Figure 2.12: The sample of different noise levels on Mackey-Glass Time series dataset

where x'_t represents the noisy value and $\mathcal{N}(0, \sigma_n^2)$ is the Gaussian distribution to gather random noise values and N is the number of values in the dataset. Thereby, a noisy dataset can be generated for each t in the dataset.

A sample of noise differences in the range of noise-free to 0 dB can be seen in Fig. 2.12

2.7.4 Evaluation

Throughout the thesis, performances of proposed methods are evaluated based on the MSE (Mean Square Error) which is the average squared difference between the estimated results and the actual values. For instance, in a time-series prediction case study, let the prediction be $P = \{p_t : t \in T\}$ and $T = \{t_i \mid 1 \leq i \leq N\}$ and the actual values are $X = \{x_t : t \in T\}$ and $T = \{t_i \mid 1 \leq i \leq N\}$. The prediction performance is evaluated by using the MSE as follows:

$$MSE = \frac{1}{N}\sum_{t=1}^{N}(p_t - x_t)^2, \tag{2.36}$$

where p is the estimated value, x is the actual value and N is the number of estimation.

Apart from MSE, the symmetric mean absolute percentage error (sMAPE) is also used for performance evaluation in Chapter 4. SMAPE is a measure of prediction accuracy of a forecasting method and it was first proposed by Armstrong [5]. Due to the sMAPE limits the error rate to 200% and is robust to outliers, it can be used an alternative to the commonly used MSE.

The sMAPE measure is calculated as follows:

$$sMAPE = \frac{100}{N} \sum_{t=1}^{N} \frac{\mid p_t - x_t \mid}{(\mid x_t \mid + \mid p_t \mid)/2} , \tag{2.37}$$

where x is the actual value, p is the estimated value and N is the number of values in the series.

Also, in Chapter 6, the recently proposed Unscaled Mean Bounded Relative Absolute Error (UMBRAE) measure its utilised [27]. UMBRAE combines the best features of various alternative measures without suffering their common issues. Specifically, UMBRAE can be considered as informative, resistant to outliers, symmetric, scale-independent and interpretable.

With UMBRAE, the performance of a proposed method can be easily interpreted: when $UMBRAE$ is equal to 1, the proposed method performs approximately the same as the benchmark method; when $UMBRAE < 1$, the proposed method performs better than the benchmark method; when $UMBRAE > 1$, the proposed method performs worse than the benchmark method.

$$MBRAE = \frac{1}{N} \sum_{t=1}^{N} \frac{\mid p_t - x_t \mid}{\mid p_t - x_t \mid + e_t^*} , \tag{2.38}$$

where x is the actual value, p is the estimated value, $e*$ is an error between a commonly used benchmark method and actual value, and N is the number of values in the series

While MBRAE is a scaled error that may not be directly interpreted as normal error ratio reflecting the error size. In order to provide a more readable or interpretable error measure, the transformation is applied as follows:

$$UMBRAE = \frac{MBRAE}{1 - MBRAE}, \tag{2.39}$$

After having detailing the datasets and evaluation methods, we move on to providing summary of the chapter.

2.8 Summary

This chapter provides background information and an overview of the existing literature that has been used in this thesis. In particular, NSFLSs have been broadly reviewed with regards to the handling of input uncertainty in determining firing strength and capturing input uncertainty adaptively in the fuzzification step.

The first aspect is to leverage the interaction between input and antecedent FSs by faithfully mapping input uncertainty to outputs. The past and current approaches in determining firing strength have been provided, and the key strengths and challenges of these approaches were highlighted.

The second aspect is to focus on modelling the input uncertainty in a dynamic adaptive manner on-the-fly. The key literature in fuzzification of NSFLSs has been reviewed, and advantages and possible limitations have been examined.

The third aspect is to maintain a given level of interpretability in FLS, while employing the input uncertainty mapping to an output of NSFLSs. Thus, the maintaining interpretability has been briefly introduced and more detailed discussion will be provided in Chapter 6.

As the test-bed for this thesis' case studies, time-series dataset generations have been outlined and noise injection procedures are detailed. Later, different evaluation procedures have been provided.

With background materials reviewed, in the next chapters, we will investigate the leverage of the mechanisms of NSFLSs. Chapter 3 mainly presents a novel approach to systematically generate firing strengths which is to leverage mapping the uncertainty affecting system inputs to outputs.

Chapter 3

Handling Input Uncertainty

In real-world circumstances, a broad range of sources of uncertainty are often directly associated with inputs of decision-support systems. NSFLSs are specifically designed for modelling the uncertainty in input FSs and handling it through the interaction between inputs and antecedent FSs in system rules. Firing strengths in fuzzy rules emerge from these interactions and play a critical role in reflecting the input uncertainty into the consequents, which in turn determine the crisp output of the system. Therefore, processes to systematically determine appropriate firing strengths become a crucially vital element to handle varying input uncertainty, which is often subject to real-world environments. Hence, in this chapter, as presented in our studies [122, 120], we focus on investigating/analysing the current firing strength determining approaches, and we put forward a novel approach to generating firing strengths which faithfully map the uncertainty affecting system inputs to outputs, addressing objective 1.

Section 3.1 discusses the background and importance of approached to determining firing strength. In Section 3.2, a critical analysis by exploring the specific behaviours of the different firing strength approaches is conducted under different input uncertainty levels. Section 3.3 puts forward an alternative subsethood based (named *sub*-NS) approach which aims to systematically determine faithful firing strengths that allow an appropriate input uncertainty mapping to outputs of NSFLSs. Later, the behaviour of the proposed *sub*-NS is compared and contrasted with the current approaches in the same case study. In Section 3.4 time series forecasting exper-

iments are employed with a different firing strength determining approach. These experiments aim to observe/compare each approach's behaviour and performance in the time series forecasting context, which contains various noise levels. Section 3.5 summarises the contribution of this chapter to this thesis.

3.1 Background and Motivation

As mentioned in Chapter 2, the first step in FLSs is to map given inputs into FSs. In singleton fuzzification, it is assumed that the input values are exact/correct values, and singleton FSs are constructed. Later, these singleton FSs are processed through rules in the inference engine step of FLSs. Due to simplicity and lower computational cost, singleton fuzzification is a commonly used design in applications. However, due to the fact that inputs are commonly exposed to sources of uncertainty, non-singleton FSs have the potential to capture the uncertainty in input data, and so may provide better results than SFLSs for the same number of rules.

In the fuzzification of NSFLSs, given inputs are mapped into non-singleton FSs to capture input uncertainty. Traditionally, widths of constructed input FSs are associated with the level of uncertainty in input values. For instance, when a sensor measures a distance from a wall, if the received measurement is always the same (e.g. 5 meters), a singleton fuzzification may be constructed with the assumption that the measurement is exact/correct (Fig. 3.1a). However, as there might be sources of uncertainty (e.g. sensor imprecision or environmental noise), this measurement value may not be determined as an exact crisp value. In that case, the measurement can be represented as non-singleton FSs by taking into account the uncertainty. For example, the measurements may fluctuate with a proportionally *low* rate which results in a relatively narrow width in input FSs (Fig. 3.1b). If the sensor exposed to a *high* degree of uncertainty causing fluctuation at the broader level, a wider width is constructed to capture that uncertainty in measurements (Figs. 3.1c or 3.1d). Hence, the distance from the wall is represented by input FSs modelling which captures the possible uncertainty in the provided measurements.

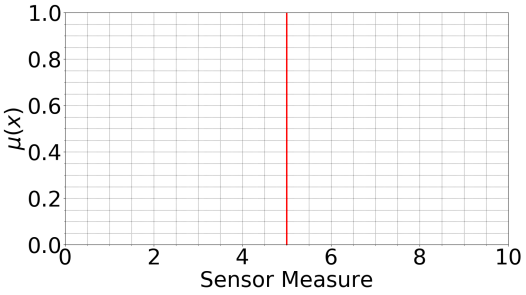

(a) Sensor measurement with noise-free exact value.

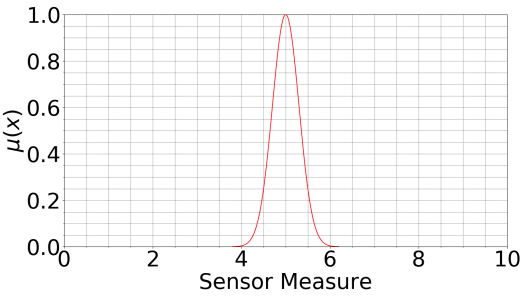

(b) Sensor measurement with a 'low' uncertainty

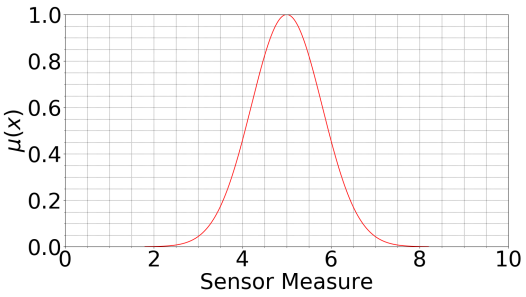

(c) Sensor measurement with a 'high' uncertainty

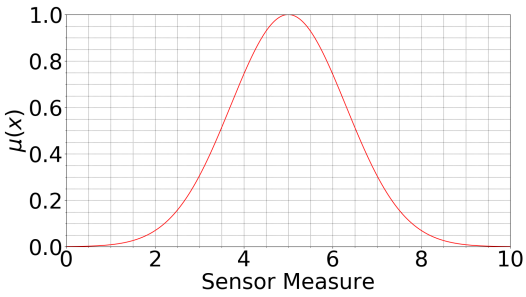

(d) Sensor measurement with a 'higher' uncertainty.

Figure 3.1: Representing a distance sensor measures as input FSs under four different uncertainty levels.

In the inference engine step of NSFLSs, inputs are processed with respect to the system rules through interaction between the input and antecedent FSs. These interactions result in rule firing strengths where input uncertainty is directly reflected on the determined firing strengths in NSFLS. Hence, particularly in NSFLS designs, the firing strength has a vital role in terms of input uncertainty handling. Considering that the real-world usually contains sources of uncertainty, systematically determining firing strength -by mapping various uncertainty information from inputs to outputs- becomes an essential component of NSFLS applications.

The traditional inference approach is for the firing strength to be equal to the maximum membership degree of the intersection between input and antecedent FSs [94]. While this approach is standard for singleton inference, a broad body of work has explored the use of other approaches to establishing what is effectively the compatibility between FSs through various measures [16, 34, 36, 44, 59, 86].

As the initial firing strengths focused studies, Turksen et al. [167, 168] proposed the Approximate Analogical Reasoning Schema (*AARS*) in rule firing decision, such that if the calculated similarity measure between input and antecedent FS is greater than a pre-defined threshold, the rule is fired. Chen et al. [28, 29] employed another similarity measures and [185] utilised subsethood measure with the same threshold strategy in medical diagnosis application. Later, the AARS is applied in NSFLSs [132] with the same threshold mechanisms as well. Following these studies, [133] extended the previous AARS works by proposing a new similarity measure which is used in fuzzy relations and in the practical application, a threshold is also defined to make a decision on rule firing. Even though the aforementioned studies are related to firing strength levels, they have mostly adhered to the strategy of firing rules based on predefined threshold values rather than determining firing strength levels to map input uncertainty to the output of FLSs.

In addition that an initial work [116] on the fuzzy neural system is implemented and extended in various forms [118, 155, 160]. In these studies, firing strengths between input and the system weight MFs are defined by using the mutual subsethood measure (2.30). Even though these studies aim to handle input uncertainty with firing strength, the mutual subsethood measure may not fully focus on the given input uncertainty levels, because of the symmetric property. For instance, a mutual subsethood measure between a *wide* input MF and a *narrow* system weight MF (which overlaps at the centre) provides the same measure for the case of vice-versa. However, having the same firing strength for both cases may not intuitively be expected as there are different input uncertainty in compare to the given weight MF. Therefore, traditionally, using mutual subsethood measure may not determine firing strengths faithfully, which is also the case of the Jaccard similarity measures as detailed in Section 3.2.

More recently, in the context of input uncertainty handling of NSFLSs, a variety of methods have been explored to capture the interaction between input and antecedent FSs faithfully. In the centroid-based inferencing approach, focuses on the area of intersection between input and antecedent FSs [130, 131]. The centroid of the intersection between input and antecedent FSs is calculated. Then, the membership degree in the antecedent FS corresponding to the centroid on the intersection is used as the firing strength. Later another study explored the use of sim-

ilarity measures itself as firing strengths in NSFLSs in order better to capture the interaction between input and antecedent FSs [176]. Later, these approaches have been used in unmanned aerial vehicle applications successfully [51, 52]. The main objective of utilising centroid-based and similarity-based composition approaches is to provide more faithful firing strength degrees which are sensitive to input uncertainty changes. So that various input uncertainty information can be systematically reflected into the output of FLSs. These approaches will be critically analysed in the next sections, and behaviours will be explored under different input uncertainty levels.

As mentioned above, in the real-world, system inputs are often affected by sources of uncertainty. Firing strengths in NSFLS designs have a significant role in mapping input uncertainty to the output of systems. Therefore, in this chapter, first, we analyse the current firing strength composition approaches by critically investigating behaviours under different input uncertainty levels. Second, as presented in our studies [120, 122], we propose an alternative approach which employs a subsethood measure (named *sub*-NS) between non-singleton input and antecedent FSs for determining firing strength which allows a systematic and faithful mapping of various uncertainty information from inputs to the outputs. These investigations and the proposed alternative approach address objective 1 of the thesis, as detailed in the following sections.

3.2 A Critical Analysis of the Current Firing Strength Determining Approaches

In this section, first, the current firing strength determining approaches (standard, centroid and similarity-based) are introduced by a critically analysis the specific behaviours of these approaches in mapping various input uncertainty on a single antecedent FS. Second, a case study to further investigate these approaches is presented in subsection 3.2.4. Later, a novel approach is introduced and a comprehensive comparison with different samples of uncertainty levels is presented in subsection 3.2.4 along with the possible advantage and disadvantages for tradi-

tional NSFLS designs.

As mentioned in the previous section, input data is usually corrupted by uncertainty in most real-world scenarios. When systems contain different levels of uncertainty, inputs can be fuzzified into non-singleton FSs to capture uncertainty [105]. In this regard, it is generally assumed that the received input x is the value which is centred in the non-singleton FSs. After that, the width of the input FSs are determined based on the uncertainty level of systems. Based on this observation, there is usually an association between the uncertainty level and the input FS's width. As the Gaussian FS is one of the commonly used designs, it has been chosen to carry out experiments throughout the thesis.

The next subsections will investigate the current firing strength determining approaches and explore behaviours under various input uncertainty levels.

3.2.1 Standard Composition-Based Approach

As the most common composition-based technique (named *sta*-NS), in the standard inference method, the maximum membership degree grade of the intersection between the input and antecedent FSs is determined as the firing strength. Throughout this thesis, the acronym *sta*-NS will be used to refer to this standard composition based approach.

Let a given input $x_1 \in X$ is constructed as I_1 FS to capture the uncertainty. When the constructed I_1 is processed through the antecedent FSs (A) in a rule, as detailed in subsec-

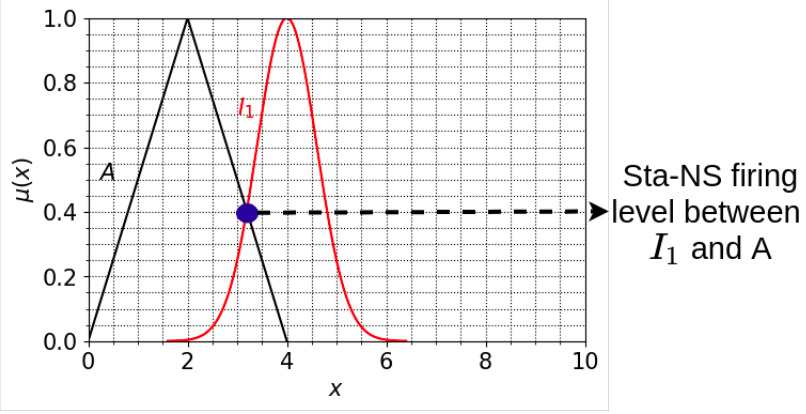

Figure 3.2: An illustration of firing strength between antecedent (A) and input FSs (I_1)

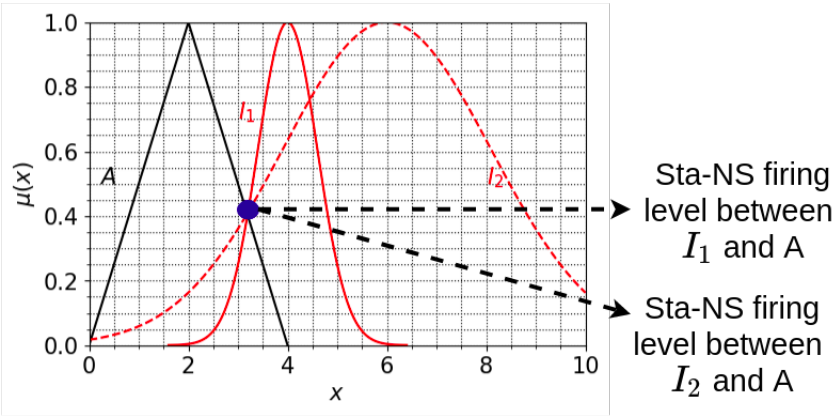

Figure 3.3: An illustration of two distinct input fuzzy sets having the same intersection level with A

tion 2.3.2.3, the given input uncertainty is directly reflected into the firing strengths. This firing strength calculation is employed by using the supremum over $\mu_{I_1}(x_i) \star \mu_A(x_i)$. Sample of this operation can be seen in Fig. 3.2, between antecedent A and the input I_1.

However, adopting the maximum point of the intersection to determine the firing strength may risk information loss in terms of the interaction of the input and antecedent FSs [131]. For example, in addition to the I_1, if another input (x_2) is given with higher uncertainty. This new input FS (I_2) results in a wider width to capture that higher uncertainty. However, as shown in Fig. 3.3, these two input FSs (I_1 and I_2) may intersect the antecedent (A) at the same membership grade, resulting in the same firing level, despite the fact that these input FSs are clearly different.

Recent work, including Pourabdollah et al. [130, 131] and Wagner et al. [176] have attempted to address this issue by introducing alternatives which employ the centroid of the intersection and similarity measures between input and antecedent FSs, respectively. Both of these approaches will be analysed and discussed further in sections below -as alternatives to the *sta*-NS approach.

3.2.2 Centroid-Based Composition Approach

The centroid-based approach (name *cen*-NS) focuses on the area of intersection between input and antecedent FSs. Firstly, the centroid of intersection between input FS (I) and antecedent

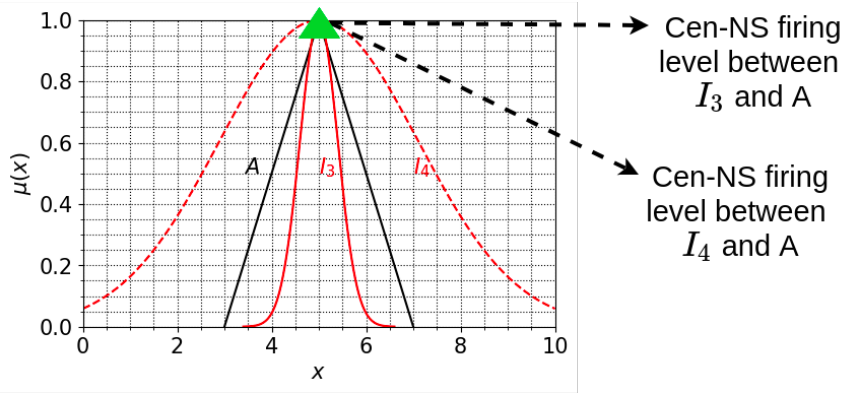

Figure 3.4: An illustration of firing level obtained using the *cen*-NS method for two different levels of uncertainty -I_3 low and I_4 high on the antecedent A.

FS (A) is calculated:

$$x_{cen}(I \cap A) = \frac{\int_{x \in X} x \, \mu_{I \cap A}(x) d_x}{\int_{x \in X} \mu_{I \cap A}(x) d_x} \tag{3.1}$$

where x_{cen} is the centroid of the intersection input and antecedent FSs ($I \cap A$).

Then, the corresponding membership degree of the position of the centroid ($x_{cen}(I \cap A)$) on the membership function of the intersection is defined to be the firing strength:

$$\mu_{I \cap A}(x_{cen}(I \cap A)) \tag{3.2}$$

Even though *cen*-NS may address the 'imperceptiveness' of the *sta*-NS (See in Fig. 3.3), *cen*-NS design may not fully reflect changes in uncertainty levels under different circumstances. For example, as shown in Fig. 3.4, in which two different input FSs are shown, lying at the same point x on the universe — I_3 having low uncertainty (expressed as the width of the input FS) and I_4 having more uncertainty (larger width). Even though the two cases' uncertainty levels are different, they both result in the same firing strength *(one)* where traditionally, one may intuitively expect to be different. In the case I_4, there is a fair possibility that the actual input can even exist outside of the antecedent A. Indeed, regardless of the level of uncertainty in I_4, a firing strength of *one* is always obtained.

3.2.3 Similarity-Based Composition Approach

A similarity measure on fuzzy sets is a function that determines to what degree (in the interval of [0,1]) two fuzzy sets contain the same values with the same degree of membership. Wagner et al. [176] suggested that any similarity measure between input FS and antecedent FS can be used to define the firing strength. In the initial work [176], they focused on the Jaccard similarity measure:

$$S(I, A) = \frac{\int_{x \in X} min(\mu_A(x), \mu_I(x))}{\int_{x \in X} max(\mu_A(x), \mu_I(x))} \tag{3.3}$$

where the input FS is (I) and the antecedent FS is (A).

Employing the proposed *sim*-NS in determining firing strengths can overcome having the same firing level in the given examples of Figs. 3.3 and 3.4. However, under particular input uncertainty levels, the *sim*-NS may generate undesirable firing strengths depending upon the model designs. For example, featuring an input x with two different levels of uncertainty, depicted by I_5 and I_6, is shown in Fig. 3.5. In the case of A and I_6, it may seem intuitive to obtain a firing strength value around 0.6, as there is relatively high uncertainty in the given input. In the A and I_5 pair, the *sim*-NS method gives a firing strength of close to zero. Indeed, as the uncertainty in x reduced further to the extreme situation of a singleton input at x, the firing strength given by *sim*-NS reduces to zero as well.

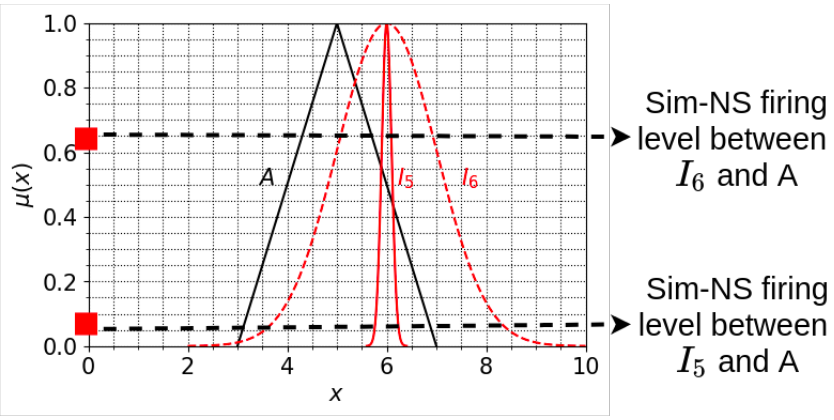

Figure 3.5: An illustration of firing level obtained using the *sim*-NS method, of input x, in the case of two different levels of uncertainty, I_3 (low) and I_4 (high) on the antecedent A.

Traditionally, in singleton input FSs or 'low' uncertainty levels in input FSs, firing strength would be expected to be higher than zero -if input and antecedents are intersected at some points, such as on the centre. Yet, *sim*-NS tend to produce firing levels which are zero or close to zero regardless of the intersections between input and antecedent FSs. It is also worthwhile noting that, in some FLS designs, antecedent and input FSs can be desired to compatible or similar. For instance, an FLS design may be built to investigate the compatibility of people opinions. Such that a person *X* may state an opinion about a restaurant. If the FLS is to seek for the opinion compatibility to the given antecedents FSs in rules, then *sim*-NS is to investigate the similarity between the given opinion from person *X* and antecedents FSs. Thus, in those particular designs, it can be said that *sim*-NS produce intuitive firing levels, i.e. *one* if only both input (opinion) FS and antecedent FS are equal.

After the three different firing strengths determining approach are critically analysed in the first set of samples, we now proceed with more comprehensive test cases where more uncertainty levels are tested on a single antecedent FS.

3.2.4 Exploration of the Current Techniques

In this section, the aforementioned firing strength determining approaches are examined, and a comprehensive comparison with 50 samples of input uncertainty levels are presented with the aim to observe the overall behaviours of each approach.

In order to investigate the current approaches, an input value x is fixed, and different uncertainty levels (standard deviations [SDs]) are investigated in the firing strength definition aspect. The input value x is chosen as the same value, which is 5, of the mean of the antecedent FS A, as shown in Fig. 3.6. In this way, this experiment allows us to observe different firing strength approaches' behaviours under different uncertainty levels when the system input and antecedent are coincidental on the centre. 50 different sequential SDs (from 0 to 3.0) values are explored in the experiment and three samples of these inputs I (with SD 0.3, $0.1.2$ and 3.0) are illustrated, together with the antecedent A, in Fig. 3.6. The firing strengths from each of the three proposed methods (*sta*-NS [blue circle], *cen*-NS [green triangle], *sim*-NS [red square]) is calculated for

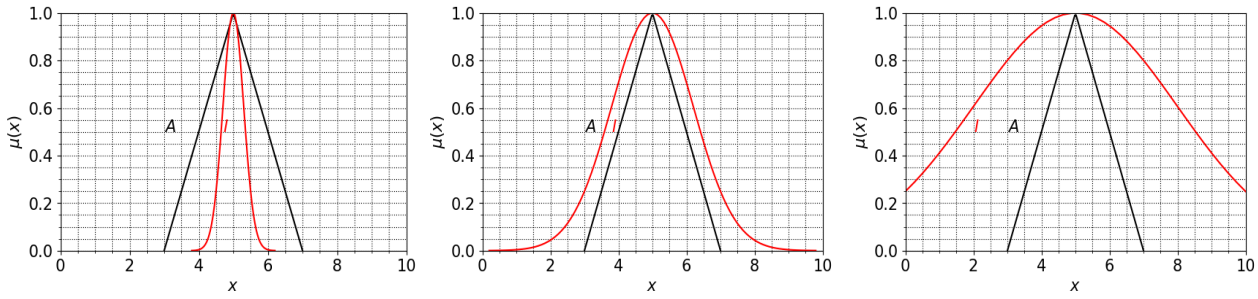

(a) σ = 0.3 (b) σ=1.2 (c) σ=3.0

Figure 3.6: An illustration of increased SDs in the input FSs (I) over the defined antecedent A.

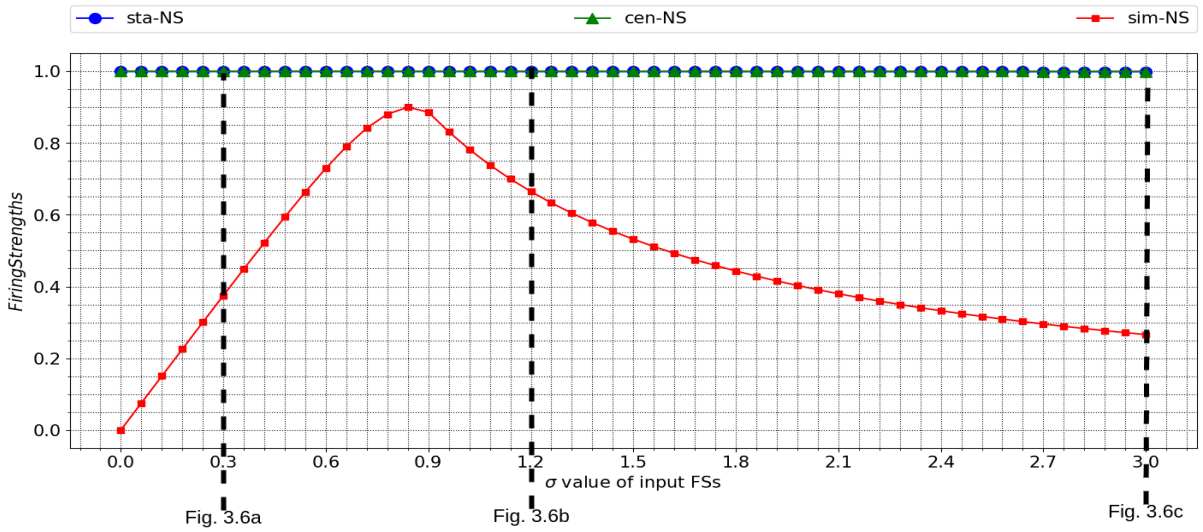

Figure 3.7: Comparison of the current firing strength determining approaches in each intersection of I-A based on changes in standard deviations of inputs I.

each level of SD and illustrated in Fig. 3.7. For instance, the dashed vertical line on the left-hand side of Fig. 3.7 represents the produced firing strengths in the case when I has the SD value of 0.3 as in Fig. 3.6a. Also, the middle and right-hand side dashed vertical lines show the produced firing strengths values for each approach from Figs. 3.6b and 3.6c, respectively.

Fig. 3.7 shows that as the uncertainty level increase (from the left to the right-hand side), the *sta*-NS and *cen*-NS approaches always produce the single firing strength (of one), regardless of the standard deviation in the input I. When the input contains a low level of uncertainty (left-hand side of the Fig. 3.7), traditionally, it is intuitive to gather the firing strength level one as the input and antecedent FSs have the same mean. However, it can be observed that the *sta*-NS and *cen*-NS methods are not designed to take into consideration higher input uncertainty levels (towards the right) in the systems, as there is a fair possibility that the actual input can even exist outside of the antecedent A.

When the produced firing strengths by *sim*-NS are scrutinised in Fig. 3.7, we observe from Fig. 3.6 that when the input has comparatively low uncertainty levels (towards to left), the produced firing strengths are close to zero. When the input width and antecedent FS width are getting close (the middle), the firing strength gradually increases to reach a maximum value. Then, when input uncertainty keep increasing (towards the right), the firing strength gradually decreases. Traditionally, when the input uncertainty increase (towards the right), considering the possibility of actual input may exist outside of the antecedent A, it may be intuitive to expect a low firing strength levels which are in line with *sim*-NS. However, when the input has a low-level of uncertainty and the input overlap on the centre of antecedent FSs (towards to the left), *sim*-NS may not provide traditionally expected firing levels. For example, when the input I has a *low* level of uncertainty (e.g. SD of 0.05), the *sim*-NS generates a firing strength close to zero. Therefore, we argue that in a traditional control sense, *sim*-NS may not efficiently design to consider low levels of uncertainty. However, if the design is built based on the compatibility of input and antecedent FSs (e.g. seeking similarity of a provided word [input] on the antecedent FSs in CWW), it should be noted that *sim*-NS can provide intuitive firing levels.

In summary, traditionally, while adopting either the *sta*-NS or *cen*-NS approaches may be helpful under low level of uncertainty (left-hand side of Fig. 3.7), they may not generate intuitively expected firing strength levels under the high level of uncertainty (right-hand side of Fig. 3.7). Conversely, while *sim*-NS can handle the high level of input uncertainty (right-hand side of Fig. 3.7) in traditional designs, it may be less helpful under low level of uncertainty (left-hand side of Fig. 3.7). We here note that these assumptions about being helpful are made based on a traditional control sense. In some particular designs (e.g. measuring similarity between input and antecedents FSs) the *sim*-NS and other approaches can also provide appropriate firing strengths and be helpful as well.

3.3 An Alternative - Subsethood Based Approach

Uncertainty levels that are associated with inputs are often changes in real-world settings. Therefore, a viable alternative approach that can systematically reflect different input uncertainty to firing levels can enhance the capacity of NSFLSs in coping with real-world settings. Hence, in this section -by considering the critical analyses in the previous case study (Section 3.2.4)-, an alternative subsethood-based composition approach (named *sub*-NS) is put forward with the aim of systematically determining faithful firing strengths that allow an appropriate input uncertainty mapping to the output of NSFLSs.

The subsethood measure [189] determines a ratio degree to which an FS is a subset of another fuzzy set. Various subsethood measures have been extensively studied by researchers over the years [46, 78, 158, 173]. In this thesis, we focus on one of the early definitions of subsethood measure as given by Kosko [78].

Perhaps the simplest way to express subsethood of set I in set A can be expressed as the ratio of the cardinality of the intersection of the two sets over that of set I, i.e.:

$$s_{SH}(I, A) = \frac{|A \cap I|}{|I|} \tag{3.4}$$

where $||$ refers to cardinality. This ratio can be formulated as follows:

$$s_{SH}(I, A) = \frac{\int_{x \in X} min(\mu_A(x_i), \mu_I(x_i)) d_x}{\int_{x \in X} \mu_I(x_i) d_x} \tag{3.5}$$

In this thesis, we propose to utilise the subsethood ratio between antecedent and input FSs, which is directly taken as the firing level $(s_{SH}(I, A))$ of these two FSs. As the number of elements from the input set I, which are part of the intersection, increases, the subsethood ratio will rise and eventually reach one when I is covered by A entirely. Likewise, as the set I moves further from A, meaning the non-intersecting number of elements increases, the subsethood ratio decreases and reaches zero when there is no intersection between the two sets at all.

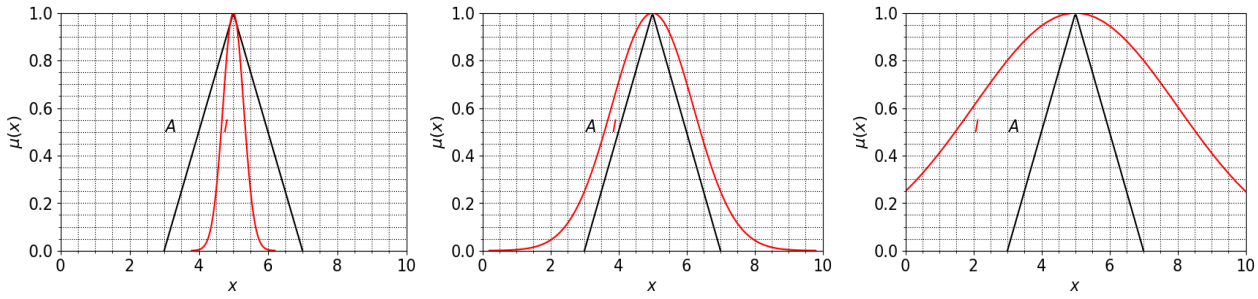

(a) σ = 0.3 (b) σ=1.2 (c) σ=3.0

Figure 3.8: An illustration of increased SDs in the input FSs (I) over the defined antecedent A.

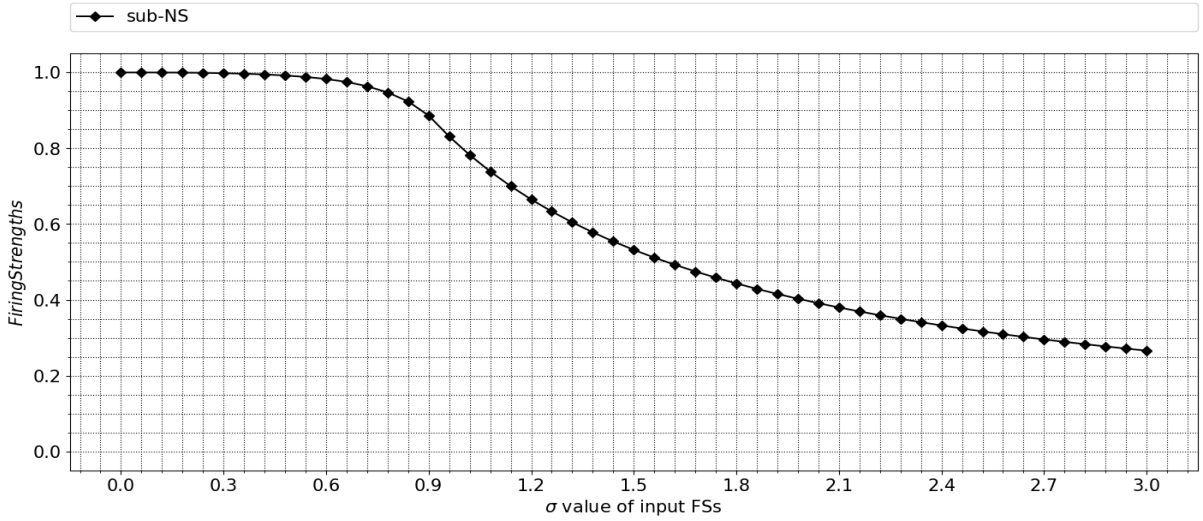

Figure 3.9: The proposed *sub*-NS firing strength determining approaches in each intersection of I-A based on changes in standard deviations of inputs I.

3.3.1 Exploration of the Alternative Subsethood Based Approach

In this subsection, the same case study settings from Section 3.2.4 are followed, and the proposed *sub*-NS is employed over the different input uncertainty levels.

When Fig. 3.9 is scrutinised, the alternative *sub*-NS show traditionally expected firing levels under both low and high levels of uncertainty. The proposed *sub*-NS (diamond) firing levels are reduced as the uncertainty level increases in the fixed input x values (towards the right). Furthermore, when the uncertainty level is decreased (toward the left), the determined firing levels are increased as it is traditionally be expected (e.g. singleton input and antecedent FS are coincidental on the centre). For example, while a noise-free singleton FS result in firing strength *one*, the higher input uncertainty (e.g. 3.0 SD) leads to lower firing levels, as there is the possibility of actual input may exist outside of the antecedent A.

Table 3.1: Firing strength determining approaches

sta-NS	*cen-NS*	*sim-NS*	*sub-NS*
$sup(\mu_I(x) \star \mu_A(x))$	$\mu_{I \cap A}(x_{cen}(\mu_I(x) \star \mu_A(x)))$	$\frac{\int_{x \in X} min(\mu_A(x), \mu_I(x))}{\int_{x \in X} max(\mu_A(x), \mu_I(x))}$	$\frac{\int_{x \in X} min(\mu_A(x), \mu_I(x)) d_x}{\int_{x \in X} \mu_I(x) d_x}$

Taken together, different firing strength determining approaches (Table 3.1) are explored with respect to the specific behaviour of the mapping input uncertainty to firing strengths. As shown in Fig. 3.10, traditionally, *sta*-NS and *cen*-NS provide faithful firing strengths on the left-hand side, whereas *sim*-NS cause a gradual decrease in firing levels. When the input has higher uncertainty levels (right-hand side), *sim*-NS traditionally produces expected firing levels as it gradually decreases, yet *sta*-NS and *cen*-NS kept firing level constant regardless of input uncertainty increase. In *sub*-NS approach, as shown in Fig 3.10, while lower input uncertainty produces high firing levels (left-hand side), high input uncertainty leads to a gradual decrease which is in line with the expectation in a traditionally designed NSFLSs for both left and right-hand side of the figure.

To evaluate and validate the alternative *sub*-NS approach's characteristics, a time-series forecasting experiment is carried out in the next section.

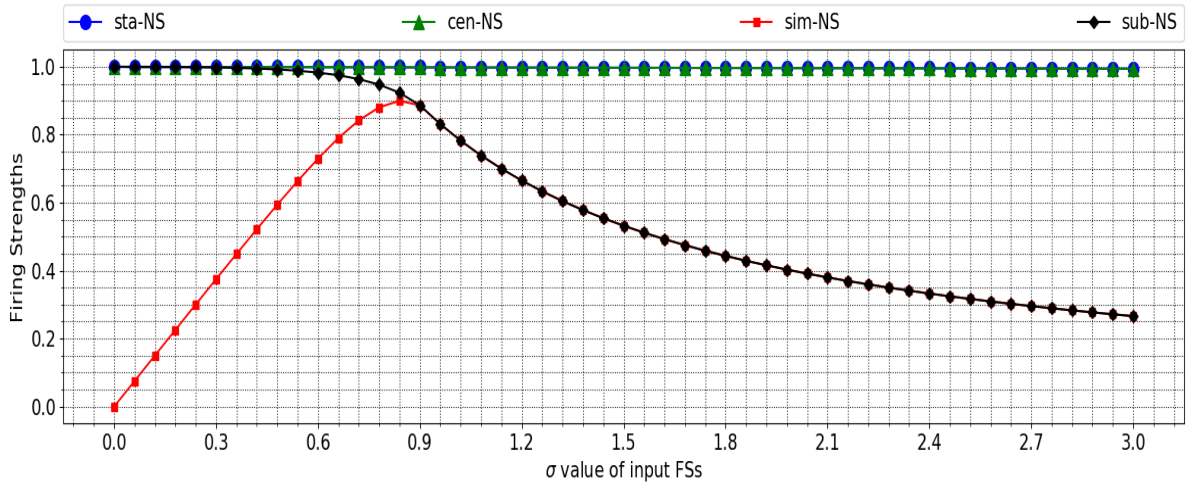

Figure 3.10: Comparison of different firing strength determining approaches, including *sub*-NS, in each intersection of I-A based on changes in standard deviations of inputs I.

3.4 Experiments

The alternative *sub*-NS is proposed to determine firing strengths under different input uncertainty levels systematically. Synthetically generated time series can provide an ideal testbed -with the potential to accurately control the levels of uncertainty. Therefore, the systematic evaluation of *sub*-NS and also the current approaches, are implemented on time series forecasting experiments under different uncertainty levels.

Throughout the experiments, six different noise levels are used, and the performance/behaviours of each firing strength determining approach are reported. As the time-series datasets, the commonly used chaotic Mackey-Glass (MG) [85], Lorenz [84] time series, which exhibits chaotic behaviour (Details can be found in Section 2.7), have been chosen to implement time-series predictions by using Mamdani Fuzzy model [88]. In the inference step of FLSs, the standard min as t-norm and max as t-conorm operators are used, and the centroid defuzzification method is utilised in the last step of FLSs.

3.4.1 Time-Series Partitioning

In order to generate the respective datasets, initially 2000 samples (from $t = -999$ to $t = 1000$) are generated and, in order to avoid fluctuations in the initial part of the time series, only the last 1000 (from $t = 1$ to $t = 1000$) points are preserved for use in the experiments. So that we obtain two chaotic time series which are denoted by $X = \{x_t : t \in T\}$ and $T = \{t_i \mid 1 \leq i \leq 1000\}$. More details on the time series generation reported in Section 2.7. In this chapter, the values $\tau = 30$, $a = 0.2$ and $b = 0.1$ are set for MG and $\sigma = 10$, $b = \frac{8}{3}$ and $p = 28$ are set for Lorenz time series. The system rule generation is completed over the first 700 ($\{x_i \mid 1 \leq i \leq 700\}$) points (training dataset) of the total 1000 values and the remained 300 points are used for testing under different noise levels for both MG and Lorenz time series.

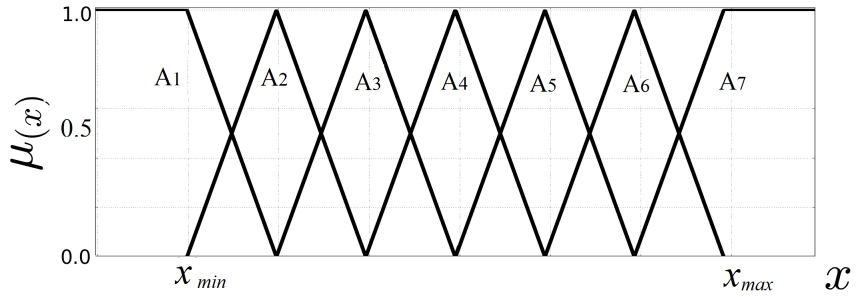

Figure 3.11: An illustration of the seven antecedent MFs used.

3.4.2 Rule Generation

The rule generation is performed on the first 70% of the time-series samples by using one of the most common rule generation technique – the *one-pass* Wang-Mendel method [179], as follows:

- Firstly, the minimum (x_{min}) and maximum (x_{max}) values of the noise-free training time series are obtained to determine the domain interval $[x_{min}, x_{max}]$. Then, the defined $[x_{min}, x_{max}]$ interval is equally divided into regions to represent the support for antecedent FSs. In the experiments, seven antecedents are defined $(A_1, A_2, ..., A_7)$. As such, seven evenly spaced antecedent FSs are generated as shown in Fig. 3.11.

- After constructing the antecedent FSs, nine past values are used as inputs and the following (10^{th}) value is used as prediction, i.e. it is the output. Examples of the input-output pairs can be seen in (3.6).

$$\begin{aligned}
&\mathbf{x}^1 = [x_1, x_2 ... x_9] \quad y^1 = x_{10} \\
&\mathbf{x}^2 = [x_2, x_3 ... x_{10}] \quad y^2 = x_{11}. \\
&... \\
&\mathbf{x}^N = [x_{n-9},\ x_{n-8} ... \ x_{n-1}] \quad y^N = x_n,
\end{aligned} \tag{3.6}$$

  where $n = 700$ is the number of value in the training set and N is the paired data value.

- The input-output pairs $((\mathbf{x}^1 : y^1), (\mathbf{x}^2 : y^2), ..., (\mathbf{x}^N : y^N))$ are created for each value in

the training time series and the inputs $(\mathbf{x}^i)$ for each input-output pair are assigned to the corresponding FSs $(A_1, A_2, ..., A_7)$ (See Fig. 3.11) based on their maximum membership degree. As it is practised in the Wang-Mendel *one-pass* method, for the consequent FSs, the same seven FSs are used and the outputs $(\mathbf{y}^i)$ are assigned to the corresponding FSs as well. After that, a rule reduction procedure is implemented on the conflicting rules. For details, please see [179].

- A sample of the generated rules can be seen in (3.7).

$$Rule^1 = IF\, x_1\, is\, A_1\, AND ... IF\, x_9\, is\, A_4\, THEN\, y_1\, is\, A_3 \tag{3.7}$$

where $x_1, x_2..., x_9$ are the input variable and $A_1, A_2, ..., A_9$ are the antecedent FSs.

3.4.3 Testing

In order to test the uncertainty handling performance of the proposed *sub*-NS over the current approaches, 6 different Gaussian noise $(0, 2, 3, 5, 10$ and 20 dB) are injected to both MG and Lorenz testing time series ($\{x_i \mid 701 \leq i \leq 1000\}$). SNR noise injection details can be found in 2.7.3.

As mentioned in section 3.2, the time series's noise is captured in defined Gaussian non-singleton input FSs, and the width/standard deviation of these input FSs correspond with the injected noise in the testing time series. For instance, when the 20 dB noisy set is used, the SD of Gaussian becomes 'lower' to capture that level of noise and when the 0 dB noisy set is used, the SD value is set to be 'wider', accordingly. For illustrative purposes,a sample of $x = 3$ constructed input FSs under 6 different noise levels can be seen in Fig. 3.12.

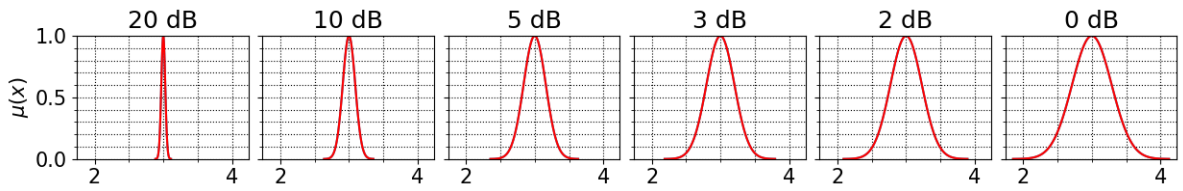

Figure 3.12: input FSs under 6 different noise.

After setting up rules and system parameters, the forecasting experiments are employed by using different firing strength definition approaches (*sta*-NS, *cen*-NS, *sim*-NS, *sub*-NS) each time. In order to mitigate the effect of randomness in the results, each experiment is repeated 30 times for all case scenarios and the average of generated Mean Square Errors (MSEs) are calculated.

3.4.4 Results for Mackey-Glass Time Series

After implementing the rule generation, 184 rules are obtained by using Wang-Mendel implementation. Then 20 dB noise is added, and the Standard deviation of 20 dB SNR value is set as the SD of non-singleton Gaussian input FSs (Fig. 3.12). Then the prediction experiment is implemented by employing the *sta*-NS in the inference engine. Following that, the same experiment is repeated by using *cen*-NS, *sim*-NS and the proposed *sub*-NS to generate firing strengths in the prediction. As shown in Fig. 3.13 and Table 3.13, the MSE results from the 20 dB noisy experiments show that while the *sta*-NS approach is produced average MSE value 0.0023, the *sub*-NS technique MSE reduced to 0.0020 which shows that the system uncertainty handling performance is improved by 13% in the case using *sub*-NS in comparison the traditional *sta*-NS technique. In addition to *sta*-NS approach, the other degree of subsethood measure (i.e. (*cen*-NS and *sim*-NS) to define firing levels are investigated, and the comparison of the results can be seen in Table 3.2.

Table 3.2: Mackey-Glass time series prediction, average MSE values over different firing strength definition approaches

	***sta*-NS**	***cen*-NS**	***sim*-NS**	***sub*-NS**
20 dB	0.0023	0.0024	0.0023	**0.0020**
10 dB	0.0073	0.0067	0.0068	**0.0065**
5 dB	0.0151	0.0142	0.0141	**0.0138**
3 dB	0.0201	0.0190	0.0189	**0.0185**
2 dB	0.0224	0.0213	0.0212	**0.0208**
0 dB	0.0288	0.0277	0.0280	**0.0274**

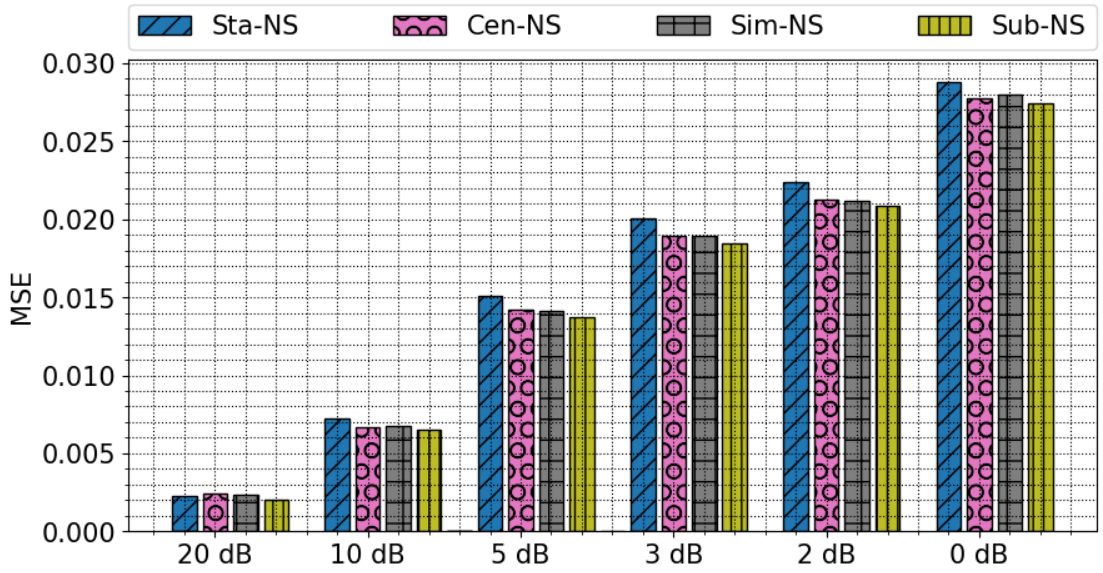

Figure 3.13: The illustration of Mackey-Glass time series prediction, average MSE values over different firing strength definition approaches

The experiments with the exact same rule set and parameters are continued under another five noise levels, and each noise level is tested with all firing strength definition approaches as well. At the end of the experiment, in comparison with the *sta*-NS approach, *sub*-NS technique is improved system accuracy by 10%, 9%, 8%, 7% and 5% under 10dB, 5dB, 3db, 2dB and 0 dB, respectively (Table 3.2 and Fig. 3.13).

Table 3.3: Lorenz Time series prediction, average MSE values over different firing strength definition approaches

	sta-NS	*cen*-NS	*sim*-NS	*sub*-NS
20 dB	1.2030	1.1968	**1.0165**	1.0855
10 dB	4.4244	4.1681	4.0737	**4.0008**
5 dB	8.8446	8.4495	8.3506	**8.2384**
3 dB	11.0766	10.7439	10.7340	**10.6505**
2 dB	13.6672	13.4096	13.4588	**13.3842**
0 dB	17.9265	**17.7147**	17.7973	17.7769

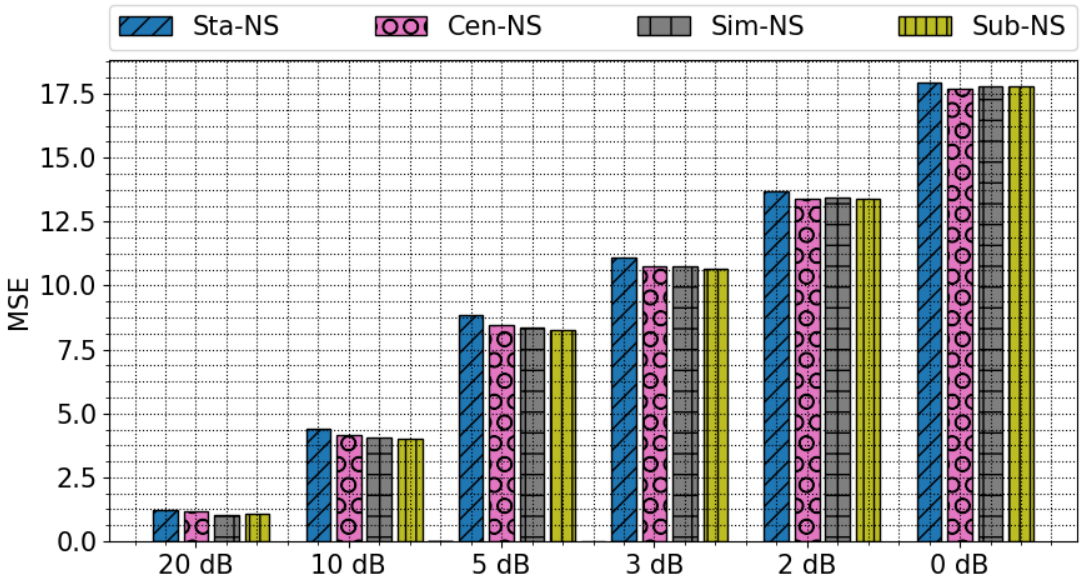

Figure 3.14: The illustration of Lorenz time series prediction, average MSE values over different firing strength definition approaches

3.4.5 Results for Lorenz Time Series

Further experiments are carried out on the Lorenz chaotic time series, and the 174 rules are generated by using the aforementioned rule generation procedure. By following the same experiment steps, different predictions are implemented under six different noise levels. These experiment results can be seen in Table 3.3 and Fig. 3.14.

3.4.6 Discussion

In order to examine the proposed alternative *sub*-NS over the current NSFLSs firing strength determining approaches, the source of the observed MSE improvements in the described time-series prediction FLSs is compared.

When the MG and Lorenz time series prediction performances are examined under all six different levels of noise, the alternative *sub*-NS approach, generally, outperforms the other current firing strength definition techniques under different noise levels (See Figs. 3.13 and 3.14). Especially in comparison to the standard *sta*-NS approach, the *sub*-NS performances show a clear performance improvement in regards to the MSE values obtained.

Also, when the alternative *sub*-NS is compared to the *cen*-NS and *sim*-NS, overall, when the uncertainty level increases the performances between the *sim*-NS and the *sub*-NS becomes more similar.

Overall, this particular set of results shows a better estimation of the actual value by the *sub*-NS compared to the other approaches in the context of NSFLSs.

3.5 Summary

As real-world settings contain many sources of uncertainty, faithful handling of uncertainty is an important asset for decision-support systems. NSFLSs are specifically designed to handle input uncertainty where it is directly reflected into the firing strength level through the interaction of input and antecedent FSs. In Section 3.2, current firing strength determining approaches (standard, centroid and similarity-based) are investigated, and a critical analysis of the specific behaviours are reported.

Firing strengths have a vital role in mapping input uncertainty to the outputs of FLSs. Thus in this chapter, as presented in our studies [120] and [122], an alternative subsethood-based firing strength determining approach (*sub*-NS) is introduced with the aim to systematically and faithfully mapping different levels of uncertainty information from inputs to outputs. A case study (Section 3.3), is implemented with the alternative *sub*-NS approach in comparison to the current firing strength determining approaches (standard, centroid and similarity-based) and underpin the possible advantages.

After presenting the critical investigation from the case study, to observe/compare behaviours of *sub*-NS and the current approaches, artificially generated chaotic time series prediction experiments are carried out under different noise levels. The experiment results point towards the idea that the *sub*-NS can also be a suitable approach to generate appropriate firing levels which provide the ability of mapping different uncertainty levels from input to output of FLSs.

Even though *sub*-NS can handle different input uncertainty levels and produce appropriate firing levels between the input and antecedent FSs, the question of 'which parameters should be used in constructing input FSs of NSFLSs to capture the uncertainty' still remains. Thus, in the next chapter, we will introduce a framework to capture input uncertainty adaptively on-the-fly, and we will integrate this framework with the proposed *sub*-NS in later sections.

Chapter 4

ADaptive Online Non-Singleton Fuzzy Logic Systems -*ADONiS*-

As mentioned in the previous chapter, uncertainty is a pervasive component in input of applications and *sub*-NS have been proposed to handle input uncertainty by systematically determining firing strengths in the inference-engine step of NSFLSs. While handling input uncertainty is a vital task for NSFLSs, capturing it properly in the fuzzification step is also another essential factor in mapping various levels of input uncertainty to the outputs which can leverage capacity of NSFLSs. Considering the fact that a broad range of sources of uncertainty can vary greatly in magnitude over time, the adaptation of NSFLSs to the varying environments can provide an efficient and effective solution for input uncertainty mapping to outputs of NSFLSs. Therefore, as presented in our studies [121, 124], this chapter introduces an end-to-end framework to adaptively configure non-singleton input FSs on-the-fly to the changing uncertainty levels in an online manner.

Section 4.1 discuss the background and motivation for capturing the input uncertainty in an online manner. Section 4.2 first introduces the proposed framework in a general perspective (addressing objective 2 in Section 1.5) then proceeds to develop one specific instance for a time-series domain. In Section 4.3, the proposed ADONiS framework is explored in two time series forecasting experiments: (i) comparing the proposed framework ADONiS over the non-adaptive

counterparts, and (ii) the ADONiS is integrated with different inferencing approaches, including the proposed alternative *sub*-NS (from Chapter 3), and comparative results are provided. In doing so, this chapter addresses objective 2 of this thesis. Lastly, Section 4.4 summaries the contribution of this chapter to the thesis.

4.1 Background and Motivation

In the previous chapter, the alternative approach *sub*-NS is proposed to leverage capacity of uncertainty mapping from inputs to outputs by systematically determining firing strengths in the inference engine step of NSFLSs. Following the *sub*-NS approach, we now focus on dynamically capturing and modelling different input uncertainty levels on-the-fly in the fuzzification step which also has a primary role for uncertainty mapping in NSFLSs. Later in Chapter 5, we will extend this capacity to capture both uncertainty and the variation in the uncertainty by means of an extra degree of freedom in input FSs.

In the literature, several studies focus on defining input FS parameters with procedures of tuning or with a priori knowledge of level of uncertainty. Initial work was carried out to change NSFLS parameters dynamically by implementing a training process [105, 106]. Later on, several studies were conducted to expedite the convergence speed of the NSFLSs training [38, 99, 138] NSFLSs have been used in many different applications, such as control of DC motors [2], control of a stepper motor [135], pattern classification [17, 32], and state space identification of UAV [150]. While these studies showed promising results, they are dependent on the availability of a training data set which is expected to accurately reflect all real-world potential operating conditions, and they are generally limited to the selection of one type of FS model to capture the input uncertainty. As the real-world circumstances are prone to change over time, depending on a single parameter for input FSs may not conveniently capture various uncertainty levels. Also, availability of a training dataset, which reflects all the real-world potential circumstances, may not be feasible.

Apart from the offline training studies, recently, a noise handling study in UAV was carried out [51] and range of different trials were implemented to determine parameters of input FSs in the fuzzification step. Also, time-series forecasting experiments with NSFLSs were performed [130, 131, 176] and in those studies, it was assumed that the uncertainty levels are already known a priori and used to define parameters of input FSs. Later on, the WMA technique was used to update the input value of NSFLSs [129]. Input FSs are constructed around these updated inputs in the fuzzification step of NSFLSs. However, similarly, it was assumed that the synthetic and stable noise levels were known a priori. While a priori knowledge of the uncertainty level can be efficient to define parameters, this approach is invariably dependent on the availability of this knowledge and does not allow the modelling of levels of uncertainty which vary over time.

Considering the varying circumstances of real-world settings, determining input FS width parameters in an offline manner (i.e. tuning or a priori knowledge) prevents NSFLSs from being able to adapt to the changing uncertainty levels in the real-world. Therefore, in this chapter, a complete ADaptive ONline Non-Singleton Fuzzy Logic System (*ADONiS*) framework is proposed to dynamically configure input FSs, in an online manner on-the-fly. In the ADONiS, input FS parameters are continuously adapted based on information gained from an iterative uncertainty level estimation process over a sequence of observations. A representative of this adaptive behaviour can be seen in Fig. 4.1. In doing so, ADONiS provides the ability to adapt to varying circumstances without requiring pre-training procedures or a priori knowledge of

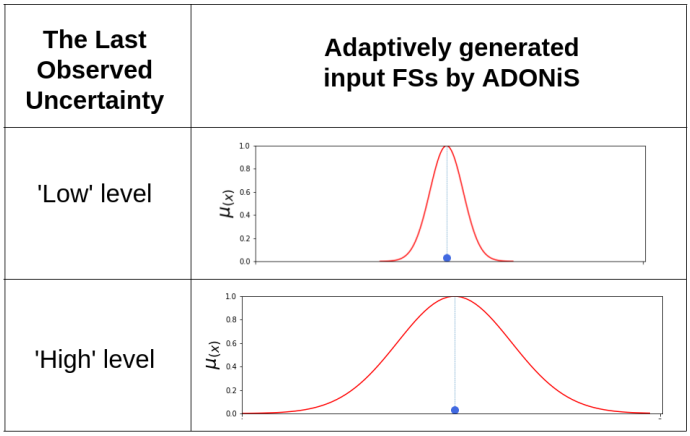

Figure 4.1: The ADONiS framework's adaptive behaviour to capture input uncertainty in the generated input FSs which is associated with the crisp input measured.

uncertainty levels. Also, by means of the online adaptive ability of ADONiS, the systems can be built upon *'pure'* rules -for instance, defining rules based on noise-free circumstances- which removes the apprehension for the varying uncertainty levels in real-world settings.

Taken together, following the input uncertainty handling by *sub*-NS in the previous chapter, we now propose the ADONiS framework with the aim of capturing different input uncertainty levels at run-time (addressing objective 2) that collectively enhance uncertainty mapping from input to outputs of NSFLSs, as detailed in the next sections.

4.2 The Proposed Framework -ADONiS-

In this section, first, we will introduce the general framework structure which is applicable for general real-world applications where uncertainty levels affecting system inputs vary in magnitude over time, such as signal processing, robotics, medical applications and forecasting etc. Second, since time-series datasets offer the potential to accurately control the levels of uncertainty affecting system inputs at any given time, a specific instance of the ADONiS will be employed on a time series case. Later, in Section 4.3, it will be linked and validated with time series forecasting experiments.

4.2.1 General Framework Structure of ADONiS

The ADONiS framework is designed to associate an online uncertainty detection technique with the parameterization of the non-singleton input FSs. In the proposed framework, input FS parameters are continuously adapted based on an uncertainty level estimation process over a sequence of observations. By doing so, ADONiS provide the capability of reflecting different uncertainty levels into widths of corresponding input FSs adaptively on run-time without requiring a priori knowledge or offline training procedure. Therefore ADONiS can adapt itself to different environmental conditions where inputs are exposed to various uncertainty sources which vary over time.

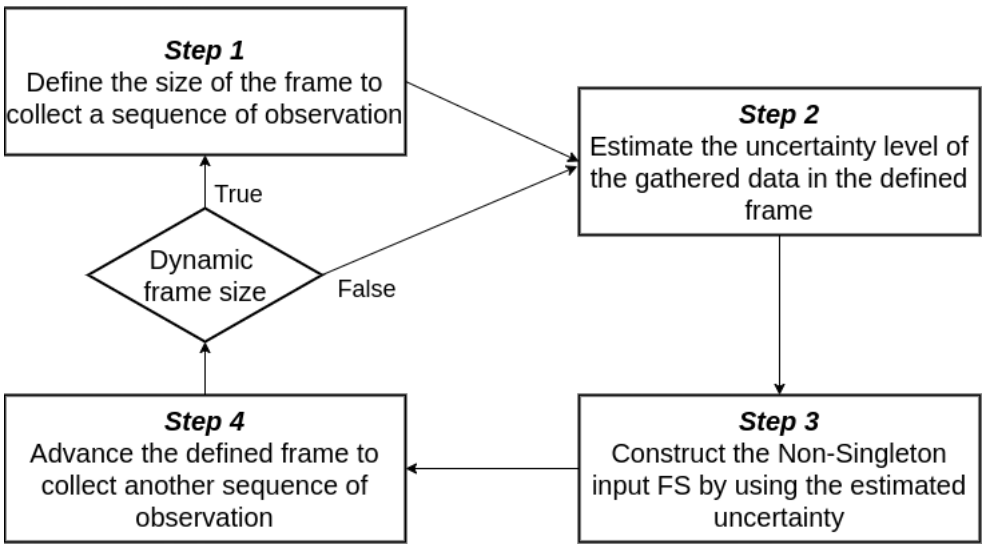

Figure 4.2: The four main steps of the proposed ADONiS framework.

The overall the ADONiS structure can be encapsulated in four main steps, as also shown in Fig. 4.2.

Step 1 - Define the size of the frame: First, a number of observations (e.g. a sequence of a signal or a patch of an image) are collected into a frame. The number of the collected observation defines the frame size which can be dynamic throughout application or can be stable based on design choice (See Fig. 4.2). For example, when using sensors, such as in a robotics context, the size of the frame may be selected in respect to the sampling rate of the sensors or based on a fixed time frame. While an expert opinion can determine the frame size, it can also be defined by following data-driven procedures. For instance, in a time series prediction context, a search algorithm can be utilised to determine optimal frame size.

After defining the frame size, the collected observations will be utilised to cooperate with the input FSs in the following steps.

Step 2 - Estimate the uncertainty: In this step, the collected observations in the defined frame are used to estimate the uncertainty levels. A suitable uncertainty estimation technique can be chosen by designers and it is employed across the gathered values in the frame. According to the input structure of the NSFLS, the uncertainty detection can be implemented by considering different features such as actual input variance vs expected variance, over time, for each input individually or together.

Step 3 - Construct Input FSs: As mentioned in the previous section, widths of input FSs are related to the existed uncertainty level in input values. Therefore, the estimated uncertainty from the defined frame is utilised to inform widths of input FSs. For example, Gaussian FSs can be defined and the detected uncertainty level can be used as the σ value of the Gaussian input FSs. By doing so, the uncertainty is captured by reflecting the estimation in widths of the input FSs.

Step 4 - Advance the defined frame: After constructing the input FS(s) for the current iteration, the generated input FS(s) proceed to the inference engine step and the given task is implemented. Following that the defined frame is advanced. This frame-advancing operation can be employed *step-by-step* (i.e. advancing the frame one by one to inform each observed value individually) or *piece-by-piece* (i.e. advancing the frame chunk by chunk to inform observed values jointly). The latter provides the same width to the group of input values which may cause a less sensitivity in uncertainty changes. In this chapter's experiments, we implement *step-by-step* frame advancing as detailed in the next sections. Later, in Chapter 5, both the frame advancing strategy will be detailed and implemented to construct adaptive IT2 input FSs.

Input uncertainty is one of the principal uncertainty in applications and generally, based on circumstances (e.g. environmental conditions), level of input uncertainty vary over time. Non-singleton input FSs provide the capacity of capturing the input uncertainty. Traditionally, studies confine input FS parameters to selecting a single value (i.e. stable width for all input FSs) which does not allow the modelling of different levels of uncertainty. For example, in a robotic context, the environmental noise can vary from 'low' to 'high' and resume to 'low' again, as the conditions are changed. In these circumstances -which prone to occur in the real-world- limiting input FSs to a single parameter can not effectively capture the varying noise levels. The proposed four-step process enables ADONiS to adapt to different levels of uncertainty affecting a system's inputs. In each iteration, inputs are associated with a given non-singleton FS, for which the parameters are determined directly by the levels of uncertainty detected over the observed/selected values (frame). Thus, different levels of input uncertainty can be captured at run-time and dynamically updated FLSs to account for changes, addressing objective 2.

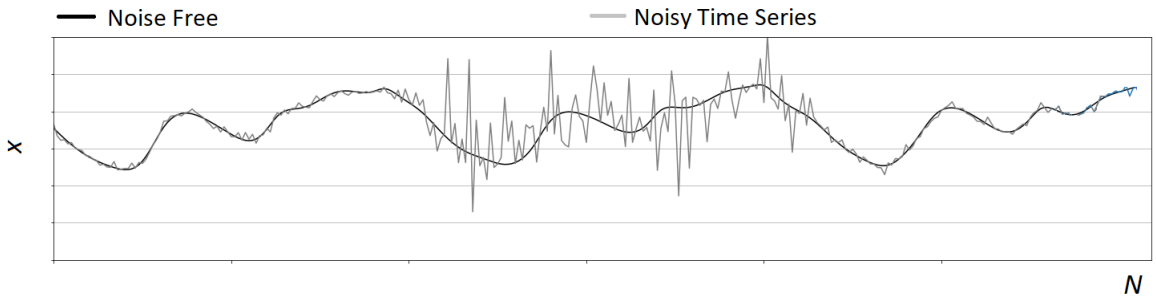

Figure 4.3: The generated noisy time-series.

After having the four steps ADONiS details in terms of the general applicability, in order to provide a detailed concrete explanation, we now proceed with the ADONiS on a time-series instance in the next subsection. As the uncertainty level can be increased or decreased effortlessly, we will also employ time-series forecasting experiments in the following Section 4.3.

4.2.2 ADONiS for Time-Series Analysis

In this subsection, in order to provide an illustration, we focus on applying the proposed ADONiS framework to the context of time series analysis. As such, we provide an instance of the generic ADONiS framework steps tailored to time series. Giving that the ADONiS is designed to capture different levels of input uncertainty, we artificially generate a time series $X = \{x_t : t \in T\}$ and $T = \{t_i \mid 1 \leq i \leq N\}$ which contain 'low' and 'high' level of noise. By doing so, the proposed ADONiS framework's behaviour can be demonstrated and illustrated under different input noise levels. The sample of the entire X can be seen in Fig. 4.3.

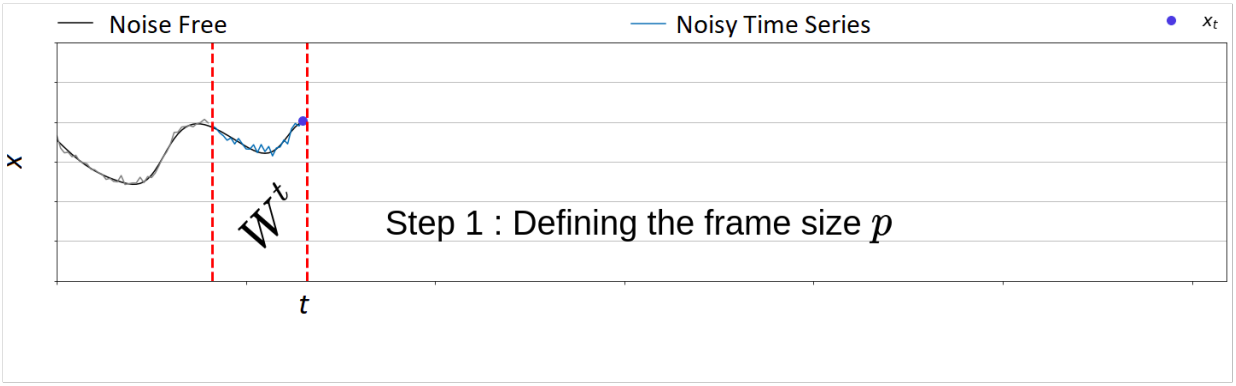

Figure 4.4: ADONiS Step 1: Defining the frame.

Step 1 - Define the size of the frame A sequence of observations collected into a frame and the quantity of these observations defined the frame size. Since the data is an univariate time-series, the frame will be slid and therefore, it can also be called a *window* for this specific instance. As illustrated in Fig. 4.4, the defined window is depicted as red dashed lines and denoted as the set W^t at the assumed current time t. The window size is referred to as p and defined as follows:

$$W^t = \{x_i \quad | \quad t \in T \wedge t - p < i \leq t\} \tag{4.1}$$

where W^t is the defined frame at the time t.

Step 2 - Estimate the uncertainty After obtaining the input data within the window W^t, the uncertainty level over the gathered values is estimated, as shown in Fig. 4.5. In this instance, we denote the corresponding uncertainty level as σ^t at the time t. Note that, in this step, based on preference, different uncertainty estimation techniques can be utilised.

$$\sigma^t = f(W^t) \tag{4.2}$$

where f is the chosen uncertainty estimation function and σ^t is the estimated uncertainty level at the time t.

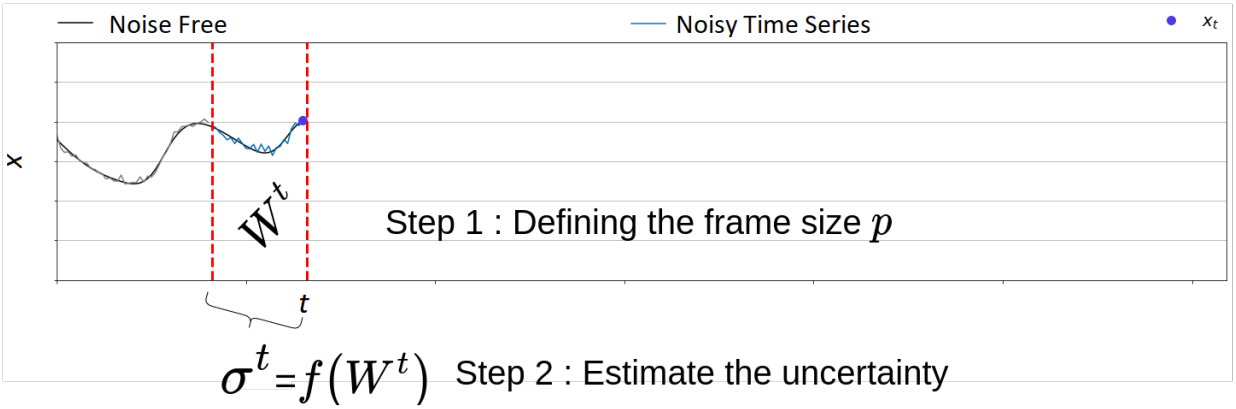

Figure 4.5: ADONiS Step 2: Estimating the noise.

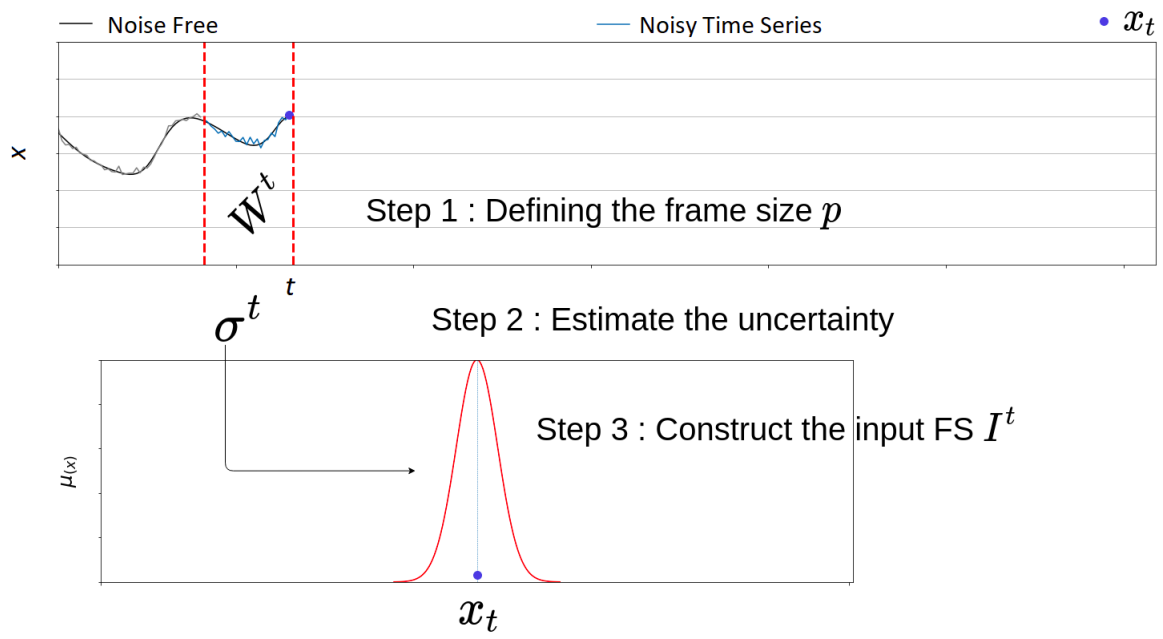

Figure 4.6: ADONiS Step 3: Constructing input FS.

Step 3 - Construct Input FSs The uncertainty estimation (σ^t) is leveraged to inform the non-singleton FS (I^t) which is associated with input(s) in the window. In this instance, the Gaussian shape is chosen for the input FS (See Fig. 4.6) and we note that other shapes can be used by reflecting the estimated uncertainty into the width of the input FSs.

$$I^t = ((x, \mu_{I^t}(x))|x \in U), \tag{4.3}$$

where

$$\mu_{I^t}(x) = \exp\left[-\frac{1}{2}\left(\frac{x_t - x'}{\sigma^t}\right)^2\right], \tag{4.4}$$

where σ^t is the width or standard deviation of the FS and x' are the neighbouring values of the mean which is located at x_t in the universe of U.

Figure 4.6 details the constructed input FSs which is based on the last observed value (x_t) in the defined frame.

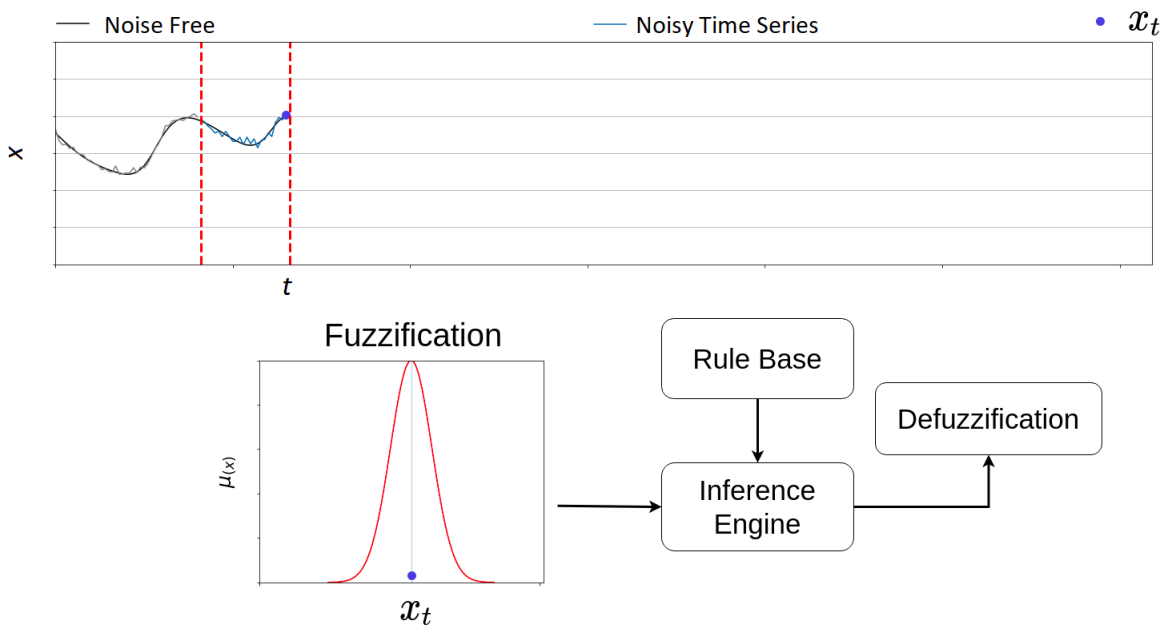

Figure 4.7: ADONiS Step 4: Employing the input FSs in the fuzzy model and advancing the frame.

Step 4 - Advance the defined frame After, the input FS (I^t) at the time t is generated for the current window, it is proceeded to the NSFLS to implement the defined task such as prediction or classification etc. A SISO sample of these procedures is illustrated in Fig. 4.7.

In the time series, as time past and more data is generated, the defined window is advanced by the step size (denoted by λ) and the same procedure is repeated. Depending on design choice, the window size can be re-adjust or remain the same as the previously defined size.

Algorithm 1: Constructing adaptive input FSs by means of sliding window noise estimation.

Input : the input value x_t at the most recent time step t
Output: the corresponding input FS I^t for the input x_t

Function `uncertaintyEstimation` (W^t)**:**
  $\sigma^t \leftarrow f\left(W^t\right)$ ▷ f is a chosen uncertainty estimation function;
  return σ^t;
Function `fuzzifyInput` (x_t, σ^t)**:**
  $I^t \leftarrow$ Gaussian FS with mean x_t and s.d. σ^t;
  return I^t ;
repeat
  $p \leftarrow frameSize$ ▷ Defining the frame size;
  $W^t \leftarrow [x_{t-p+1}, x_t]$; ▷ W^t is the current frame;
  $\sigma^t \leftarrow uncertaintyEstimation(w_t)$;
  $I^t \leftarrow fuzzifyInput(x_t, \sigma^t)$;
until $x_t = end$;

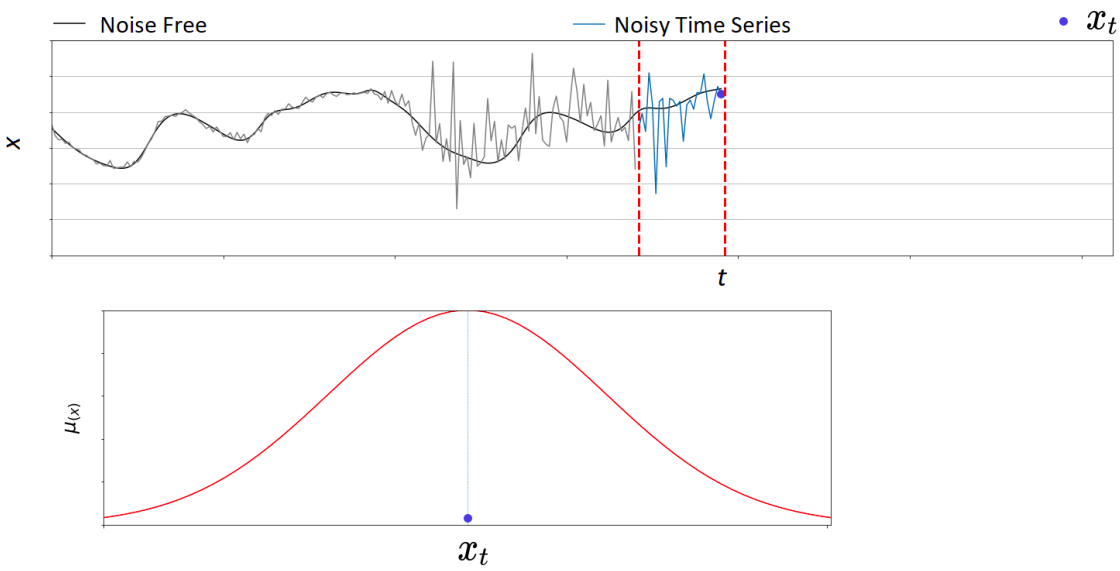

Figure 4.8: The demonstration of the capturing *high* uncertainty in the input FS t run-time.

Algorithm 1 presents the pseudo-code of the proposed adaptive input FSs fuzzification in the context of time-series analysis.

In Fig. 4.7, a sample of constructing input FSs where a 'low' level of noise leads to a narrow width/s.d. is visualised. As time past and new values are observed, the window can be advanced by one (leads to a sliding window practically), and the same steps are repeated. As another sample is illustrated in Fig. 4.8, when the input is disturbed by 'higher' noise level than the previous sample, input FS width is dynamically informed by following the ADONiS steps and a wider FSs is constructed, in turn, providing the capacity of capturing different levels of noise in an online manner without any a priori knowledge. An animated illustration of the complete process can be seen online at `https://ieeexplore.ieee.org/document/8790770/media` or at `https://bit.ly/3deRA1r`.

After having a detailed explanation of the ADONiS on a time-series instance, we now proceed to time-series forecasting experiments in order to demonstrate ADONiS behaviour in the context of forecasting under varying input noise levels.

4.3 Experiments

As was mentioned in previous chapters, time-series forecasting provides an ideal test-bed for the systematic evaluation (offering the potential to accurately control the levels of uncertainty/noise affecting system inputs at any given time) of techniques designed to deal with input uncertainty. Thus, this section validates the practical impact of the proposed ADONiS framework by empirically evaluating it across non-linear chaotic time-series predictions under various levels of noise. Mainly, two different experiments are carried out as *Experiment 1* and *Experiment 2*.

In *Experiment 1*, we aim to illustrate ADONiS adaptive behaviours where inputs of systems are corrupted at different levels of noise and how does that varying input uncertainty are adaptively captured and mapped to outputs of the system, addressing objective 2. In these experiments, a comparison of the adaptive behaviour of ADONiS against different non-adaptive counterparts is reported.

In *Experiment 2*, we integrate ADONiS with different firing strength generation techniques - including the proposed *sub*-NS (See details in Chapter 3)- and comparative prediction results are provided. In this experiment, the same time-series dataset (with varying noise levels) are used and we aim to observe the behaviours of ADONiS with different inference engine techniques as part of the broader architecture.

In the next subsection, we present the general experimental set-up and in the next section, we will specify each experiment individually.

4.3.1 Experimental Set-Up

This subsection will provide overall the key design aspects in the experimental set-up for both Experiment 1 and Experiment 2 by detailing the used time-series datasets, rule generation procedures, fuzzification and overall predictions in NSFLSs.

4.3.1.1 Time Series Generation

In both experiments, two commonly used chaotic (Mackey-Glass and Lorenz) time-series are used to implement time-series forecasting. The details of the used time-series generation and partitioning can be found in Section 3.4.1. Following that procedures, the values $\tau = 30$, $a = 0.2$ and $b = 0.1$ are set for MG and $\sigma = 10$, $b = \frac{8}{3}$ and $p = 28$ are set for Lorenz time-series in the generation. By doing do, chaotic behaviours are provided in the datasets and ADONiS design can be tested in those particular chaotic circumstances.

4.3.1.2 Rule Generation

In the literature, different rule generation techniques are exist [80, 61, 113]. As it was practised in the previous section, one of the most common rule generation technique – the *one-pass* Wang-Mendel method is implemented on the first 70% of the time-series samples, using a commonly adopted FLS architecture [179] with seven antecedents based on evenly spaced MFs. The prediction is implemented by using nine past points and the 10^{th} value is predicted. The rule generation's details can be found in Section 3.4.2. Two key training approaches are explored for both experiments to generate system rules: *Noise-Free Time Series* based rule generation and *Noisy Time Series* based rule generation.

The noise-free time series rule generation aims to design the system with 'pure' rules and test the ADONiS behaviour under different noisy testing settings. The objective of this strategy is to mimic a real-world application case where there is no a priori knowledge for the level of noise on run-time. For instance, in a robotics context, rules are defined based on noise-free laboratory conditions and the robot is tested under noisy real-world environments. By doing so, the system rules can be relatively less 'complex', while ADONiS can dynamically handle unseen noisy conditions from input to output of models on-the-fly, addressing objective 2.

The noisy time-series rule generation aims to design a system where there is only noisy data available. In this case, we aim to report ADONiS behaviour and robustness within the design of noisy rules. In this rule generation, training time-series samples are injected with a predefined

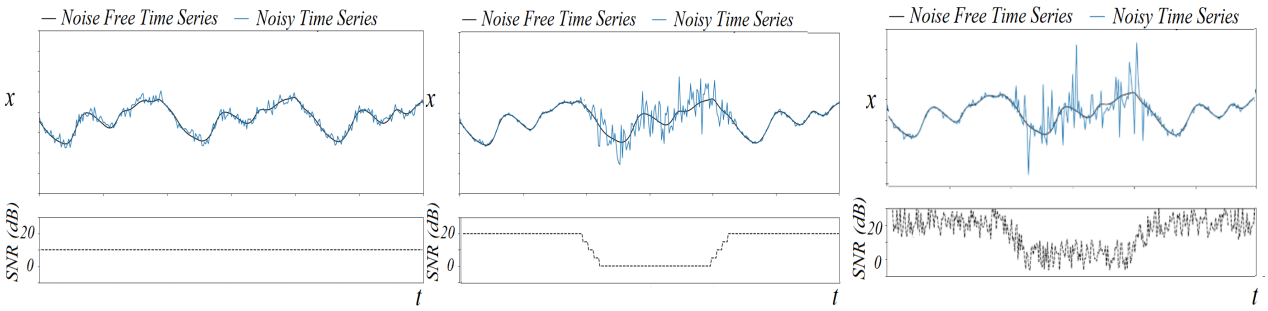

(a) Stable Noise (b) Mixed Stable Noise (c) Variable Noise

Figure 4.9: An Illustration of the three instances of a test time series generated with different noise level scenarios. The bottom figures shows the corresponding noise levels in the time series.

noise levels, as detailed in the given experiments.

4.3.1.3 Test Time Series Generation

In order to test the performance of the proposed ADONiS, the remaining 30% of the time series dataset is used in three different scenarios: using a stable 10 dB level of Gaussian white noise (see Fig. 4.9a); a mixed scenario where the Gaussian noise varies from a very low and stable 20 dB to a period of high, but stable 0 dB, before returning to 20 dB (see Fig. 4.9b); the low and high noise levels from the previous testing series are perturbed randomly in magnitude (by 10 dB) itself which is illustrated in Fig. 4.9c.

By generating these pattern of noise variation, we attempt to mimic real-world situations where an unexpected disturbance suddenly occurs in the signal data (e.g. light variation affecting a camera). By doing so, the ADONiS adaptive behaviour can be illustrated with respect to varying uncertainty mapping from input to outputs of model.

4.3.1.4 Fuzzification

In Experiment 1, both the adaptive input FS generation approach and a simpler a priori input FS definition approach are used to implement a comparative study between the proposed ADONiS framework and non-adaptive approach performances.

In Experiment 2, in each variant, the proposed adaptive input FS generation approach is used and it is integrated with different firing strength generation techniques (*sta*-NS, *cen*-NS,*sim*-NS and the proposed *sub*-NS).

In the ADONiS fuzzification case, since, the forecasting is done with nine past points, we define the window size (p) to be nine as well and the noise estimation function is adopted from [136] and implemented on the each past nine points $\mathbf{x}^t = (x_{t-8}, x_{t-7}, ..., x_t)$. Note that, based on designer choice, different noise estimation techniques and different window size can be utilised in this step. While smaller window size may provide more sensitive noise estimation, we follow the main structure and nine past points are taken to estimate the noise levels. The noise estimation is implemented as follows:

$$\mathbf{y}^t = \frac{1}{\sqrt{2}}(x_{i+1} - x_i) \quad \forall\, i \in W^t, \tag{4.5}$$

where W^t is the defined window at the time t and $\mathbf{y}^t$ is the calculated difference vector from the W^t at the time t.

Then the standard deviation of the difference vector is calculated as follows:

$$\sigma^t = \sqrt{\frac{1}{p-1}\sum_{i=1}^{p-1}(y_i - \bar{y})^2}, \tag{4.6}$$

where $\bar{y}$ is the mean of the difference vector and σ^t is the estimated noise.

Then the estimated noise (σ^t) is used as the standard deviation parameter of the x_t non-singleton Gaussian input FSs and the estimated noise level is captured in the constructed input FS. In this instance, we advance the window *step-by-step* ($\lambda = 1$) and each input FS is always be associated with the estimated (σ^t) value. For example, the input $x_{t-5} \in \mathbf{x}^t$ is associated with the uncertainty of the frame W^{t-5}. Note that the window W^{t-5} is the set of $\{x_i \quad | \quad t-5-p < i \leq t-5\}$ where p is defined as nine. Considering the input vector contains nine values, the association can be 'formulated' as follows:

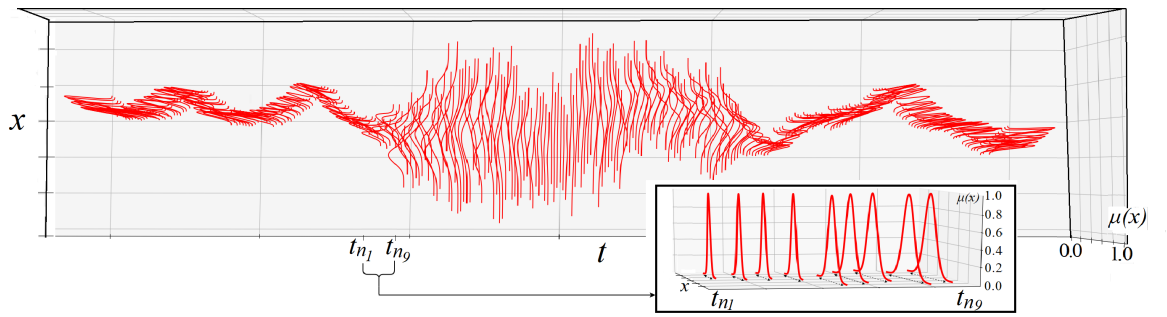

Figure 4.10: A sample set of the all generated input FSs in the *Stable Noise* series (Fig. 4.9b). Note: the inset figure it tilted for better visibility.

$$
\begin{aligned}
(W^{t-9} \sim x_{t-9}) &\rightsquigarrow I^{t-9} \\
(W^{t-8} \sim x_{t-8}) &\rightsquigarrow I^{t-8} \\
&\dots \\
(W^{t} \sim x_{t}) &\rightsquigarrow I^{t}
\end{aligned}
\tag{4.7}
$$

where the symbol $\sim$ refers the association between the defined window and the corresponding input. The $\rightsquigarrow$ notation is used to represent 'leads to' the corresponding input FS.

Overall, fuzzification is implemented in an online learning manner and the input FSs are adapted without requiring any a priori knowledge about the noise levels or any offline procedures. In Fig. 4.10, the adaptive framework is illustrated with the generated input FSs ($\lambda = 1$ *step-by-step* process) by implementing on the *Stable Noise* time-series dataset (Fig. 4.9b).

The pseudo-code of this specific implementation can be seen in Algorithm 2.

4.3.1.5 Prediction

After generating the adequate input FSs to be associated with the most recent crisp input to the (NS)FLSs, the last 9 $(I^{t-9+1}, I^{t-9+3}, ..., I^{t})$ input FSs are processed to predict the next crisp point in the time series (and thus the crisp input for the next iteration).

In the used (NS)FLS models, the min and max operators are used for the t-norm and t-conorm, respectively. Then the centre of gravity technique is utilised in the defuzzification

Algorithm 2: Constructing adaptive input FSs by means of sliding window noise estimation (4.5) and (4.6) [136].

Input : the input value x_t at the most recent time step
Output: the corresponding input FS I_t for the input x_t

Function `noiseEstimation(`W^t`)`**:**
  $index \leftarrow 1$;
  $y \leftarrow []$ ▷ y is the list for the difference list;
  repeat
    $y[index] \leftarrow \frac{1}{\sqrt{2}} \left(W^t[index+1] - W^t[index]\right)$;
    $index = index + 1$;
  until $index = p - 1$;
  $\sigma^t \leftarrow s.d(y)$ ▷ Standard deviation of the y;
  return σ^t ;
Function `fuzzifyInput(`$x_t, \widehat{\sigma}_n$`)`**:**
  $I_t \leftarrow$ Gaussian FS with mean x_t and s.d. σ^t;
  return I_t ;
$t \leftarrow 0$;
repeat
  $p \leftarrow frameSize$ ▷ Defining the frame size;
  $W^t \leftarrow [x_{t-p+1}, x_t]$; ▷ W^t is the current frame;
  $\sigma^t \leftarrow noiseEstimation(W^t)$;
  $I_t \leftarrow fuzzifyInput(x_t, \sigma^t)$;
  $t \leftarrow t + 1$;
until $x_t = end$;

step. Since structurally different NSFLSs (adaptive and non-adaptive) are compared in the experiment, scaled performance results may provide a more feasible comparison. Therefore, the performance of each FLS is assessed using the Symmetric Mean Absolute Percent Error (sMAPE) [90] which provides a result between 0% and 200%. Also, as one the most common error measures, Mean Square Error (MSE) based results are included in Appendix A.2.

In order to mitigate the randomness in the results, each time series is generated 30 times and at the end of each experiment set the average sMAPE values are provided, while the MSE results are provided in Appendix A.2. Also, statistical analyses for both experiment are included in Appendix A.3.

After having detailed the experimental setup for both experiments, we now proceed to the implementation of experiments along with the obtained results.

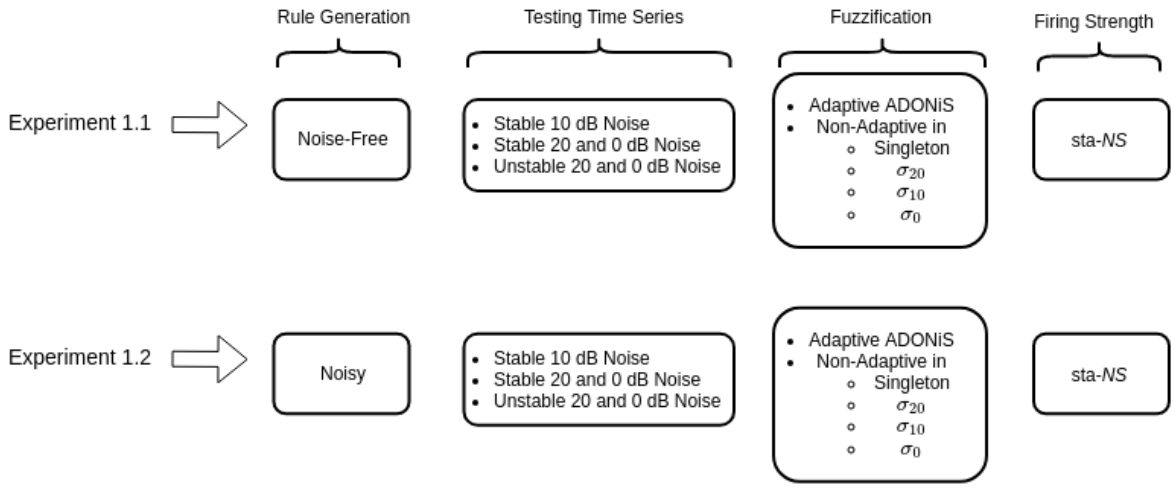

Figure 4.11: Experiment 1 with two sub-stages.

4.3.2 Experiment 1 - Adaptive and Non-Adaptive Comparison

In the real-world, a broad range of noise sources are common and while these sources have an affect on inputs of models, they vary in magnitude over time. As regards to the objective 2 of this thesis, dealing with varying input uncertainty can provide performance benefits for the models. In Experiment 1, we focus on testing ADONiS behaviour under different level of noise that is injected to the input of models. The overall experimental steps can be seen in Fig. 4.11. Regarding the rule generation of the systems, two sub-experiments *Experiment 1.1* and *Experiment 1.2* are conducted as noise-free rule generation and noisy rule generation, respectively.

In the non-adaptive design of the counterpart (NS)FLSs, the inputs FSs are constructed manually giving rise to four different comparative systems: a singleton FLS using singleton input FSs, and three distinct NSFLSs, using input FSs configured for 20 dB (σ_{20}), 10 dB (σ_{10}) and 0 dB (σ_0) noise levels respectively. In the experiments, the comparison of each variant is provided to ensure that the proposed adaptive fuzzification technique is challenged against different non-adaptive approaches.

4.3.2.1 Experiment 1.1 Noise-Free Rule Generation Results

In *Experiment 1.1*, noise-free rule generation is conducted, and the ADONiS framework's performance is reported compared to the different non-adaptive counterparts. This experiment's

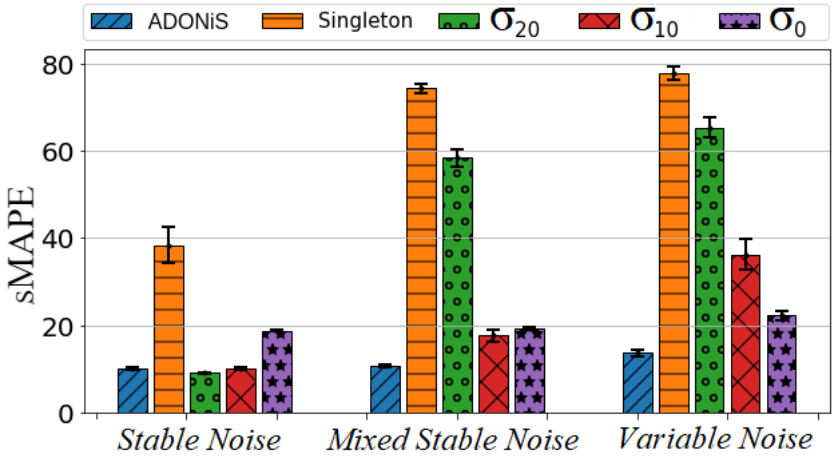

Figure 4.12: Experiment 1.1- MG Noise-free rule generation with ADONiS and Non-Adaptive fuzzifications, sMAPE prediction result comparison. Confidence intervals shown as black lines

main rationale is that generating rules in a 'pure' version and capture/handle noise in the testing phase on run-time. This setting aims to investigate ADONiS adaptive behaviours under 'unseen' noise levels and how it compares to manually designed counterparts.

After generating noise-free rules, the three test datasets (Fig. 4.9) are used for individual forecasting experiments.

First, the *Stable Noise* test series (Fig. 4.9a) is used to compare the adaptive and non-adaptive approaches. The prediction results are reported at the left-hand side of Fig. 4.12 for MG and Fig. 4.13 for Lorenz Time series. As can be seen, the adaptive fuzzification prediction results are quite similar to the σ_{20} and σ_{10} fuzzification value results and provide generally low error

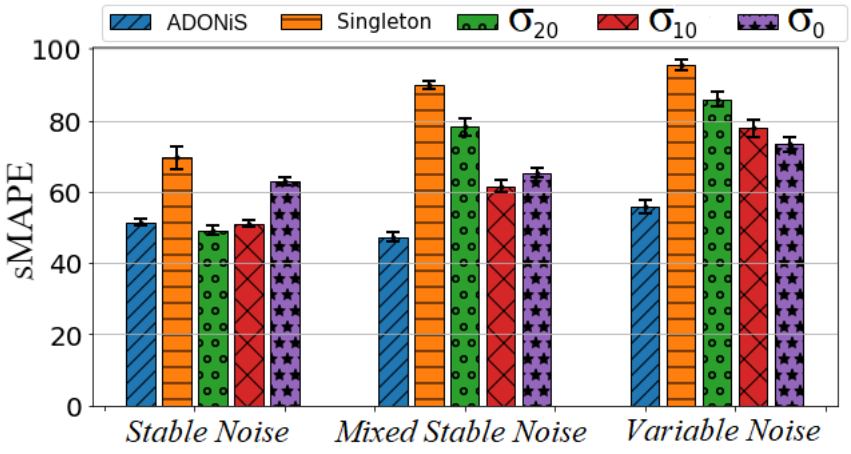

Figure 4.13: Experiment 1.1-Lorenz Noise-free rule generation in with ADONiS and Non-Adaptive fuzzifications, sMAPE prediction result comparison.

(which is intuitive as 10dB noise was injected into this time series), while the singleton approach and the σ_0 fuzzification lead to higher error levels.

Second, the *Mixed Stable Noise* test series (Fig. 4.9b) is used in the testing. The sMAPE result comparisons are provided in the middle of Figs. 4.12 and 4.13 which show that the adaptive technique has a clear performance benefit over each case of non-adaptive systems.

Third, the more challenging test series (*Variable Noise* as shown in Fig. 4.9c) is used in testing with results shown at the right-hand side of Figs. 4.12 and 4.13. Here, again, the adaptive technique outperforms each of the non-adaptive systems.

Each corresponding experiment MSE results can be seen in Appendix A.2.

4.3.2.2 Experiment 1.2 Noisy Rule Generation Results

After completing three sets of experiments with the noise-free rule settings, a more challenging context is established by generating rules by using noisy datasets (See Fig. 4.11). Three training datasets, which follow a similar structure as the corresponding test datasets, are generated. For example, if the model will be tested with the *Stable noise* from Fig. 4.9b, the training dataset is generated based on the same structure and noise levels. . This experiment's main rationale is to test ADONiS behaviour compared to the other non-adaptive designs under different rule generation circumstances. The prediction sMAPE results are shown in Fig. 4.14 for MG and

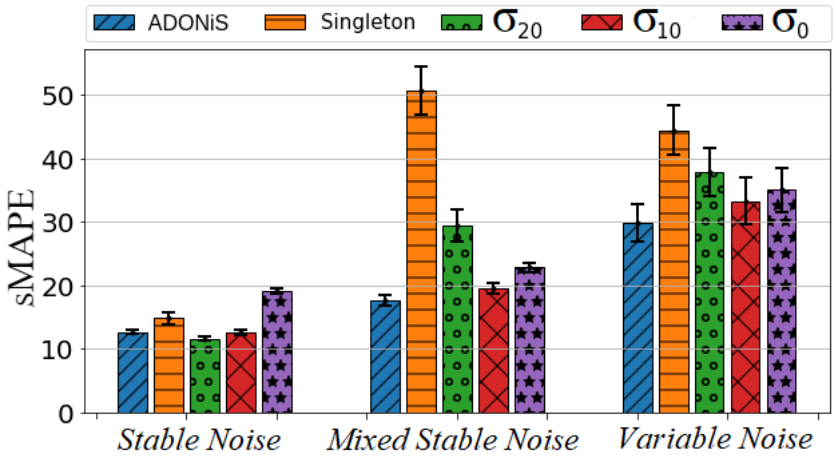

Figure 4.14: Experiment 1.2 - MG Noisy rule generation with ADONiS and Non-Adaptive fuzzifications, sMAPE prediction result comparison.

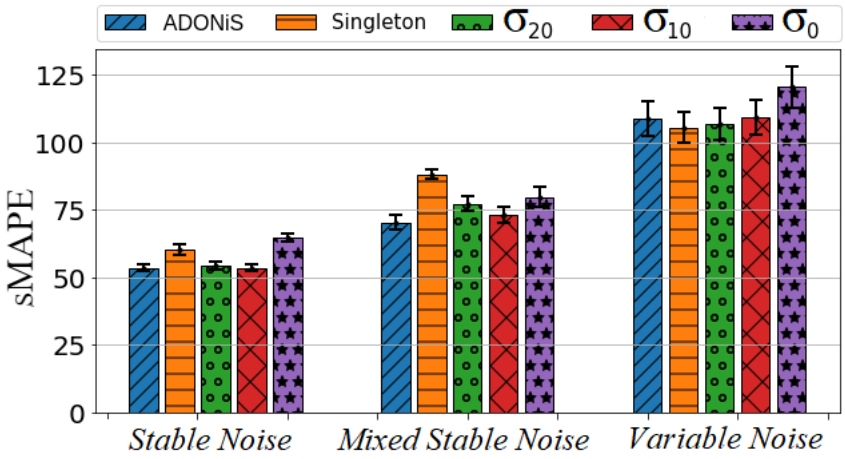

Figure 4.15: Experiment 1.2 - Lorenz Noisy rule generation with ADONiS and Non-Adaptive fuzzifications, sMAPE prediction result comparison.

Fig. 4.15 for Lorenz Time-series predictions. MSE results are reported in Appendix A.2.

In these experiments, first, 10 dB noise is injected into the training datasets and the system rule generation is completed. Then, the corresponding *Stable Noise* test dataset which includes 10 dB noise is used in the testing. The sMAPE results are shown at the left hand-side of Fig. 4.14 and Fig. 4.15. ADONiS and the two non-adaptive (σ_{20} and σ_{10}) fuzzification techniques produce similar sMAPE results.

For the second scenario, another training dataset is generated to correspond to the *Mixed Stable Noise* time series structure (Fig. 4.9b). This training series is used to generate system rules, and the resulting systems are tested using the *Mixed Stable dB Noise*. The results for both ADONiS and non-adaptive systems are shown in the middle of Fig. 4.14 and Fig.4.15. Though a variety of pre-fixed σ values are evaluated as bases of comparison for the adaptive technique, the proposed adaptive technique has the lowest sMAPE values.

Further, for the third case, a similar dataset to the *Variable Noise* (Fig. 4.9c) dataset is used for training. As the results are shown at the right hand-side of Fig. 4.14 and Fig. 4.15, the ADONiS approach produces the lowest or close to the lowest sMAPE values.

Overall, in both Experiment 1.1 and Experiment 1.2, the ADONiS adaptive input uncertainty handling capacity are compared to other non-adaptive counterparts under varying noise levels. Generally, as can be seen, the ADONiS framework provides the best or close the best perfor-

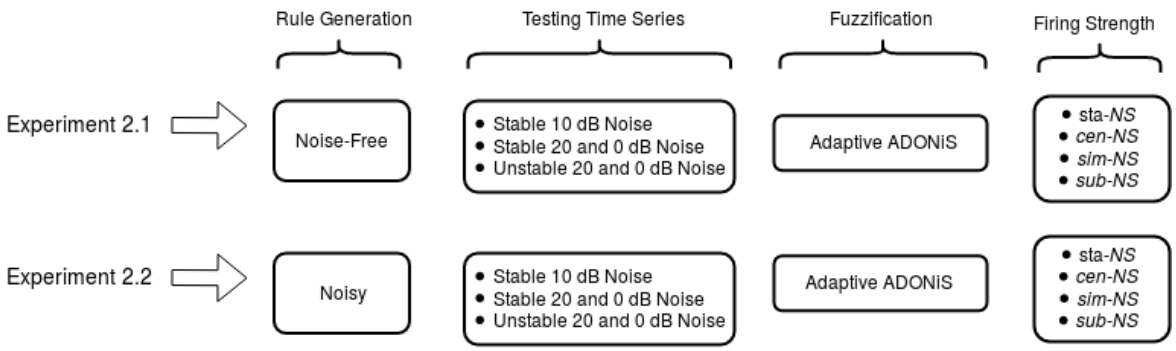

Figure 4.16: Experiment 2 with two sub-stages.

mance, as will be detailed in the discussion. We now proceed with a further ADONiS analysis in Experiment 2, where it is integrated with different firing strength-determining approaches.

4.3.3 Experiment 2 - ADONiS Integrated with Firing Strength Determining Techniques

In Experiment 1, we focused on ADONiS compared to non-adaptive systems under circumstances where input noise varies over time.

In Experiment 2, we focus on integrating the ADONiS framework with *sta*-NS, *cen*-NS, *sim*-NS and the proposed *sub*-NS firing strength determining approaches where input noise vary over time. In each variant of experiment, ADONiS is integrated with a different firing strength determining architecture (See Fig. 4.16) and the performance of each ADONiS framework is compared. The rationale for these experiments is to investigate further and leverage ADONiS framework performance while capturing input uncertainty in fuzzification and handling it in the inference engine of NSFLSs, specifically mapping uncertainty from input to output of FLSs.

In each variant of the experiments, first, the *sta*-NS approach is implemented and then the same experiments are repeated by using *cen*-NS, *sim*-NS and the proposed *sub*-NS composition methods within the NSFLSs. As shown in Fig. 4.16, in two subsequent experiments, ADONiS is implemented for noise-free and noisy rule generations, respectively, for both the MG and Lorenz time series.

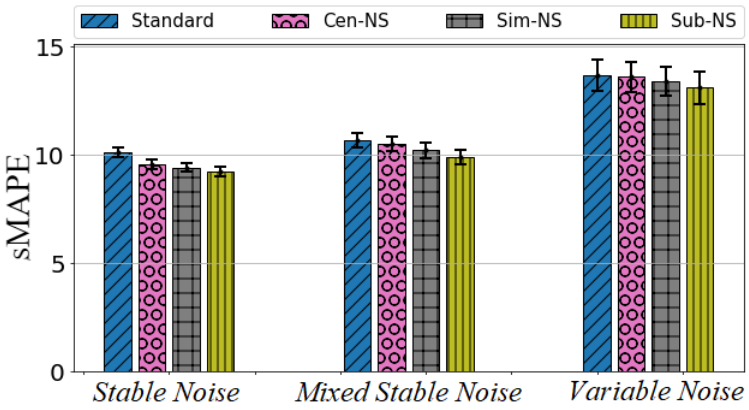

Figure 4.17: Experiment 2.1 - MG Noise-Free trained ADONiS integrated with advanced *sta*-NS, *cen*-NS, *sim*-NS and *sub*-NS prediction results with adaptive NSFLSs.

4.3.3.1 Experiment 2.1 Noise-Free Rule Generation Results

The models' rules are generated by using noise-free training datasets for both MG and Lorenz time series and subsequently evaluated for all three testing noise scenarios captured in Fig. 4.9. The results for all three scenarios and both time series are shown in Figs. 4.17 and 4.18.

As shown in the figures, when the *sub*-NS approach is integrated with the ADONiS framework, it produces slightly better sMAPE values than the rest of *sim*-NS, *cen*-NS and *sta*-NS NSFLSs counterparts.

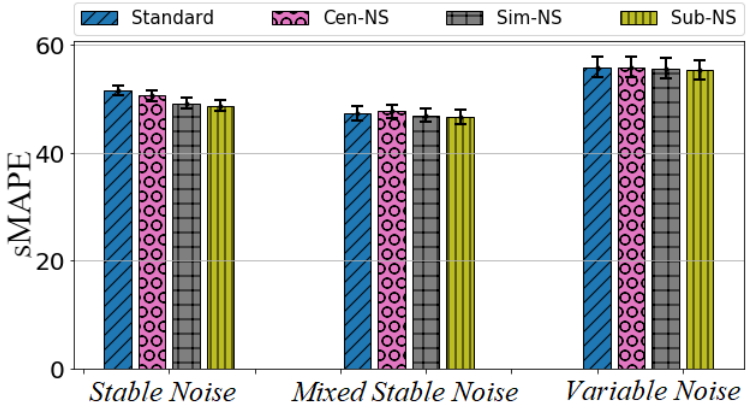

Figure 4.18: Experiment 2.1 - Lorenz Noise-free trained ADONiS integrated with advanced *sta*-NS, *cen*-NS, *sim*-NS and *sub*-NS prediction results with adaptive NSFLSs.

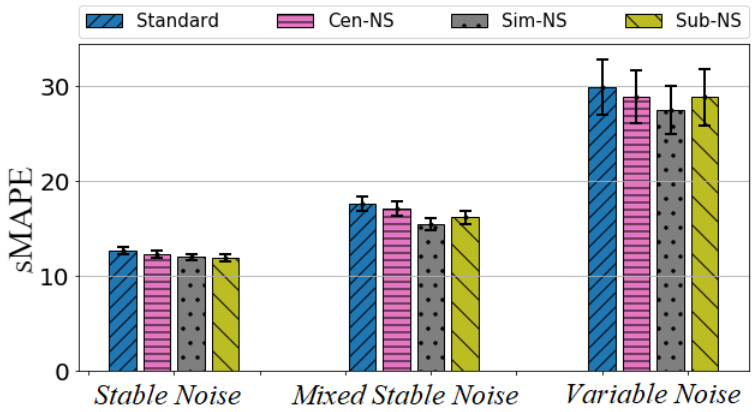

Figure 4.19: Experiment 2.2 - MG Noisy trained ADONiS integrated with advanced *sta*-NS, *cen*-NS, *sim*-NS and *sub*-NS prediction results with adaptive NSFLSs.

4.3.3.2 Experiment 2.2 Noisy Rule Generation Results

In the noisy rule generation experiments (See Figs. 4.19 and 4.20), while the *sub*-NS shows better performance under stable noise level in testing, the *sim*-NS outperforms it under unstable Mixed Stable Noise and Variable Noise testing conditions.

4.3.4 Discussion

When the model rules are generated from noise-free time-series (Experiment 1.1, see Figs. 4.12 and 4.13), the noise levels in the test series can be considered as unexpected/unseen for the model. When a stable 10 dB noise level is used in the testing dataset (the left hand-side of Figs. 4.12 and 4.13), both ADONiS and some non-adaptive systems provide similar results for

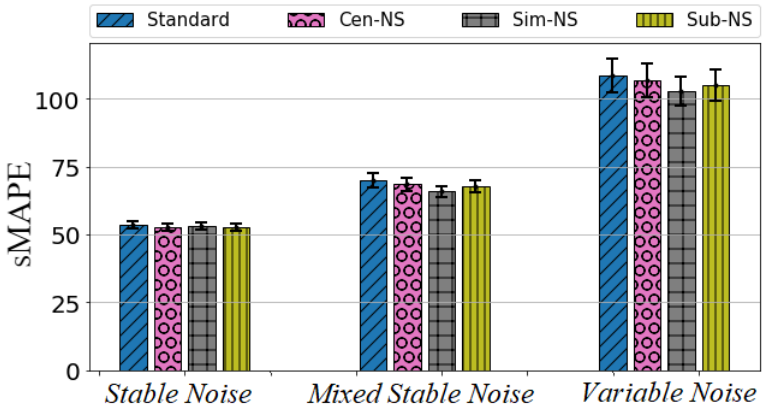

Figure 4.20: Experiment 2.2 - Lorenz Noisy trained ADONiS integrated with advanced *sta*-NS, *cen*-NS, *sim*-NS and *sub*-NS prediction results with adaptive NSFLSs.

both the MG and Lorenz experiments. In the non-adaptive implementation, as the test series contains 10 dB noise level, manually adjusting input FSs to the 10 dB σ_{10} values can be argued to provide an unfair or at least unreasonable advantage to the non-adaptive technique. Such that in the real world, of course, the actual level of noise/uncertainty cannot commonly be known in advance. In contrast, the proposed ADONiS framework does not require any a priori information about the noise levels. The proposed framework is shown to be advantageous to capture and handle unseen noise levels compared to the non-adaptive variants in the set of Experiments 1.1.

In Experiment 1.2, we explore the scenario where pre-defined noise levels are employed during rule generation (Figs. 4.14 and 4.15). Even though we test the NSFLSs with a series of noise levels which include the actual noise levels for which the non-adaptive NSFLSs were training, the proposed ADONiS framework produces either the lowest or close to the lowest sMAPE values in all experimental scenarios.

In addition, experiments 1.1 and 1.2 are repeated under uniform noise injection rather than the Gaussian type noise injection. The results of these experiments are presented in Appendix A.1. As shown in those results, the proposed framework shows the similar prediction performance as a Gaussian noise type and generally outperforms manually designed NSFLS counterparts.

As a core part of the rationale underpinning this chapter is the strong focus on appropriate managing of uncertainty affecting system inputs, we have explored (Experiment 2) different inference engine approaches (*sta*-NS, *cen*-NS, *sim*-NS and the alternative *sub*-NS). As shown in Figs. 4.17 and 4.18, the *sub*-NS architecture can achieve slightly better sMAPE values in comparison to other integrated ADONiS designs under noise-free rule-generation. Figs. 4.19 and 4.20 show that in the noisy training conditions both *sub*-NS and *sim*-NS have a performance benefit. Based on these experiments, there is strong potential for integrating the proposed ADONiS framework with the other inference architectures in real-world application with varying noise levels.

In order to assess the statistical reliability of these results, a series of paired sample t-tests are conducted and reported in AppendixA.3. Divergence of results is found depending upon

the type of error measure used (sMAPE vs MSE), and according to noise levels both in testing and training. However, in general, *sub*-NS is found to be the best performing technique. This is particularly true within the noise-free training conditions, in which it performs significantly better than all other measures in 10 out of 12 conditions. In noisy training conditions, *sub*-NS is found to be significantly better in only 3 out of 12 conditions, while *sim*-NS is found to be best in 8. The detailed results can be found in AppendixA.3.

Overall, the experiments show that while in some specific (constant and low-noise) cases, offline (pre-defined) fuzzification for a noise level of σ_{20} or σ_{10} is superior, for cases where the uncertainty levels are unstable, the proposed ADONiS framework delivers superior results across the extensive variety of scenarios explored. Given that real-world environments are subject to a broad range of uncertainty sources, input of models is affected at different levels over time. The proposed ADONiS framework dynamically adjusts input FSs on-the-fly, in an online manner, which directly benefits applications subject to unstable and/or unknown noise levels as are common in real-world circumstances which address objective 2 of the thesis.

4.4 Summary

Since real-world environments are influenced by a broad range of input-affecting uncertainty sources -which can vary greatly in magnitude over time-, the availability of a priori knowledge of varying circumstances may not be possible for models. Even though it is assumed that a priori knowledge is available (e.g. training dataset covering all real-world circumstances), input FS tuning procedures are generally limited to selecting one type of FS model to capture the input uncertainty. This aspect tends to prevent NSFLSs dependent on offline tuning from being able to adapt to the breadth of changing uncertainty levels inherent in real-world applications.

In this chapter, a complete framework (ADONiS) is proposed to configure NSFLS input FSs, in an online manner, by applying an uncertainty detection technique to a sequence of recent observations. In doing so, ADONiS enables constructing input FSs which can dynamically capture different levels of uncertainty on the run-time, in turn providing capacity to adapt the

breadth of changing uncertainty levels inherent to real-world applications.

The results from Experiment 1 (the comparison of the proposed ADONiS and non-adaptive techniques) suggests that the proposed approach of dynamically changing input FSs is a suitable approach for handling input noise, especially where input noise levels vary. In particular, when there is no a priori knowledge of the future noise levels (Experiment 1.1), the ADONiS can be built on noise-free rules and still be able to map varying input uncertainty to outputs of NSFLSs.

Further, in Experiment 2, four firing strength generation techniques -designed to handle the interaction of input and antecedent FSs with high fidelity- are evaluated in conjunction with ADONiS. Here, the results show that combining ADONiS with advanced NSFLS inference mechanisms can deliver better input uncertainty mapping in comparison to the traditional NSFLS inference.

Overall, as presented in our studies [121, 124], the experiment results in different scenarios, highlighting the ADONiS framework's generality and performance benefits under unexpected/unseen or seen noise levels for the model. Therefore, by addressing objective 2; ADONiS is capable of capturing uncertainty at run-time and dynamically updating FLSs to account for changes in the uncertainty affecting inputs.

As the limitations of the particular ADONiS framework version which is used in this chapter, although a significant accuracy increase was achieved in the presented forecasting experiments, given the small set of experiments and adoption of a single noise estimation algorithm, these results can only represent an initial step towards a general conclusion and a real-world application. Furthermore, in order to make a plausible uncertainty level estimation, defined frames (in step 1 of the ADONiS) should contain adequate information. If parameters of frame size can not contain a reflective information, input FS may not efficiently capture the current uncertainty. In addition, in the case of using a large frame and a complex uncertainty detection technique, the increase in the computational cost may limit the applicability of the framework, depending on applications. It is worthwhile noting that, defining frame size can be implemented based on expert knowledge or by using various data-driven procedures.

So far, in Chapter 3, we have proposed an alternative approach (*sub*-NS) to handle input uncertainty in the inference engine step of NSFLSs. In this chapter, we have proposed the ADONiS framework to dynamically adapt input FSs to different uncertainty levels dynamically on-the-fly. While capturing different uncertainty levels in the last observed values can provide benefits to ADONiS, another mechanism to capture variation in the uncertainty levels over time can also be beneficial for decision support systems. Thus, in the next chapter, we will elaborate on the ADONiS with IT2 input FSs to capture both uncertainty in the last observed value(s) and the uncertainty levels' variation over time.

Chapter 5

Adaptive Interval Type-2 Input FSs

In the previous chapter, the ADONiS framework is proposed to capture uncertainty in the last observed value(s) at run-time. The environments of real-world circumstances are often subject to change over time. While some uncertainty sources may exist in a period of time, it may not linger afterwards. Furthermore, the uncertainty effect of each source may vary in magnitude over time as well. These real-world settings put serious challenges forward to decision-support systems due to the uncertainty of inputs that can vary broadly over time. ADONiS demonstrates promising results in capturing the level of uncertainty from the last observed value(s), yet an extra mechanism for assembling the varying circumstances can provide additional benefits. For instance, in a robotics application environment where uncertainty varies considerably, the last observed value may have a 'low' level of uncertainty which results in a narrow input FS. However, as the environmental conditions vary, there is a possibility that the uncertainty may increase again. Hence, the extra degree of freedom can provide the capacity for capturing the degree of variation over time in environmental conditions. Therefore, in this chapter, by addressing objective 3, we focus on extending the ADONiS structure by capturing both the uncertainty in the last observed value(s) and also the degree of variation in uncertainty levels over time, as presented in our study [123].

Section 5.1 introduces the background and motivation of this chapter. Section 5.2 provides the extended ADONiS framework to capture both the last observed uncertainty and variation

in uncertainty levels which addresses objective 3. Section 5.3 presents a time-series forecasting case study to demonstrate the behaviour of the extended framework. Lastly, Section 5.4 summarises the contribution of this chapter to this thesis.

5.1 Background and Motivation

Most real-world environments are subject to different uncertainty sources in which each source may exist/affect the inputs simultaneously or partially/individually in different time scales. In particular, the variations in the uncertainty levels makes estimating and handling uncertainty a complex and challenging task which may results in non-optimal outcomes. So far in this thesis, in Chapter 3, the alternative approach *sub*-NS is proposed to further develop the capacity of uncertainty mapping from inputs to outputs by systematically determining firing strengths in the inference engine step of NSFLSs. In Chapter 4, the ADONiS framework is proposed to adaptively capture input uncertainty levels from the last observed value(s) which also has a primary role for input uncertainty mapping to outputs of NSFLSs. While input uncertainty handling and capturing is a crucial element of decision-support systems, additionally capturing the variation in uncertainty levels over-time can also potentially provide performance benefits with regards to properly responding to circumstantial changes in decision-support systems.

While Type-1 FSs are designed to capture uncertainty [189], Type-2 (T2) FSs [191] are an extension of the T1 FSs, where each degree of membership is a FS rather than a crisp number (Details can be found in Section 2.1.2). Due to this extra degree of freedom, generally, T2 FSs can provide a better ability to capture variation in uncertainty levels [35, 49, 91, 152, 174, 182, 192].

In the literature, many attempts have been made with the purpose of defining Type-2 input FS parameters with offline training procedures or a priori knowledge assumptions in NSFLSs [25, 72, 89, 96, 97, 164, 183, 192]. Even though plausible results have been acquired, the parameter determining for Type-2 input FSs can be regarded as impractical, as both the width and the extra degree of freedom in input FSs mainly rely on either offline training procedures or a priori

assumptions about the uncertainty levels. Considering the different uncertainty levels which are omnipresent in real-world applications, Type-2 input FS designs should be fully adaptive to stable/unstable environments, e.g. variation in uncertainty levels.

Apart from that several studies [146, 147, 148, 149] put forward another method in adaptive IT2 input FSs generation which were later extended in later studies [140, 141]. In these studies, some pre-trials have been conducted by applying different conditions (changing temperature, sound noise, and wind) while recording a robotics sensor measurements at a fixed distance. Based on the gathered sensor measurements, a non-specified convex shaped piece-wise linear T1 input FSs are generated and repeating these process different T1 input FSs are utilised to construct IT2 input FSs in those pre-trials. After defining the IT2 with a variety of distances in the pre-trials, on the run-time of the actual experiments, five consecutive crisp measurements from sensors are collected and the average of these 5 measurements is interpolated with the originally constructed T2 FSs. In those studies FOUs of input FSs are used to model the uncertainty associated with the measurements. Even though the adaptive manner in those studies is very plausible and endorsed by experiments, since the original T2 FSs are defined by employing pre-trials experiments, this findings are still limited to the chosen pre-trial conditions.

In real-world circumstances, as varying levels of uncertainty source may disturb input data at different levels/times, capturing and handling this variation in uncertainty levels can be a useful step for applications. In order to capture these different circumstances adaptively, this chapter puts forward the extension of the ADONiS framework; while capturing the last observed input uncertainty adaptively in the principal T1 FS, the extra degree of freedom (i.e. FOU) of IT2 is used to capture/model the variation in uncertainty levels in an adaptive manner (addressing objective 3 stated in 1.5). In doing so, for instance, in an environment where the circumstances change drastically, the FOU is automatically be adjusted to be wider to capture these variations in uncertainty levels. Additionally, in an environment where the circumstances are stable, the FOU is automatically be adjusted to be narrower.

ADONiS and the extended IT2 ADONiS behaviours are compared in Fig. 5.1 by depicting four different case scenarios. As can be seen in the first two rows, the last observed uncertainty

The Last Observed Uncertainty	Variation in Uncertainty Over-Time	ADONiS	IT2 Extended ADONiS
'Low' level	'Low' variation	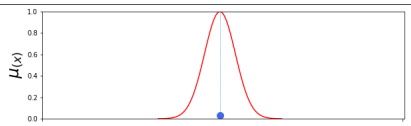	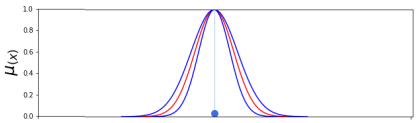
'Low' level	'High' Variation	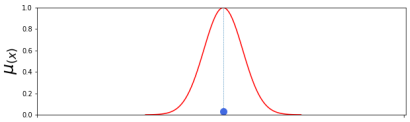	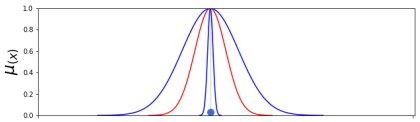
'High' level	'Low' variation	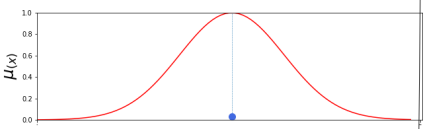	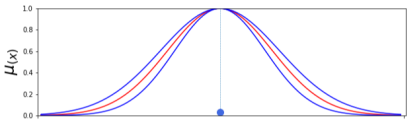
'High' level	'High' Variation	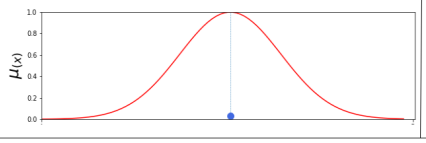	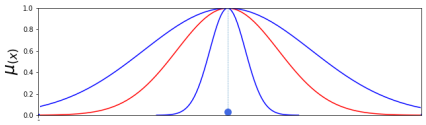

Figure 5.1: ADONiS and the IT2 extended ADONiS input FSs comparison under four different sample secanrios.

levels are relatively similar (labelled as ‘low’) and variations in uncertainty levels are different (’low’ in the first row, ’high’ in the second row). While the ADONiS framework leads to quite similar T1 input FSs, the extended framework produces two distinct IT2 input FSs by also capturing the variation in the uncertainty levels. For instance, in a robotics context, the first row can be portrayed as a steady environment where noise levels are low and stable over time. The second row can be depicted as the environmental conditions are unstable and subject to change, even though the last observed value(s) contain ’low’ uncertainty. In doing so, by means of FOU, the variation in uncertainty levels is also captured around the constructed T1 FSs enabling the system to respond properly to changes in its inputs. Similar scenarios can be characterised for the third and fourth rows in Fig. 5.1 as well.

Dynamically having different widths and FOU values on generated input FSs, -without requiring a priori knowledge- can enable models to be being *prepared* for drastic changes in environments. Furthermore, when uncertainty can not be fully reflected on the T1 input FSs, the dynamically adjusted FOU can also provide performance benefits and robustness for the model, as detailed in the next section.

5.2 The Extended ADONiS Framework

Considering both the advantages of ADONiS and Type-2 FS designs in respect to input FSs, in this section, we extend the proposed ADONiS framework with a strategy to design adaptive IT2 input FSs at a run-time. In the extended proposed framework, first, the last observed uncertainty level is captured and principal T1 input FSs are constructed as in Chapter 4. Second, the variation of uncertainty levels is also captured and reflected as FOU (standard deviation uncertainty) on the constructed principal T1 input FSs.

As mentioned and illustrated in Fig. 5.1, in the previous section, in an unstable environment, the generated FOU will adapt itself by widening. Simultaneously, the widths of the principal T1 input FSs are adapted itself to the last observed uncertainty level as well. In doing so, the FOU is utilised to capture the variation in uncertainty levels, while the core T1 input FS is utilised to capture the last observed uncertainty level. Likewise, in a stable environment where uncertainty levels are durable, the generated FOU adapts itself by narrowing and the width of the principal T1 input FSs are adapted itself to the last observed stable uncertainty level which can be high or low. Note that, in the ADONiS application case, both T1 FSs would have a similar structure as shown in the first and second rows or third and fourth rows of Fig. 5.1. However, by employing the extended framework, environmental conditions are sufficiently captured in the IT2 input FSs of the NSFLSs which can be helpful in environments where uncertainty levels are not stable.

In the next subsection, we will elaborate on each point of the extended framework where each step can be followed in Fig. 5.2.

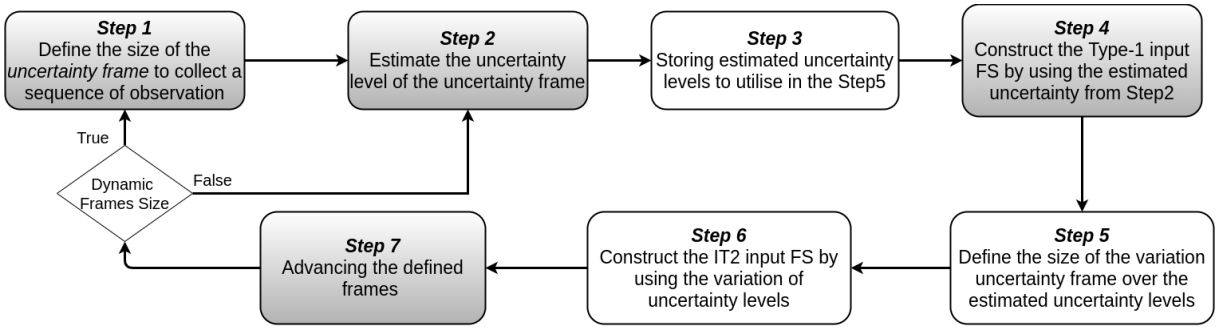

Figure 5.2: The extended ADONiS framework to generate adaptive IT2 input FSs. Grey colour highlighted steps are the same procedures in ADONiS implementation.

5.2.1 General Framework Structure

As shown in Fig. 5.2, the extended ADONiS framework is completed in seven steps. While 4 of these steps are employed same as the ADONiS framework (see the grey colour highlighted Steps 1,2,4 and 7), the remained steps are additionally implemented to construct IT2 input FSs. As the extension of the ADONiS framework, in this version, two different time frames are defined. In order to prevent confusion, the first frame will be referred to as *Uncertainty Frame* and the second frame is *Variation Uncertainty Frame* throughout this chapter.

Step 1 - Define the size for the uncertainty frame: This step is the same as in the ADONiS framework implementation. A sequence of observations from the input source are collected over a given frame which is referred as *Uncertainty Frame*. For instance, in a robotics context, this frame size can be set as stable containing sensor measurements every 1-second time-frame or it can be set to contain a certain number of values (e.g. every 100 values). Also, based on the design choice, the size/length of this frame can be dynamically changed, as shown in Fig. 5.2.

This proposed extended framework is can be utilised in different applications such as signal processing, robotics, medical applications and forecasting etc. As the time-series instance provide a suitable testbed, in this subsection, the general framework is illustrated on a time-series instance. So that following the implementation in 4.2.2, the dataset is denoted as $X = \{x_t : t \in T\}$ and $T = \{t_i \mid 1 \leq i \leq N\}$. The defined *uncertainty frame* (red vertical dashed lines) is denoted as the set W^t, where $W^t \subseteq X$, and is shown as follows:

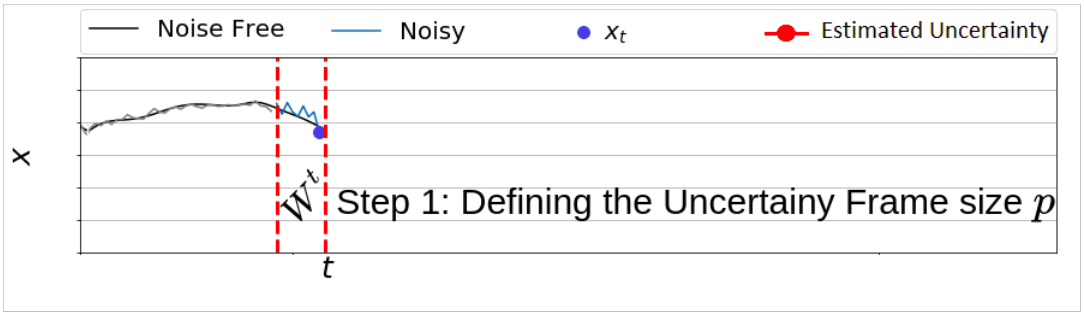

Figure 5.3: Step 1 defining the uncertainty frame size in the extended ADONiS framework to generate IT2 input FSs.

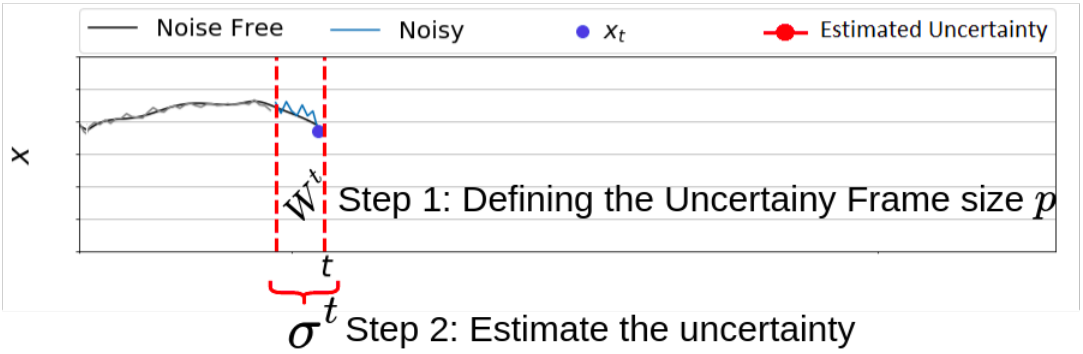

Figure 5.4: Step 2 the last observed uncertainty estimation in the extended ADONiS framework to generate IT2 input FSs.

$$W^t = \{x_i \mid x \in X \ , \ t - p < i \leq t\} \tag{5.1}$$

where t is the last observed time, p is the size of the frame.

A time-series sample of this frame can be seen in Fig. 5.3 as the red dashed line.

Step 2 - Estimate Uncertainty: Same as in the ADONiS framework, an uncertainty detection technique is implemented to estimate the last observed uncertainty level over the collected observations. In this step, different techniques can be utilised. As is practised in Chapter 4, a chosen algorithm is used to estimate the uncertainty level of the defined *uncertainty frame* (red vertical dashed lines) and this step is also following the same procedure from Chapter 4, as shown in Fig. 5.4.

$$\sigma^t = f(W^t) \tag{5.2}$$

where f is the chosen uncertainty estimation function and σ^t is the estimated uncertainty level at the time t.

Step 3 - Storing the estimated uncertainty: Unlike the ADONiS framework, in this step, estimated uncertainty levels are stored for each *uncertainty frame*. Thus, as the *uncertainty frame* advances, a new estimation will be stored for each new step. In doing so, the record of these estimated uncertainty changes can provide insight into 'how much stable is the environment?' which in turn can be utilised to prepare the input FSs. The estimation set is denoted by Q

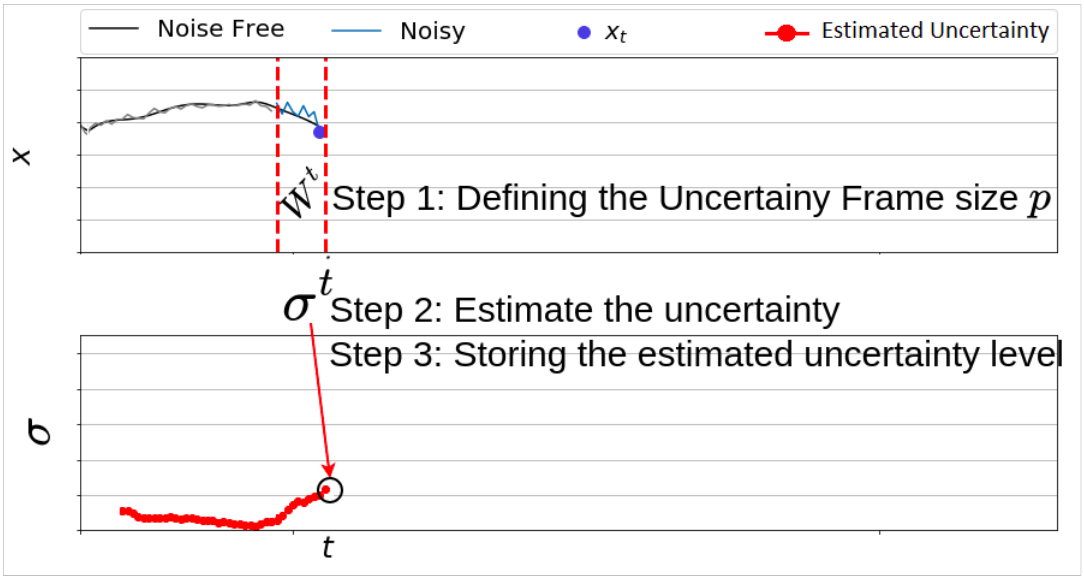

Figure 5.5: Step 3 storing the last observed uncertainty estimation in the extended ADONiS framework to generate IT2 input FSs.

and while the uncertainty estimation is operated, each estimation is added to this defined set as follows:

$$Q^t = Q^{t-1} \cup \sigma^t, \tag{5.3}$$

where Q is the set of estimated uncertainty level values, t is the current time and σ^t is the estimated uncertainty level at the time t.

The stored uncertainty levels -along with the previous estimations- are illustrated at the bottom of in Fig. 5.5, as σ.

Step 4 - Construct a Type-1 input FS: By following the same procedures from the ADONiS framework, a principal Type-1 input FS is constructed by using the last estimated uncertainty level of the *uncertainty frame* frame. This estimated uncertainty (σ) can be used, for example, with Gaussian FSs to inform their width/standard deviation. In doing so, this T1 input FS can capture the last observed uncertainty level which will be the core of the generated IT2 later. The illustration of the T1 input FS generation is shown in Fig. 5.6.

$$I^t = \{(x, \mu_{I^t}(x)) \mid \forall x \in U\}, \tag{5.4}$$

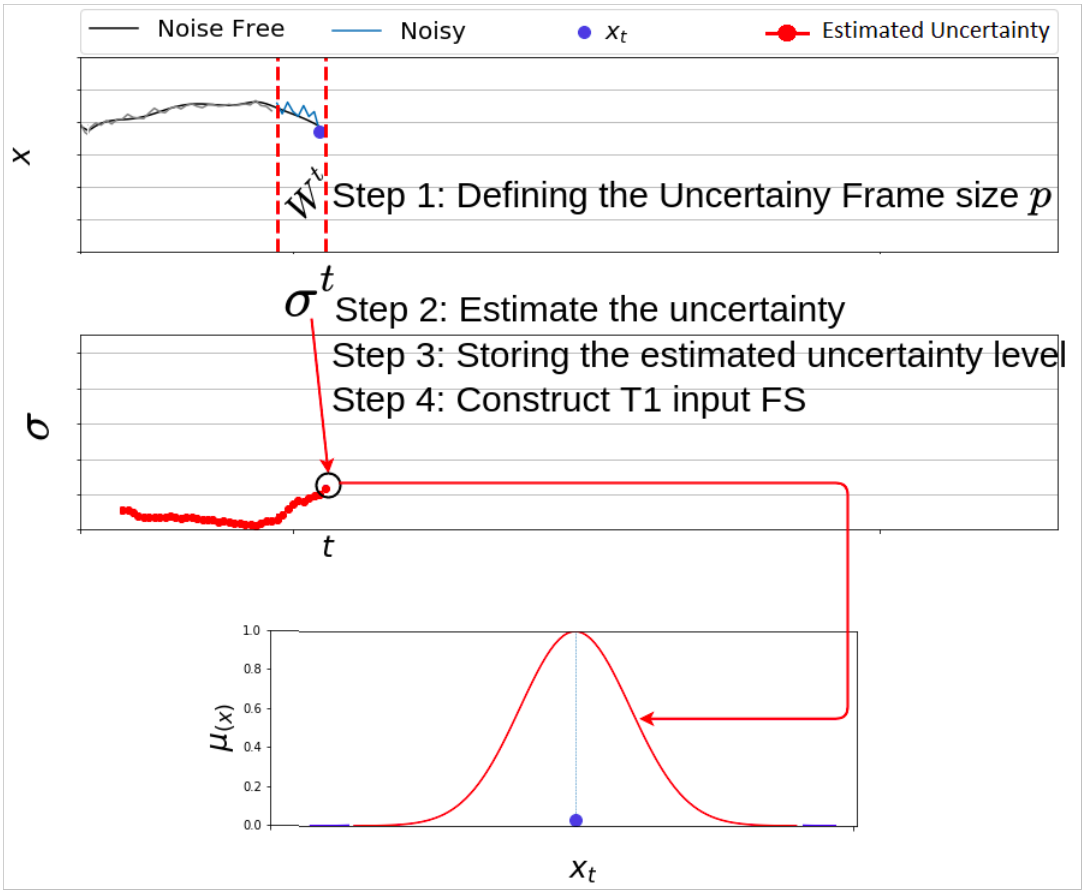

Figure 5.6: Step 4 constructing T1 input FSs in the extended ADONiS framework to generate IT2 input FSs.

where $\mu_{I^t}(x)$ is degree of membership.

Step 5 - Define the size for the variation uncertainty frame: Unlike the ADONiS implementation, another frame is defined in this step. The reason for defining this frame is to observe the environmental changes over time and utilise these observed circumstances (e.g. unstable or stable) in IT2. By doing so, generated IT2 input FSs will be able to capture variation over-time which enables the system to respond properly to changes in its inputs. For instance, in a sudden uncertainty change, the principal T1 input FS may not fully capture these changes; however, by means of FOU, the extra degree of freedom can provide additional ability to capture these uncertainty changes.

This frame is referred as *variation uncertainty frame* (vertical blue dashed lines) and depending on the design choice, the size/length of the frame can be changed or stable according to the application. In this instance, we denote the *variation uncertainty frame* as V, where $V \subseteq Q$,

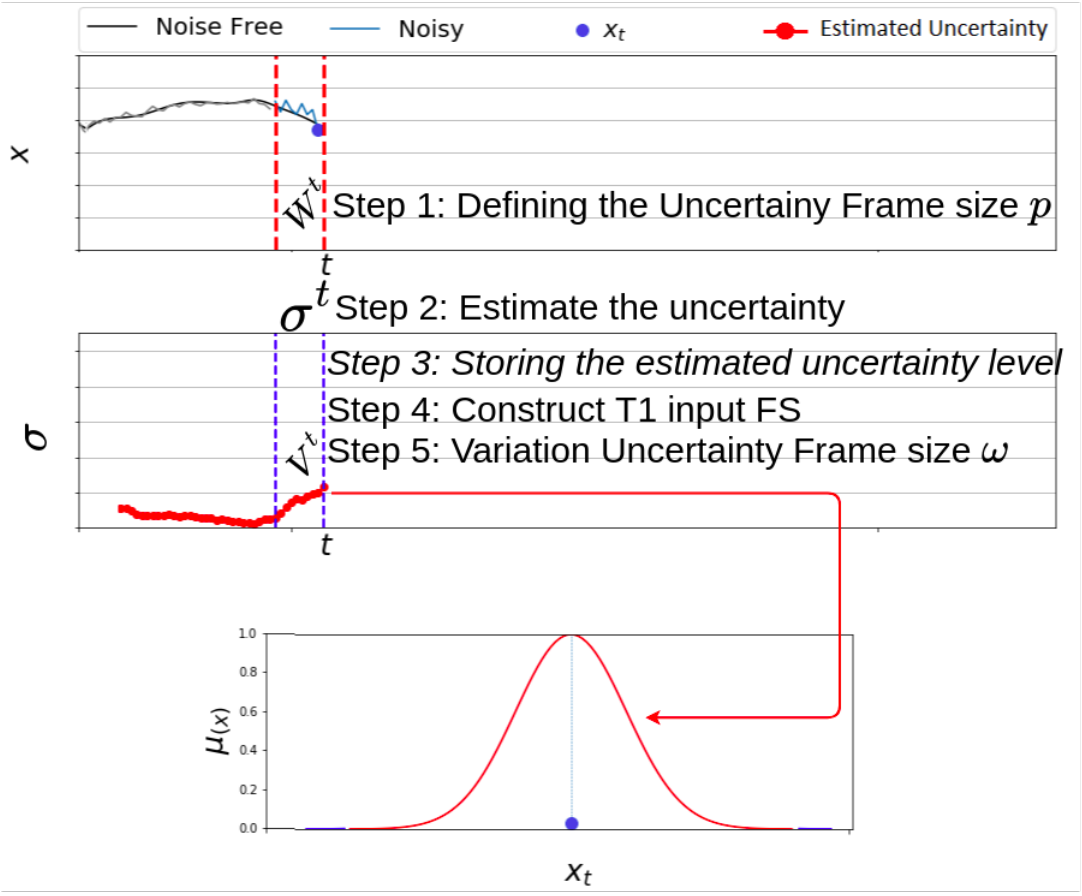

Figure 5.7: Step 5 defining variation uncertainty frame in the extended ADONiS framework to generate IT2 input FSs.

and the size of this frame is denoted as ω. This frame over the stored estimated uncertainty levels is defined as follows:

$$V^t = \{\sigma^i \mid \sigma \in Q \ , \ t - \omega < i \leq t\} \tag{5.5}$$

This *variation uncertainty frame* is illustrated as blue dashed line at the middle figure of Fig. 5.7.

Step 6 - Construct an Interval Type-2 input FS: Here, the variation of the uncertainty levels over the *Variation Uncertainty frame* is computed and is used to specify the size of the IT2 FOU around the initial T1 (principal) MF generated in Step 4. In doing so, in an environment where the uncertainty keeps changing, the variation lead to be high which in turn creates wider FOU values. Conversely, if uncertainty levels are kept constant (regardless of being high or low)

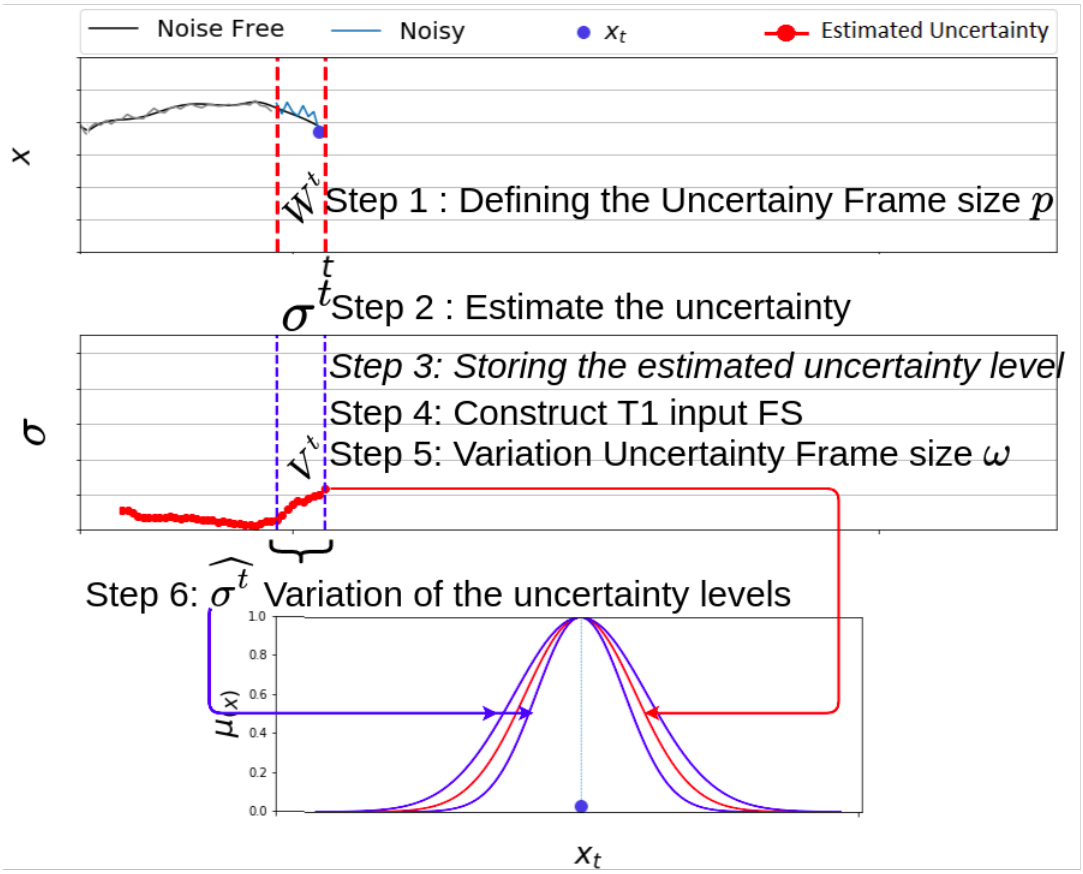

Figure 5.8: Step 6 defining FOU as the variation in uncertainty levels.

over time, the variation leads to low which in turns generating narrower FOU values. A sample of generated FOU value on the IT2 FSs can be seen as blue at the bottom Fig. 5.8. This can provide the ability to capture varying circumstances and the IT2 construction is implemented as follows:

$$\widehat{\sigma^t} = \sqrt{\frac{1}{\omega}\sum_{i=1}^{\omega}(\sigma^i - \bar{\sigma})^2}, \quad \forall\, i \in V^t, \tag{5.6}$$

where $\bar{\sigma}$ is the mean of the *uncertainty variation set* (V^t), ω is the size of the set and $\widehat{\sigma^t}$ is the variation in the uncertainty frame at the time t.

$$\widetilde{I}^t = \{((x,u), \mu_{\widetilde{I}^t}(x,u)) \mid x \in U\ ,\ u \in J_x \subseteq [0,1]\}, \tag{5.7}$$

where J_x is the primary membership

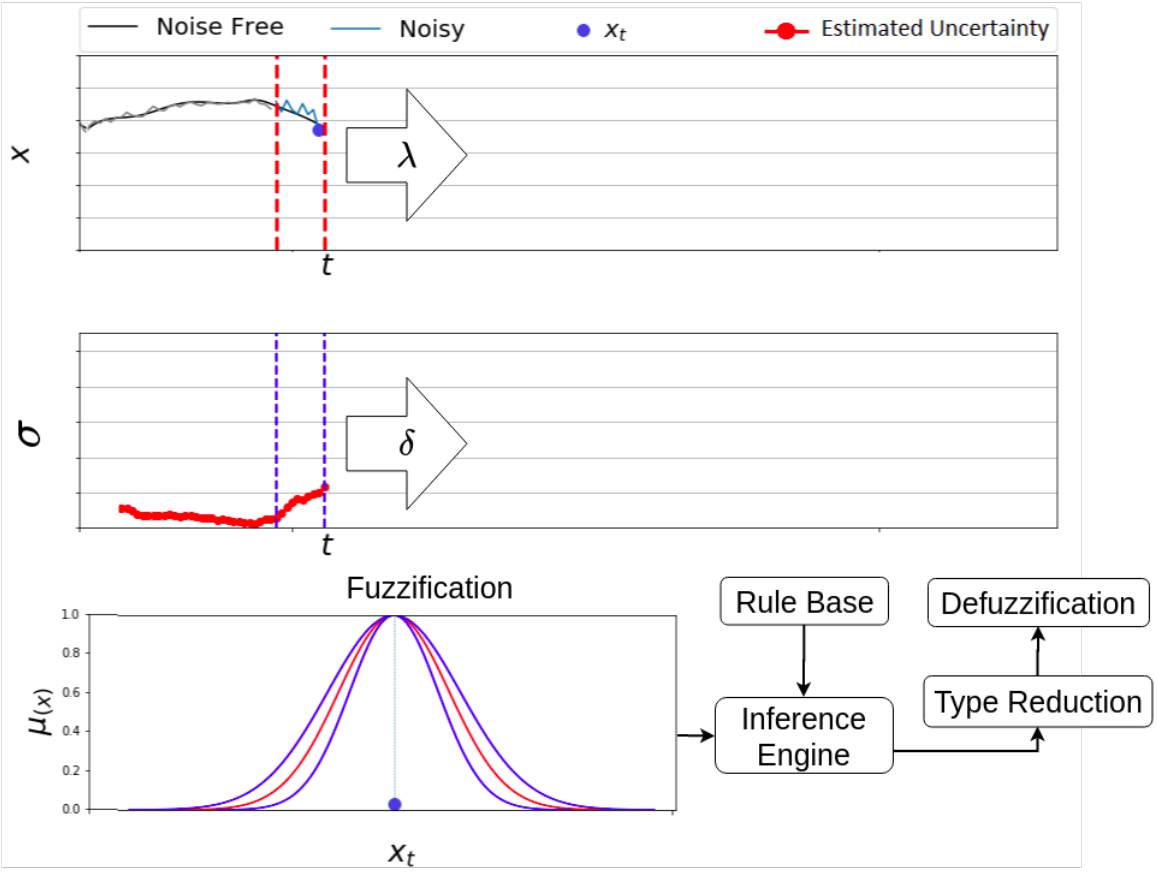

Figure 5.9: Step 7 processing the generated IT2 input FS(s) and advance the frames.

Step 7 - Advancing the defined frame:

After generating the IT2 input FS(s) for the current frame, the generated input FS(s) are proceeded to the NSFLS to implement the defined task such as prediction. A sample of SISO can be seen in Fig. 5.9. As time pass and more data is gathered, the defined *uncertainty frame* and the *variation uncertainty frame* are advanced by defined steps. The step size of the each frame is denoted as λ for the *uncertainty frame* and δ for the *variation uncertainty frame* steps. So that the extended framework is completed for 7 steps and the same procedures are repeated.

Overall, the proposed framework can be employed in a variety of applications where the input is subject to both uncertainty and varying uncertainty levels over time. The extended ADONiS strategy is employed by leveraging the seven-step methodology over the generated time-series, as shown in Fig. 5.8. By following the uncertainty estimation algorithm, the last observed noise level (σ^t) is detected in the *Uncertainty frame* (red dashed lines W^t in Fig. 5.8) and it is stored along with the previously detected noise levels. To construct Type-1 input FS,

the detected uncertainty (σ^t) is utilised as the standard deviation of the Gaussian FS. Then, *Variation Uncertainty Frame* (blue dashed line V^t in Fig. 5.8) is defined and the variance $(\widehat{\sigma^t})$ for the estimates within this frame is calculated. The gathered variance is used to generate FOU of the constructed T1 input MF resulting in IT2 input (blue MFs in Fig. 5.8). The well known *uncertain standard deviation* technique is performed by simply adding and subtracting the gathered noise variance from the actual $(\sigma^t \pm \widehat{\sigma^t})$ value to calculate the standard deviation of upper and lower MFs of the IT2 input MF.

In order to illustrate the adaptive behaviour, two samples of this extended 7 steps strategy

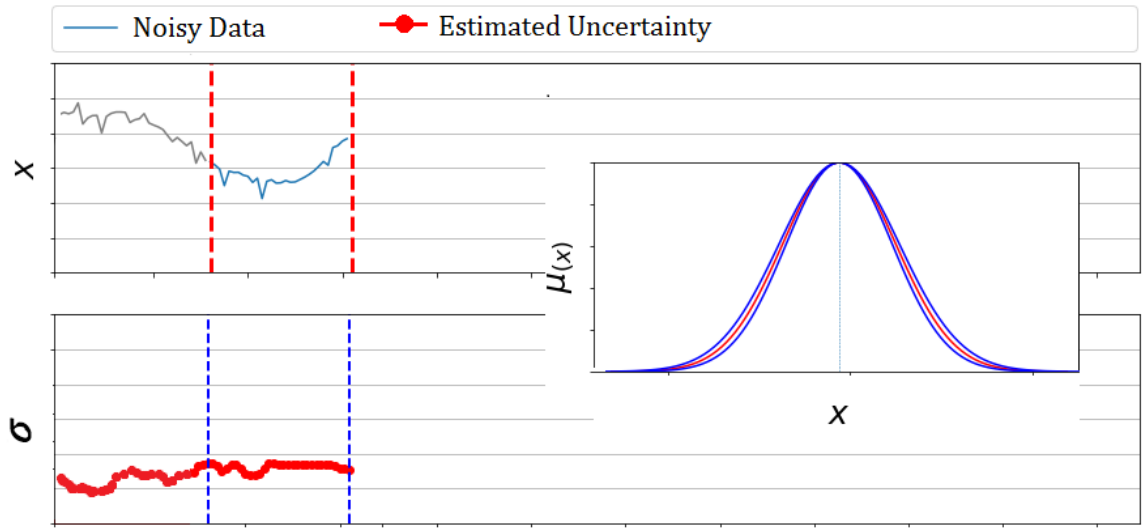

(a) FOU Generation under stable noise

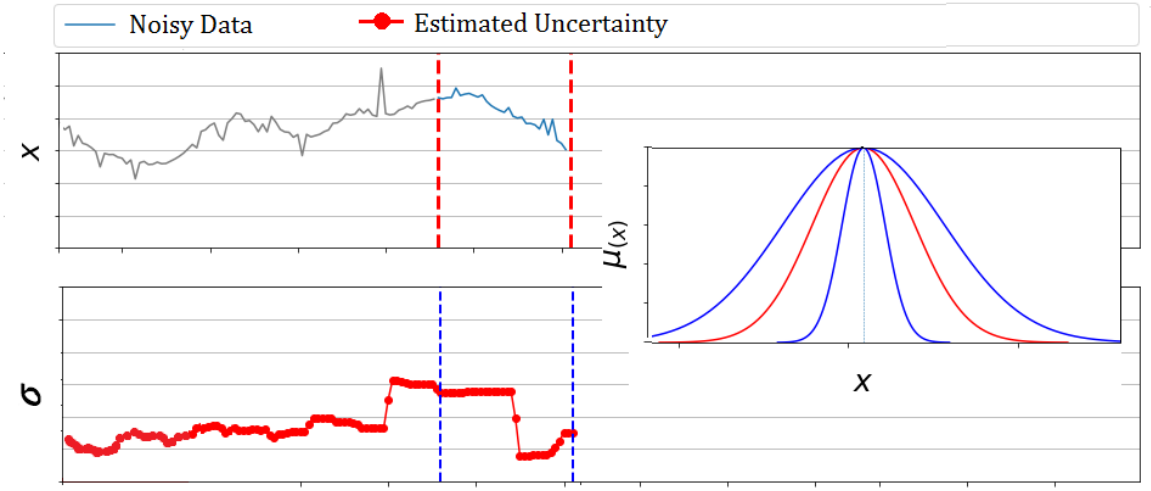

(b) FOU Generation under highly varying noise

Figure 5.10: Illustration of different generated IT2 input MFs.

is shown in Fig. 5.10. Even though the noise level estimated in the last observed values are similar in both examples, the variation of the noise over the frame differs substantially in both cases (note, here, both the frames are of equal size for simplicity). Specifically, in Fig. 5.10a and Fig. 5.10b, the last observed noise levels (σ^t) are similar for both cases. While in Fig. 5.10a these estimations are steady over-time, in Fig. 5.10b, it is not steady and varying over time. The adaptive input FS and FOU generation thus lead to two very different IT2 input MFs, with a smaller FOU generated for the more stable case on the right of Fig. 5.10a and a wider FOU for the more unstable case on the right of Fig. 5.10b. The animated illustration of this adaptive behaviour can be seen on `https://bit.ly/37LV4sG`.

As shown in the time-series instance, the proposed approach is to *'envelop'* (using the FOU) the variation of noise levels affecting a system over time and it is designed to capture the often strong variation of encountered by real-world systems. For example, if the environmental conditions are unstable in a robotics application (e.g. a light sensor is exposed to a flickering light occasionally), the inputs values vary considerably, leading to varying uncertainty levels. The adaptive FOU provides the degrees of freedom to capture this variation. If the circumstances tend to be more stable, then the variation of the uncertainty levels is smaller, resulting automatically in narrower FOUs more akin to type-1 MFs, enabling the system to respond properly to changes in its inputs.

After having detailed implementation of the extended framework on time-series instances, in the following section, time-series datasets will be utilised in order to demonstrate and explore the proposed strategy in forecasting experiments.

5.3 Experiments

The time-series generation is an easily manageable test-bed since the noise injection can be implemented with easily controllable operations. As the aim of the proposed extended framework is to capture both uncertainty and the variation in uncertainty levels, these conditions can be accommodated in time-series dataset conveniently. Therefore, in this section, the pro-

posed extended strategy is tested and the practical impact is shown in time-series forecasting by demonstrating the ability of capturing both uncertainty and the variation in uncertainty levels (addressing objective 3 in Section 1.5). In doing so, the different noise level conditions can be captured in input FSs by means of extra degree freedom which provide a robust prediction in the case of varying noise levels.

As it was practised in Chapters 3 and 4, the same time-series datasets (MG and Lorenz time-series), are chosen to perform forecasting. Two different experiments are carried out and in both experiments, the proposed adaptive strategy is compared to different non-adaptive counterparts. 9 inputs are used to predict 10^{th} value in [179], the frame sizes (*uncertainty frame* [p] and *uncertainty variation frame* [ω]) are set to be 9 to contain 9 variables. In the type-reduction step, the well known EKM algorithm is used, details can be seen found in [181]. In the rule generation, the same procedures from sections 3.4.1 and 3.4.2 are followed by using the first 70% of the noise-free time-series.

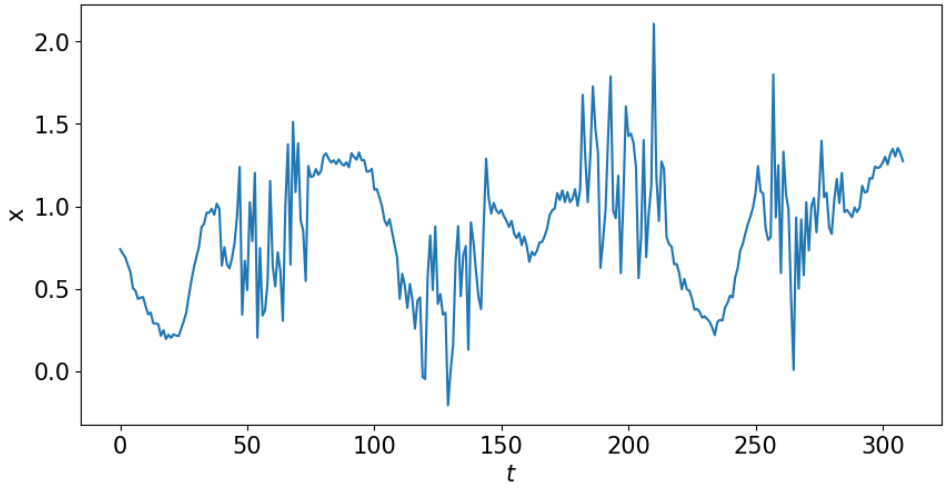

(a) A sample of the generated time-series which contain high and low noise.

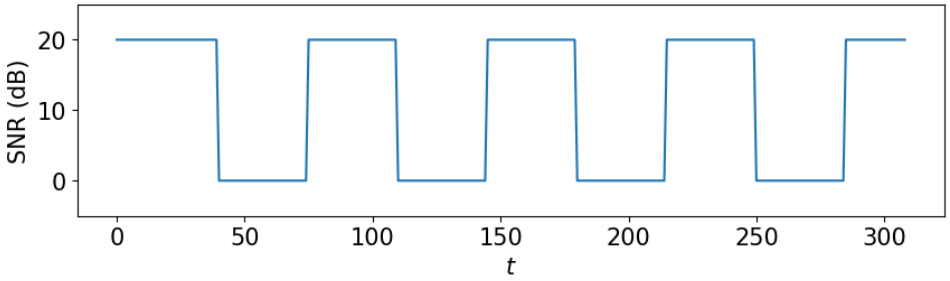

(b) The injected corresponding noise levels

Figure 5.11: Illustration of testing time-series and corresponding noise levels.

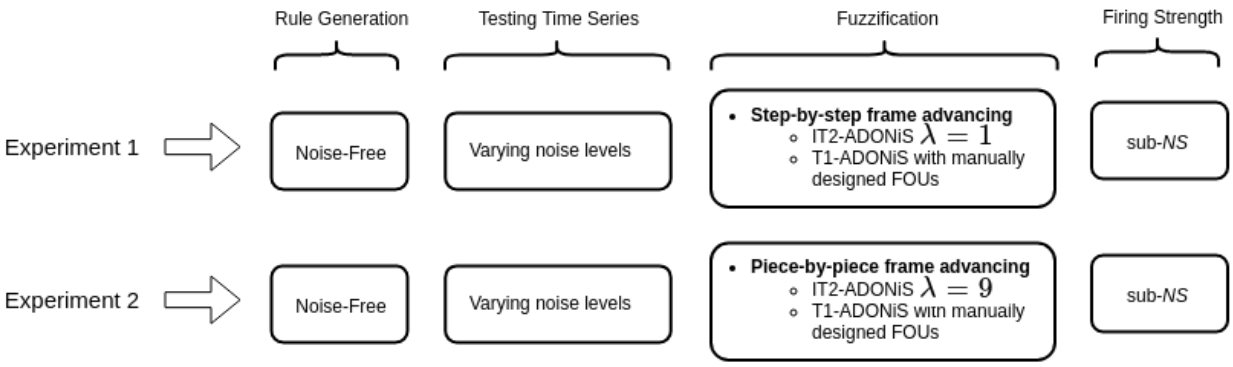

Figure 5.12: Experiment 1 and Experiment 2 scenarios.

In the test time-series generation, in order to provide the varying circumstances, mixed noise levels (*low, high,...,low*) are used in the testing time-series. The low and high noise injections are implemented more frequently over the times series and varying circumstances are created. A sample of this time-series can be seen in Fig. 5.11. While the upper figure shows the produced time-series (Fig. 5.11a), the bottom figure shows the corresponding used noise levels 5.11b in the time-series as 20 and 0 dBs. In doing so, the proposed extended framework can be tested on time-series which contains both low-high uncertainty levels and which vary over-time as well.

5.3.1 Experimental Set-Up

As illustrated in Fig. 5.12, two different experiments are carried out to evaluate the extended ADONiS framework. Both experiments largely followed the similar structure, as was practised in the previous chapters. In both experiments, after evaluating the adaptive approach (IT2-ADONiS), a follow-on set of non-adaptive experiments is conducted where a set of predefined FOU sizes are used, rather than automatically adapting the FOU size. In non-adaptive designs, T1 FSs are generated by following the first 4 steps of the extended framework (see Section 5.2), after that the performance of the NSFLS for 10 fixed FOU sizes, i.e. for values between 0.01 and 0.1 for MG and between 0.5 and 3.5 for Lorenz time-series are evaluated. In doing so, the adaptive IT2-ADONiS forecasting performance is compared with different non-adaptive counterparts.

The differences between the two experiments are the step size of the uncertainty frame (λ).

Algorithm 3: Constructing adaptive IT2 input FSs by means of sliding window noise estimation (4.5) and (5.6) and variation in noise levels.

Input : the input value x_t at the most recent time step
Output: the corresponding IT2 input FS $\widetilde{I}^t$ for the input x_t

Function `variationNoise(`V^t`)`**:**
  $\widehat{\sigma^t} \leftarrow s.d(V^t)$ ▷ Standard deviation of the V^t;
  return $\widehat{\sigma^t}$;
Function `noiseEstimation(`W^t`)`**:**
  $index \leftarrow 1$;
  $y \leftarrow []$ ▷ y is the list for the difference list;
  repeat
    $y[index] \leftarrow \frac{1}{\sqrt{2}} \left(W^t[index+1] - W^t[index]\right)$;
    $index = index + 1$;
  until $index = p - 1$;
  $\sigma^t \leftarrow s.d(y)$ ▷ Standard deviation of the y;
  return σ^t ;
Function `fuzzifyT1Input(`$x_t, \widehat{\sigma}_n$`)`**:**
  $I_t \leftarrow$ Gaussian FS with mean x_t and s.d. σ^t;
  return I_t ;
Function `fuzzifyIT2Input(`$I^t, \widehat{\sigma^t}$`)`**:**
  $\widetilde{I}^t \leftarrow$ The uncertain standard deviation on the Gaussian FS I^t with $\sigma^t \pm \widehat{\sigma^t}$
  return $\widetilde{I}^t$;
$t \leftarrow 0$;
repeat
  $p \leftarrow frameSize$ ▷ Defining the uncertainty frame size;
  $W^t \leftarrow [x_{t-p+1}, x_t]$; ▷ W^t is the current uncertainty frame;;
  $\sigma^t \leftarrow noiseEstimation(W^t)$;
  $I^t \leftarrow fuzzifyT1Input(x_t, \sigma^t)$;
  $\omega \leftarrow frameSize$ ▷ Defining the variation uncertainty frame size;
  $V^t \leftarrow [\sigma^{t-\omega+1}, \sigma^t]$; ▷ V^t is the variation frame;
  $\widehat{\sigma^t} \leftarrow variationNoise(V^t)$;
  $\widetilde{I}^t \leftarrow fuzzifyIT2Input(I^t, \widehat{\sigma^t})$;
  $t \leftarrow t + 1$;
until $x_t = end$;

In the variants of Experiment 1 the *uncertainty frame* is advanced *step-by-step* where the λ and ω step size set to be 1 which practically, result in sliding windows. This sliding operator allows the principal T1 FSs to be sensitive to any changes in the last observed uncertainty levels. Algorithm 3 presents the pseudo-code of the proposed adaptive IT2 input FSs fuzzification in the context of this experiment.

Experiment 2 is designed to evaluate the specific aspect of using adaptive FOU in compare to non-adaptive FOUs. In this experiment, the assumption is made that the principal T1 input FS may not be able to fully capture the last observed uncertainty changes. For instance, in a robotic sensor context, the uncertainty frame size can be set to 5 seconds time-frame. However, uncertainty levels are changed drastically within that 5 second time-frame and the principal T1 input FSs may not fully capture these changes. In order to portrayed this scenarios, in Experiment 2, the principal T1 FSs are constructed in a less sensitive manner and adaptive FOU(s) are built on these T1 FSs. So that the question of "Can adaptive FOU provide optimum performances, in the case of T1 FSs cannot capture the last observed uncertainty levels sensitively?. Hence, the *uncertainty frame* is advanced *piece-by-piece* where the $\lambda = 9$ and $\omega = 1$ step size. In doing so, the principal T1 FSs are to change in every 9 steps, rather than each step.

Having detailed both experiments rationales and general settings in this subsection, we now proceed to experiments and results in the following subsections.

5.3.2 Experiment 1 - Advancing the frame Step-by-Step

As mentioned above, in this experiment, first, the proposed 7 step strategy is utilised to complete prediction of time-series which contains varying noise levels. The defined frames are advanced by using step-by-step ($\lambda = 1$ and $\omega = 1$) approach where it is advanced for each value in the time-series. The association of each window to each IT2 input FSs can be seen in (5.8) and illustrative sample can be seen in Fig. 5.13.

$$\begin{aligned}
(V^{t-8} \sim W^{t-8} \sim x_{t-8}) &\rightsquigarrow \widetilde{I^{t-8}} \\
(V^{t-7} \sim W^{t-7} \sim x_{t-7}) &\rightsquigarrow \widetilde{I^{t-7}} \\
&\dots \\
(V^{t} \sim W^{t} \sim x_{t}) &\rightsquigarrow \widetilde{I}^{t}
\end{aligned} \tag{5.8}$$

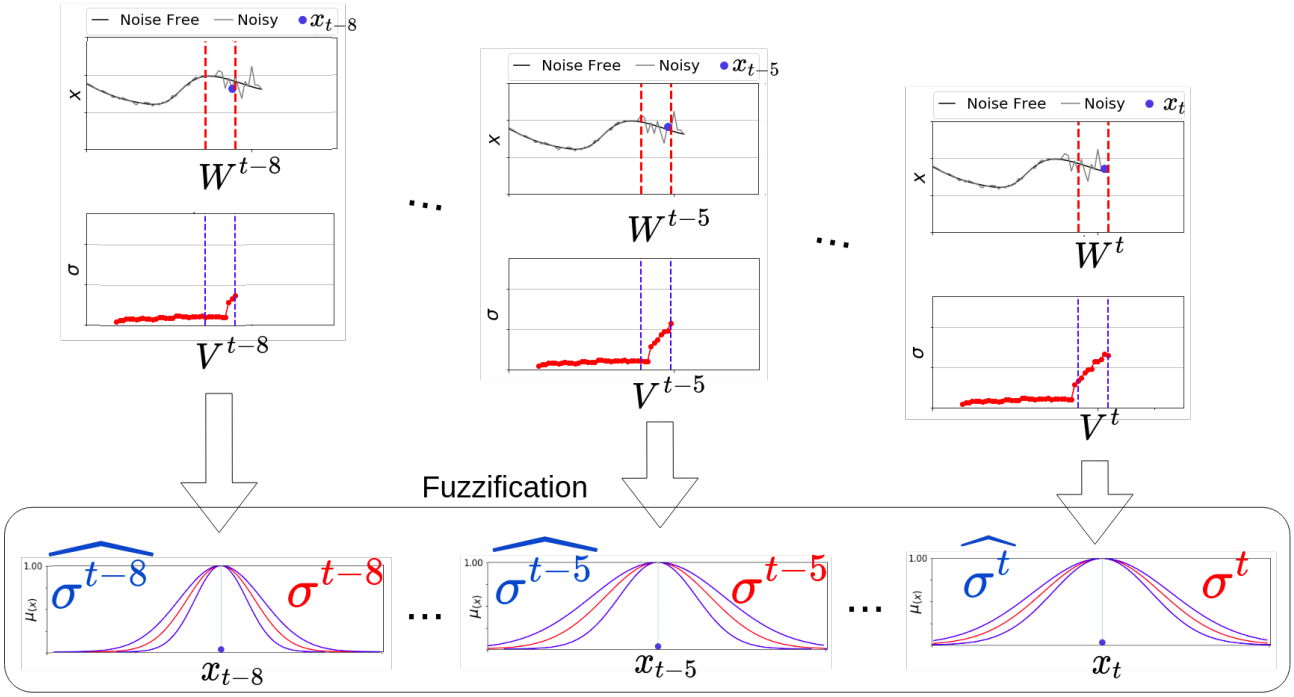

Figure 5.13: Experiment 1 - Each input FSs having different width and FOU values

where W is the *uncertainty frame* (red dashed line in Fig. 5.13),V is the *variation uncertainty frame* (blue dashed line in Fig. 5.13), x refers to corresponding input value, $\widetilde{I}$ is the constructed IT2 input FS, the symbol $\sim$ refers only the association between the defined windows and the corresponding inputs. The $\rightsquigarrow$ notation is to denote 'leads to' the corresponding IT2 input FS.

The animated samples of Experiment 1 can be seen in `https://bit.ly/2KOWv0D`. The experiment is repeated for both MG and Lorenz time-series.

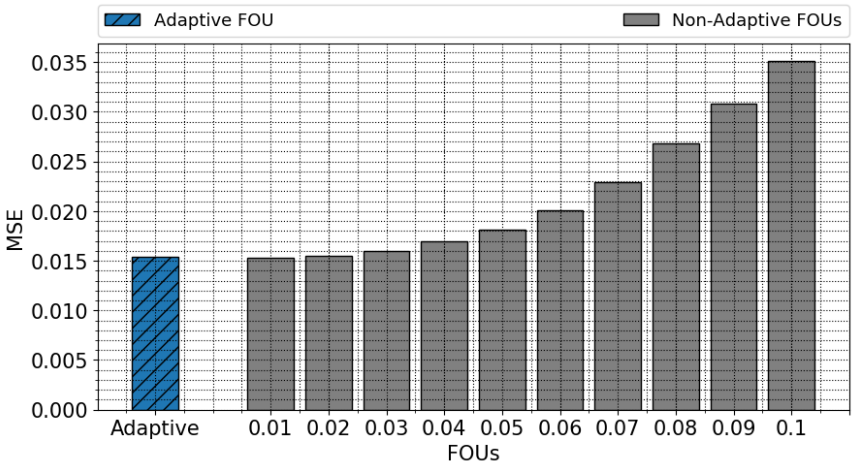

Figure 5.14: Experiment 1 - MG time-series the MSE prediction result comparison of adaptive and non-adaptive FOU generation in the test set which contains varying noise levels

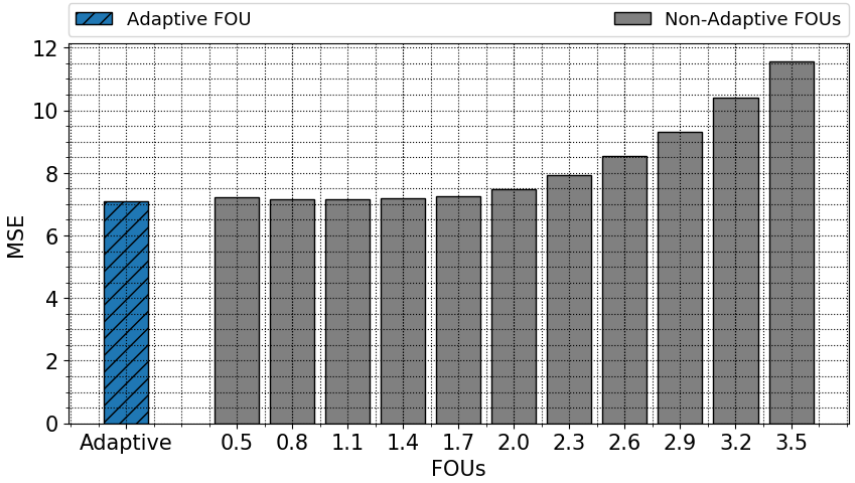

Figure 5.15: Experiment 1 - Lorenz Time-series the MSE prediction result comparison of adaptive and non-adaptive FOU generation in the test set which contains varying noise levels

5.3.2.1 Experiment 1 Results

As shown in Fig. 5.14 for MG and 5.15 for Lorenz time-series, the least FOU values (0.01 for MG and 0.5 for Lorenz) provide the best prediction performance among the other 10 manually set FOU values. In the adaptive approach, similar MSE results are produced, indicating an accurate adaptation of the FOU size. The detailed discussion will be provided in Section 5.3.4.

5.3.3 Experiment 2 - Advancing the frame Piece-by-Piece

In this experiment, the *uncertainty frame* is advanced *piece-by-piece* where after each 9 input value is received, the frame is advanced over that 9 inputs at once ($\lambda = 9$). So that the same estimated uncertainty levels are applied to the 9 input FSs. In other words, each 9 T1 input FS will have the same width. Note that in the previous experiment, each input FS has different width to capture the last observed uncertainty. However, in this experiment, each individual uncertainty capturing become less sensitive for the core T1 FSs. The association to construct IT2 inputs can be seen in (5.9) and the illustrative sample is shown in Fig. 5.16. As it is shown, the window W^t is associated with each input. Animated illustration of this example can also be seen on `https://bit.ly/3nKUSPT`.

$$
\begin{aligned}
(V^{t-8} \sim W^t \sim x_{t-8}) &\rightsquigarrow \widetilde{I^{t-8}} \\
(V^{t-7} \sim W^t \sim x_{t-7}) &\rightsquigarrow \widetilde{I^{t-7}} \\
&\dots \\
(V^{t} \sim W^t \sim x_{t}) &\rightsquigarrow \widetilde{I}^t
\end{aligned}
\tag{5.9}
$$

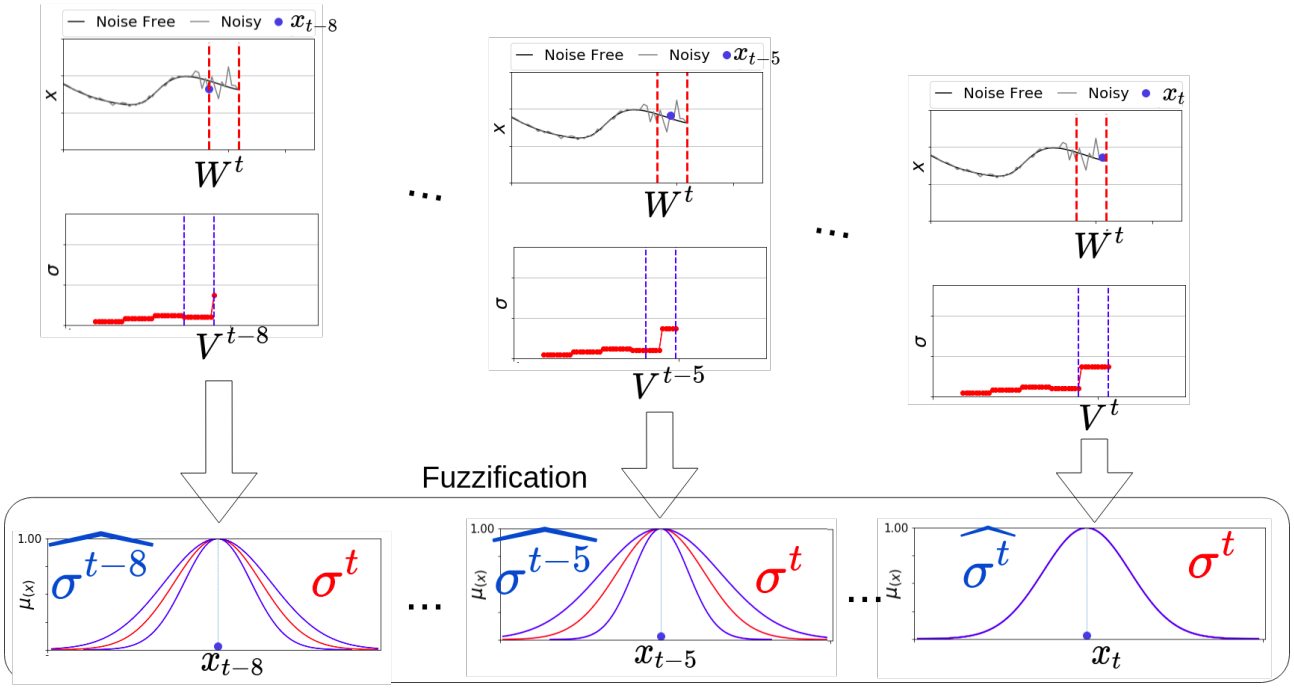

Figure 5.16: Experiment 2- Each principal T1 input FSs having the same width (σ^t) and different FOU values.

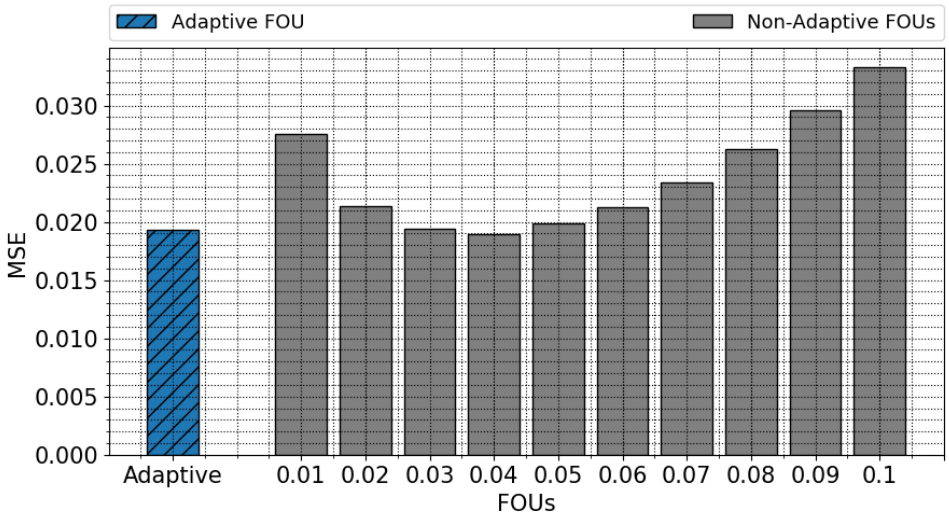

Figure 5.17: Experiment 2 - MG Time-series the MSE prediction result comparison of adaptive and non-adaptive FOU generation in the test set which contains varying noise levels

where W is the *uncertainty frame* (red dashed line in Fig. 5.16), V is the *uncertainty variation frame* (blue dashed line in Fig. 5.16), x refers to corresponding input value, $\widetilde{I}$ is the constructed IT2 input FS, the symbol $\sim$ refers only the association between the defined windows and the corresponding inputs. The $\rightsquigarrow$ notation is to denote 'leads to' the corresponding input FS.

Note that, in (5.9) and Fig. 5.16, the W frame association differs from Experiment 1 (Fig. 5.13). As it is advanced by *piece-by-piece*, each input FSs have the same width (σ^t) which is the estimated uncertainty level in the uncertainty frame (W^t red dash lines). Additionally, each input FS have different FOU values which is the variation in the *variation uncertainty frame* (blue dash lines).

5.3.3.1 Experiment 2 Results

As can be seen in Fig. 5.17 for MG and Fig. 5.18 for Lorenz time-series, the best performance is provided by the FOU value 0.04 of MG and 1.7-2.3 of Lorenz time-series among the 10 different manually performed FOU value. When the proposed adaptive approach is implemented, it provides similar performance with the best manually adjusted approach. The detailed discussion will be provided in the next subsection.

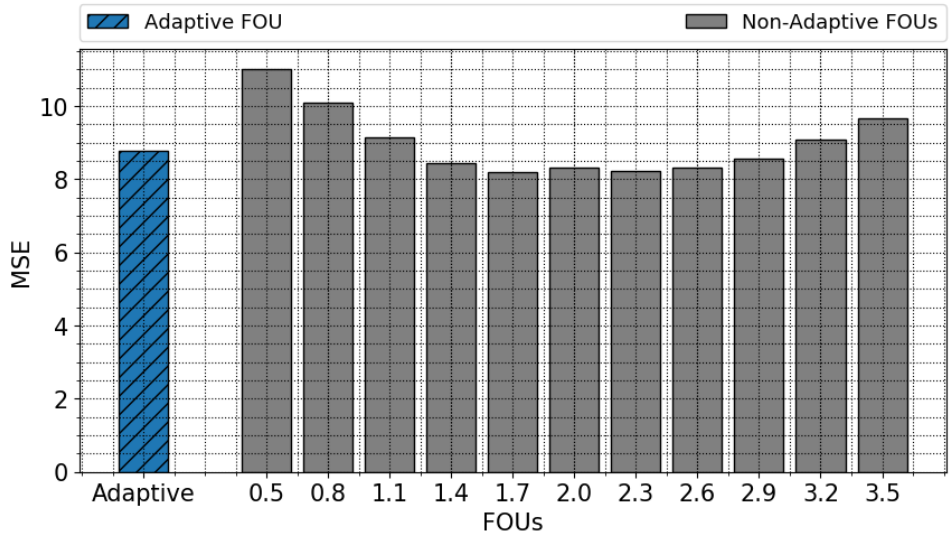

Figure 5.18: Experiment 2 - Lorenz Time-series the MSE prediction result comparison of adaptive and non-adaptive FOU generation in the test set which contains varying noise levels

5.3.4 Discussion

In Experiment 1, the *uncertainty frame* is advanced step-by-step ($\lambda = 1$) which allows each T1 input FS(s) to have different widths corresponding to the last observed estimated uncertainty levels. Thus, this step-by-step technique provides sensitivity to the last observed uncertainty level changes in T1 input FSs. In the adaptive IT2-ADONiS variants of Experiment 1, the T1 principal FSs are extended with an adaptive FOU to generate IT2 input FSs. The size of the FOU is driven by variation in uncertainty levels as measured over an *Uncertainty Variation Frame* and the FOU is applied to T1 input FSs which provides an adaptive behaviour. In the non-adaptive variants of Experiment 1 (T1-ADONiS manually designed FOUs), 10 different sequential FOU values are employed manually to T1 input FSs to investigate the 'optimum' FOU value in prediction performances.

As shown in Figs. 5.14 and 5.15, the manually adjusted FOU value 0.01 and 0.5 provides the optimum performance which is also similar to the performance of the proposed extended ADONiS strategy. It is crucial to note that when we use the extended ADONiS framework, we do not need to know any a priori information about the noise levels, their variation or any specific FOU sizes. So that without 'brute-forcing' different FOU values, the optimum performance can be gained by simply using the extended ADONiS framework.

Having the *uncertainty frame* advancing *step-by-step* can provide the ability to capture the uncertainty of individual inputs which may induce sensitive T1 input FSs in uncertainty changes. As shown in the previous sections (Fig. 5.13), each principal T1 input FSs have different widths to capture each estimated uncertainty, enabling uncertainty modelling in a 'sensitive' manner. As shown in Experiment 1's results, in both cases, the least FOU value -as well as the adaptive approach- provides the best performance among all other variants. As the principal T1 input FSs are sensitive to the uncertainty changes, this led us to consider that IT2's extra degree of freedom may not be crucially necessary at this level of sensitivity. Therefore, in the second experiment, to specifically investigate FOU values-performance association, we opted to reduce the T1 input FS sensitivity by advancing the frame *piece-by-piece* rather than on each input.

In Experiment 2, to evaluate the specific FOU adaptiveness aspect of each IT2 input FSs, the principal T1 input FSs are generated in a less sensitive manner and optimum performance is investigated with the extended framework and non-adaptive counterparts. In this experiment, the *uncertainty frame* is advanced *piece-by-piece* where the step size is set to 9 ($\lambda = 9$). This leads each T1 input FSs in the *uncertainty frame* to have the same width (See Fig. 5.16) which cause relatively less sensitivity in each uncertainty level change. In both variants of Experiment 2 (adaptive extended IT2-ADONiS and non-adaptive counterparts), T1 input FSs are generated by following this technique.

As shown in Figs. 5.17 and 5.18, the optimum performances are provided by the FOU value 0.04 for MG and 2.3 for Lorenz time-series and the proposed adaptive framework also produces similar performances. As was the case in Experiment 1, the ADONiS framework does not require any extra manual adjustments in FOU to reach the optimum performance.

In both experiments, the proposed adaptive approach results are compared to counterpart Type-2 systems. In these comparison different sequential FOU width values are applied on these Type-2 systems in a *brute-force* to find the *optimum* performance value. As results show that the optimum valued Type-2 system and the proposed adaptive systems can achieve the relatively similar performance. Even though both performance are similar the proposed approach does not require the sequential trials but adapt itself based on conditions automatically on-the-fly. On the other hand the counterpart Type-2 system required many trials to find the optimum width which would provide the optimum performance. However, in a real-world context, it may not be possible to run all different FOU sizes sequentially/manually. Furthermore, it is worthwhile noting that, these optimum FOU values are valid for the specifically used testing time-series. In other testing-sets, the optimum FOU parameters would change depending on noise levels as well. Since the extended adaptive approach does not require any manual parameters settings, it can be said that the proposed approach for its automatic adaption would be strongly useful in a real-world setting where uncertainty varies over-time.

5.4 Summary

The real-world encompasses different uncertainty sources and these sources may vary vastly which cause either major or minor impact on a system's inputs at different times. Even though in Chapter 4, the ADONiS framework provides promising results in capturing uncertainty in the last observed value(s), it is the variations in the uncertainty levels, in particular, which makes estimating and handling uncertainty a complex and challenging task.

Considering the potential advantages of NSFLSs and Type-2 designs in respect to input FSs, in this chapter, we, therefore, extended the ADONiS framework and put forward a strategy to design IT2 input FSs of NSFLSs at run-time. Specifically, while Chapter 4 has shown how individual levels of last observed uncertainty can be captured by T1 input FSs, this chapter explore whether the additional degrees of freedom of IT2 FSs can be used to capture a variety of (varying) levels of input uncertainty as are commonly encountered in real-world applications, –as presented in our study [123].

In the extended framework, principal T1 input FSs are generated by detecting uncertainty within an *Uncertainty Frame*. Further, the variations in uncertainty levels are measured over an *Uncertainty Variation Frame* and it is used to generate FOU on the T1 FSs resulting in the comprehensively adaptive IT2 input FSs. Even though the T1 FSs capture the last observed uncertainty level properly, because of the variation in uncertainty levels, the last observed uncertainty capturing may not fully reflect the environmental conditions overall. The extended framework's main aim is to capture the variation in uncertainty levels (using the FOU) and enable systems to respond properly to changes in its inputs.

The proposed extended framework is evaluated in MG and Lorenz time-series prediction experiments. In the testing time-series dataset, 'low' (20 dB) and 'high' (0 dB) noise levels are used and they are injected to the dataset in a 'low','high',...,'low','high' manner to design an environment where the noise levels vary over-time. Two different experiments are conducted by comparing performances between the adaptive extended IT2 ADONiS framework and non-adaptive counterparts. In both experiments, it has been shown that the extended IT2 ADONiS

framework provides the optimum performance compared to non-adaptive trials. It is worthwhile noting that in these experiments, the proposed extended IT2 ADONiS framework does not require an extensive *brute-force* FOU parameters trials to achieve the optimum performance, whereas non-adaptive IT2 counterparts requires to employ some trials to find the optimum FOU and performance conclusively.

Overall, the proposed strategy ensures that IT2 input FSs are designed dynamically on-the-fly, removing the requirement of a priori knowledge of uncertainty levels and training procedures in parameter definitions. Also, as shown in Experiment 1 and Experiment 2's results, by modelling the variation of the uncertainty levels, the conditions affecting a system's inputs are captured appropriately in input FSs (addressing objective 3 of this thesis). For instance, in a robotics application, if environmental conditions are unstable and the uncertainty levels vary considerably, the adaptive FOU provides the degrees of freedom to capture this variation. If the circumstances tend to be more stable, then the variation of the uncertainty levels is smaller, resulting automatically in narrower FOUs more akin to T1 input FSs, enabling the system to respond accordingly to changes in its inputs.

The limitations of the conducted experiments can be listed as follows: (i) Only a small set of experiments are carried out on commonly used two chaotic time series. (ii) A single noise estimation algorithm is conducted. Based on the used dataset type (e.g. sensor signals or stock market data), an appropriate noise estimation algorithm should be selected accordingly. (iii) The method to determine width of FOUs which is depending on the selection of *variation uncertainty frame* parameter (ω). In order to define the FOU(s) properly, the size of *variation uncertainty frame* should be determined adequately to reflect the variation of environments. (iv) The computational burden. As the *variation uncertainty frame* is used to calculate variation in uncertainty levels, it may cause an extra computational burden which, therefore, frame sizes should be chosen optimally. Overall, we note that there are an enormous number of different settings that can be implemented (e.g. different noise designs, different parameters in frames or predictions). Hence, it should be noted that these results can only represent an initial step towards a general conclusion and a real-world application. Considering these limitations, in the future, different settings will be explored with different settings and datasets.

So far in this thesis, input uncertainty handling (Chapter 3) in the inference engine steps, input uncertainty capturing (Chapter 4) in the fuzzification steps and extended varying input uncertainty capturing (in this chapter) are investigated and evaluated. In general, case studies have shown that the performance improvements of FLSs are promising. Besides the uncertainty handling capacity of FLSs, interpretability is the other main key aspect of using FLSs; having an insight into decision processes that humans can comprehend can facilitate overall operations of models in various aspects. Therefore, in Chapter 6, we will explore the interpretability mechanism of NSFLSs and we will investigate whether the given interpretability can be 'protected' while the performance is increased by using the proposed approach/frameworks in this thesis.

Chapter 6

Maintaining Levels of Interpretability

A key aspect of the vision of interpretable AI is to have decision-making models which can be understood and evaluated by humans. Hence, while a decision-making model delivers a good performance, providing an insight into the decision process is also an important asset in terms of having trust or allowing a 'debug' process in decisions. Even though the interpretability of AI is widely acknowledged to be a critical issue, it still remains a challenging task. FLSs are considered to possess mechanisms which can provide a degree of interpretability. FLSs building process can be done by experts or by using data-driven approaches and a level of interpretability can be provided in the initial design -by benefiting expert insights or by following interpretability taxonomies (e.g. rule parsimony in rule base or completeness, distinguishability, complementarity in MFs partitioning etc.). Yet, when accuracy-oriented adaptive learning processes are used on the designed FLSs, initially given interpretation of the FLSs cannot always be guaranteed due to the altering key parameters and conflicting objectives of accuracy and interpretation [21, 23, 62, 64, 100, 111]. In this chapter, as presented in our study [119], the focus is expanded to encompass interpretability, considering specifically whether the mechanisms developed in Chapters 3-5 can be usefully applied in the sense of minimising the changes that affect the key interpretability components. Hence, while the proposed methods allow NSFLSs to achieve better performance by coping with input uncertainty in the fuzzification and inference engine steps, the initially given level of interpretability degree can be maintained without altering the structure or key parameters of given FLSs.

Section 6.1 discusses the background and motivation for maintaining interpretability of FLSs. Section 6.2 explores the capability of maintaining interpretability in the ADONiS. Section 6.3 presents steps of the conducted case study and a discussion of the findings is given in Section 6.4. Lastly, in Section 6.5 a summary of this chapter is presented.

6.1 Background and Motivation

FSs are generally designed with respect to linguistic labels and are interconnected by linguistic rules [191]. Therefore, FLSs are frequently referred to as 'interpretable' systems. Early research in FLSs focused on building rules with expert knowledge reflecting experts insights inherently which provide a degree of interpretability in systems. Later, when expert knowledge is not available, data-driven approaches are started utilising to design FLSs. In order to provide a degree of interpretability in those data-driven designed systems some taxonomies are proposed. For instance *low-level interpretability* and *high-level interpretability* in regards to overall interpretability degree assessment of FLSs [54, 194]. Low-level interpretability is mostly related to the semantics associated with the used MFs in a given model. This low-level interpretability can be achieved by imposing constraints on the MFs or approaches considering measures such as distinguishability, coverage, etc. The high-level interpretability is more related to the number of rules, variables, labels per rule etc.

Even though the level of interpretability degree can be provided by experts and/or data-driven techniques, the varying real-world circumstances -which contain different levels of uncertainty- require approaches that bring challenges regarding the interpretability levels of models.

To deal with varying circumstances of real-world settings, different approaches have been developed over the years. Such approaches are mostly inherited from numerical learning techniques, such as ANFIS [70] or TSK models [162]. Traditionally, models use parametric equations and/or statistical optimisation techniques to tune parameters based on data-driven approaches. As depicted in Fig. 6.1, while these optimisation procedures provide performance benefits, they often cause alteration in fuzzy rule sets, rule parameters, MFs or fuzzy partition-

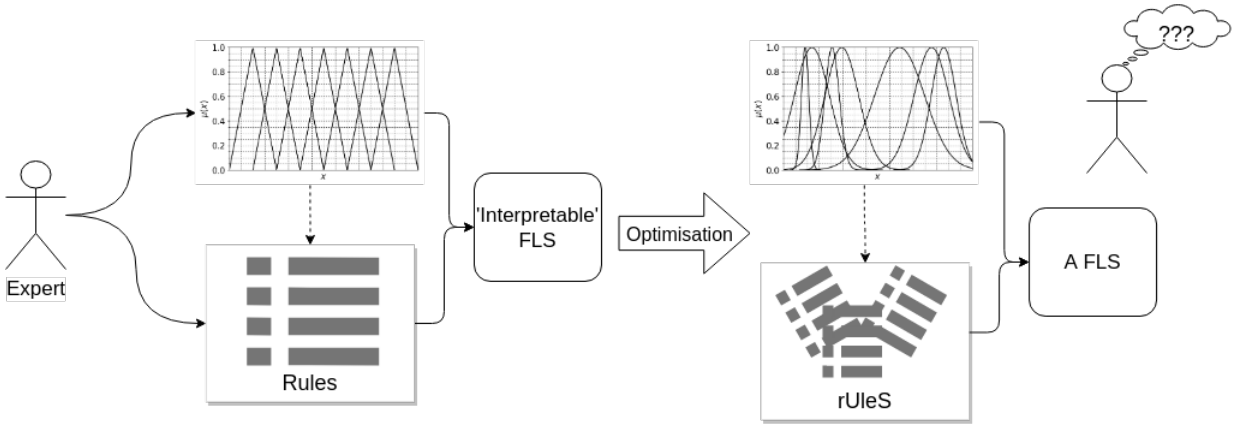

Figure 6.1: An illustration of building an interpretable FLS and applying optimisation procedures which may affect MFs and/or rules resulting in high accuracy but poorer interpretability.

ing structures with high accuracy but commonly do not consider whether the resulting model is interpretable or not [4, 22, 153]. This poses an interesting question for the tuning of FLSs: can we improve the performance of FLS without negatively affecting the given FLSs' interpretability? In other words, can we have both: interpretability and good performance?

In recent years an increasing number of studies have started to focus on fundamental questions such as what *interpretability* is, in general, and in particular in respect to FLSs? How many rules or how many variables per rule are interpretable? Or to which degree are properties of the partitioning of the variables key for interpretable FLSs? [4, 71, 57, 82, 137]. In the literature, various taxonomies have been suggested to explore interpretability degree of FLSs [4, 54, 93] and nowadays, FLSs research focuses on combining the high performance and interpretability of models [22, 56, 60, 194].

So far in this thesis, in Chapter 3, an alternative inference engine method is proposed; in Chapter 4, the ADONiS framework is proposed; and in Chapter 5, the ADONiS framework is extended with the aim of leveraging performance of FLSs. Overall, input uncertainty is captured/adapted in the fuzzification stage and handled in the inference engine step at run-time that delivers good performance in the face of varying input uncertainty conditions. Therefore, as shown in the previous Chapters, these proposed frameworks can provide performance benefits in comparison to the counterparts models. Additionally, while providing performance benefits, the proposed methods confine the tuning procedures into the fuzzification stage, leaving other components (e.g. the rules, defined MFs etc.) of the system 'untouched', thus providing a

fundamental requirement for maintaining the given interpretability. As the capacity for interpretability is one of the main assets of FLSs and is often one of the key motivations to use FLSs in decision-support [137], in this chapter, the ADONiS framework usage is explored in the context of whether it can usefully be applied to maintain the interpretability level of systems. Later, ADONiS usage in comparison to a commonly used tuned counterpart (ANFIS) model is compared and contrasted in response to varying noise levels in a time-series prediction context.

In the next section, ADONiS implementation is evaluated in the context of overall maintaining interpretability in FLSs.

6.2 Maintaining the Given Level of Interpretability with ADONiS

Model interpretability can be characterised such that a human can comprehend and validate why/how results are produced in a given system. As mentioned in Chapter 2, interpretability is a complex field where multiple components take part in multiple views. A growing body of literature has been examined to assess interpretability of FLSs [4, 54, 93, 194] and different taxonomies proposed to cover multiple aspects to consider interpretability of FLSs, such that the FS-based interpretability (e.g. labels, distinguishability, a moderate number of FSs etc) or the rule-based interpretability (readability of a single rule and parsimony of rule-set etc.).

In an FSs-based constructing process, if expert knowledge is available, experts can design MFs, labels and parameters etc. based on their knowledge in their field and the semantics of these FSs can be understood by humans. In doing so, FSs-based interpretability is instinctively provided by experts. If expert knowledge is not available, the FSs can be constructed by following generally acknowledged properties such as distinguishability, complementarity etc. By following general properties, the semantics of FSs can be built and interpretability of the generated FSs can be enabled.

In a rule-base constructing process, experts can define system rules based on the generated

FSs. Since experts use their field knowledge, these rules' interpretability can be provided commonly as experts design them. If expert knowledge is not available, data-driven approaches can be utilised to generate rules and the interpretability of these rules can be achieved by following the generally accepted properties such as rule simplicity, consistency etc.

As an example, consider an FLS is designed by collaborating medical experts and computer scientists to model a decision. The FSs are constructed by medical experts which provides meaningful designs to them. Also, the rules are defined based on medical knowledge. In doing so, the overall interpretability can be provided in the initial design of the FLS. However, the real-world has different conditions which cause varying circumstances on the run-time. Even though the initial FLS design is interpretable by medical experts, varying patient inputs (e.g noise in the heart rate sensor) may not fully correspond to the given FSs or rules (e.g. none of the rules may not be fired in the face of of noisy inputs). Therefore, uncertainty in real-world data may not *match* with the given system. Traditionally, in order to deal with these uncertainties in environments, data-centric optimisation procedures can be employed at different stages of FLSs, e.g. altering FSs parameters, increasing/decreasing rule numbers etc. This usually provides performance benefits, yet since the FSs and/or rules are altered in a data-driven way, medical experts may no longer understand it. Thus, the initial interpretability of FLS may deteriorate.

In the ADONiS design, the performance increase is achieved by enabling to model uncertainty 'where it arises' and handled through the given rules. Particularly, input uncertainty (e.g. noise in the heart rate sensor) is captured adaptively in the fuzzification step and handled in interactions between input and antecedent FSs in the inference engine step. In doing so, while the performance increase is achieved, ADONiS limits any optimisation impact to the fuzzification and the inference engine steps. Therefore, different components of FLSs such as MFs, antecedents, consequent etc. remain 'untouched'. An illustrative figure can be seen in Fig. 6.2. Thus, while dealing with different input uncertainty levels on run-time, the initially given interpretability is protected and the FSs or rules remain meaningful to experts.

Furthermore, since the ADONiS is designed to provide adaptive behaviours by capturing and handling different circumstances on the run-time, the rule-base can be constructed based

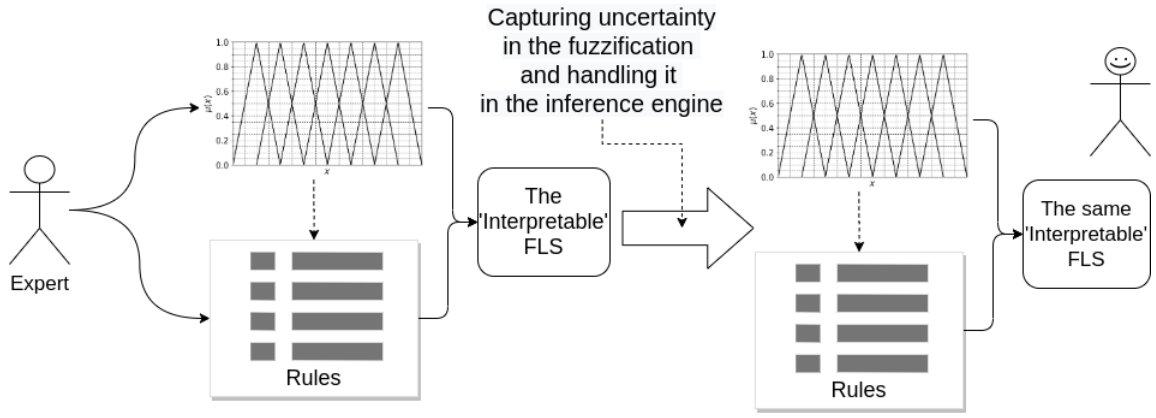

Figure 6.2: An illustration of building the ADONiS FLS where input uncertainty is captured in the fuzzification and handled in the inference engine steps at run-time. While having an increase performance, the other key parameters are 'untouched' which leads to maintaining the initially given interpretability degree.

on noise-free circumstances and ADONiS can integrate input with the given rules. This characteristic allows having a simpler rule-set which can also contribute to the interpretability of models.

To recapitulate, since input data is affected by uncertainty sources in the real-world, traditionally, models use offline optimisation procedures to cope with these changing environments. Such optimisation procedures traditionally use a training dataset and lead to changes of the same key parameters which are vital for interpretability, thus delivering improved performance at the cost of poorer interpretability. However, the ADONiS framework adapts itself to the changing uncertainty levels by tuning input FS parameters in the fuzzification step on run-time and deliver performances. While the performance is increased, it also preserves the valuable interpretable structure, namely the rules, antecedents and consequents, addressing objective 4.

In the next section, we will investigate ADONiS employment in respect to accuracy-interpretability by comparing another commonly used model.

6.3 Experiment in Comparing ADONiS to Optimisation Based Methods

This section compares and contrasts the ADONiS adaptation framework and commonly used the ANFIS model in response to varying noise levels in a time-series prediction experiment. This case study's main aim is not to find which approach delivers the best time-series prediction but rather to assess to which extent ADONiS can actually deliver both good performance and interpretability in the face of varying levels of noise - through comparison to optimisation based techniques. Specifically, in the course of experiment implementation under different noise levels, the key parameters of interpretability (FSs, antecedents and consequents etc) status are examined with a question that 'to which degree the original parameters are preserved?' for both ADONiS and ANFIS models.

As mentioned in previous chapters, as the time-series provide a convenient test-bed in terms of generating dataset and adding noise in a controllable manner, we have chosen the time-series prediction case study in this chapter as well.

6.3.1 Time Series Generation

MG time-series is generated and 1009 noise-free values are obtained for t from 100 to 1108. One of the common models for noise is additive white Gaussian noise [81]. Three different signal-to-noise ratios (20 dB, 5 dB and 0 dB) are used to generate noisy time-series with additive Gaussian white noise. These four (noise-free and noisy) datasets are split into 70% (rule generation/training) and 30% (testing) samples to be used in different variants of the experiments. In the MG generation, τ value is set to be 17 to exhibit chaotic behaviour. Details of time-series generation and noise adding procedures can be found in Sections 2.7 and 2.7.3.

6.3.2 Rule Generation

Regarding the rule generation in the experiments, while different approaches have been introduced [31, 80], in this particular case study, we follow the well established Wang-Mendel [179] rule generation technique. We acknowledge that other approaches may be equally or more viable, for example, in the given domain of time-series prediction, nevertheless, for this study, our key objective was to generate one basic rule base which is maintained identical across all FLSs, thus providing a basis for systematic comparison. Further, we note that the specific antecedent and consequent FSs used here are selected to evenly partition the domain of the variables, and thus are not meaningful in a traditional linguistic sense, yet followed the low-level interpretability properties [194].

The MFs generation in this case study is implemented by following similar FLS architecture in [179]:

First, the domain of the training set $[x_{min}, x_{max}]$ is defined. In order to capture all inputs (including the ones, which can be outside of the input domain, in testing), the defined domain is expanded by 10% and the *cut-off* procedure is implemented for the inputs which are outside of this domain in testing.

Then the input domain is evenly split into seven regions, and bell-shaped antecedents are generated. As shown in Fig. 6.3, these constructed MFs are linguistically labelled as *Further Left (FL), Medium Left (ML), Close Left (CL), Medium (M), Close Right (CR), Medium Right (MR), Further Right (FR)*. Here, by designing the FSs in this form, the following low-level

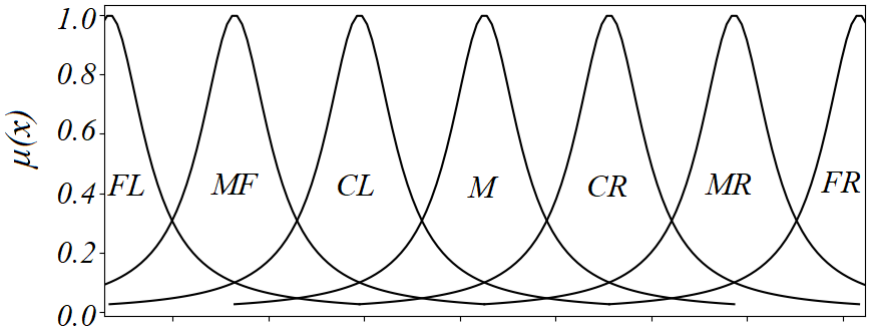

Figure 6.3: An illustration of the seven antecedent MFs used.

interpretability properties are provided.

- ***Distinguishability:*** In order to conceive a clear semantics meaning, FSs are clearly defined in a distinctive range in the universe of discourse, as shown in Fig. 6.3. In a case of FSs were overlaps; as a result, it might be difficult to assign distinct linguistic labels and semantic meaning to these FSs. Note that when the MFs are defined by experts, overall semantic meaning can be interpretable by that particular expert. Yet, in our data-driven approach, the distinguishability feature of these FSs becomes more influential in the overall interpretability of the FLSs.

- ***Moderate number of MFs:*** Considering human cognitive psychology, the number of defined FSs are defined to not exceed the short-term memory capacity, which is 7 ± 2 [101]. So that a human can efficiently conceive the overall process of the FSs and related components. Thus, 7 MFs are defined as shown in Fig. 6.3.

- ***Coverage or completeness of fuzzy partitioning:*** Every data point should belong to at least one MF in the entire universe of discourse which means the membership degree of the data point should not be zero. This can be possible with a design of MFs which covers all the universe. Thus, min and max values are selected as the centre of *Further Left* and the *Further Right* MFs, as shown in Fig. 6.3. As mentioned before, the data-driven optimisation approaches may confine this coverage, as it heavily depends on the given training dataset and the testing domain may not match under varying circumstances of real-world settings.

- ***Normalisation:*** In general, having at least one data point with a membership degree equal to one can represent a clear semantic meaning for the particular MF, that should be normal MF. Thus, we have designed MFs to be normal FSs.

- ***Complementarity:*** *Strong fuzzy partitioning* are widely assumed to have high semantic interpretability in the sense of keeping clear and transparent structures. For this reasons, the defined MFs are evenly distributed and also ensured that the sum of all its membership values are 1 or close to 1.

We consider the preservation of the original shape of the FSs (post-tuning) as important (as it is that shape which will be meaningful in applications of FLSs such as in medical decision support, common control applications, etc.).

For the rule generation and the prediction, as in [179], nine past values are used as inputs and the following (10^{th}) value is predicted, i.e. the output. After forming the input-output pairs as $((\mathbf{x}^1 : y^1), (\mathbf{x}^2 : y^2), ..., (\mathbf{x}^N : y^N),)$ each input value within the pair is assigned to the corresponding antecedent FS $(FL, .., M, .., FR)$. As practised in the Wang-Mendel *one-pass* method, the same seven FSs are used for the consequent FSs, and the outputs $(\mathbf{y}^i)$ are assigned to the corresponding FSs $(FL, .., M, .., FR)$ as well. A sample of the generated rules can be seen in (6.1). For details of rule generation, please refer [179].

$$R^1 = \textbf{IF}\, x_1\, is\, MR\, \textbf{AND} ...\ x_9\, is\, M\ \textbf{THEN}\, y_1\, is\, CR \tag{6.1}$$

In the rule generation, the data-driven interpretability is provided by following some of the *high-level* interpretability properties [194] below.

- ***Rule base parsimony and simplicity:*** According to the principle of Occam's razor (the best model is the simplest one fitting the system behaviours well). By following the procedure from the key study [179], rule reduction procedure is applied to obtain the rule-set.
- ***Readability of single rule:*** As mentioned, the number for the human cognitive skills should be 7 ± 2. To achieve the understanding, the premises in the rules are followed the same principle.
- ***Completeness:*** By covering the whole domain and also by using non-singleton input FSs, at least one rule are fired in the system.

The used data-driven system design approach [179] follows the aforementioned *low* and *high* level properties. This allows the FLS to have a level of interpretability; even though the system

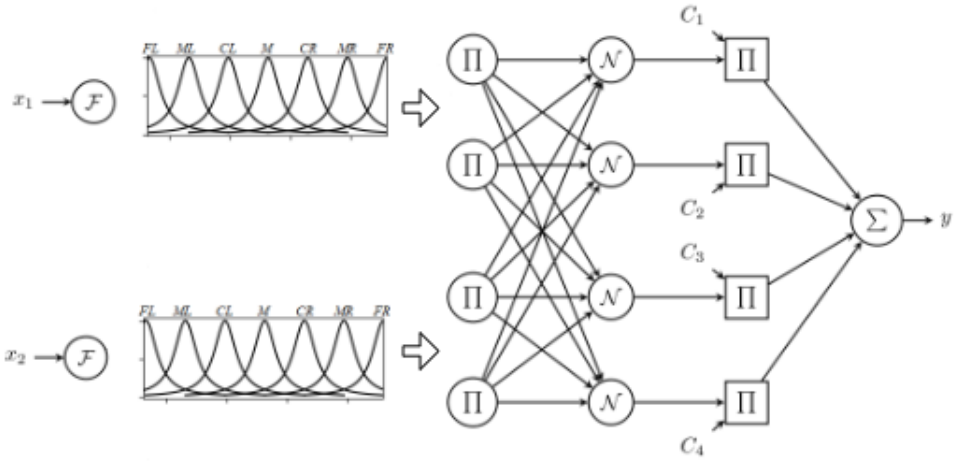

Figure 6.4: An initial ANFIS structure with MFs.

is designed by using the data-driven approach. We consider the preservation of the original shape of the MFs (post-tuning) leading the preservation of rule-set.

6.3.3 Parameters Tuning

6.3.3.1 ADONiS

When implementing ADONiS, the varying circumstances are captured in the fuzzification step (with sliding window $\lambda = 1$) and handled in the inference step. By doing so, no offline optimisation procedure is used on the key parameters of FLS to deal with noise in the dataset. Thus, previously established MFs $(FL, .., M, ..FR)$ and previously generated model rules remain 'untouched' which provides ADONiS the ability to maintain the given interpretability. Here, it is worthwhile noting that the given interpretability level might be 'high' or 'low'. Regardless of the interpretability level, ADONiS is to preserve the model component to maintain the given interpretability degree and details will be discussed in Section 6.4.4.

6.3.3.2 ANFIS Optimisation

As one common model, ANFIS is widely used in many applications to improve the performance of FLSs [7, 8, 43, 73]. ANFIS uses optimisation on model parameters which aims to 'fine-tune'

to obtain more accurate approximation than a initially defined system. The optimisation is conducted by using a given training dataset with the objective to deliver good performance, i.e. minimum error. In doing so, if the training dataset covers noisy conditions, the parameters are altered accordingly and the model is 'prepared' for the upcoming noisy environment in testing settings.

In the ANFIS implementation of this experiments, each of the seven antecedent MFs are assigned an input neuron (See Fig. 6.4) [26]. The gradient descent optimisation technique is then implemented to update the antecedent MF parameters and the consequent linear functions. In the meantime, the least-squares estimation method [161] is used to update the parameters of consequent linear functions in each training epoch. During each epoch, the antecedent FS parameters are updated for each input. Therefore, as a sample in Fig. 6.5 illustrates, while beginning with only seven antecedents, after optimisation, different antecedent FSs are generated. This alteration are implemented for each set of 7 FSs corresponding to each 9 inputs. Thus, theoretically 9x7=63 different or similar FSs are obtained for each inputs –with the associated increase in model complexity which will be discussed in Section 6.4.4.

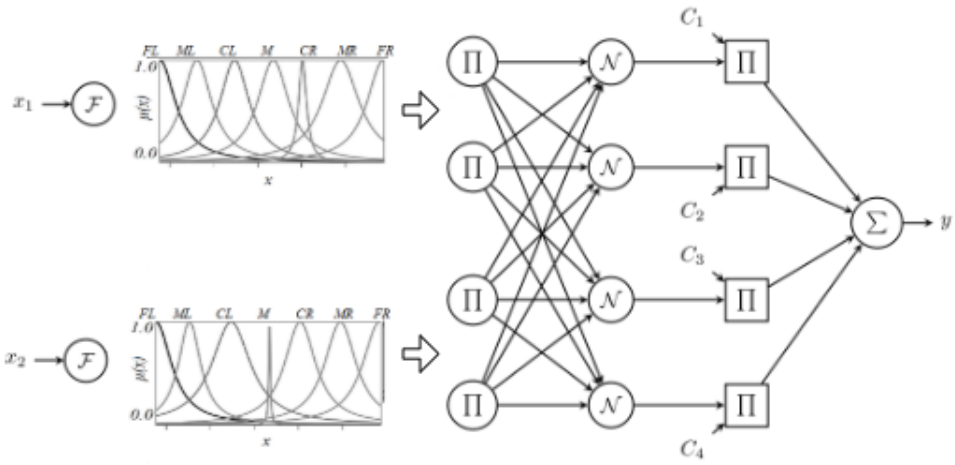

Figure 6.5: After optimisation, the ANFIS structure with the altered MFs.

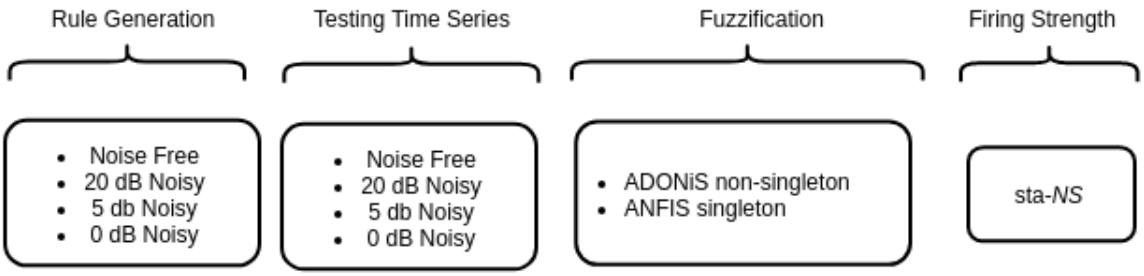

Figure 6.6: Experiment scenarios.

6.3.4 Performance Evaluation

In order to assess the noise handling capability of each model, we calculate the difference between model predictions and noise-free data values at each time-point. Both ADONiS and ANFIS performances are measured by using the common root-mean-squared-error (RMSE) and in addition, the recently proposed Unscaled Mean Bounded Relative Absolute Error (UMBRAE) [27]. UMBRAE combines the best features of various alternative measures without suffering their common issues, e.g. being infinite or undefined under certain circumstances, high sensitivity to outliers.

To use UMBRAE, a benchmark method needs to be selected. In this case study, the benchmark method simply uses the average of input values as predictions. With UMBRAE, the performance of a proposed method can be easily interpreted: when $UMBRAE$ is equal to 1, the proposed method performs approximately the same as the benchmark method; when $UMBRAE < 1$, the proposed method performs better than the benchmark method; when $UMBRAE > 1$, the proposed method performs worse than the benchmark method.

6.4 Results and Discussion

In total, 4 x 4 = 16 different experimental scenarios are implemented, using different noise levels in both rule generation/optimisation and testing phases. Specifically, four different training sets (noise-free, 20, 5 and 0 dB) and four different testing sets (noise-free, 20, 5 and 0 dB) are used–to represent a variety of potential real-world noise levels. Experiment setup can be seen

in Fig. 6.6.

In each variant of experiments, while both model's performance is compared, the exploration also focuses to 'how does the interpretability is affected?' e.g. the meaningfulness of antecedent MFs during the prediction.

In the ADONiS implementation, the first 700 values are used to generate rules and the remaining 300 values are used for testing. Note that as ADONiS uses 9 inputs to construct input FSs, the first 9 values of the testing set are omitted, leaving only the final 291. In ANFIS, while using the exact same rules as ADONiS, the first 400 data pairs are used as the training set; the following 300 data pairs are used as a validation set; and the final 291 of the remaining 300 data pairs are used as the testing set.

6.4.1 Experiment 1 - Noise-free Rule Generation Results

In the first experiment, the rule set is generated using the noise-free time-series dataset. Four different testing datasets (noise-free, 20, 5 and 0 dB) are used.

RMSE results of the ADONiS prediction experiment, with noise-free testing, can be seen on the left-hand side of Fig. 6.7a, as blue colours bars. Note that since there is no noise in the testing dataset, the generated input FSs tend to be a singleton FS. Thus, the traditional singleton prediction is implemented in this particular experiment.

After completing noise-free testing and using the same rule-set (from the noise-free training dataset), the 20 dB testing dataset is used in the prediction experiment of the ADONiS. The RMSE results of this experiment are shown in Fig. 6.7a. Thereafter, the remaining 5 dB and 0 dB testing datasets are used with the same rule set–RMSE results are shown in Fig. 6.7a.

Following the ADONiS prediction (with noise-free rule set and four different testing datasets), ANFIS optimisation is carried out on the previously generated rule parameters, and the antecedent parameters are updated in the *'black-box'* manner. Then, these updated antecedents are used in the prediction of the noise-free testing dataset. The results of this experiment are shown in Fig. 6.7a as orange colours bars and as can be seen that ANFIS performance outper-

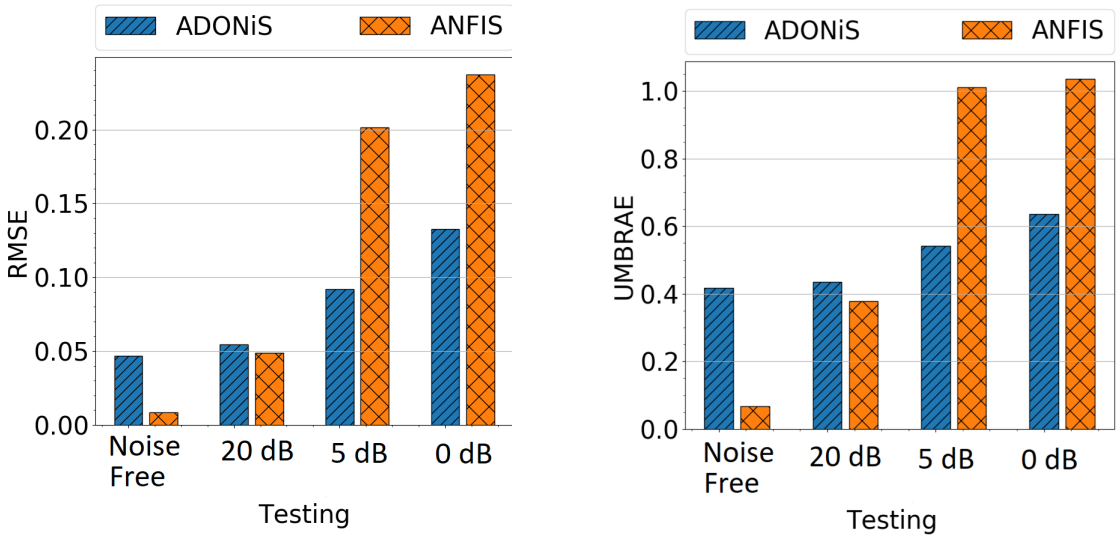

(a) RMSE results

(b) UMBRAE results

Figure 6.7: Experiment 1: Noise-Free rule generation

forms ADONiS significantly in this particular experiment.

After that, the same updated rules from the noise-free training dataset are used with the 20 dB testing dataset. The performance of ANFIS is reported in Fig. 6.7a. As can be seen, ADONiS and ANFIS have similar performances under the 20 dB noisy testing variant.

Following this, 5 dB and 0 dB noisy datasets were used in testing–RMSE results are illustrated in Fig. 6.7a. As shown, in both of these noisy conditions, ADONiS outperform ANFIS substantially.

As the second error measure, UMBRAE is used to compare ADONiS ANFIS based on a benchmark prediction performance. These sets of experimental results can be seen in Fig. 6.7b and the result trend similar to the RMSE results. Yet, under 5 dB and 0 dB testing conditions, ANFIS provides UMBRAE error measure of around 1 which indicates that this ANFIS performance is only as good as the used benchmark method that is simply averaging the inputs.

6.4.2 Experiment 2 - 20 dB Noisy Rule Generation Results

In this experiment, rule generation is completed by using the 20 dB noisy time-series dataset. The resulting rules are then used in ADONiS predictions on the noise-free, 20 dB, 5 dB and 0

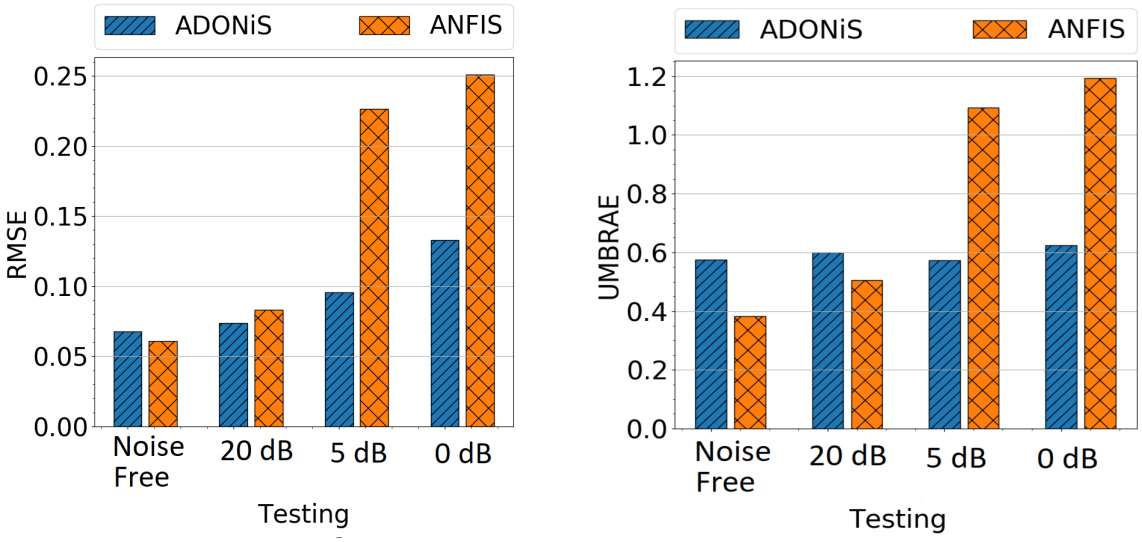

(a) RMSE results

(b) UMBRAE results

Figure 6.8: Experiment 2: 20dB Noisy rule generation

dB noisy testing datasets. The RMSE experiment results are shown in Fig. 6.8a.

After ADONiS implementation, ANFIS optimisation is implemented on the antecedents' parameters, according to the 20 dB noisy training dataset. Then the ANFIS predictions are performed on the same four (noise-free, 20 dB, 5 dB and 0 dB) different datasets. These prediction results are illustrated in Fig. 6.8a. These findings show a clear trend that ADONiS and ANFIS provide similar performances under noise-free or low-noise conditions. Under higher noise levels (5 and 0 dB), ADONiS has a clear performance advantage.

As evaluated using the UMBRAE error measure, equivalent results are illustrated in Fig. 6.8b. These UMBRAE results show that while ADONiS produces the error measure of around 0.6.

6.4.3 Experiment 3 and 4 - 5 and 0 dB Noisy Rule Generation Results

The same procedures from the previous experiments are followed. First, rules are generated based upon the 5dB noisy time-series datasets. Next, ADONiS performance is tested with the four (noise-free, 20 dB, 5 dB and 0 dB) testing datasets. Afterwards, ANFIS optimisation is used to update the antecedent parameters and ANFIS predictions are completed on the same four (noise-free, 20 dB, 5 dB and 0 dB) testing datasets. 5dB rule generation results are shown

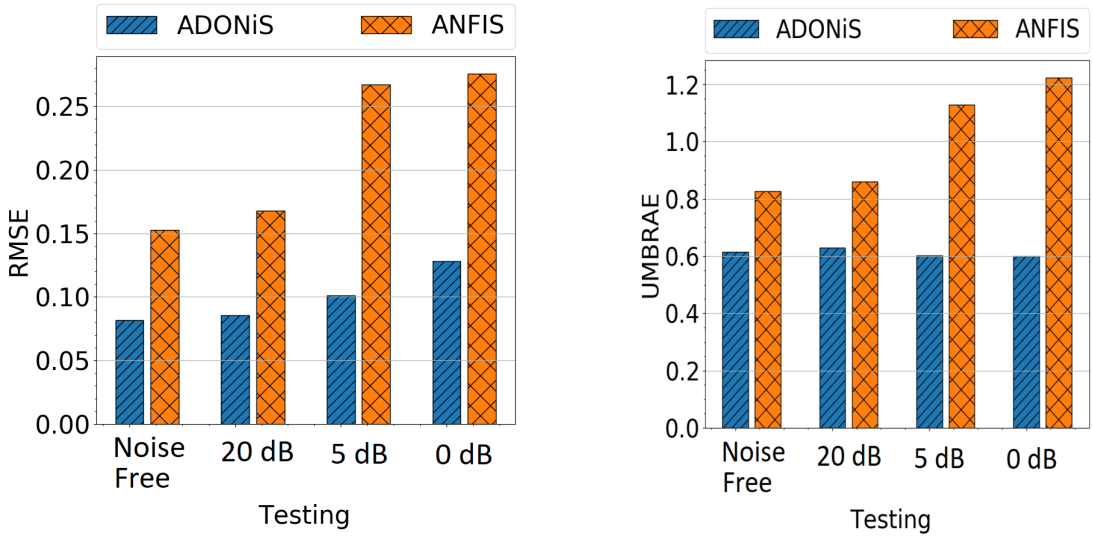

(a) RMSE results (b) UMBRAE results

Figure 6.9: Experiment 3: 5 dB Noisy rule generation

in Fig. 6.9 for RMSE and UMBRAE. Thereafter, 0 dB rule generation is completed and the four different testing results are illustrated in Figs. 6.10. These two experiment results show that the performance of the ADONiS is better than ANFIS under all the conditions.

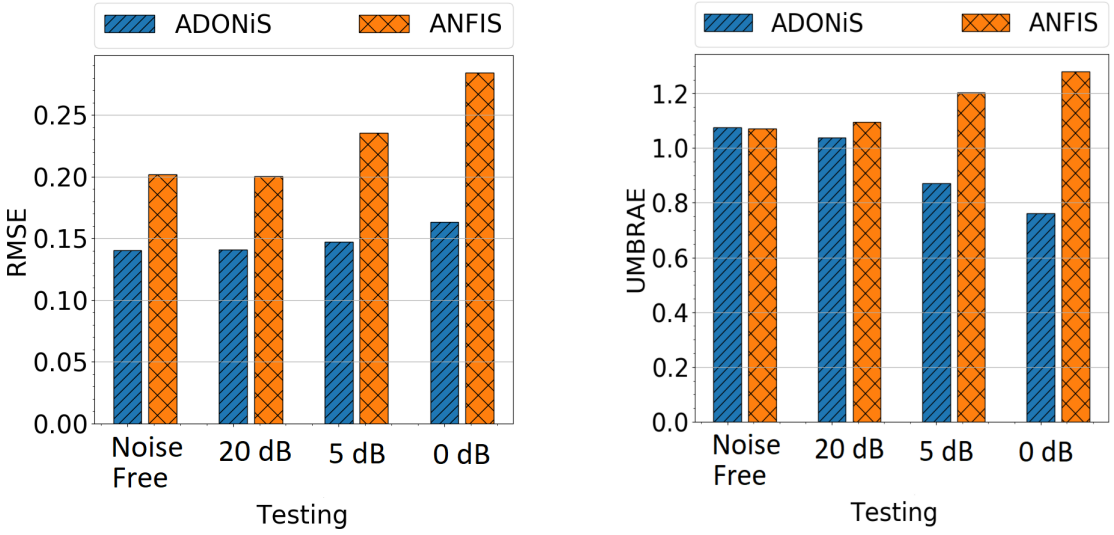

(a) RMSE results (b) UMBRAE results

Figure 6.10: Experiment 4: 0 dB Noisy rule generation

6.4.4 Discussion

Overall, the interpretability of a fuzzy model builds upon several components, e.g. rules, antecedents and/or consequent numbers, and the semantics at the fuzzy partitioning level, MFs etc. Traditionally, while optimisation techniques may provide a better performance, this leads to changing the parameters (e.g. antecedents FSs) based on a training dataset which results in a less interpretable model. However, since FLSs have mechanisms to provide interpretability, changing these parameters in a data-driven way can negatively affect the interpretability of models. For example, it may cause a loss of complementarity, coverage or distinguishability of FSs across a universe of discourse and the meaningfulness of the used FSs. Conversely, tuning parameters in the fuzzification step can maintain interpretability as well as provide performance benefits.

In the experiment, we first explore the ADONiS model, which targets the fuzzification step by confining the optimisation effect but handling noise 'where it arises'. Second, traditional ANFIS optimisation is used. In this section, after a brief performance comparison, the interpretability is discussed for both models.

Overall, when all the results are scrutinised all together (Figs. 6.7, 6.8, 6.9, 6.10), it can be seen that ADONiS and ANFIS provide comparable performances. While ANFIS shows better performance in the noise-free training and noise-free testing cases, especially under high levels of noise, ADONiS' performance is better than that of the ANFIS-tuned FLS.

In the experiments, the input domain is equally divided into 7 antecedents which are linguistically labelled from *Further Left* to *Further Right* $(FL, .., M, .., FR)$ (See Fig.6.3) and each input is assigned with these antecedents as shown on the left-hand side of Fig. 6.11. The same rule set is generated once. In the ADONiS approach, no optimisation procedure is performed offline (all tuning is done online through adaptation) and all the rules, antecedents and consequents remain intact. As can be seen on the right-hand side of Fig. 6.11, the same antecedents and consequents are used in the testing stage for ADONiS. Here, the input uncertainty is captured and handled throughout the fuzzification and inference engine process rather than optimising antecedent or consequent parameters. We note that this is intuitive as changes affecting

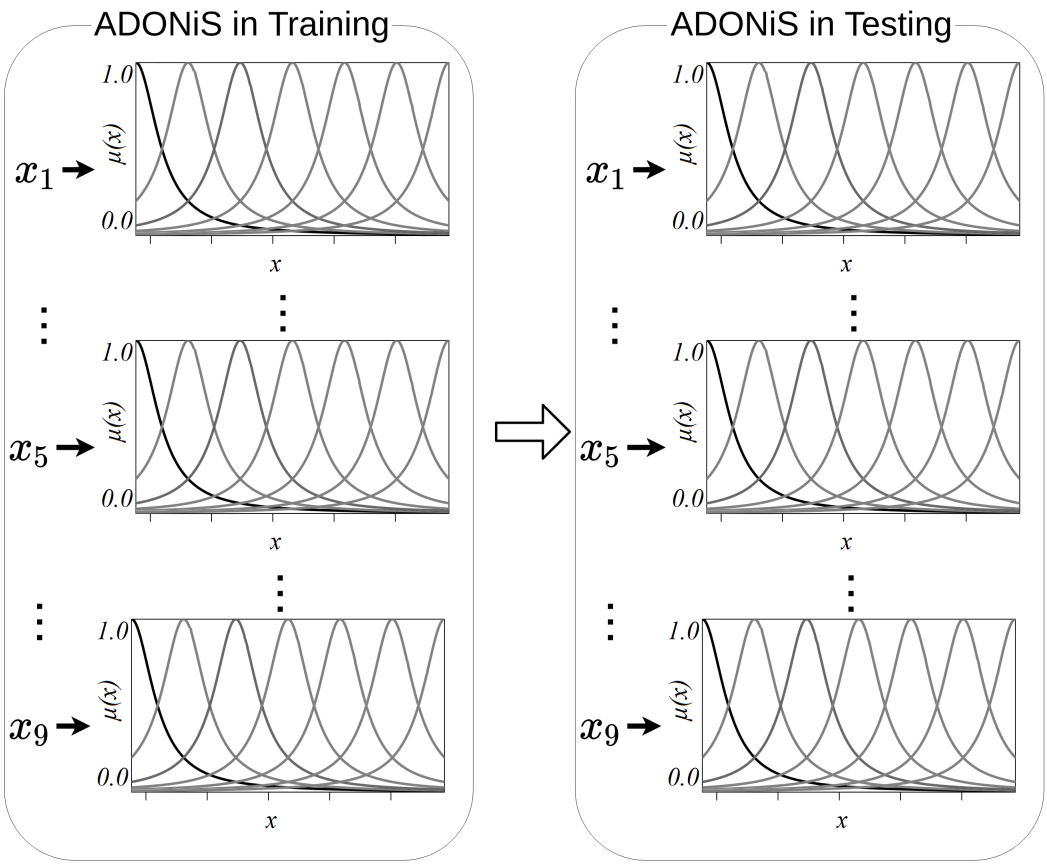

Figure 6.11: Comparison of Antecedents in ADONiS implementation which highlights that the antecedent MFs remain identical throughout the experiments.

the inputs should not affect the linguistic models of antecedents and consequents - preserving interpretability. For example, when a rule is examined in (6.2), all the *Medium* (M) MFs are the same as in Fig. 6.3 and it can be observed that the given sample inputs x_1 and x_9 are processed using the same MFs. In doing so, the initially designed 7 antecedent are used in the whole prediction process.

$$IF\, x_1\, is\, M ... \, x_5\, is\, MR ... \, x_9\, is\, M\; THEN\; y_1\, is\, CR \tag{6.2}$$

On the other hand, in the ANFIS implementation, although the same rules are used (see the left-hand side of Fig. 6.12) the optimisation procedure focuses on the antecedent parameters. Thus, the parameters are changed in respect to the training data, changing the antecedent and thus necessarily making it different to the original (considered interpretable) model (see the right-hand side of Fig. 6.12). Also, since each set of 7 MFs are altered for each corresponding

inputs, different set of 7 MFs are obtained for each input. Overall, this can affect both the semantics and the complexity at the fuzzy partitioning level. For example, the *Medium* MF is changed through the optimisation procedure. As can be seen in Fig. 6.12 and rule (6.3), the *Medium'* (M') and *Medium"'* (M''') are not the same for inputs x_1 and x_9 which inhibits the interpretability of the model.

$$IF\, x_1\, is\, \textbf{\textit{M'}} \ldots x_5\, is\, \textbf{\textit{MR"}} \ldots x_9\, is\, \textbf{\textit{M"'}}\; THEN\; y_1 \tag{6.3}$$

Overall, these initial results show that both models can provide comparable prediction results under different levels of noise. As shown, traditionally, the ANFIS model is to change key parameters of FLSs in the optimisation procedure. These parameters changes can provide increase in accuracy but cause poorer interpretability as the key parameters are altered in a data-driven way. However, while the ADONiS provides a comparable accuracy increase, it also

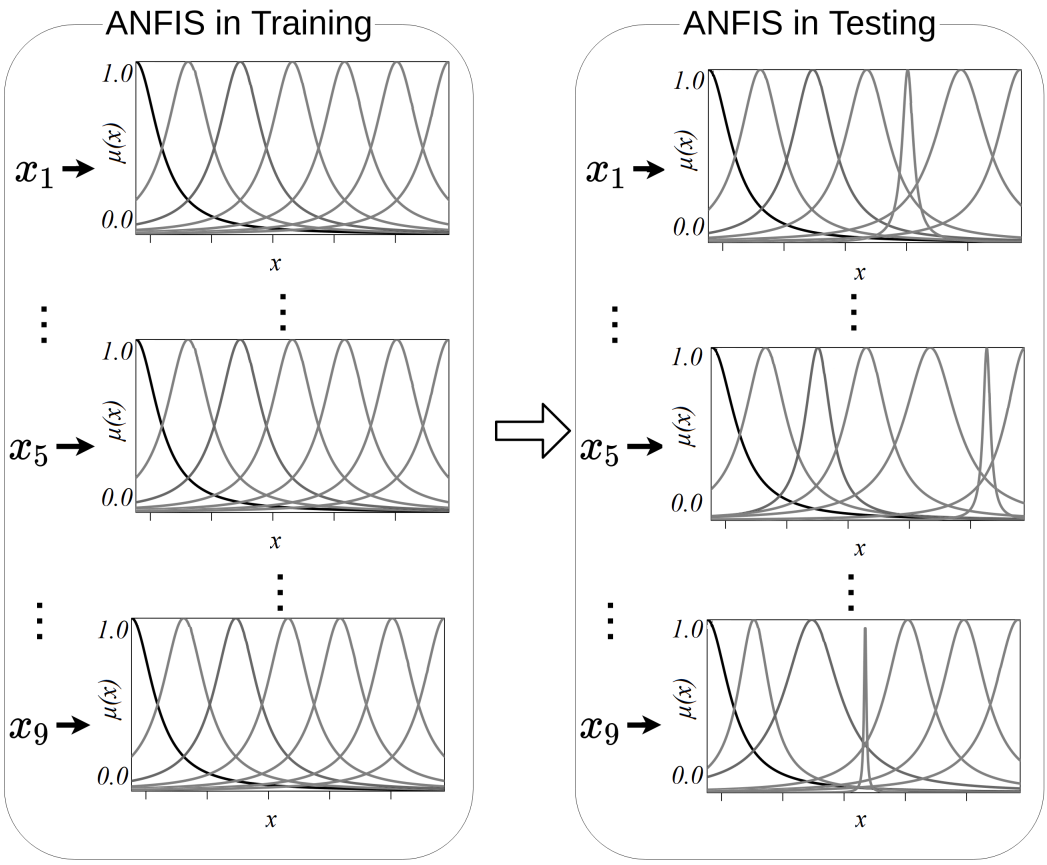

Figure 6.12: Comparison of Antecedents in ANFIS implementation which highlights that the antecedent MFs are altered in optimisation of the experiments and each input has a new different set of MFs.

provides the ability to tune parameters in the fuzzification stage which can help to maintain the interpretability –such that there is no alteration in MFs or rule parameters etc.

6.5 Summary

One of the key motivations to use FLSs is that their interpretability ability which is highly related to both MFs based and rule-based aspects. These aspects can be provided by using hand-crafted methods or data-driven techniques. In regard to the performance of FLSs, while optimisation techniques can be applied to deliver improved performance, such optimisation has traditionally lead to changes of the some key parameters which are vital for interpretability, thus delivering improved performance at the cost of poorer interpretability.

In this chapter, the focus is expanded to encompass the interpretability capacity of the ADONiS framework. While ADONiS provides performance improvements in the face of different input uncertainty levels, it also preserves its given interpretable levels, namely the rules (kept constant), antecedents and consequents, addressing objective 4.

Through a set of time-series prediction experiments, the potential of the ADONiS framework, which handles input noise where it arises, is explored in comparison to a traditional ANFIS optimisation approach. Both approaches' behaviour and performance are analysed with a view to informing future research aimed at developing FLSs with both high performance and high interpretability. It should be noted that experimental investigation has been limited to time-series predictions with a comparison of a single ANFIS model in terms of interpretability capacities. We believe that these initial results highlight a very interesting research direction for FLSs, which can maintain interpretability by modelling complexity only in specific parts (i.e. fuzzification or inference engine) of their structure.

So far, in this thesis, we have shown the ADONiS and the extended framework performance improvements and maintaining interpretability capacity in the context of chaotic time-series prediction experiments. In the next chapter, a set of experiments will be carried out to systematically evaluate the robustness and capability of the proposed frameworks in both controlled

and simulated real-world settings, addressing objective 5.

Chapter 7

Real-world Deployment of ADONiS - a Medical Case Study

So far, in this thesis, both a priori and adaptive approaches to faithfully handling input uncertainty have been introduced and evaluated in the context of time-series prediction experiments, along with the aim of maintaining a given degree of interpretability for FLSs. This chapter moves beyond time series prediction towards a real-world case study which was in part motivated by the international COVID-19 crisis in 2020: the automated control of breathing (oxygenation) support for neonatal babies. The case study was designed to test the deployability of ADONiS in a real-world setting and to provide initial insight in respect to its viability in replacing traditional approaches, in particular standard, singleton fuzzy logic control systems.

In this application, the model parameters (MFs and rules) are determined by medical experts and sensory inputs (heart rate, oxygen saturation levels and given oxygen levels) are processed as inputs to provide the following oxygen level suggestions as output. The particularly interesting aspect of the application is that there is an expectation from the medical professionals to be able to understand the decision making underpinning the oxygen flow, thus ideally, the model parameters and rules should be preserved – unless the medical experts themselves decide to change them. This provides the challenge of how best to deal with input (sensor) uncertainty affecting the control system and thus an ideal case study for ADONiS. The chapter explores a number of scenarios and experiments, addressing objective 5.

In Section 7.1, a general overview of the medical application is provided. In Section 7.2, the methodology and thus the data collection, model construction of systems used (SFLS and ADONiS frameworks) are presented. Section 7.3 presents a set of scenarios and associated experiments which are conducted using simulated datasets to ascertain and illustrate the ADONiS framework compared to the SFLS counterpart. Experiments on real-world datasets -captured in a neonatal ward at the University of Nottingham and Queen's Medical Centre (QMC)- are conducted and evaluated both in terms of their actual output performance and their overall 'qualitative' behaviour. Lastly, Section 7.5 presents the summary of the chapter.

7.1 Neonatal Baby Study Overview

Estimations show that around 15 million premature birth incidents happen around the world annually [151] and a significant proportion of these premature infants need mechanical respiratory support for a period following their birth [11]. During respiratory support, O_2 levels in their blood is a highly critical *parameter* being associated with the risk of severe complications such as chronic diseases and even mortality. Thus, in order to provide ideal O_2 support, the systematic and timely monitoring of infants' condition is critical. The amount of oxygen in the bloodstream (Oxygen saturation [SpO_2]) and heart rate (HR) can be measured by sensors such as skin probe pulse oximeters as shown in Fig. 7.1 [177]. Based on the monitoring, the O_2 support level is determined in order to maintain the SpO_2 level in the targeted range.

While O_2 support level decisions are generally made by bedside caregivers (nurses), studies show that this manual adjustment process is not very effective [47, 79]. For instance, when a baby's state changes to a 'low' SpO_2, a manual adjustment of the O_2 support requires the bedside caregiver to both be present and to notice the drop in SpO_2, and then make the necessary adjustment to O_2.

Reports show that manual O_2 level adjustments often cause infants to spend a significant amount of time outside of the targeted range [37], and the average proportion of time spent within the target range can be as low as 30%-40% of time [33]. Thus, automated decision-

Figure 7.1: Pulse oximetry devices on newborn babies reproduced from [177]

support to provide O_2 level suggestions can be a useful tool, especially in comparison with manual adjustment.

However, the automatic adjustment of O_2 levels is a challenging task. Sensors, which measure a baby's condition (e.g. SpO_2 or HR), can be affected by various factors at different scales and time-periods. The wavelength of light, measurement site, contact force, ambient light intensity, ambient temperature, or electromagnetic interference can cause inaccurate sensors measurements [128]. Furthermore, motion artefacts reduce the accuracy of continuous long-term monitoring. Since infants exhibit more movement than adults typically, it can be more difficult to measure vital signs accurately in neonatal babies [172]. Considering these real-world circumstances, standard hospital hardware provides signal quality parameters for the measured values to indicate the accuracy of readings. Nevertheless, while different approaches have been developed to assess the quality of signals leveraging this information [33, 42, 144], it remains a challenging and thus far unsolved area [109].

Furthermore, as alluded to above, due to safety, trustworthiness and ethical aspects of clinical tests, the interpretability of the automated decisions are also an essential aspect [20, 67], and automated control approaches which do not afford the interpretability of the automated decisions might seriously limit the usability of the approaches in practice [171].

Overall, while an automated tool can provide an advantage to maintain the targeted O_2 range for infants, two main requirements have been identified: (i) the model should have a capacity to cope with real-world uncertainty/noise in sensor data and, (ii) the model should be interpretable

for medical professionals to comprehend the decision-support process.

Following this overview of O_2 level modelling in neonatal babies, we now systematically address the capability of the proposed ADONiS framework in addressing the requirements, at the same time, addressing objective 5.

7.2 Methodology

In this case study, neonatal baby O_2 support level suggestions are modelled by collaborating with an academic neonatologist and his team at the University of Nottingham and QMC hospital. As detailed in subsection 7.2.2, the models are designed based on their expertise, including for the design of the FLSs MFs and rules.

7.2.1 Dataset Collection

As mentioned, generally, baby O_2 support level adjustments are performed by bedside caregivers based on a baby's condition which is captured using sensors. In the specific context of this case study and data-collection process, a CARESCAPE Monitor B850 transmission mode pulse oximeter is used to gather HR and SpO_2 levels every second, while the given O_2 levels are recorded simultaneously. In total, six babies' parameters were anonymously collected for various periods of time. A sample of the dataset is visualised in Fig. 7.2 where the left Y-axis shows the baby's HR which is represented by a solid black line and the right Y-axis shows SpO_2 levels, represented by a solid red line. Also, the *ideal* range -which is stated by medical professionals- for both parameters is illustrated by dashed lines (black dashed lines for HR and red dashed lines for SpO_2). Note that HR readings in the dataset reported as 1 were removed from the dataset as a pre-processing step.

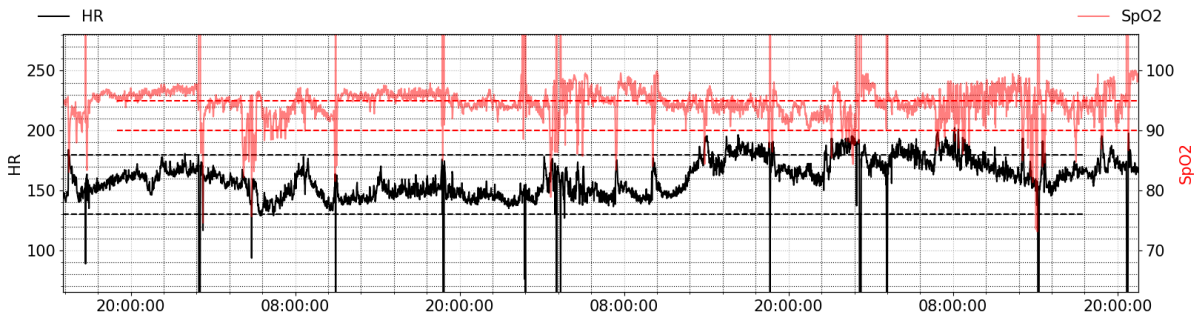

Figure 7.2: A baby HR and SpO_2 values over a time interval

7.2.2 Model Construction - Membership Functions and Rules

O_2 suggestion decisions are made for every minute and for each suggestion, at the current time (t), heart rate ($HR(t)$), oxygen saturation ($SpO_2(t)$), and the currently given oxygen ($O_2(t)$) levels are used as inputs to make the suggestion of the next oxygen support level ($O_2(t+1)$).

As the first step of constructing the model, *Low*, *Moderate* and *High* MFs were defined by hand for HR, SpO_2 and O_2 by the academic neonatologist. Later, these provided MFs are approximately replicated using linear MFs, which are used in the FLSs. A sample of manually provided MFs for the SpO_2 can be seen in Fig. 7.3a and the approximated, linear MFs are shown in Fig. 7.3b.

Based on the hand-drawn MFs, system rules are defined by the academic neonatologist. A sample of the created rule can be seen in 7.1. As the given sample rule suggest, if a baby has *low* HR (t) (Bradycardia) and *moderate* SpO_2 (t), and currently the given O_2 (t) support is *moderate*, then the next O_2 (t+1) support should be *high*.

$$IF\ HR(t)\ is\ \textbf{Low}\ AND\ SpO_2(t)\ is\ \textbf{Moderate}\ AND\ O_2(t)\ is\ \textbf{Moderate}\ THEN\ O_2(t+1)\ is\ \textbf{High} \tag{7.1}$$

In total, 24 rules are created to model the O_2 support level suggestions (All the created rules can be found in appendix B in Table B.1).

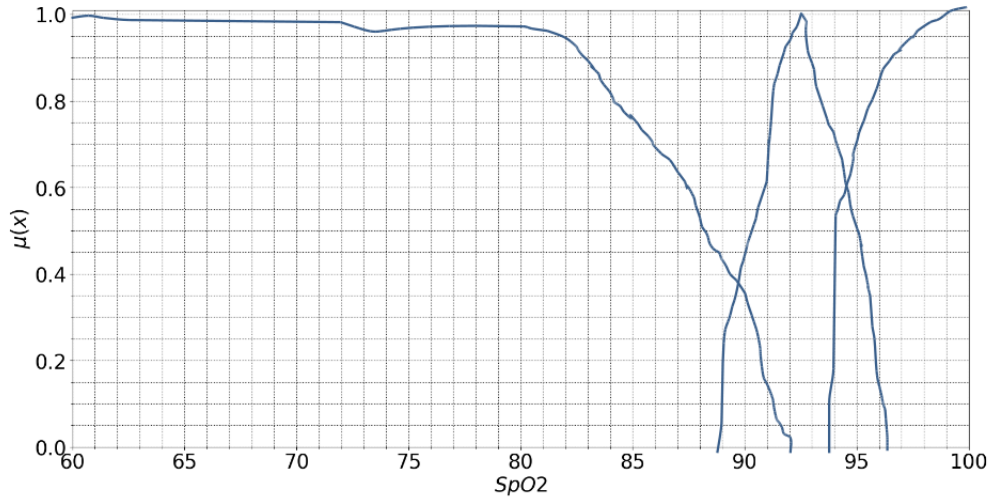

(a) The given MFs for SpO_2

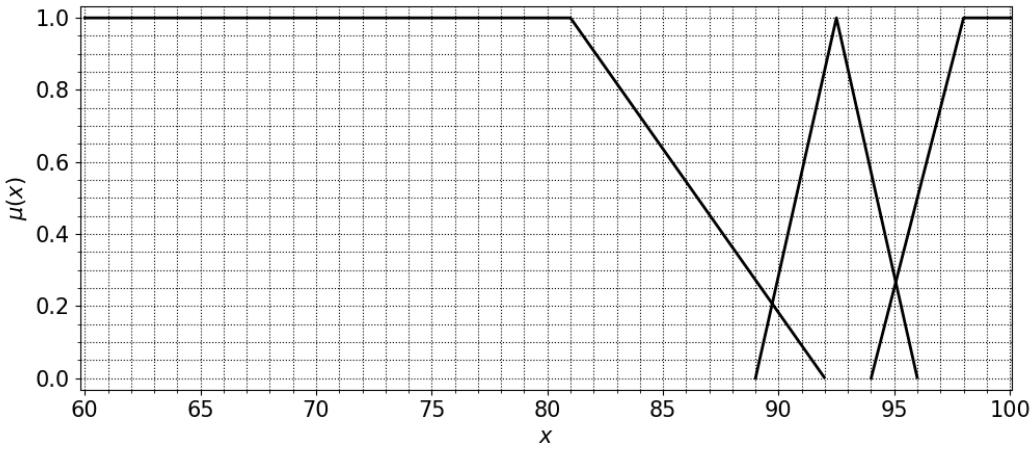

(b) The approximated MFs for SpO_2

Figure 7.3: Illustration of low, moderate and high MFs for SpO_2.

7.2.3 Singleton Fuzzy Logic Systems and ADONiS

In this section, SFLS outputs, i.e. O_2 level suggestions are compared to those generated by the ADONiS framework. Both FLSs use the exact same MFs and rules as outlined in the previous subsection.

As discussed in Chapter 2, for the SFLS, model inputs are modelled as singleton FSs. The resulting control surface of this model (HR in compare to SpO_2 levels) can be seen in Fig 7.4. Overall, as shown in Figs 7.4, SFLSs O_2 suggestions exhibit 'sharp' changes between some parameters (e.g. step descent if the SpO_2 value crossed 90).

In the traditional NSFLS designs, inputs of systems are fuzzified into non-singleton FSs

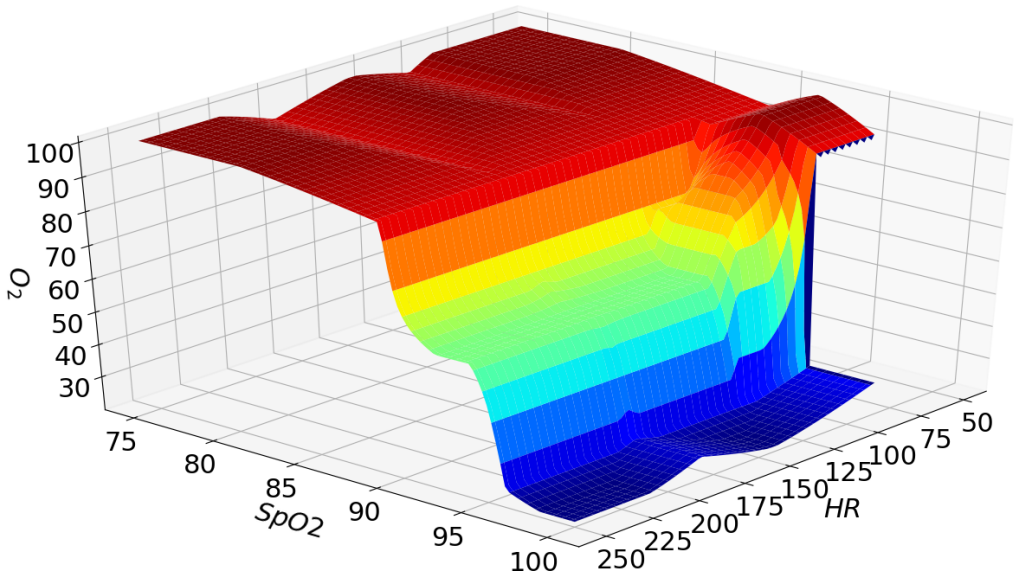

Figure 7.4: The control surface (HR and SpO_2) of the SFLS based on generated MFs and rules.

which are associated with the level of input uncertainty. Naturally, the question arises that what should be the width parameters for input FSs to model the input uncertainty which may highly be associated to different factors at different times (e.g. ambient temperature, electromagnetic interference or motion artefact)?

In order to highlight the effect of input FS width parameter selection, two standard NSFLS systems' -with the same rules and MFs- control surface are visualised and compared. In the first instance (named $NSFLS_1$), to exemplify a 'low' noisy environments, input widths are set to be 'narrow' manually and the control surface is re-generated with the same rules and MFs. The generated control surface for this particular $NSFLS_1$ can be seen in 7.5a. Later, in another example design (named $NSFLS_2$), to depict a higher noisy environment, input widths are set to be wider and the control surface is re-created by the exact same rules and MFs which is shown in Fig. 7.5b. In order to illustrate the difference between these two NSFLSs ($NSFLS_1$ and $NSFLS_2$), the provided O_2 suggestion levels difference between $NSFLS_1$ and $NSFLS_2$ is also visualised in Fig. 7.6. Note that to visually highlight the differences, the O_2 axes scale is set to 0-30. As it is shown in Fig. 7.6, naturally, the width parameters in input FSs have an effect on the behaviour of systems and it should be determined properly being based on the uncertainty level of system inputs.

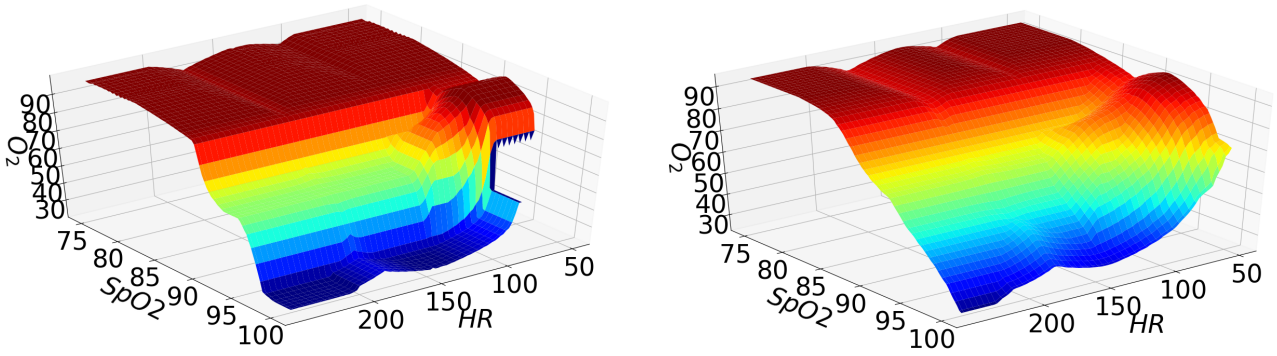

(a) $NSFLS_1$. (b) $NSFLS_2$.

Figure 7.5: $NSFLS_1$ and $NSFLS_2$ control surfaces (HR and SpO_2) based on the generated MFs and system rules.

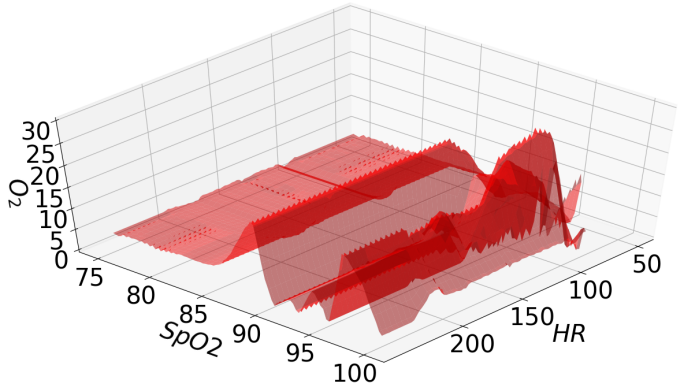

Figure 7.6: O_2 suggestion differences between $NSFLS_1$ and $NSFLS_2$.

As mentioned in Chapter 2, in the literature, traditionally data-centric optimisation procedures are used to adjust FSs, rule parameters or input FSs widths of FLSs. However, in the context of using non-singleton input FSs, relying on optimisation procedures may lead to a single width parameter for input FSs which prevent models from being able to adapt to different noise levels over time. As discussed in Chapter 4, due to the heterogeneity and diversity of real-world conditions, uncertainty levels tend to vary. Thus any system adopting one uncertainty level set a priori (resulting in one parameter set for the fuzzification stage in the case of NSFLSs) is unable to adjust to variation in said noise level at runtime – making the online adaptation to changing noise levels, as offered by ADONiS, desirable.

Additionally, with respect to systems interpretability, when a data-centric optimisation is applied to a model, changing MFs or rules (which are designed by the neonatologist initially) may negatively impact the interpretability of these MFs, rules and thus the overall model. However,

the ADONiS framework employs an online learning method to continuously update input FSs. While this procedure can provide an improved capacity to deal with input-affecting uncertainty, it can also facilitate maintaining the interpretability of given MFs and rules which are designed based on by the neonatologist initially.

In order to conveniently explore the behaviour of the ADONiS framework in these setting (uncertainty handling and interpretability capacity), we deploy it, selecting a window size of 5 minutes (i.e. the sliding window W size is set to 5) for inputs HR (W_{HR}), SpO_2 (W_{SpO_2}) and O_2 (W_{O_2}). Thus, the ADONiS framework will take the input data (and associated variation and noise) over 5 minutes into account to inform input the widths of the Gaussian input FSs. The same noise estimation algorithm (1) as outlined in Chapter 4 is used. We note that different window sizes, different frequencies (e.g. every 30 seconds) or different estimation algorithms could, of course, be used in this implementation as well.

The focus of the experiment is to ascertain and illustrate the behaviour of the dynamic adaptation in ADONiS in the context of the application. In other words, we are not looking to determine the optimal set of parameters leading to optimal outcome. We note that for the given application and dataset, no ground truth is available which would enable determining whether such an optimum had been reached.

In each experiment, SFLS's O_2 level suggestion results are compared to those generated by ADONiS framework. Since ground truth is not available for the given application, the experiment results are evaluated by showing results of ADONiS and SFLSs O_2 suggestions to the neonatologist to get his opinion. After providing the results, the question "*Which models' suggestion is better or preferable? and Why?*" was asked, then, behaviours of systems and the provided opinions are discussed.

Following this overview of the methodology, we now proceed to the experiments.

7.3 Experiments

In each experiment, SFLS's O_2 level suggestion results are compared to those generated by ADONiS framework. In order to observe behaviours of these systems under controllable environments, we first created artificial datasets where each are designed to mimic a case of a baby who exhibits different conditions. In total, we established five different case scenarios where five different datasets are generated for each. The datasets are designed to contain 60 values where each value can be regarded as a time unit (e.g. 1 minute etc.). The created case scenarios are summarised below and the rationale for each established scenario will be explained in the following subsections.

- Case Study 1: The simulated HR and SpO_2 levels are kept within the *ideal* range (defined by the neonatologist) throughout the experiment.
- Case Study 2: For a single value in the dataset, the simulated HR and SpO_2 levels are changed on the *edge* of ideal ranges (e.g SpO_2 level changed to 90% for *short* time).
- Case Study 3: For multiple values, the simulated HR and SpO_2 levels are changed on the *edge* the ideal ranges (e.g SpO_2 levels keep changing around 90% for a *longer* time interval).
- Case Study 4: For a single value, the simulated HR and SpO_2 levels are changed *significantly* (e.g. HR around 50 and SpO_2 around 85% for a *short* time.)
- Case Study 5: For multiple values, the simulated HR and SpO_2 levels are changed significantly (e.g. HR around 50 and SpO_2 around 85% for a longer time interval.)

After completing synthetic 5 case studies, SFLS and ADONiS framework models are used on the real-world dataset to report the behaviours of each model. Later, case studies and real-world experiment results are evaluated as detailed in the next subsection.

7.3.1 Results Evaluation

Since there is no ground truth available to validate and compare the suggested O_2 levels from the ADONiS and SFLSs, there is a reliance on opinions from experts to verify results. In the experiments, in particular, a form is prepared to demonstrate each case study and real-world experiments scenarios along with the O_2 suggestion results by providing visualisations and results. Later this form is sent to Prof. Don Sharkey who is an academic neonatologist at the University of Nottingham and Queen's Medical Centre (QMC). For each case study and the real-world experiment results, Prof. Don Sharkey's opinion was asked by stating *What is your comment on these models' O2 suggestions?*, *Which models' suggestion is better or preferable?* and *Why?* in the form. Each response and opinion from Prof. Don Sharkey is provided in each corresponding case study and real-world experiments in the following sections.

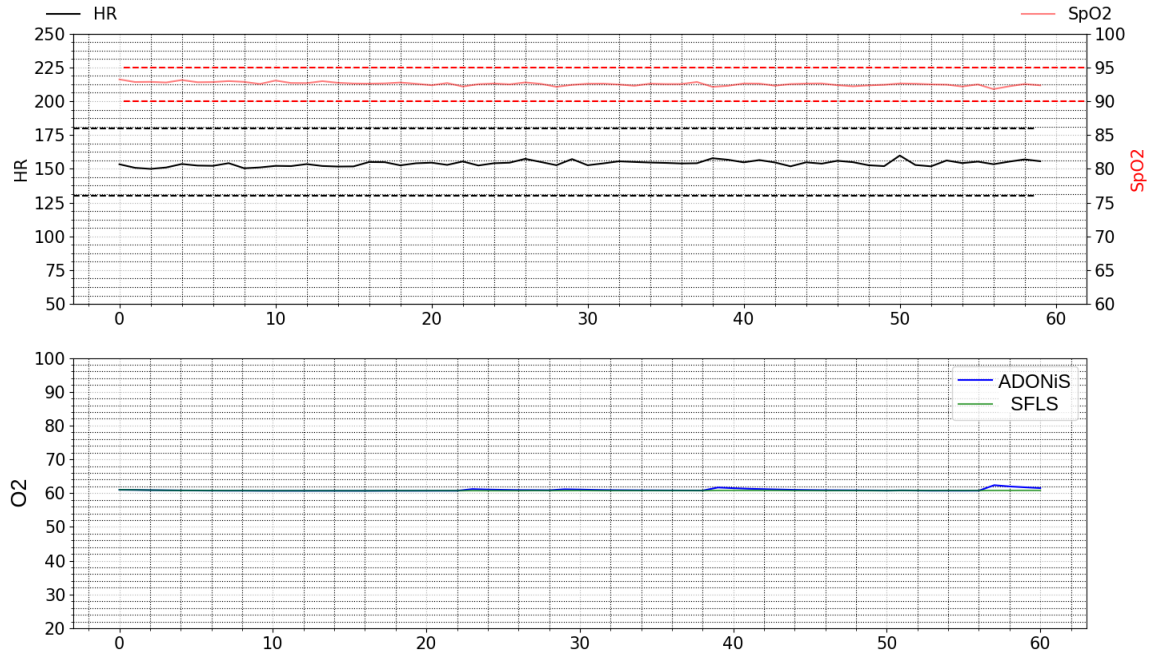

Figure 7.7: ADONiS and SFLS 2 models O_2 support level suggestions

7.3.2 Case Study 1 - Normal Conditions

In this case study, we considered a scenario where HR and SpO_2 levels are simulated to be within the ideal ranges throughout the experiment. This scenario is designed to mimic the case of a baby whose HR and SpO_2 levels are in normal conditions.

Throughout the synthetic dataset can be seen at upper Fig. 7.7 where the left y-axis shows HR levels (a solid black line) and the right y-axis shows the SpO_2 levels (a solid red line). Also, the *ideal* range for both parameters are illustrated by dashed lines (a black dashed line for HR and a red dashed line for SpO_2). The horizontal axis is to represent the 60 values index.

As mentioned, two different model O_2 support suggestions are investigated. The bottom Fig. 7.7 shows the corresponded O_2 suggestion levels for both systems, ADONiS (a blue line) and SFLS (a green line).

As the bottom Fig. 7.7 shows, both models provide similar O_2 support suggestions which are stable and around 60% for the created dataset where the case scenarios are to mimic a baby whose HR and SpO_2 levels are within the ideal range throughout the experiment. It can be said that the created rule (7.2) (*rule 11* from the Table B.1) -by the neonatologist- was the main driver in this O_2 suggestion process.

$$IF\ HR(t)\ is\ \textbf{Moderate}\ AND\ SpO_2(t)\ is\ \textbf{Moderate}\ AND\ \ O_2(t)\ is\ \textbf{Moderate}\\ THEN\ O_2(t+1)\ is\ \textbf{Moderate} \tag{7.2}$$

Since there is no high variation or uncertainty in the created dataset, the online adaption capacity of ADONiS results in the non-singleton input FSs to be similar to singleton FSs, naturally.

Since no ground truth available to evaluate the systems' behaviours, the results are shown to the neonatologist Prof. Don Sharkey and the questions of "*Which models' suggestion is better or preferable? and Why?*" were asked.

The following opinion/answer were stated:

> "If the baby is very stable in 60% oxygen this would suggest significant lung disease. Here the model prediction remaining static is important as the other variables don't change. Equally, the model could say 25% or 100% as long as it didn't vary"

As Prof. Don Sharkey pointed out, the stability of suggestions are the key expected behaviours and both systems are followed this static behaviour. In terms of the suggested percentage (60%), we note that it can be adjusted by changing the output FSs parameters.

7.3.3 Case Study 2 - A *short* change on the 'edge'

In this case study, we have created HR and SpO_2 levels within ideal range; however, a sudden short change (for 1 value in the dataset) occurs on the edge of the ideal range of the parameters. This scenario is designed to mimic the case of a baby whose HR and SpO_2 values are somehow *slightly* affected (e.g. electromagnetic interference, a minor motion artefact or even a real 'slight' change for a short time) while the simulated baby's overall conditions are within the ideal range.

7.3.3.1 Case Study 2.1 - A *short* drop on the 'edge'

In case study 2.1, a short drop for both HR and SpO_2 values are synthetically created. which can be seen at upper Fig. 7.8.

Experiments are repeated by using this synthetically created dataset and both systems (ADONiS and SFLS) O_2 suggestions results can be seen at the bottom Fig 7.8.

As it is shown, ADONiS O_2 support suggestion (a blue line) is increased to around 70%, which is less than the SFLSs suggestion (around 95% [a green line]). As shown in Fig. 7.9a, ADONiS framework adaptively results in non-singleton input FSs to be wider where it interacts with different antecedent FSs (i.e. both *Moderate* SpO_2 MF and *Low* SpO_2 MF) whereas singleton input FS only interact with the Low SpO_2 MF (Fig. 7.9b). This non-singleton input

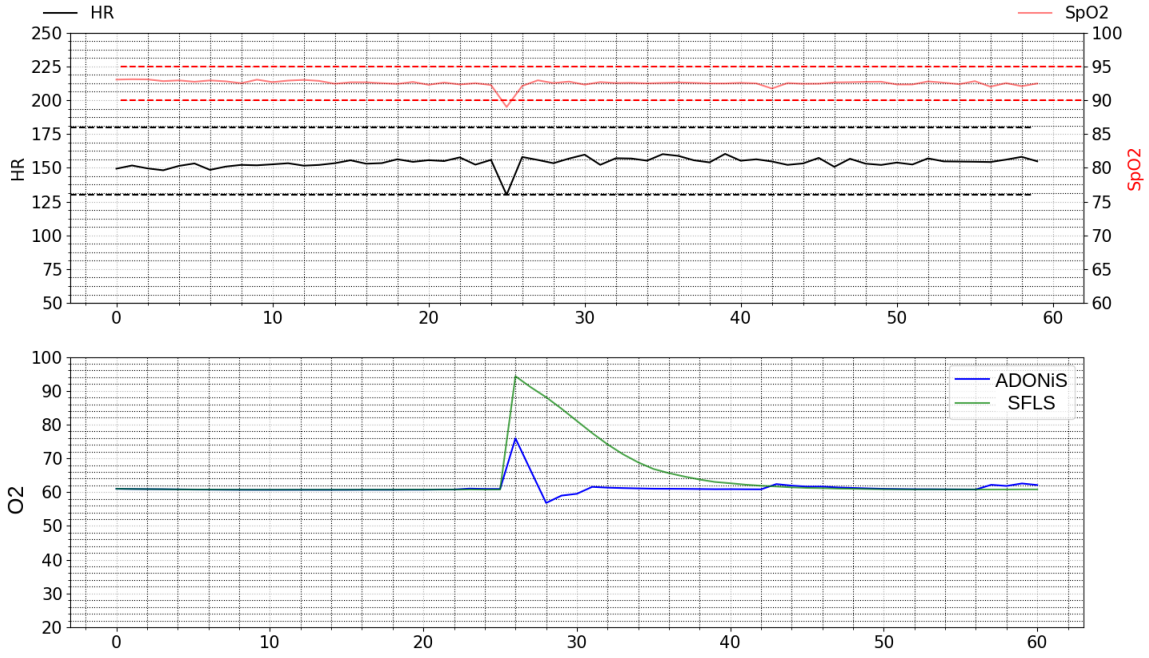

Figure 7.8: Dataset of a short drop and both models (ADONiS and SFLS) O_2 support level suggestions in the Case Study 2.1.

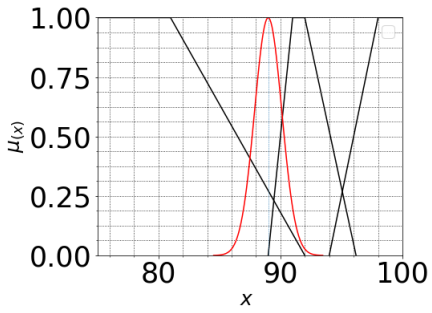

(a) The adaptively created non-singleton input FS (red) interacts with both HR Low MF (black) and SpO_2 Moderate MF (black)

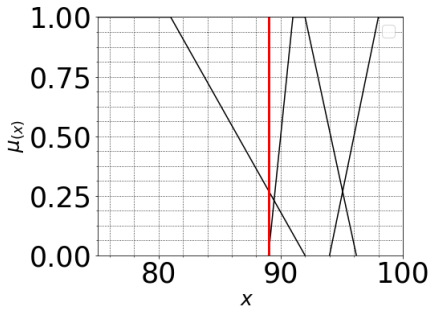

(b) The singleton input FS (red) interacts with only SpO_2 Low MF (black)

Figure 7.9: Non-singleton and Singleton input FS interaction with SpO_2 Low, Moderate and High MFs.

FS interaction results in O_2 suggestion to have a lower magnitude than singleton input FS case. The overall interaction of this non-singleton input FS over the created 24 rules can be seen in Appendix B Fig. B.1.

Also, after the drop occurs for 1 value in the synthetically created dataset and when the simulated HR and SpO_2 levels return to the 'normal', ADONiS O_2 suggestions recovers faster

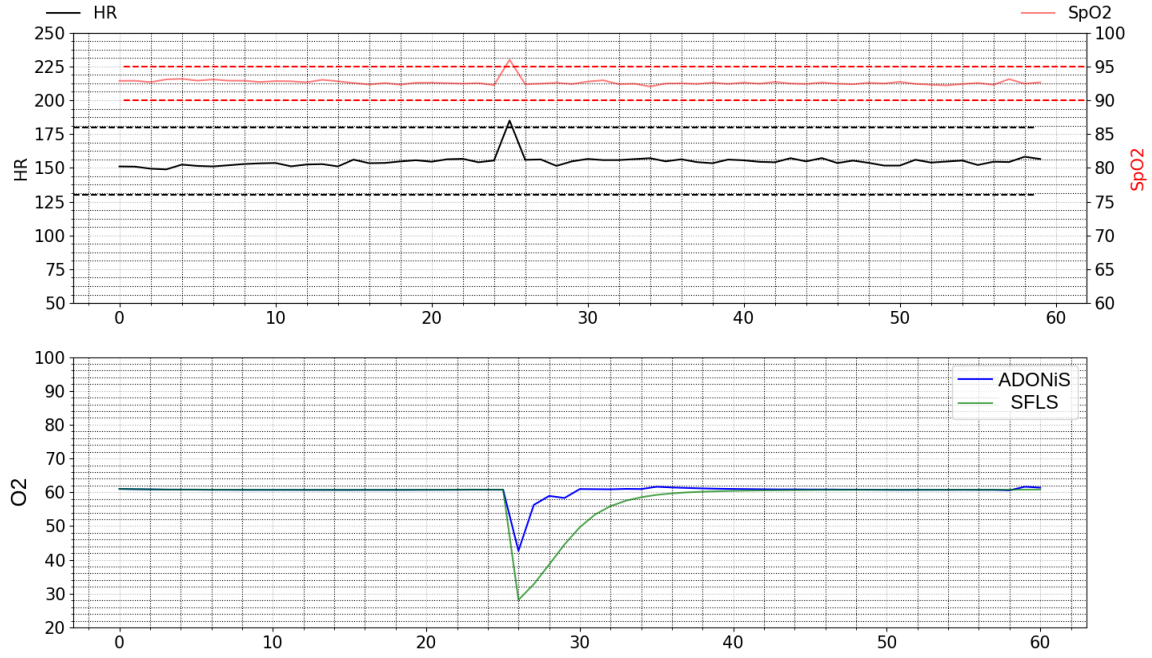

Figure 7.10: Dataset of a short increase and both models (ADONiS and SFLS) O_2 support level suggestions in the Case Study 2.2.

than the SFLS. Note that the third input ($O_2(t)$) has a role in this recovery time and typically, a standard NSFLS designs are to 'recover' slower than the SFLS.

7.3.3.2 Case Study 2.2 - A *short* increase on the 'edge'

In this case study, another synthetic dataset was created where HR and SpO_2 levels within the ideal range; however, a short sudden increase occurs in the middle of the synthetically created dataset which both HR and SpO_2 can be seen at the top of Fig. 7.10.

Experiments are repeated by using this dataset and both models (ADONiS and SFLS) O_2 suggestions results can be seen at the bottom of Fig 7.10. Similar to the Case study 2.1 (subsection 7.3.3.1), ADONiS and SFLS provide similar patterns. While ADONiS O_2 support suggestion is changed (decreased to around 45%) less than SFLS (around 30%). Also, when the increase occurs for 1 step and the simulated HR and SpO_2 levels return to the 'normal', ADONiS recovers faster than the SFLS.

Both case study 2.1 and 2.2 results were shown to Prof. Don Sharkey by asking "*Which models' suggestion is better or preferable? and Why?*". The response was that in both case studies (2.1 and 2.2), the ADONiS framework provides more preferable O_2 level suggestions then SFLSs, because of the fact that small change in baby conditions leads to proportionally small changes in suggestions.

7.3.4 Case Study 3 - A *longer* changes on the 'edge'

In this case study, for multiple values of both HR and SpO_2 levels are artificially changed on the 'edge' of the ideal ranges. This scenario is designed to mimic the case of a baby whose HR and SpO_2 conditions are changed and continued for a longer time.

7.3.4.1 Case Study 3.1 - A *longer* drop on the 'edge'

In the case study 3.1, the synthetically created dataset can be seen at the upper Fig. 7.11. Both systems O_2 support suggestions can be observed at the bottom figure of Fig. 7.11.

As can be seen in bottom Fig. 7.11, when both HR and SpO_2 levels are dropped, both models react by increasing the O_2 support suggestion levels. Overall, while SFLS has more and/or fluctuating suggestions, the ADONiS framework provides less and/or smooth suggestions throughout the drops of HR and SpO_2.

As indicated in the control surface of SFLS in section 7.2.3, sharp changes between some values are demonstrated. Thus, as the HR and/or SpO_2 levels are crossed the ideal range borders, SFLS O_2 level outputs increase sharply. However, because of the ADONiS adaptive non-singleton input FS designs, these changes are formed in a more gradual manner, such as not changing the O_2 suggestions from 60% to 90% immediately.

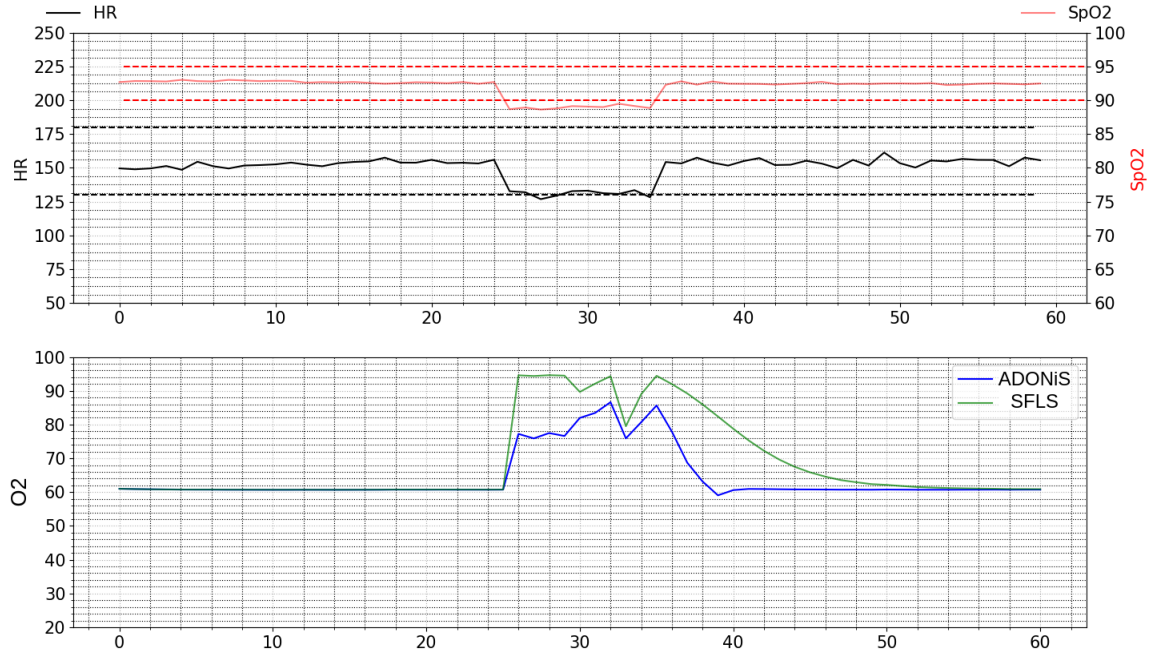

Figure 7.11: Dataset for longer drop and both models (ADONiS and SFLS) O_2 support level suggestions in the Case Study 3.1.

7.3.4.2 Case Study 3.2 - A *longer* increase on the 'edge'

In this case study, both HR and SpO_2 levels are artificially increased on the edge of ideal ranges for multiple values in the dataset (See the upper Fig. 7.12) and both models O_2 support suggestions can be observed at the bottom figure of Fig. 7.12.

As can be seen in bottom Fig. 7.12, when HR and SpO_2 levels are increased, both models react by increasing the O_2 support suggestion levels. Overall, while SFLS provides less O_2 level outputs (between 25% to 35% [the green line]), ADONiS framework provides more O_2 level outputs (between 35% to 45%) throughout the increase of HR and SpO_2 where the results are inline with the previous Case Study 3.1.

According to Prof. Don Sharkey, in both case studies (3.1 and 3.2), ADONiS provides more preferable O_2 level suggestions then SFLSs, because of the fact that "vital signs remain just outside normal range so no need to adjust significantly".

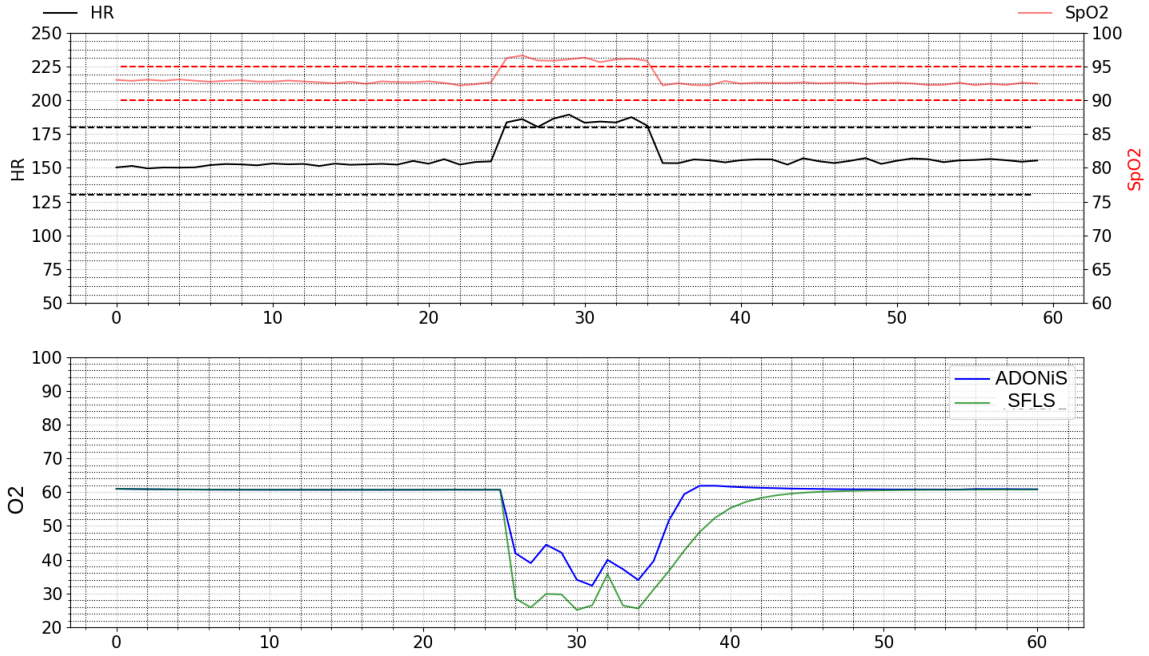

Figure 7.12: Dataset for longer increase and both models (ADONiS and SFLS) O_2 support level suggestions in the Case Study 3.2

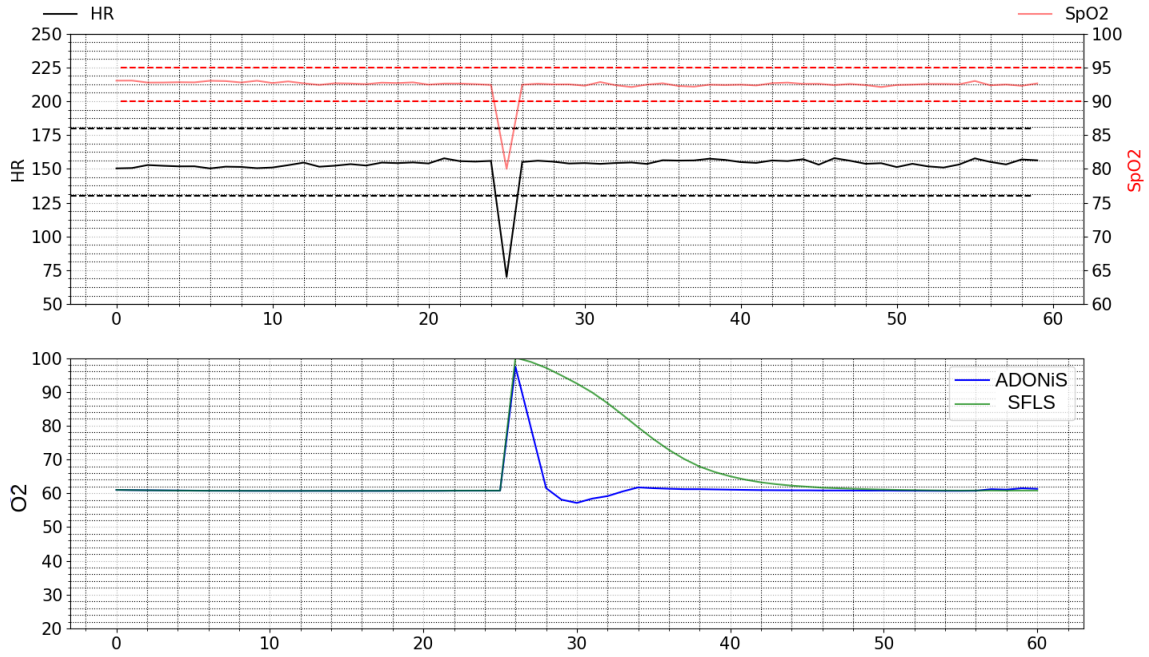

Figure 7.13: Dataset for a significant drop and both models (ADONiS and SFLS) O_2 support level suggestions in the Case Study 4.1.

7.3.5 Case Study 4 - A *short significant* change

In this case study, HR and SpO_2 levels are overall simulated to be within the ideal range; however, a sudden *significant* change (for 1 value) occurs in the middle of the created dataset. This scenario is similar to Case study 2, but in this case, it is designed to mimic the case of a baby whose HR and SpO_2 values are *significantly* affected for a short time while the simulated baby overall conditions are within the ideal range.

7.3.5.1 Case Study 4.1 - A *short significant* drop

In this case study, the simulated HR and SpO_2 levels are dropped *significantly* for a single step.

Both models (ADONiS and SFLS) reactions are compared at the bottom figure of Fig. 7.13 and as can be seen, both models O_2 suggestion is increased to around 95-100%. The reason for these similar reactions is that even though the ADONiS's adaptive behaviour provides a 'wide' non-singleton input FS, it falls within a single antecedent FS and does not interact with other antecedents. Thus, the results become similar to SFLS. In such case, if input values (mean of non-singleton FSs) are that 'low' and the input uncertainty (width of non-singleton FSs) is not enough to interact with other antecedents, intuitively, it can be expected to obtain a similar behaviour of SFLSs.

While ADONiS suggestion is slightly less than the SFLS initially, when the simulated HR and SpO_2 levels go back to normal range (after a single step drop), ADONiS O_2 suggestions get back to normal (60%) faster than the SFLS. As noted in Case Study 2.1, this faster recovery time for the ADONiS model is due to the third non-singleton input ($O_2(t)$).

7.3.5.2 Case Study 4.2 - A *short significant* increase

In this case study, the simulated HR and SpO_2 levels are increased *significantly* for a single step.

Both models (ADONiS and SFLS) reactions are compared at the bottom figure of Fig. 7.14,

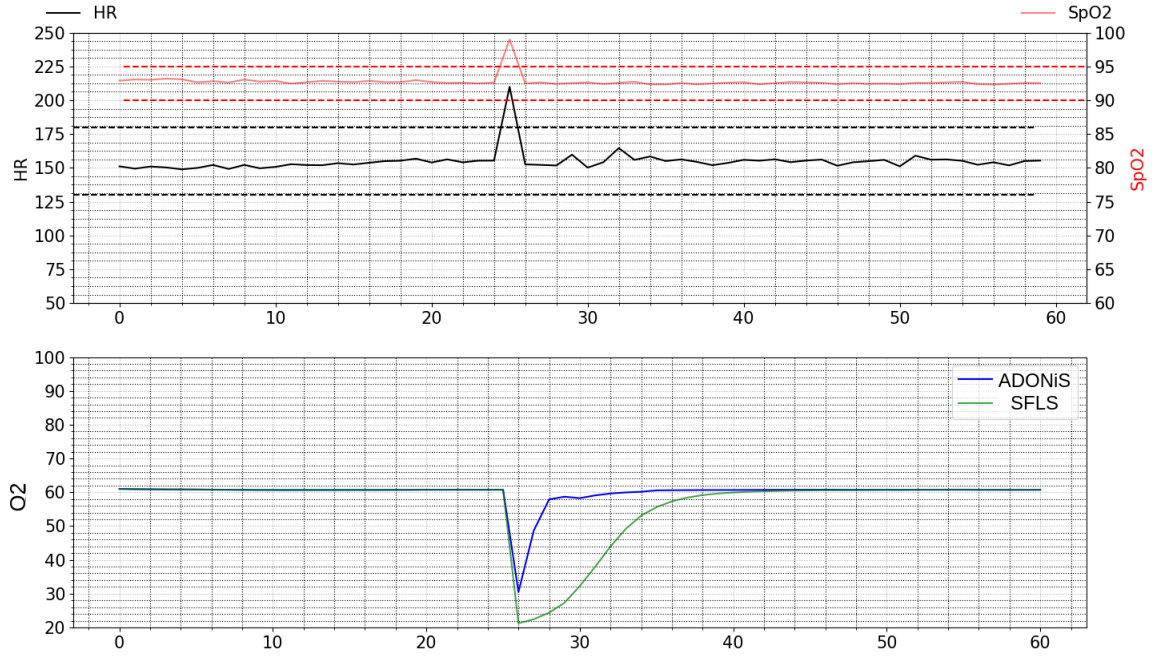

Figure 7.14: Dataset for a increase drop and both models (ADONiS and SFLS) O_2 support level suggestions in the Case Study 4.2.

and the results are in line with the previous Case study 4.1 results.

According to Prof. Don Sharkey, for the case study 4.1, the ADONiS provides more preferable O_2 level outputs then SFLSs as stated:

> "Brief increase in O_2 is all that is required before return to baseline. SFLS isn't realistic in that the long 'tail' as return to baseline O2 would result in an overshoot of SpO_2 to 100%"

Also, similar to the case study 4.1, SFLS might cause the SpO_2 to drop after returning into the normal range which may not be preferable. Thus, ADONiS provides more preferable results for case study 4.2 as well.

7.3.6 Case Study 5 - A *longer significant* change

In this case study, the *significant* changes are simulated for longer time intervals for both HR and SpO_2 levels.

7.3.6.1 Case Study 5.1 - A *longer significant* drop

The simulated dataset can be seen in the top figure of 7.15.

As shown in the bottom figure of Fig. 7.15, both models (ADONiS and SFLS) reacted in a similar manner. Both models are reached 100% O_2 suggestion levels. While SFLS reaches that point immediately, ADONiS took time and reaches 100% suggestions gradually. The reason for this taking time is that while the similar condition last (e.g. low SpO_2), the non-singleton input FSs widths are gradually decreased and become more certain about the conditions or sensor readings. This can be interpreted as the ADONiS model is more cautious about the changes.

Also, as the simulated HR and SpO_2 levels get back to the ideal range, the ADONiS sugges-

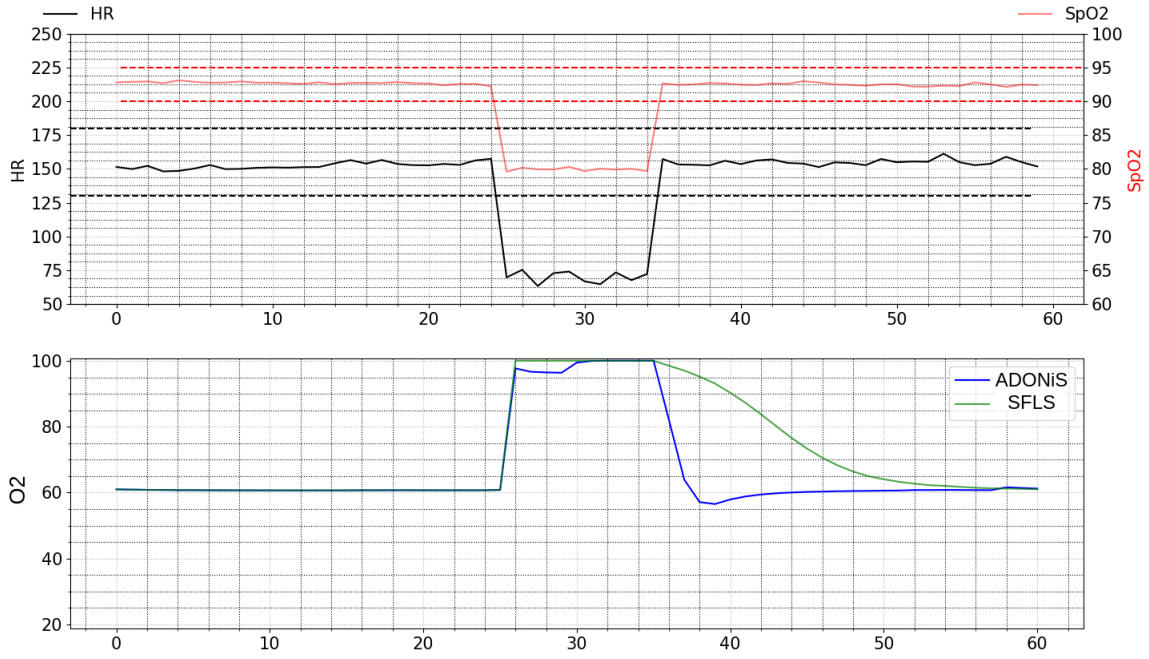

Figure 7.15: Dataset for a longer drop and both models (ADONiS and SFLS) O_2 support level suggestions in the Case Study 5.1.

tions returned to the 60% levels faster than the SFLS.

7.3.6.2 Case Study 5.2 - A *longer significant* increase

The simulated dataset can be seen in the top figure of 7.16. As shown in the bottom figure of Fig. 7.16, both models (ADONiS and SFLS) reacted in a similar manner which is in line with the previous Case Study 5.1.

According to Prof. Don Sharkey, "the actual model in reality would probably fall between both models of ADONiS and SFLS. The rapid increase in O_2 is appropriate, the return to baseline is either too short or too long and should be somewhere in-between of the provided suggestions.

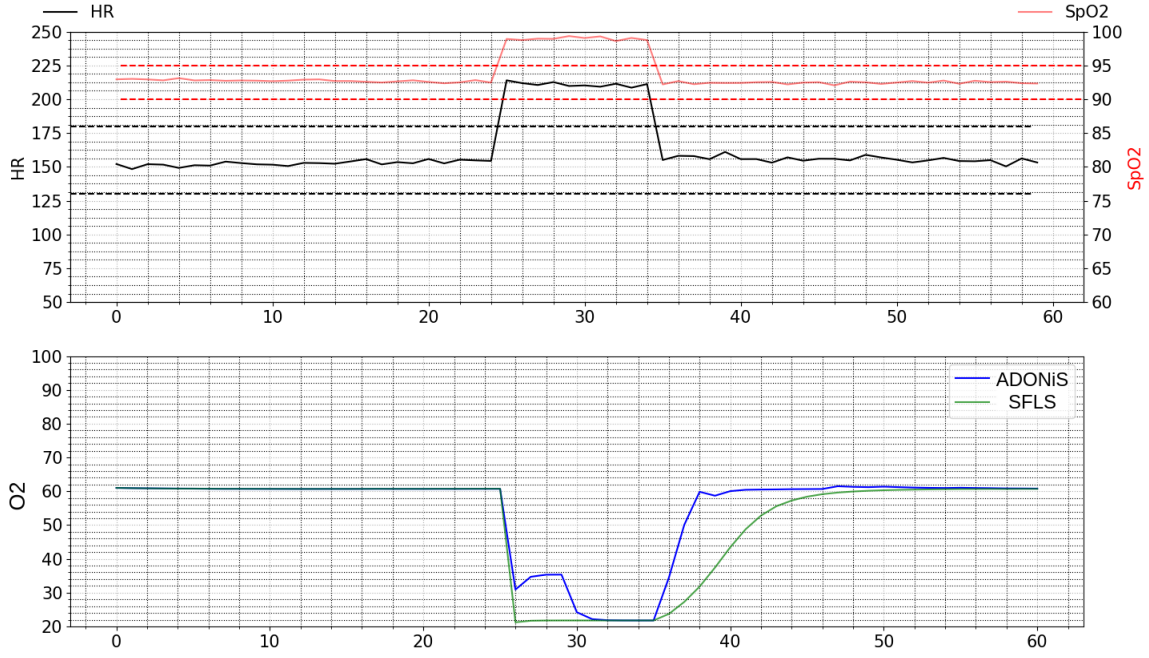

Figure 7.16: Dataset for a longer increase and both models (ADONiS and SFLS) O_2 support level suggestions in the Case Study 5.2.

7.3.7 Actual Dataset Experiment

After completing the case studies and observing/comparing both models (ADONiS and SFLS) behaviours, the given real-world datasets are used to make suggestions of O_2 support levels. As an illustrative sample, a baby dataset (named as *25.csv*) roughly one-hour raw data (per second) is shown in Fig. 7.17.

As the data is collected per second, the illustrated raw one-hour data contains roughly 3600 values for both HR and SpO_2 levels.

In the used models, the O_2 suggestions are implemented every minute. Thus the average of each 60 seconds data is calculated. So that the O_2 suggestions will be delivered for each minute, this averaged dataset can be seen at the top of Fig. 7.18. Note that this averaging procedure leads to 600 values in the dataset. For instance, while the indexing of roughly 3600 HR values was denoted as set $HR(t - \sim 3600), HR(t - \sim 3599), ..., HR(t - 1), HR(t)$, after averaging it is denoted as $HR(t - \sim 3600), HR(t - \sim 3540), ..., HR(t - 60), HR(t))$.

In this datasets, both ADONiS and SFLS O_2 suggestions are illustrated at the bottom of Fig. 7.18. As can be seen, the overall ADONiS model O_2 level suggestions are provided in a *smoother* manner over time.

According to Prof. Don Sharkey, ADONiS provides more preferable O_2 support suggestions. Because "It isn't excessive and allows the baby to return to normal in a more natural way".

The rest of the datasets with O_2 support suggestions for all the collected data can be found in

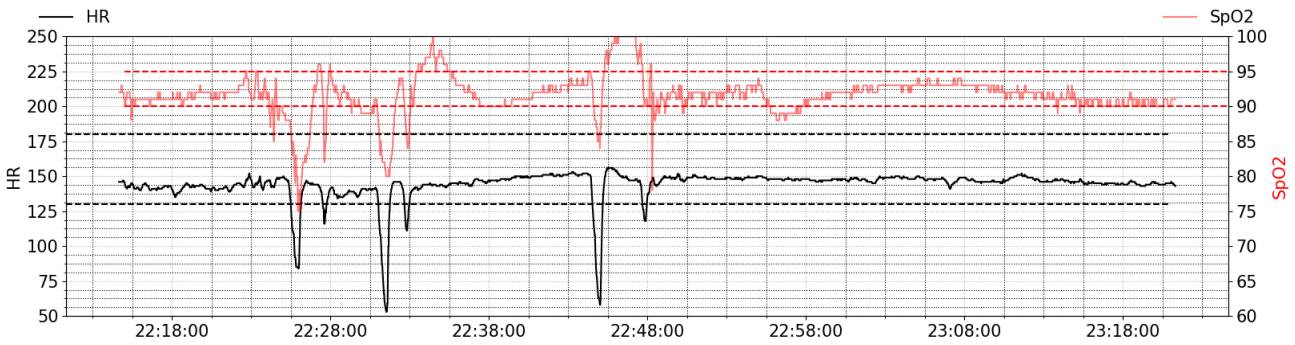

Figure 7.17: Roughly 1 hour HR and SpO_2 levels (per second) of the baby *25*.

Appendix B Section B.3.

7.4 Overall Discussion

As can be seen in the case studies and the real-world data, ADONiS and the SFLS differ in some aspects (e.g. reaction time and O_2 levels outputs).

When HR and SpO_2 levels are synthetically changed for a short time (e.g. as synthetically created in Case Studies 2 and 4), the ADONiS model's initial O_2 level output changes are less than those of the SFLS. Due to the width of the non-singleton input FSs automatically widening (in the case where data has variation), the interaction between input FSs model antecedents leads the initial reaction to be less than SFLS. It can be said that motion artefact or noise from the environments may negatively affect the sensor readings and may cause this type of changes in the HR and SpO_2 input levels. Thus, ADONiS initial reactions are more *cautious* and tend to observe conditions for a determined time interval (window size). Also, while SFLS O_2

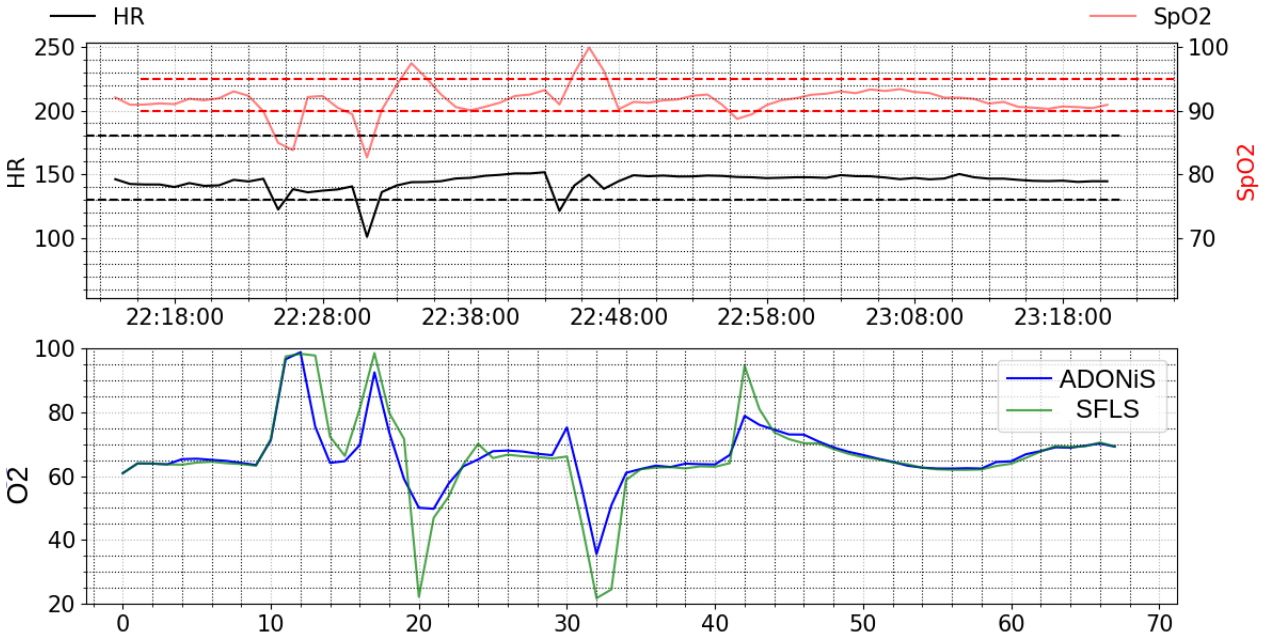

Figure 7.18: 1 hour HR and SpO_2 levels (per minute) of the baby *25* and both models suggestions.

suggestions have sharp changes (e.g. slightly crossing the ideal range [Case Study 2]), due to the adaptive input FSs, ADONiS provides more gradual O_2 outputs changes over the HR and SpO_2 levels domain.

If a baby's condition is changed and continued for a longer time interval (i.e. Case Studies 3 and 5), the O_2 output of the ADONiS model gradually reaches the same values as that of the SFLS. For example, if HR values show a bradycardia condition (lower HR levels than the ideal range), both models react immediately, but initial ADONiS O_2 level outputs are initially not as high as the SFLS. If the HR values are kept at bradycardia levels in the determined time interval, then ADONiS gradually reaches the same O_2 level outputs as SFLS.

Considering no ground truth is available which would enable determining whether an optimal output has been achieved, the academic neonatologist Prof. Don Sharkey were asked to evaluate the outputs. Based on the given opinions, overall, it can be said that ADONiS provides more preferable O_2 level suggestions compared to SFLSs. We note that the focus of this application is to ascertain and illustrate the behaviour of the ADONiS and SFLS and the obtained results appear to be well supported by the medical professional. We note that the results do not enable a general claim in terms of either approach being ideal; nevertheless, based on the empirical case studies and their evaluation, the overall behaviour of the ADONiS system in this setting was deemed to be acceptable by the neonatologist, and more so than the behaviour of a comparable SFLS.

7.5 Summary

Overall, keeping infants' conditions within the targeted range is a crucial task being associated with the risk of severe complications such as chronic diseases and even mortality [156]. As bedside caregivers may not be present and to notice to adjust the O_2 support levels constantly, an automated control design can be beneficial to maintain babies' conditions.

However, this automated control decision-support process is a challenging task in terms of two main aspects. First, it should have the capacity to cope with real-world uncertainty/noise in

sensor data because of the fact that sensors, which measure a baby's condition, can be affected by various factors at different scales and time-periods. Second, there is an expectation from medical professionals to be able to understand the decision making underpinning the oxygen flow in terms of safety, trustworthiness and ethical aspects of clinical tests. Traditionally, while the real-world uncertainty handling capacity is increased in a model, it is likely to cause alteration in model structure (e.g. different MFs or different rules etc.) which may cause poorer interpretability, –as shown in Chapter 6.

In the automated control of breathing support for neonatal babies, the deployability of ADONiS is tested to ascertain and illustrate initial insight in respect to its viability in replacing traditional approaches, in particular standard SFLS. As our aim is to provide initial insights of the deployability of ADONiS, further research and evaluations are required for the implementation of ADONiS to control the O_2 levels of real-world babies.

So far the results show that both models provide reasonable O_2 suggestions based on the created MFs and rules by the academic neonatologist. While the ADONiS model provides more smooth and gradual changes, the SFLS shows more 'agile' patterns in O_2 level suggestions. We note that for the given application and dataset, no ground truth is available which would enable us to determine whether such an optimum has been reached. Since ground truth is not available, the experiment results are evaluated by showing them to the neonatologist to get his opinion on both models' given results.

According to the neonatologist, overall, the ADONiS provides more preferable O_2 level suggestions compared to the traditional SFLS in this particular experimental setting. We note that different experts' opinion may vary based on their experiences. Thus, having opinions from only one medical expert may not be adequate to apply ADONiS in real-world modelling O_2 support. Also, different possible designs in ADONiS structure (e.g. different window size or uncertainty estimation algorithms) can be applied for further research and evaluations.

After having a detailed application of ADONiS on the neonatal baby O_2 support modelling, we now proceed to the conclusion of this thesis.

Chapter 8

Conclusions and Future Work

Due to the diversity of real-world conditions, input uncertainty is one of the principal uncertainties in applications and it often varies in magnitude over-time. Thus, coping with varying input uncertainty becomes a critical task in decision-support systems. Although there is a vast amount of literature on the uncertainty handling in decision-support systems, there are still key aspects to enhance, in particular in respect to maintaining the given interpretability of these systems while handling uncertainty. Fuzzy set theory provides the basis for FLSs which are often associated with the ability of both handling uncertainty and having a capacity of interpretability. In particular, Non-Singleton Fuzzy Logic Systems (NSFLSs) are designed to cope with uncertainty that affects input which is one of the main uncertainty sources in real-world systems. In this thesis, the aim is to further develop input uncertainty capturing and handling capacity while also maintaining 'interpretability' level of systems. In order to achieve this aim, we pursued the following specific list of objectives throughout the thesis.

1. To conduct a critical analysis of the specific behaviour of different firing strength determining approaches in mapping input uncertainty to outputs of NSFLSs, and to put forward a novel approach to generating firing strengths which faithfully handles the uncertainty affecting system inputs.

2. To develop a framework that enables capturing different levels of input uncertainty - as one of the principal sources of uncertainty - and to model the input uncertainty dynami-

cally, on-the-fly, where it arises.

3. To extend the proposed framework with an extra mechanism of adaptation to the magnitude of uncertainty change over time, achieving a compromise between reactivity and smoothness. Thus, to capture both the uncertainty in the last observed value(s) and uncertainty levels variation over time by means of the extra degree of freedom.

4. To maintain the interpretability level of the FLSs through the preservation of the key parameters for interpretability, while also providing an increase in performance of FLSs.

5. To test the deployability of the proposed framework to provide initial insight in respect to its viability in real-world applications.

In the following sections of this chapter, the main contributions of this thesis are summarised, highlighting how the individual objective and thus overall the aim have been addressed throughout the thesis. After that, the limitations and future research direction are presented. In the final section, the list of publications from this thesis is given.

8.1 Contributions and Publications

Chapter 2 outlined an overview of background material and existing literature that were used and referred to in this thesis. A review of the current NSFLS studies was presented with a focus on inference engine and fuzzification steps which are traditionally associated with input uncertainty handling and capturing, respectively. The chapter also highlighted the current research gaps in further developing input uncertainty capacity of NSFLSs. Lastly, the application employed to evaluate the proposed technique and framework in this thesis was also reviewed.

In the inference engine step of NSFLSs, inputs are processed with respect to the system rules through interaction between the input and antecedent FSs. These interactions result in rule firing strengths where input uncertainty is directly reflected on the determined firing strengths in NSFLS. Hence, particularly in NSFLS designs, the firing strength has a vital role in terms of input uncertainty handling.

- **Contribution 1: An alternative subsethood-based composition approach**

  Chapter 3 addressed objective 1, by proposing a novel alternative approach to systematically determine firing strengths. In Chapter 3, we focused on investigating the current and an alternative approach to faithfully mapping input uncertainty to the outputs of systems. First, a critical compare-contrast analysis was carried out on the current firing strength determining techniques and potential challenges in certain conditions were stated which addressed part of objective 1 ('To conduct a critical analysis in exploring the specific behaviour of different firing strength determining approaches in mapping input uncertainty to outputs of NSFLSs'). Building on the critical analysis outcome of the current methods, we then put forward a novel alternative subsethood-based composition approach (named *sub*-NS) with the aim of systematically determining firing strengths that allows an appropriate input uncertainty handling and mapping to the output of NSFLSs –as presented in our studies [120, 122] below.

  [122] **PEKASLAN, D.**, KABIR, S., GARIBALDI, J. M., AND WAGNER, C. Determining firing strengths through a novel similarity measure to enhance uncertainty handling in non-singleton fuzzy logic systems. *In Proceedings of the 9th International Joint Conference on Computational Intelligence - Volume 1: IJCCI, (2017)*, INSTICC, SciTePress, pp. 83–90. (Contribution to Chapter 3)

  [120] **PEKASLAN, D.**, GARIBALDI, J. M., AND WAGNER, C. Exploring subsethood to determine firing strength in non-singleton fuzzy logic systems. *In Fuzzy Systems (FUZZ-IEEE), IEEE International Conference on (2018),* IEEE.(Contribution to Chapter 3)

  In doing so, we fulfil objective 1 ('to put forward a novel approach to generating firing strengths which faithfully handles the uncertainty affecting system inputs.')

As pointed out throughout the thesis, in real-world conditions, a broad range of uncertainty sources can affect inputs and they may vary greatly in magnitude over time. Considering these circumstances of real-world settings, the adaptation of NSFLSs to the varying environments can provide an efficient and effective solution for input uncertainty mapping to outputs of NSFLSs.

- **Contribution 2: The initial version of the ADONiS Framework**

  Chapter 4 addressed objective 2, by developing a framework that enables to dynamically capture different levels of input uncertainty on-the-fly. Therefore, in Chapter 4, we proposed an end-to-end framework (ADaptive Online Non-SIngleton Fuzzy Logic System [ADONiS]) to adaptively configure non-singleton input FSs to the changing uncertainty levels in an online manner. The ADONiS framework can continuously adapt input FS parameters based on information gained from an iterative uncertainty level estimation process over a sequence of observations –as presented in our studies [121, 125, 124] below.

  [121] **PEKASLAN, D.**, GARIBALDI, J. M., AND WAGNER, C. Noise parameter estimation for non-singleton fuzzy logic systems. In *2018 IEEE International Conference on Systems, Man, and Cybernetics (SMC) (2018)*, pp. 2960–2965. (Contribution to Chapter 4 and Chapter 5).

  [125] **PEKASLAN, D.**, WAGNER, C., GARIBALDI, J. M., MARIN, L. G.,AND SÁEZ, D. Uncertainty-aware forecasting of renewable energy sources. *In 2020 IEEE InternationalConference on Big Data and Smart Computing (BigComp)(2020)*, IEEE, pp. 240–246

  [124] **PEKASLAN, D.**, WAGNER, C., AND GARIBALDI, J. M. Adonis—adaptive online non-singleton fuzzy logic systems. *IEEE Transactions on Fuzzy Systems 28, 10 (2020)*, 2302–2312. (Contribution to Chapter 4).

  Thus, ADONiS can provide the ability to dynamically adapt to varying circumstances at run-time without requiring pre-training procedures or a priori knowledge of uncertainty levels in an online manner. Also, by means of the online adaptive ability of ADONiS, the systems can be built upon ‘pure’ rules -for instance, defining rules based on noise-free circumstances- which removes the apprehension for the varying uncertainty levels in real-world settings. In doing so, we fulfilled objective 2 (‘To develop a framework that enables capturing different levels of input uncertainty - as one of the principal sources of uncertainty - and to model the input uncertainty dynamically, on-the-fly, where it arises.’)

The environments of real-world circumstances are often subject to change over time. While some uncertainty sources may exist in a period of time, they may not linger afterwards. Furthermore, the effect of each sources of uncertainty may vary in magnitude over time as well. These real-world settings put serious challenges forward to decision-support systems due to the fact that input uncertainty can vary broadly and drastically over-time. The ADONiS framework demonstrated promising results in capturing levels of uncertainty from the last observed value(s) in input FSs and yet an extra mechanism to capture the varying circumstances can provide additional benefits.

- **Contribution 3: Extending the ADONiS Framework**

  Chapter 5 addressed objective 3, by extending the proposed ADONiS framework with an extra mechanism for capturing the varying circumstances. Therefore, in Chapter 5, we put forward the structure by capturing both the uncertainty in the last observed value(s) and also the variation in uncertainty levels over time. While capturing the last observed input uncertainty adaptively in the principal T1 input FS, the extra degree of freedom (FOU) of IT2 input FSs were used to capture/model the variation in uncertainty levels in an adaptive manner. For instance, in an environment where the circumstances changed drastically, the FOU were automatically adjusted to be wider to capture these variations in uncertainty levels. Additionally, in an environment where the circumstances were stable, the FOUs were automatically adjusted to be narrower. Having different widths and FOUs values dynamically -without requiring a priori knowledge or tuning- can enable models to be being prepared for drastic changes in environments on run-time. Furthermore, when uncertainty can not be fully reflected to the T1 input FSs, the dynamically adjusted FOUs can also provide performance benefits and robustness for the model -as presented in our study [123].

  [123] **PEKASLAN, D.**, WAGNER, C., AND GARIBALDI, J. M. Leveraging IT2 Input Fuzzy Sets in Non-Singleton Fuzzy Logic Systems to Dynamically Adapt to Varying Uncertainty Levels. *IEEE International Conference on Fuzzy Systems 2019-June (2019*). (Contribution to Chapter 5)

In doing so, we fulfilled objective 3 ('To extend the proposed framework with an extra mechanism of assembling the varying circumstances. To capture uncertainty in the last observed value(s) at run-time and also provide the capacity for capturing the variation in environmental conditions as an extra degree of freedom.')

FSs are generally designed with respect to linguistic labels and are interconnected by linguistic rules in FLSs. Thus, FLSs are frequently referred to as 'interpretable' systems which builds one of the key motivations to use FLSs. However, to deal with varying circumstances of real-world settings, approaches mostly inherited numerical learning techniques (e.g. parametric equations or statistical optimisation techniques) to tune parameters based on data-driven approaches. While these procedures provide performance benefits, they often cause alteration in key parameters, such as fuzzy rule sets, rule parameters, MFs or fuzzy partitioning structures with high accuracy but commonly do not consider whether the resulting model is interpretable or not.

- **Contribution 4: Maintaining Interpretability**

  Chapter 6 addressed objective 4, by maintaining the given interpretability level while increasing the performance of FLSs. Therefore, in Chapter 6, the focus was expanded to encompass interpretability, considering specifically whether the mechanisms developed in Chapters 3 - 5 can be usefully applied to maintain given interpretability of models by minimising altering the given FLS parameters. The performance increase was achieved by enabling to model uncertainty 'where it arises' and handling it through the given rules. Particularly, input uncertainty (e.g. noise in the heart rate sensor) was captured dynamically in the fuzzification step and handled in interactions between input and antecedent FSs in the inference engine step. Thus, while the performance increase was achieved, ADONiS frameworks limited any optimisation impact to the fuzzification and inference engine steps -as presented in our study [119].

  [119] **PEKASLAN, D.**, CHEN, C., WAGNER, C., AND GARIBALDI, J. M. Performance and interpretability in fuzzy logic systems – can we have both? *In Information Processing and Management of Uncertainty in Knowledge-Based Systems (Cham, 2020)*,

M.-J. Lesot, S. Vieira, M. Z. Reformat, J. P. Carvalho, A. Wilbik, B. Bouchon-Meunier, and R. R. Yager, Eds., Springer International Publishing, pp. 571–584. (Contribution to Chapter 6)

In doing so, different components of FLSs such as MFs, antecedents, consequent etc. remained 'untouched'. Thus, while dealing with different input uncertainty levels on run-time, the initially given interpretability degree can be protected and the FSs or rules remain meaningful –if they were understood well initially. In doing so, we fulfilled objective 4 ('To maintain the interpretability level of the FLSs through the preservation of the key parameters for interpretability, while also providing an increase in performance of FLSs.')

As the next step, the deployability of the proposed framework is tested to provide initial insight in respect to its viability in real-world applications. As this thesis writing period was carried out during the international COVID-19 crisis in 2020, a related automated control of breathing support for neonatal babies experiments were conducted. Estimations show that around 15 million premature birth incidents happen around the world annually and a significant proportion of these premature infants need mechanical respiratory support in a period following their birth. Reports show that manual O_2 level adjustments often cause infants to spend a significant amount of time outside of the targeted range which may cause chronic diseases and even mortality. Thus, automated decision-making to provide O_2 level suggestions can be a useful tool while it involves the following aspects (i) handling uncertainty in sensor measurements (ii) an expectation from the medical professionals to be able to understand the decision making underpinning the oxygen flow.

- **Contribution 5: The deployability of ADONiS in a Medical Case Study**

  Chapter 7 moved beyond time-series prediction towards a real-world case study which was in part motivated by the international COVID-19 crisis in 2020. Objective 5 addressed by implementing ADONiS in the aforementioned automated control of oxygenation support for neonatal babies which tested the deployability to ascertain and illustrate initial insight in respect to ADONiS viability in replacing traditional approaches, in par-

ticular standard SFLS. While the system (i.e. rules and MFs) was designed by medical professionals, the sensory input (i.e heart rate and SpO_2) uncertainty was captured and handled in the fuzzification and inference engine steps. Thus, while input uncertainty was handled on-the-fly, the initially given interpretability was preserved. The ADONiS O_2 level suggestion results were verified by asking opinions from the medical professionals. In doing so, we fulfilled objective 5 ('To test the deployability of the proposed framework to provide initial insight in respect to its viability in real-world applications.')

After providing a detailed conclusion and contributions for each chapter, we will now discuss the limitations and future works of this thesis.

8.2 Limitations and Future Works

In decision-support models, various uncertainty types exist and input uncertainty is one of the primary sources of uncertainty in real-world applications. In this thesis, we focused specifically on further developing input uncertainty capturing and handling capacity through the mapping from input to the outputs of FLSs. Thus, this thesis does not address all sources of uncertainty types. Furthermore, while applying the proposed approaches to increase performances, we focused specifically to preserve the interpretability of FLSs. Thus, this thesis does not address the interpretability concept in different systems but specifically focused on FLSs.

In Chapter 3, an alternative *sub*-NS approach is proposed to generate firing strengths which can enhance handling input uncertainty of NSFLSs. Although a faithful input uncertainty mapping has been achieved and generally better time-series prediction performances (MSEs) have been obtained by using *sub*-NS approach, if a model was specifically built on 'agreement' between input and antecedent FSs, we note that other approaches' (e.g. *sim*-NS) firing strengths may produce intuitively expected firing levels. Furthermore, the proposed alternative approach has only been investigated in time-series forecasting application with only two commonly used chaotic time-series datasets. Therefore, the future research direction will require *sub*-NS to be analysed over different datasets and moreover, a variety of application areas where inputs are af-

fected by uncertainty sources (e.g. robotics) will be explored. If the results from such datasets and different applications will demonstrate the ability of faithful input uncertainty mapping to the outputs of systems, this will point towards the idea that the *sub*-NS can be a suitable approach to be used in applications where inputs may contain different levels of uncertainty. However, we acknowledge that these investigations would go beyond this thesis research.

In Chapters 4 and 5, the ADONiS and the extended IT2 ADONiS framework have been proposed which used the noise estimation algorithm -to inform input FSs- over an iterative frame of a sequence of observations. Although an increase in accuracy has been achieved and interesting insights have been obtained in time-series forecasting studies, given the small set of experiments and adoption of the single noise estimation algorithm, these results can only represent an initial step towards the general conclusion and real-world applications eventually. Therefore, further experimental investigations will be carried out in a variety of application domains by also employing different components (e.g. different noise estimation algorithms or dynamic frame sizes) of the ADONiS and the extended IT2 ADONiS frameworks.

In Chapter 6, the proposed framework implementation has been explored in the context of whether it can be usefully applied to maintain the interpretability level of systems. As mentioned, the uncertainty is captured in fuzzification and it is handled through the system rules without altering the model's interpretability parameters (e.g. MFs, number of rules or rule parameters etc.). The experimental investigation has been limited to time-series predictions. Furthermore, only a single model (ANFIS) has been used to make a comparison in terms of interpretability. We believe that these initial results highlight an interesting research direction for FLSs which can maintain interpretability by modelling complexity only in specific parts of their structure (e.g. the fuzzification or the inference engine steps). Future work will concentrate on expanding the experimental evaluation with different models, datasets on different domains while broadening the capacity for optimisation beyond the specific design of ADONiS frameworks. Also, interpretability indices will be explored to evaluate the comparison of different models regarding performance and interpretability ability.

In Chapter 7, a limited number of experiments have been implemented on a single application

of the neonatal baby O_2 support modelling without any real-world deployment. Furthermore, these experiments have been limited by the fact that there is no ground truth available to validate the suggested O_2 levels from the ADONiS and SFLSs. Therefore, there has been a reliance on opinions from the neonatologist to verify the results. It should also be noted that having opinion from a single expert may not be adequate as different experts may have different opinion or uncertainty in opinions. Multiple expert opinion is naturally lead to a Type-2 system which would would go beyond this thesis research. In order to deploy the proposed ADONiS framework in the future, we will seek to expand different medical datasets which have ground truth for evaluation. Also, the maintained interpretability aspects will be evaluated by gathering expert opinions. After these comprehensive evaluations on both the accuracy and interpretability of the system, ADONiS can be a useful aid in modelling O_2 support.

Additionally, in Chapter 5, one of the time-series forecasting experiments has demonstrated that the least chosen FOU sizes provided the optimal performance –where the principal T1 input FSs were designed by ADONiS (please see 5.3.2 for details). Hence, in the future, an additional analysis of the T1 ADONiS framework compared to traditional T2 FLSs will be further evaluated to explore an answer to the question of 'If the input uncertainty is properly captured in T1 input FSs, would traditional T2 systems (T2 inputs or antecedent FSs) be still more advantages than T1 systems?' We note that this study would involve a large body of work which would go beyond this thesis.

On a wider level, thus far, the experimental settings have been limited to time-series datasets and the real-world evaluation were limited to only a single medical case study. Intuitively, one future project would be to explore the integration of the proposed *sub*-NS into the ADONiS frameworks for further evaluation in different application domains which may further inform the suitability of using the integrated ADONiS and *sub*-NS frameworks.

Bibliography

[1] "uncertainty". *Cambridge Advanced Learner's Dictionary & Thesaurus* (2020). Accessed on: Jun. 8, 2020. [Online] Available at `https://dictionary.cambridge.org/dictionary/english/uncertainty`.

[2] AKPOLAT, Z. H. Non-singleton fuzzy logic control of a dc motor. *Journal of Applied Sciences 5*, 5 (2005), 887–891.

[3] ALONSO, J. M., CASTIELLO, C., AND MENCAR, C. *Interpretability of Fuzzy Systems: Current Research Trends and Prospects*. Springer Berlin Heidelberg, Berlin, Heidelberg, 2015, pp. 219–237.

[4] ALONSO, J. M., MAGDALENA, L., AND GONZÁLEZ-RODRÍGUEZ, G. Looking for a good fuzzy system interpretability index: An experimental approach. *International Journal of Approximate Reasoning 51*, 1 (2009), 115 – 134.

[5] ARMSTRONG, J. S. Measures of Accuracy. In *Long-Range Forecasting: From Crystal Ball to Computer*, A Wiley-Interscience Publication. Wiley, 1985, pp. 346–354.

[6] ARSLAN, A. *İlkçağ felsefe tarihi: Sokrates öncesi Yunan felsefesi*. İstanbul Bilgi Üniversitesi Yayınları, 2006.

[7] ATSALAKIS, G. S., AND VALAVANIS, K. P. Forecasting stock market short-term trends using a neuro-fuzzy based methodology. *Expert Systems with Applications 36*, 7 (2009), 10696–10707.

[8] AZADEH, A., SABERI, M., GITIFOROUZ, A., AND SABERI, Z. A hybrid simulation-adaptive network based fuzzy inference system for improvement of electricity consumption estimation. *Expert Systems with Applications 36*, 8 (2009), 11108–11117.

[9] BAI, Y., AND WANG, D. Fundamentals of fuzzy logic control—fuzzy sets, fuzzy rules and defuzzifications. In *Advanced Fuzzy Logic Technologies in Industrial Applications*. Springer, 2006, pp. 17–36.

[10] BALAZINSKI, M., CZOGALA, E., AND SADOWSKI, T. Control of metal-cutting process using neural fuzzy controller. In *[Proceedings 1993] Second IEEE International Conference on Fuzzy Systems* (1993), pp. 161–166 vol.1.

[11] BANCALARI, E., AND CLAURE, N. Advances in respiratory support for high risk newborn infants. *Maternal health, neonatology and perinatology 1*, 1 (2015), 1–10.

[12] BENEDETTI, M., CASAGRANDA, A., DONELLI, M., AND MASSA, A. An adaptive multiscaling imaging technique based on a fuzzy-logic strategy for dealing with the uncertainty of noisy scattering data. *IEEE Transactions on Antennas and Propagation 55*, 11 (2007), 3265–3278.

[13] BOJADZIEV, G. *Fuzzy logic for business, finance, and management*, vol. 23. World Scientific, 2007.

[14] BOOLE, G. *The mathematical analysis of logic*. Philosophical Library, 1847.

[15] BORAN, F. E., GENÇ, S., KURT, M., AND AKAY, D. A multi-criteria intuitionistic fuzzy group decision making for supplier selection with topsis method. *Expert Systems with Applications 36*, 8 (2009), 11363–11368.

[16] BOUCHON-MEUNIER, B., DELECHAMP, J., MARSALA, C., AND RIFQI, M. Several forms of fuzzy analogical reasoning. In *Proceedings of 6th International Fuzzy Systems Conference* (July 1997), vol. 1, pp. 45–50 vol.1.

[17] BOUHID, A. Q. Z., AMARAL, R. P. F., DA FONSECA, L. G., AND DE AGUIAR, E. P. Classification of faults in a switch machine using type-1 and non-singleton fuzzy logic system trained by hestenes and stiefel's conjugate gradient method.

[18] BUROKER, J. Port royal logic.

[19] CARA, A. B., WAGNER, C., HAGRAS, H., POMARES, H., AND ROJAS, I. Multiobjective optimization and comparison of nonsingleton type-1 and singleton interval type-2 fuzzy logic systems. *IEEE Trans. Fuzzy Syst. 21*, 3 (June 2013), 459–476.

[20] CARUANA, R., LOU, Y., GEHRKE, J., KOCH, P., STURM, M., AND ELHADAD, N. Intelligible models for healthcare: Predicting pneumonia risk and hospital 30-day readmission. In *Proceedings of the 21th ACM SIGKDD international conference on knowledge discovery and data mining* (2015), pp. 1721–1730.

[21] CASILLAS, J., CORDÓN, O., HERRERA, F., AND MAGDALENA, L. *Accuracy Improvements to Find the Balance Interpretability-Accuracy in Linguistic Fuzzy Modeling: An Overview*. Springer Berlin Heidelberg, Berlin, Heidelberg, 2003, pp. 3–24.

[22] CASILLAS, J., CORDÓN, O., HERRERA, F., AND MAGDALENA, L. Interpretability Improvements to Find the Balance Interpretability-Accuracy in Fuzzy Modeling: An Overview. 3–22.

[23] CASTELLANO, G., FANELLI, A. M., AND MENCAR, C. A neuro-fuzzy network to generate human-understandable knowledge from data. *Cognitive Systems Research 3*, 2 (2002), 125 – 144. Integration of Symbolic and Connectionist Systems.

[24] CASTRO, J. R., CASTILLO, O., MELIN, P., AND RODRÍGUEZ-DÍAZ, A. A hybrid learning algorithm for a class of interval type-2 fuzzy neural networks. *Information Sciences 179*, 13 (2009), 2175 – 2193. Special Section on High Order Fuzzy Sets.

[25] CAVALLARO, E., MICERA, S., DARIO, P., JENSEN, W., AND SINKJÆR, T. On the intersubject generalization ability in extracting kinematic information from afferent nervous signals. *IEEE Transactions on Biomedical Engineering 50*, 9 (2003), 1063–1073.

[26] CHEN, C., JOHN, R., TWYCROSS, J., AND GARIBALDI, J. M. An extended ANFIS architecture and its learning properties for type-1 and interval type-2 models. In *Proceedings IEEE International Conference on Fuzzy Systems* (2016), pp. 602–609.

[27] CHEN, C., TWYCROSS, J., AND GARIBALDI, J. M. A new accuracy measure based on bounded relative error for time series forecasting. *PLOS ONE 12*, 3 (2017), 1–23.

[28] CHEN, S. M. A new approach to handling fuzzy decision-making problems. *IEEE Trans. Syst., Man, Cybern. 18*, 6 (Nov 1988), 1012–1016.

[29] CHEN, S.-M. A weighted fuzzy reasoning algorithm for medical diagnosis. *Decision Support Systems 11*, 1 (1994), 37 – 43.

[30] CHENG-JIAN LIN, TZU-CHAO LIN, AND CHIN-LING LEE. An asymmetry subsethood-based neural fuzzy network. In *The 2006 IEEE International Joint Conference on Neural Network Proceedings* (2006), pp. 2852–2858.

[31] CHI, Z., WU, J., AND YAN, H. Handwritten numeral recognition using self-organizing maps and fuzzy rules. *Pattern Recognition 28*, 1 (1995), 59 – 66.

[32] CHUA, T. W., AND TAN, W. W. Non-singleton genetic fuzzy logic system for arrhythmias classification. *Engineering Applications of Artificial Intelligence 24*, 2 (2011), 251–259.

[33] CLARKE, A., YEOMANS, E., ELSAYED, K., MEDHURST, A., BERGER, P., SKUZA, E., AND TAN, K. A randomised crossover trial of clinical algorithm for oxygen saturation targeting in preterm infants with frequent desaturation episodes. *Neonatology 107*, 2 (2015), 130–136.

[34] CORNELIS, C., AND KERRE, E. Inclusion-based approximate reasoning. pp. 221–230.

[35] COUPLAND, S., GONGORA, M. A., JOHN, R., AND WILLS, K. A comparative study of fuzzy logic controllers for autonomous robots. 1332–1339.

[36] CROSS, V., AND SUDKAMP, T. Geometric compatibility modification. *Fuzzy Sets and Systems 84*, 3 (1996), 283–299.

[37] DANI, C. Automated control of inspired oxygen (fio2) in preterm infants: Literature review. *Pediatric Pulmonology 54*, 3 (2019), 358–363.

[38] DE AGUIAR, E. P., DE A. NOGUEIRA, F. M., VELLASCO, M. M. B. R., AND RIBEIRO, M. V. Set-membership type-1 fuzzy logic system applied to fault classification in a switch machine. *EEE Trans. Intell. Transp. Syst. 18*, 10 (Oct 2017), 2703–2712.

[39] DOMBI, J. A general class of fuzzy operators, the demorgan class of fuzzy operators and fuzziness measures induced by fuzzy operators. *Fuzzy Sets and Systems 8*, 2 (1982), 149 – 163.

[40] DOSHI-VELEZ, F., AND KIM, B. Towards a rigorous science of interpretable machine learning. *arXiv preprint arXiv:1702.08608* (2017).

[41] DUBOIS, D. J. *Fuzzy sets and systems: theory and applications*, vol. 144. Academic press, 1980.

[42] ELGENDI, M. Optimal signal quality index for photoplethysmogram signals. *Bioengineering 3*, 4 (2016), 21.

[43] ESFAHANIPOUR, A., AND AGHAMIRI, W. Adapted neuro-fuzzy inference system on indirect approach TSK fuzzy rule base for stock market analysis. *Expert Systems with Applications 37*, 7 (2010), 4742–4748.

[44] ESTEVA, F., GARCIA, P., GODO, L., AND RODRÍGUEZ, R. A modal account of similarity-based reasoning. *International Journal of Approximate Reasoning 16*, 3-4 (1997), 235–260.

[45] EYOH, I., JOHN, R., DE MAERE, G., AND KAYACAN, E. Hybrid learning for interval type-2 intuitionistic fuzzy logic systems as applied to identification and prediction problems. *IEEE Transactions on Fuzzy Systems 26*, 5 (Oct 2018), 2672–2685.

[46] FAN, J., XIE, W., AND PEI, J. Subsethood measure: new definitions. *Fuzzy Sets and Systems 106*, 2 (1999), 201–209.

[47] FATHABADI, O. S., GALE, T. J., OLIVIER, J., AND DARGAVILLE, P. A. Automated control of inspired oxygen for preterm infants: what we have and what we need. *Biomedical Signal Processing and Control 28* (2016), 9–18.

[48] FERRERO, A., AND SALICONE, S. Fully comprehensive mathematical approach to the expression of uncertainty in measurement. *IEEE Transactions on Instrumentation and Measurement 55*, 3 (2006), 706–712.

[49] FIGUEROA, J., POSADA, J., SORIANO, J., MELGAREJO, M., AND ROJAS, S. A type-2 fuzzy controller for tracking mobile objects in the context of robotic soccer games. In *The 14th IEEE International Conference on Fuzzy Systems, 2005. FUZZ '05.* (May 2005), pp. 359–364.

[50] FLAMM, D. History and outlook of statistical physics, 1998.

[51] FU, C., SARABAKHA, A., KAYACAN, E., WAGNER, C., JOHN, R., AND GARIBALDI, J. M. A comparative study on the control of quadcopter uavs by using singleton and non-singleton fuzzy logic controllers. In *2016 IEEE International Conference on Fuzzy Systems (FUZZ-IEEE)* (July 2016), pp. 1023–1030.

[52] FU, C., SARABAKHA, A., KAYACAN, E., WAGNER, C., JOHN, R., AND GARIBALDI, J. M. Similarity-based non-singleton fuzzy logic control for improved performance in uavs. In *2017 IEEE International Conference on Fuzzy Systems (FUZZ-IEEE)* (July 2017), pp. 1–6.

[53] FU, C., SARABAKHA, A., KAYACAN, E., WAGNER, C., JOHN, R., AND GARIBALDI, J. M. Input uncertainty sensitivity enhanced nonsingleton fuzzy logic controllers for long-term navigation of quadrotor uavs. *IEEE/ASME Transactions on Mechatronics 23*, 2 (April 2018), 725–734.

[54] GACTO, M. J., ALCALÁ, R., AND HERRERA, F. Interpretability of linguistic fuzzy rule-based systems: An overview of interpretability measures. *Information Sciences 181*, 20 (2011), 4340–4360.

[55] GAFA, C., AND COUPLAND, S. A new recursive type-reduction procedure for general type-2 fuzzy sets. In *2011 IEEE Symposium on Advances in Type-2 Fuzzy Logic Systems (T2FUZZ)* (2011), pp. 44–49.

[56] GALENDE, M., SAINZ, G., AND FUENTE, M. Accuracy-interpretability trade-off for precise fuzzy modeling using simple indices. application to industrial plants1. *IFAC Proceedings Volumes 44*, 1 (2011), 12656 – 12661. 18th IFAC World Congress.

[57] GARIBALDI, J. M., AND OZEN, T. Uncertain Fuzzy Reasoning: A Case Study in Modelling Expert Decision Making. *IEEE Transactions on Fuzzy Systems 15*, 1 (feb 2007), 16–30.

[58] GAWEDA, A. E., JACOBS, A. A., ARONOFF, G. R., AND BRIER, M. E. Perception-based expert system with application to clinical decision making. In *2004 IEEE International Conference on Fuzzy Systems (IEEE Cat. No.04CH37542)* (2004), vol. 2, pp. 907–910 vol.2.

[59] GODO, L., AND RODRÍGUEZ, R. O. *A Fuzzy Modal Logic for Similarity Reasoning*. Springer US, Boston, MA, 1999, pp. 33–48.

[60] GONZÁLEZ, J., ROJAS, I., POMARES, H., HERRERA, L. J., GUILLÉN, A., PALOMARES, J. M., AND ROJAS, F. Improving the accuracy while preserving the interpretability of fuzzy function approximators by means of multi-objective evolutionary algorithms. *International Journal of Approximate Reasoning 44*, 1 (2007), 32 – 44. Genetic Fuzzy Systems and the Interpretability–Accuracy Trade-off.

[61] GOU, J., HOU, F., CHEN, W., WANG, C., AND LUO, W. Improving wang–mendel method performance in fuzzy rules generation using the fuzzy c-means clustering algorithm. *Neurocomputing 151* (2015), 1293 – 1304.

[62] GUILLAUME, S. Designing fuzzy inference systems from data: An interpretability-oriented review. *IEEE Transactions on Fuzzy Systems 9*, 3 (2001), 426–443.

[63] GUILLAUME, S., AND CHARNOMORDIC, B. Generating an interpretable family of fuzzy partitions from data. *IEEE Transactions on Fuzzy Systems 12*, 3 (2004), 324–335.

[64] GUILLAUME, S., AND CHARNOMORDIC, B. Generating an interpretable family of fuzzy partitions from data. *IEEE Transactions on Fuzzy Systems 12*, 3 (2004), 324–335.

[65] HAYASHI, Y., BUCKLEY, J. J., AND CZOGALA, E. Fuzzy neural network with fuzzy signals and weights. In *[Proceedings 1992] IJCNN International Joint Conference on Neural Networks* (1992), vol. 2, pp. 696–701 vol.2.

[66] HIDALGO, D., MELIN, P., AND CASTRO, J. R. *Non-singleton Interval Type-2 Fuzzy Systems as Integration Methods in Modular Neural Networks Used Genetic Algorithms to Design*. Springer International Publishing, Cham, 2017, pp. 821–838.

[67] HUTTOVA, V., RAFL, J., MÖLLER, K., BACHMAN, T. E., KUDRNA, P., ROZANEK, M., AND ROUBIK, K. Model of spo2 signal of the neonate. *Current Directions in Biomedical Engineering 5*, 1 (2019), 549–552.

[68] JACCARD, P. *Nouvelles recherches sur la distribution florale*. 1908.

[69] JANG, J. . R., AND SUN, C. . Predicting chaotic time series with fuzzy if-then rules. In *[Proceedings 1993] Second IEEE International Conference on Fuzzy Systems* (1993), pp. 1079–1084 vol.2.

[70] JANG, J.-S. ANFIS: adaptive-network-based fuzzy inference system. *IEEE Transactions on Systems, Man, and Cybernetics 23*, 3 (1993), 665–685.

[71] JIN, Y. Fuzzy modeling of high-dimensional systems: Complexity reduction and interpretability improvement. *IEEE Transactions on Fuzzy Systems 8*, 2 (2000), 212 – 221.

[72] KHANESAR, M. A., KAYACAN, E., TESHNEHLAB, M., AND KAYNAK, O. Analysis of the noise reduction property of type-2 fuzzy logic systems using a novel type-2 membership function. *IEEE Transactions on Systems, Man, and Cybernetics, Part B (Cybernetics) 41*, 5 (2011), 1395–1406.

[73] KHANESAR, M. A., KAYACAN, E., TESHNEHLAB, M., AND KAYNAK, O. Extended Kalman Filter Based Learning Algorithm for Type-2 Fuzzy Logic Systems and Its Exper-

imental Evaluation. *IEEE Transactions on Industrial Electronics 59*, 11 (2012), 4443–4455.

[74] KIM, B., WATTENBERG, M., GILMER, J., CAI, C., WEXLER, J., VIEGAS, F., AND SAYRES, R. Interpretability beyond feature attribution: Quantitative testing with concept activation vectors (tcav). *arXiv preprint arXiv:1711.11279* (2017).

[75] KLIR, G., AND YUAN, B. *Fuzzy Sets and Fuzzy Logic: Theory and Applications*. Prentice Hall PTR, 1995.

[76] KLIR, G. J. *Uncertainty and Information: Foundations of Generalized Information Theory*. 2005.

[77] KNEALE, W., KNEALE, W. C., AND KNEALE, M. *The development of logic*. Oxford University Press, 1962.

[78] KOSKO, B. Fuzziness vs. probability. *International Journal of General System 17*, 2-3 (1990), 211–240.

[79] LAPTOOK, A., SALHAB, W., ALLEN, J., SAHA, S., AND WALSH, M. Pulse oximetry in very low birth weight infants: can oxygen saturation be maintained in the desired range? *Journal of perinatology 26*, 6 (2006), 337–341.

[80] LI-XIN WANG. The wm method completed: a flexible fuzzy system approach to data mining. *IEEE Transactions on Fuzzy Systems 11*, 6 (Dec 2003), 768–782.

[81] LIU, F., AND MENDEL, J. M. An interval approach to fuzzistics for interval type-2 fuzzy sets. In *2007 IEEE International Fuzzy Systems Conference* (July 2007), pp. 1–6.

[82] LIU, H., GEGOV, A., AND COCEA, M. Complexity Control in Rule Based Models for Classification in Machine Learning Context. In *Advances in Computational Intelligence Systems* (Cham, 2017), P. Angelov, A. Gegov, C. Jayne, and Q. Shen, Eds., Springer International Publishing, pp. 125–143.

[83] LIU, X., TANAKA, M., AND OKUTOMI, M. Single-image noise level estimation for blind denoising. *IEEE Trans. Image Process. 22*, 12 (Dec 2013), 5226–5237.

[84] LORENZ, E. N. Deterministic nonperiodic flow. *Journal of the atmospheric sciences 20*, 2 (1963), 130–141.

[85] MACKEY, M. C., GLASS, L., ET AL. Oscillation and chaos in physiological control systems. *Science 197*, 4300 (1977), 287–289.

[86] MAGREZ, P., AND SMETS, P. Fuzzy modus ponens: A new model suitable for applications in knowledge-based systems. *International Journal of Intelligent Systems 4* (06 1989), 181 – 200.

[87] MAKROPOULOS, C., AND BUTLER, D. Spatial decisions under uncertainty: fuzzy inference in urban water management. *Journal of Hydroinformatics 6*, 1 (2004), 3–18.

[88] MAMDANI, E. H., AND ASSILIAN, S. An experiment in linguistic synthesis with a fuzzy logic controller. *International journal of man-machine studies 7*, 1 (1975), 1–13.

[89] MARTÍNEZ-SOTO, R., CASTILLO, O., AND CASTRO, J. R. *Genetic Algorithm Optimization for Type-2 Non-singleton Fuzzy Logic Controllers*. Springer International Publishing, Cham, 2014, pp. 3–18.

[90] MEADE, N., AND ARMSTRONG, J. Long range forecasting: From crystal ball to computer (2nd edition). *The Journal of the Operational Research Society 37* (05 1986), 533.

[91] MELIN, P., AND CASTILLO, O. A new method for adaptive control of non-linear plants using type-2 fuzzy logic and neural networks. *International Journal of General Systems 33*, 2-3 (2004), 289–304.

[92] MENCAR, C., CASTELLANO, G., AND FANELLI, A. M. Distinguishability quantification of fuzzy sets. *Information Sciences 177*, 1 (2007), 130 – 149. Zdzislaw Pawlak life and work (1926–2006).

[93] MENCAR, C., AND FANELLI, A. M. Interpretability constraints for fuzzy information granulation. *Information Sciences 178*, 24 (2008), 4585–4618.

[94] MENDEL, J. M. *Uncertain rule-based fuzzy logic systems: introduction and new directions*. Prentice Hall PTR Upper Saddle River, 2001.

[95] MENDEL, J. M., JOHN, R. I., AND LIU, F. Interval type-2 fuzzy logic systems made simple. *IEEE Transactions on Fuzzy Systems 14*, 6 (2006), 808–821.

[96] MENDEZ, G. M., AND DE LOS ANGELES HERNANDEZ, M. Interval type-2 non-singleton type-2 takagi-sugeno-kang fuzzy logic systems using the hybrid learning mechanism recursive-least-square and back-propagation methods. In *2010 11th International Conference on Control Automation Robotics Vision* (2010), pp. 710–714.

[97] MÉNDEZ, G. M., AND DE LOS ANGELES HERNÁNDEZ, M. Hybrid learning mechanism for interval A2-C1 type-2 non-singleton type-2 Takagi-Sugeno-Kang fuzzy logic systems. *Information Sciences 220* (2013), 149–169.

[98] MENDEZ, G. M., AND HERNANDEZ, A. Hybrid IT2 NSFLS-1 Used to Predict the Uncertain MXNUSD Exchange Rate. In *Hybrid Artificial Intelligence Systems* (Berlin, Heidelberg, 2008), E. Corchado, A. Abraham, and W. Pedrycz, Eds., Springer Berlin Heidelberg, pp. 575–582.

[99] MENHAJ, M. B., SURATGAR, A. A., AND KARRARI, M. A modified dynamic non-singleton fuzzy logic system for nonlinear modeling. In *IJCNN'99. International Joint Conference on Neural Networks. Proceedings (Cat. No. 99CH36339)* (1999), vol. 6, IEEE, pp. 4357–4361.

[100] MIKUT, R., JÄKEL, J., AND GRÖLL, L. Interpretability issues in data-based learning of fuzzy systems. *Fuzzy sets and systems 150*, 2 (2005), 179–197.

[101] MILLER, G. A. The magical number seven, plus or minus two: Some limits on our capacity for processing information. *Psychological review 63*, 2 (1956), 81.

[102] MISHRA, A., AND ZAHEERUDDIN. Hybrid fuzzy neural network based still image compression. In *2010 International Conference on Computational Intelligence and Communication Networks* (2010), pp. 116–121.

[103] MOHAMMADZADEH, A., GHAEMI, S., KAYNAK, O., AND KHANMOHAMMADI, S. Robust H_∞-based synchronization of the fractional-order chaotic systems by using new

self-evolving nonsingleton type-2 fuzzy neural networks. *IEEE Transactions on Fuzzy Systems 24*, 6 (2016), 1544–1554.

[104] MOUZOURIS, G. C., AND MENDEL, J. M. Non-singleton fuzzy logic systems. In *Proceedings of 1994 IEEE 3rd International Fuzzy Systems Conference* (1994), pp. 456–461 vol.1.

[105] MOUZOURIS, G. C., AND MENDEL, J. M. Nonlinear time-series analysis with non-singleton fuzzy logic systems. In *Computational Intelligence for Financial Engineering, 1995., Proceedings of the IEEE/IAFE 1995* (1995), IEEE, pp. 47–56.

[106] MOUZOURIS, G. C., AND MENDEL, J. M. Dynamic non-singleton fuzzy logic systems for nonlinear modeling. *IEEE Transactions on Fuzzy Systems 5*, 2 (1997), 199–208.

[107] MOUZOURIS, G. C. G., AND MENDEL, J. M. J. Nonsingleton fuzzy logic systems: theory and application. *IEEE Transactions on Fuzzy Systems 5*, 1 (1997), 56–71.

[108] NARAYAN, A., HIPEL, K. W., PONNAMBALAM, K., AND PAUL, S. Neuro-fuzzy inference system (asupfunis) model for intervention time series prediction of electricity prices. In *2011 IEEE International Conference on Systems, Man, and Cybernetics* (2011), pp. 2121–2126.

[109] NARAYEN, I. C., SMIT, M., VAN ZWET, E. W., DAWSON, J. A., BLOM, N. A., AND TE PAS, A. B. Low signal quality pulse oximetry measurements in newborn infants are reliable for oxygen saturation but underestimate heart rate. *Acta Paediatrica 104*, 4 (2015), e158–e163.

[110] NIE, M., AND WOEI WAN TAN. Closed form formulas for computing the centroid of a general type-2 fuzzy set. In *2015 IEEE International Conference on Fuzzy Systems (FUZZ-IEEE)* (2015), pp. 1–8.

[111] PAIVA, R. P., AND DOURADO, A. Interpretability and learning in neuro-fuzzy systems. *Fuzzy Sets and Systems 147*, 1 (2004), 17 – 38. Hybrid Methods for Adaptive Systems.

[112] PAL, A., MONDAL, B., BHATTACHARYYA, N., AND RAHA, S. Similarity in fuzzy systems. *Journal of Uncertainty Analysis and Applications 2*, 1 (2014), 18.

[113] PALIT, A. K., AND POPOVIC, D. Fuzzy logic based automatic rule generation and forecasting of time series. In *FUZZ-IEEE'99. 1999 IEEE International Fuzzy Systems. Conference Proceedings (Cat. No.99CH36315)* (1999), vol. 1, pp. 360–365 vol.1.

[114] PATERITSAS, C., PERTSELAKIS, M., AND STAFYLOPATIS, A. A som-based classifier with enhanced structure learning. In *2004 IEEE International Conference on Systems, Man and Cybernetics (IEEE Cat. No.04CH37583)* (2004), vol. 5, pp. 4832–4837 vol.5.

[115] PAUL, S., AND KUMAR, S. Fuzzy neural inference system using mutual subsethood products with applications in medical diagnosis and control. In *10th IEEE International Conference on Fuzzy Systems. (Cat. No.01CH37297)* (2001), vol. 2, pp. 728–731 vol.3.

[116] PAUL, S., AND KUMAR, S. Subsethood-product fuzzy neural inference system (SuPFuNIS). *IEEE Transactions on Neural Networks 13*, 3 (2002), 578–599.

[117] PAUL, S., AND KUMAR, S. Subsethood based adaptive linguistic networks for pattern classification. *IEEE Transactions on Systems, Man, and Cybernetics, Part C (Applications and Reviews) 33*, 2 (2003), 248–258.

[118] PAUL, S., KUMAR, S., AND SINGH, L. A novel evolutionary tsk-subsethood model and its parallel implementation. In *2008 IEEE International Conference on Fuzzy Systems (IEEE World Congress on Computational Intelligence)* (2008), pp. 1880–1885.

[119] PEKASLAN, D., CHEN, C., WAGNER, C., AND GARIBALDI, J. M. Performance and interpretability in fuzzy logic systems – can we have both? In *Information Processing and Management of Uncertainty in Knowledge-Based Systems* (Cham, 2020), M.-J. Lesot, S. Vieira, M. Z. Reformat, J. P. Carvalho, A. Wilbik, B. Bouchon-Meunier, and R. R. Yager, Eds., Springer International Publishing, pp. 571–584.

[120] PEKASLAN, D., GARIBALDI, J. M., AND WAGNER, C. Exploring subsethood to determine firing strength in non-singleton fuzzy logic systems. In *Fuzzy Systems (FUZZ-IEEE), IEEE International Conference on* (2018), IEEE.

[121] PEKASLAN, D., GARIBALDI, J. M., AND WAGNER, C. Noise parameter estimation for non-singleton fuzzy logic systems. In *2018 IEEE International Conference on Systems, Man, and Cybernetics (SMC)* (2018), pp. 2960–2965.

[122] PEKASLAN, D., KABIR, S., GARIBALDI, J. M., AND WAGNER, C. Determining firing strengths through a novel similarity measure to enhance uncertainty handling in non-singleton fuzzy logic systems. In *Proceedings of the 9th International Joint Conference on Computational Intelligence - Volume 1: IJCCI,* (2017), INSTICC, SciTePress, pp. 83–90.

[123] PEKASLAN, D., WAGNER, C., AND GARIBALDI, J. M. Leveraging IT2 Input Fuzzy Sets in Non-Singleton Fuzzy Logic Systems to Dynamically Adapt to Varying Uncertainty Levels. *IEEE International Conference on Fuzzy Systewms 2019-June* (2019).

[124] PEKASLAN, D., WAGNER, C., AND GARIBALDI, J. M. Adonis—adaptive online nonsingleton fuzzy logic systems. *IEEE Transactions on Fuzzy Systems 28*, 10 (2020), 2302–2312.

[125] PEKASLAN, D., WAGNER, C., GARIBALDI, J. M., MARIN, L. G., AND SÁEZ, D. Uncertainty-aware forecasting of renewable energy sources. In *2020 IEEE International Conference on Big Data and Smart Computing (BigComp)* (2020), IEEE, pp. 240–246.

[126] PEREZ-NEIRA, A., SUEIRO, J. C., ROCA, J., AND LAGUNAS, M. A. A dynamic non-singleton fuzzy logic system for ds/cdma communications. In *1998 IEEE International Conference on Fuzzy Systems Proceedings. IEEE World Congress on Computational Intelligence (Cat. No.98CH36228)* (1998), vol. 2, pp. 1494–1499 vol.2.

[127] PERTSELAKIS, M., AND STAFYLOPATIS, A. Dynamic modular fuzzy neural classifier with tree-based structure identification. *Neurocomputing 71*, 4 (2008), 801 – 812. Neural Networks: Algorithms and Applications 50 Years of Artificial Intelligence: a Neuronal Approach.

[128] PETTERSON, M. T., BEGNOCHE, V. L., AND GRAYBEAL, J. M. The effect of motion on pulse oximetry and its clinical significance. *Anesthesia & Analgesia 105*, 6 (2007), S78–S84.

[129] POURABDOLLAH, A., JOHN, R., AND GARIBALDI, J. M. A new dynamic approach for non-singleton fuzzification in noisy time-series prediction. In *Fuzzy Systems (FUZZ-IEEE), 2017 IEEE International Conference on* (2017), IEEE, pp. 1–6.

[130] POURABDOLLAH, A., WAGNER, C., AND ALADI, J. Changes under the hood - a new type of non-singleton fuzzy logic system. In *Fuzzy Systems (FUZZ-IEEE), 2015 IEEE International Conference on* (2015), vol. 2015–Novem, p. 1–8.

[131] POURABDOLLAH, A., WAGNER, C., ALADI, J. H., AND GARIBALDI, J. M. Improved uncertainty capture for nonsingleton fuzzy systems. *IEEE Trans. Fuzzy Syst. 24*, 6 (Dec 2016), 1513–1524.

[132] QUEK, C., AND ZHOU, R. W. Structure and learning algorithms of a nonsingleton input fuzzy neural network based on the approximate analogical reasoning schema. *Fuzzy Sets and Systems 157*, 13 (2006), 1814–1831.

[133] RAHA, S., HOSSAIN, A., AND GHOSH, S. Similarity based approximate reasoning: fuzzy control. *Journal of Applied Logic 6*, 1 (2008), 47–71.

[134] RAHA, S., PAL, N. R., AND RAY, K. S. Similarity-based approximate reasoning: methodology and application. *IEEE Trans. Syst., Man, Cybern. - Part A: Systems and Humans 32*, 4 (July 2002), 541–547.

[135] RAMOS, J., REYES, E., SANCHEZ, J. L., HERNANDEZ, J. I., AND MÉNDEZ, G. M. A professional pid implemented using a non-singleton type-1 fuzzy logic system to control a stepper motor. *Int. J. Eng. Res. Sci.(IJOER) II 2* (2016), 94–101.

[136] RANK, K., LENDL, M., AND UNBEHAUEN, R. Estimation of image noise variance. *IEE Proceedings - Vision, Image and Signal Processing 146*, 2 (Aug 1999), 80–84.

[137] RAZAK, T. R., GARIBALDI, J. M., WAGNER, C., POURABDOLLAH, A., AND SORIA, D. Interpretability and complexity of design in the creation of fuzzy logic systems — a user study. In *2018 IEEE Symposium Series on Computational Intelligence (SSCI)* (Nov 2018), pp. 420–426.

[138] RIBEIRO, M. V. Learning rate updating methods applied to adaptive fuzzy equalizers for broadband power line communications. *EURASIP Journal on Advances in Signal Processing 2004*, 16 (2004), 824326.

[139] ROSS, T. *Fuzzy Logic with Engineering Applications*. Wiley, 2016.

[140] RUIZ, G., POMARES, H., ROJAS, I., AND HAGRAS, H. The non-singleton fuzzification operation for general forms of interval type-2 fuzzy logic systems. *IEEE International Conference on Fuzzy Systems 2* (2017).

[141] RUIZ-GARCIA, G., HAGRAS, H., POMARES, H., AND RUIZ, I. R. Toward a Fuzzy Logic System Based on General Forms of Interval Type-2 Fuzzy Sets. *IEEE Transactions on Fuzzy Systems 27*, 12 (2019), 2381–2395.

[142] RUSPINI, E. H. On the semantics of fuzzy logic. *International Journal of Approximate Reasoning 5*, 1 (1991), 45 – 88.

[143] RUSSELL, B. Vagueness. *The Australasian Journal of Psychology and Philosophy 1*, 2 (1923), 84–92.

[144] SABETI, E., REAMAROON, N., MATHIS, M., GRYAK, J., SJODING, M., AND NAJARIAN, K. Signal quality measure for pulsatile physiological signals using morphological features: Applications in reliability measure for pulse oximetry. *Informatics in Medicine Unlocked 16* (2019), 100222.

[145] SAFIOTTI, A. Fuzzy logic in autonomous robotics: behavior coordination. In *Proceedings of 6th international fuzzy systems conference* (1997), vol. 1, IEEE, pp. 573–578.

[146] SAHAB, N., AND HAGRAS, H. Adaptive non-singleton type-2 fuzzy logic systems: A way forward for handling numerical uncertainties in real world applications. *International Journal of Computers, Communications and Control 6* (Sep 2011).

[147] SAHAB, N., AND HAGRAS, H. An adaptive type-2 input based nonsingleton type-2 Fuzzy Logic System for real world applications. *IEEE International Conference on Fuzzy Systems* (2011), 509–516.

[148] SAHAB, N., AND HAGRAS, H. A type-2 nonsingleton type-2 fuzzy logic system to handle linguistic and numerical uncertainties in real world environments. In *2011 IEEE Symposium on Advances in Type-2 Fuzzy Logic Systems (T2FUZZ)* (April 2011), pp. 110–117.

[149] SAHAB, N., AND HAGRAS, H. Towards comparing adaptive type-2 input based non-singleton type-2 fls and non-singleton flss employing gaussian inputs. In *2012 IEEE International Conference on Fuzzy Systems* (June 2012), pp. 1–8.

[150] SALMAN, S. A., PUTTIGE, V. R., AND ANAVATTI, S. G. Real-time validation and comparison of fuzzy identification and state-space identification for a uav platform. In *2006 IEEE Conference on Computer Aided Control System Design, 2006 IEEE International Conference on Control Applications, 2006 IEEE International Symposium on Intelligent Control* (2006), IEEE, pp. 2138–2143.

[151] SAMMOUR, I., AND KARNATI, S. Non-invasive respiratory support of the premature neonate: From physics to bench to practice. *Frontiers in Pediatrics 8* (2020).

[152] SEPÚLVEDA, R., CASTILLO, O., MELIN, P., RODRÍGUEZ-DÍAZ, A., AND MONTIEL, O. Experimental study of intelligent controllers under uncertainty using type-1 and type-2 fuzzy logic. *Information Sciences 177*, 10 (2007), 2023–2048.

[153] SETNES, M., BABUSKA, R., KAYMAK, U., AND NAUTA LEMKE, VAN, H. Similarity measures in fuzzy rule base simplification. *IEEE Transactions on Systems, Man and Cybernetics. Part B, Cybernetics 28*, 3 (1998), 376–386.

[154] SHUNMUGA VELAYUTHAM, C., AND KUMAR, S. Some applications of an asymmetric subsethood product fuzzy neural inference system. In *The 12th IEEE International Conference on Fuzzy Systems, 2003. FUZZ '03.* (2003), vol. 1, pp. 202–207 vol.1.

[155] SHUNMUGA VELAYUTHAM, C., KUMAR, S., AND PAUL, S. Evolvable subsethood product fuzzy neural network for pattern classification. *International journal of pattern recognition and artificial intelligence 16*, 07 (2002), 957–970.

[156] SILVERMAN, W. A. A cautionary tale about supplemental oxygen: the albatross of neonatal medicine. *Pediatrics 113*, 2 (2004), 394–396.

[157] SINGH, L., AND KUMAR, S. Parallel evolutionary asymmetric subsethood product fuzzy-neural inference system with applications. In *2006 IEEE International Conference on Fuzzy Systems* (2006), pp. 1858–1865.

[158] SINHA, D., AND DOUGHERTY, E. R. Fuzzification of set inclusion: theory and applications. *Fuzzy sets and systems 55*, 1 (1993), 15–42.

[159] SMITH, R. Aristotle's logic. In *The Stanford Encyclopedia of Philosophy*, E. N. Zalta, Ed., summer 2019 ed. Metaphysics Research Lab, Stanford University, 2019.

[160] SONG, H. J., MIAO, C. Y., WUYTS, R., SHEN, Z. Q., D'HONDT, M., AND CATTHOOR, F. An extension to fuzzy cognitive maps for classification and prediction. *IEEE Transactions on Fuzzy Systems 19*, 1 (2011), 116–135.

[161] SORENSON, H. W. Least-squares estimation: from Gauss to Kalman. *IEEE Spectrum 7*, 7 (jul 1970), 63–68.

[162] TAKAGI, T., AND SUGENO, M. Fuzzy identification of systems and its applications to modeling and control. *IEEE transactions on systems, man, and cybernetics*, 1 (1985), 116–132.

[163] TORRES, A., AND NIETO, J. J. Fuzzy logic in medicine and bioinformatics. *BioMed Research International 2006* (2006).

[164] TORRES, P., AND SÁEZ, D. Type-2 fuzzy logic identification applied to the modeling of a robot hand. *IEEE International Conference on Fuzzy Systems*, July (2008), 854–861.

[165] TURKSEN, I. Four methods of approximate reasoning with interval-valued fuzzy sets. *International Journal of Approximate Reasoning 3*, 2 (1989), 121 – 142.

[166] TURKSEN, I., AND TIAN, Y. Interval-valued fuzzy sets representation on multiple antecedent fuzzy s-implications and reasoning. *Fuzzy Sets and Systems 52*, 2 (1992), 143 – 167.

[167] TURKSEN, I., AND ZHONG, Z. An approximate analogical reasoning schema based on similarity measures and interval-valued fuzzy sets. *Fuzzy Sets and Systems 34*, 3 (1990), 323 – 346.

[168] TURKSEN, I. B., AND ZHONG, Z. An approximate analogical reasoning approach based on similarity measures. *IEEE Trans. Syst., Man, Cybern. 18*, 6 (Nov 1988), 1049–1056.

[169] UDDIN, M. S., SEKERCIOGLU, Y. A., AND MANI, N. Fuzzy logic systems: A classification based on capabilities in handling uncertainty. In *2007 IEEE International Conference on Systems, Man and Cybernetics* (2007), pp. 807–811.

[170] VELAYUTHAM, C. S., AND KUMAR, S. Asymmetric subsethood-product fuzzy neural inference system (asupfunis). *IEEE Transactions on Neural Networks 16*, 1 (2005), 160–174.

[171] VELLIDO, A. The importance of interpretability and visualization in machine learning for applications in medicine and health care. *Neural Computing and Applications* (2019), 1–15.

[172] VILLARROEL, M., CHAICHULEE, S., JORGE, J., DAVIS, S., GREEN, G., ARTETA, C., ZISSERMAN, A., MCCORMICK, K., WATKINSON, P., AND TARASSENKO, L. Non-contact physiological monitoring of preterm infants in the neonatal intensive care unit. *NPJ digital medicine 2*, 1 (2019), 1–18.

[173] VLACHOS, I. K., AND SERGIADIS, G. D. Subsethood, entropy, and cardinality for interval-valued fuzzy sets—an algebraic derivation. *Fuzzy Sets and Systems 158*, 12 (2007), 1384–1396.

[174] WAGNER, C., AND HAGRAS, H. A genetic algorithm based architecture for evolving type-2 fuzzy logic controllers for real world autonomous mobile robots. In *2007 IEEE International Fuzzy Systems Conference* (July 2007), pp. 1–6.

[175] WAGNER, C., AND HAGRAS, H. zslices - towards bridging the gap between interval and general type-2 fuzzy logic. pp. 489 – 497.

[176] WAGNER, C., POURABDOLLAH, A., MCCULLOCH, J., JOHN, R., AND GARIBALDI, J. M. A similarity-based inference engine for non-singleton fuzzy logic systems. In *Fuzzy Systems (FUZZ-IEEE), 2016 IEEE International Conference on* (2016), IEEE, pp. 316–323.

[177] WALKER, J. Newborn pulse oximetry screening pilot under way, 2015.

[178] WANG, L. . Stable adaptive fuzzy control of nonlinear systems. *IEEE Transactions on Fuzzy Systems 1*, 2 (1993), 146–155.

[179] WANG, L.-X., AND MENDEL, J. M. Generating fuzzy rules by learning from examples. *IEEE Transactions on systems, man, and cybernetics 22*, 6 (1992), 1414–1427.

[180] WEAVER, W. Science and complexity. In *Facets of systems science*. Springer, 1991, pp. 449–456.

[181] WU, D., AND MENDEL, J. Enhanced karnik–mendel algorithms. *Fuzzy Systems, IEEE Transactions on 17* (09 2009), 923 – 934.

[182] WU, D., AND TAN, W. W. A type-2 fuzzy logic controller for the liquid-level process. In *2004 IEEE International Conference on Fuzzy Systems (IEEE Cat. No.04CH37542)* (July 2004), vol. 2, pp. 953–958 vol.2.

[183] WU, H., AND MENDEL, J. M. Classification of battlefield ground vehicles using acoustic features and fuzzy logic rule-based classifiers. *IEEE Transactions on Fuzzy Systems 15*, 1 (2007), 56–72.

[184] YAGER, R. R. On a general class of fuzzy connectives. *Fuzzy Sets and Systems 4*, 3 (1980), 235 – 242.

[185] YEUNG, D. S., AND TSANG, E. C. Improved fuzzy knowledge representation and rule evaluation using fuzzy petri nets and degree of subsethood. *International journal of intelligent systems 9*, 12 (1994), 1083–1100.

[186] YEUNG, D. S., AND TSANG, E. C. C. A comparative study on similarity-based fuzzy reasoning methods. *IEEE Trans. Syst., Man, Cybern., Part B (Cybernetics) 27*, 2 (Apr 1997), 216–227.

[187] YEUNG, D. S., AND YSANG, E. C. C. A multilevel weighted fuzzy reasoning algorithm for expert systems. *IEEE Transactions on Systems, Man, and Cybernetics - Part A: Systems and Humans 28*, 2 (1998), 149–158.

[188] YU, Q., DIAN, S., LI, Y., LIU, J., AND ZHAO, T. Similarity-based non-singleton general type-2 fuzzy logic controller with applications to mobile two-wheeled robots. *Journal of Intelligent & Fuzzy Systems*, Preprint (2019), 1–14.

[189] ZADEH, L. A. Fuzzy sets. *Information and control 8*, 3 (1965), 338–353.

[190] ZADEH, L. A. Outline of a new approach to the analysis of complex systems and decision processes. *IEEE Transactions on Systems, Man, and Cybernetics SMC-3*, 1 (1973), 28–44.

[191] ZADEH, L. A. The concept of a linguistic variable and its application to approximate reasoning—i. *Information sciences 8*, 3 (1975), 199–249.

[192] ZHAI, D., HAO, M., AND MENDEL, J. M. A non-singleton interval type-2 fuzzy logic system for universal image noise removal using quantum-behaved particle swarm opti-

mization. In *2011 IEEE International Conference on Fuzzy Systems (FUZZ-IEEE 2011)* (June 2011), pp. 957–964.

[193] ZHAO, T., YU, Q., DIAN, S., GUO, R., AND LI, S. Non-singleton general type-2 fuzzy control for a two-wheeled self-balancing robot. *International Journal of Fuzzy Systems 21*, 6 (2019), 1724–1737.

[194] ZHOU, S. M., AND GAN, J. Q. Low-level interpretability and high-level interpretability: a unified view of data-driven interpretable fuzzy system modelling. *Fuzzy Sets and Systems 159*, 23 (2008), 3091–3131.

[195] ZIMMERMANN, H.-J. An application-oriented view of modeling uncertainty. *European Journal of operational research 122*, 2 (2000), 190–198.

[196] ZIMMERMANN, H. J. Fuzzy set theory. *Wiley Interdisciplinary Reviews: Computational Statistics 2*, 3 (2010), 317–332.

Appendix A

Appendix

A.1 Analysis of ADONiS under Uniform Noise

All experiments in the Chapter 4 have been replicated using uniformly distributed (rather than normally distributed) noise and the results are presented in this section. Here, in the noise generation, the interval of the uniform distribution is defined as $[-\delta, \delta]$ with $\delta = (\sqrt{3}\,\sigma_n)$. Note that σ_n represents the noise level. such as $\sigma_{20}, \sigma_{10} and \sigma_0$

$$x'_t = x_t + \mathcal{U}(-\delta,\, \delta) \qquad t = 1, 2, 3..., N\ , \tag{A.1}$$

where x'_t represents the noisy value, $\mathcal{U}(-\delta,\, \delta)$ is the uniform distribution to generate random noise values and N is the number of values in the dataset.

A.1.1 Experiment 1.1

The approach in Section 4.3.2.1 of the Chapter 4 is followed but the time series datasets are injected with uniform rather than Gaussian noise. Fig. A.1 is the corresponding figure of Fig. 4.12, as is Fig. A.2 for Fig. 4.13 of the Chapter 4.

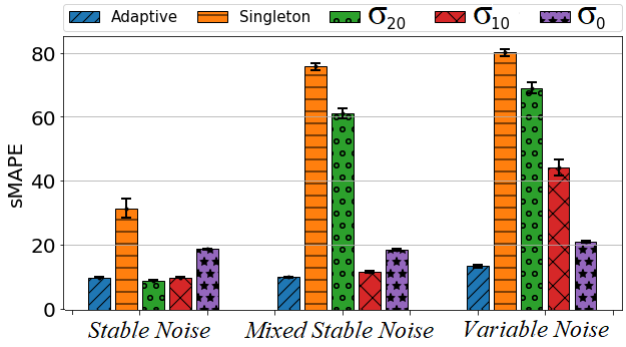

Figure A.1: Experiment 1.1- the repetition of Fig. 4.12 with uniform noise rather than Gaussian noise in the time series datasets.

A.1.2 Experiment 1.2

As for Experiment 1.1., the approach of Section 4.3.2.2 of the Chapter 4 is followed but the time series datasets are injected with uniform rather than Gaussian noise. Fig A.3 is the corresponding figure of Fig. 4.14, as is Fig. A.4 for Fig. 4.15 of the Chapter 4.

A.2 Experiment Results shown through MSE

These results follow to same approaches as described in Sections 4.3.2 of the Chapter 4. However, the FLSs performances are shown using the Mean Square Error (MSE) rather than sMAPE.

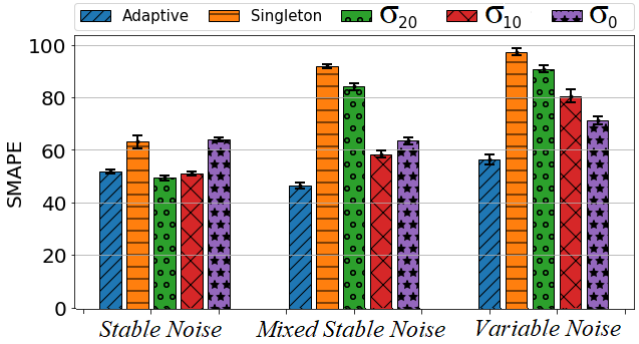

Figure A.2: Experiment 1.1- the repetition of Fig. 4.13 with uniform noise rather than Gaussian noise in the time series datasets.

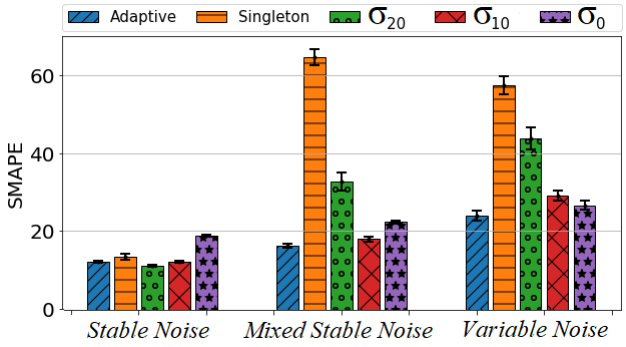

Figure A.3: Experiment 1.2- corresponding to Fig. 4.14 with uniform rather than Gaussian noise in the time series datasets.

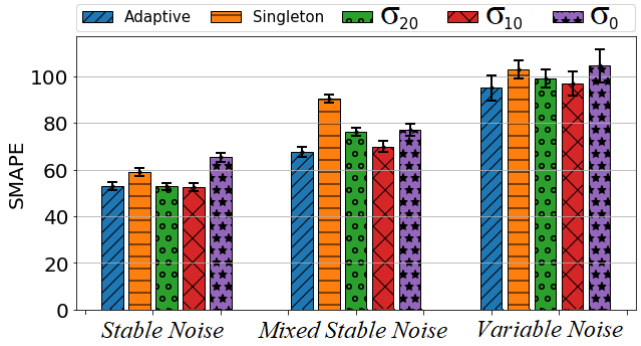

Figure A.4: Experiment 1.2- corresponding to Fig. 4.15 with uniform rather than Gaussian noise in the time series datasets.

A.2.1 Experiment 1 - the Adaptive and Non-Adaptive Comparison in MSE

A.2.1.1 Experiment 1.1 Noise Free Training

The experiment in Section 4.3.2.1 of the Chapter 4 are followed and the MSE (rather than sMAPE) is provided as a measure of prediction accuracy. Fig. A.5 provides the counterpart to Fig. 4.12 and A.6 provides the counterpart to Fig. 4.13 from the thesis.

A.2.1.2 Experiment 1.2 Noisy Training

The experiment in Section 4.3.2.2 of the Chapter 4 are followed and the MSE (rather than sMAPE) is provided as a measure of prediction accuracy. Fig. A.7 provides the counterpart to Fig. 4.14 and A.8 provides the counterpart to Fig. 4.15 from the Chapter 4.

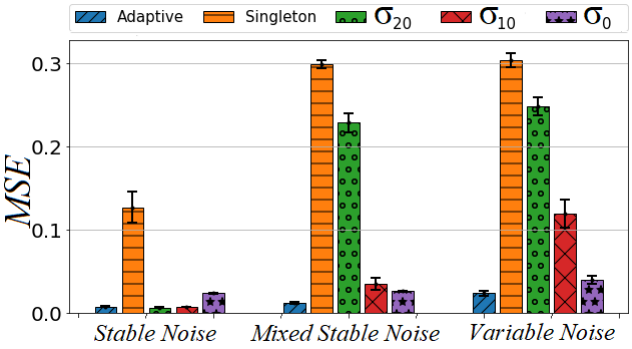

Figure A.5: Experiment 1.1- corresponding to Fig. 4.12 showing MSE rather than the sMAPE based results.

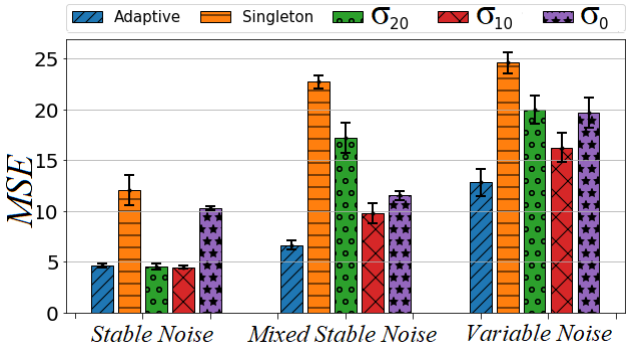

Figure A.6: Experiment 1.1 - corresponding to Fig. 4.13 showing MSE rather than the sMAPE based results.

A.2.2 Experiment 2 - Advanced NSFLSs Comparison in the ADONiS Framework in MSE

A.2.2.1 Experiment 2.1 Noise Free Training

The experiment in Section 4.3.3.1 of the Chapter 4 are followed and the MSE (rather than sMAPE) is provided as a measure of prediction accuracy. Fig. A.9 provides the counterpart to Fig. 4.17 and Fig. A.10 provides the counterpart to Fig. 4.18 from the Chapter 4.

A.2.2.2 Experiment 2.2 Noisy Training

The experiment in Section 4.3.3.2 of the Chapter 4 are followed and the MSE (rather than sMAPE) is provided as a measure of prediction accuracy. Fig. A.11 provides the counterpart to Fig. 4.19 and Fig. A.12 provides the counterpart to Fig. 4.20 from the Chapter 4.

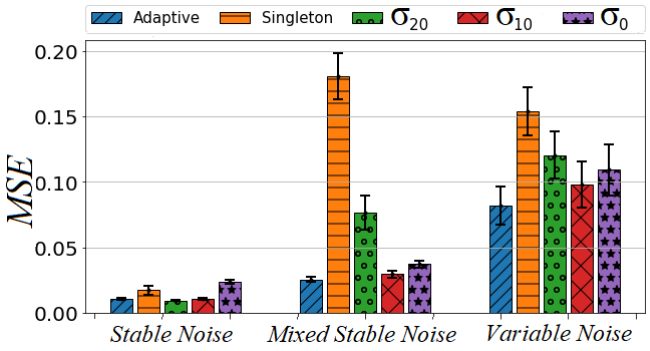

Figure A.7: Experiment 1.2 - corresponding to Fig. 4.14 showing MSE rather than the sMAPE based results.

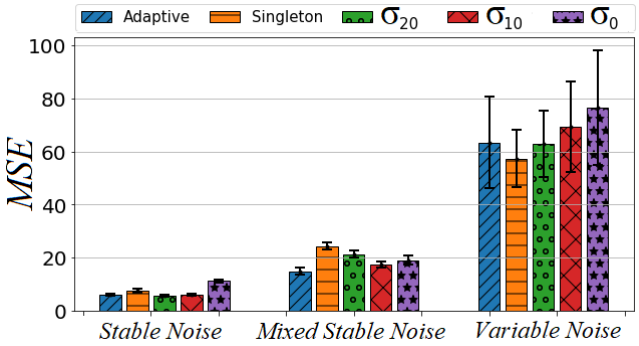

Figure A.8: Experiment 1.2 - corresponding to Fig. 4.15 showing MSE rather than the sMAPE based results.

A.3 Statistical Analyses

In this section, in order to assess the statistical reliability of these result differences, a series of paired sample t-tests are conducted. Here, the measure of performance (sMAPE or MSE) for the best performing method is compared against that of the next best. This was done within each of three conditions, for both MG and Lorenz time series experiments. These comparisons indicate that for the experiments conducted, in noise free training and when using the sMAPE measure, *sub*-NS results are significantly better than the next best performing (*sim*-NS) NSFLSs results, under all three different cases and in both time series (MG and Lorenz) (See Table. A.1). When using the MSE measure (Table A.3), *sub*-NS Noise-free training results are significantly better than the next best performing NSFLSs results in all but Variable Noise testing conditions.

When trained under noisy conditions, and according to the sMAPE measure (Table A.2), *sub*-NS is found to be significantly better than any other technique in the MG time-series Stable

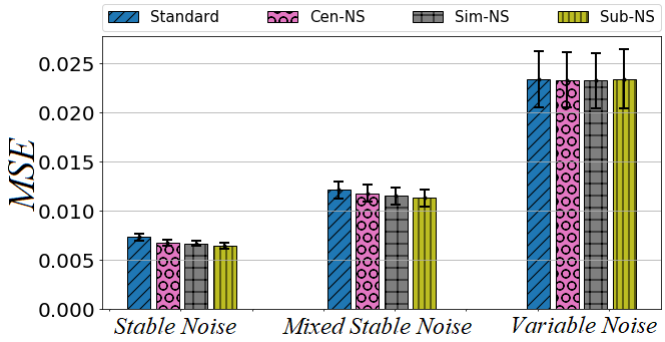

Figure A.9: Experiment 2.1 - corresponding to Fig. 4.17showing MSE rather than the sMAPE based results.

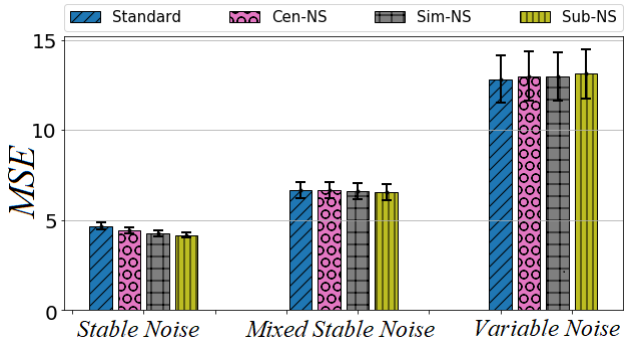

Figure A.10: Experiment 2.1 - corresponding to Fig. 4.18 showing MSE rather than the sMAPE based results.

Noise condition. However, *sim*-NS is found to be significantly the best performing technique in both Mixed Stable and Variable noise conditions (Table A.2), according to the sMAPE measure. The same pattern of results is evident when assessed under the MSE measure (Table A.4), with the exception that *sub*-NS is also found to be significantly best performing technique in the Lorenz time-series Stable Noise condition.

Table A.1: Experiment 2.1 Noise Free Training sMAPE results statistical paired sample t-test (2 tailed df=29 the least average mean shown in bold)

	MG Time Series			Lorenz Time Series	
Experiment Scenarios	t value	p value	Experiment Scenarios	t value	p value
Stable Noise (sim-NS and sub-NS)	-6.983	< .00001	Stable Noise (*sim*-NS and ***sub*-NS**)	-5.157227	0.00002
Mixed Stable Noise (*sim*-NS and ***sub*-NS**)	-9.703	< .00001	Mixed Stable Noise (*sim*-NS and ***sub*-NS**)	-2.460	0.0201
Variable Noise (*sim*-NS and ***sub*-NS**)	-4.914	0.00003	Variable Noise (*sim*-NS and ***sub*-NS**)	-2.157	0.03939

Table A.2: Experiment 2.2 Noisy Training sMAPE results statistical paired sample t-test (2 tailed df=29 the least average mean shown in bold)

	MG Time Series			Lorenz Time Series	
Experiment Scenarios	t value	p value	Experiment Scenarios	t value	p value
Stable Noise (*sim*-NS and ***sub*-NS**)	-3.485	0.00158	Stable Noise (*cen*-NS and ***sub*-NS**)	-0.546	0.58909
Mixed Stable Noise (***sim*-NS** and *sub*-NS)	9.449	< .00001	Mixed Stable Noise (***sim*-NS** and *sub*-NS)	8.799	< .00001
Variable Noise (***sim*-NS** and *sub*-NS)	3.596	0.00118	Variable Noise (***sim*-NS** and *sub*-NS)	3.914	0.00051

Table A.3: Experiment 2.1 Noise Free Training MSE results statistical paired sample t-test (2 tailed df=29 the least average mean shown in bold)

	MG Time Series			Lorenz Time Series	
Experiment Scenarios	t value	p value	Experiment Scenarios	t value	p value
Stable Noise (*sim*-NS and ***sub*-NS**)	-10.719	< .00001	Stable Noise (*sim*-NS and ***sub*-NS**)	-5.124	0.00002
Mixed Stable Noise (*sim*-NS and ***sub*-NS**)	-5.874	< .00001	Mixed Stable Noise (*sim*-NS and ***sub*-NS**)	-2.591	0.01483
Variable Noise (***cen*-NS** and *sim*-NS)	-0.725	0.4741	Variable Noise (***sta*-NS** and *sim*-NS)	2.532	0.017

Table A.4: Experiment 2.2 Noisy Training MSE results statistical paired sample t-test (2 tailed df=29 the least average mean shown in bold)

	MG Time Series			Lorenz Time Series	
Experiment Scenarios	t value	p value	Experiment Scenarios	t value	p value
Stable Noise (*sim*-NS and ***sub*-NS**)	-3.617	0.00112	Stable Noise (*sim*-NS and ***sub*-NS**)	-4.975	0.00003
Mixed Stable Noise (***sim*-NS** and *sub*-NS)	9.056	< .00001	Mixed Stable Noise (***sim*-NS** and *sub*-NS)	6.602	< .00001
Variable Noise (***sim*-NS** and *sub*-NS)	4.524	0.00009	Variable Noise (***sim*-NS** and *sub*-NS)	3.263	0.00283

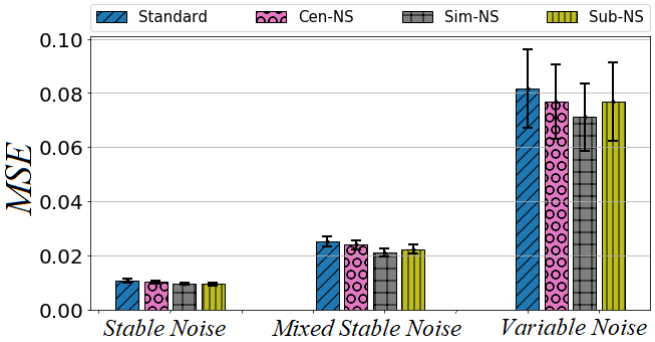

Figure A.11: Experiment 2.2 - corresponding to Fig. 4.19 showing MSE rather than the sMAPE based results.

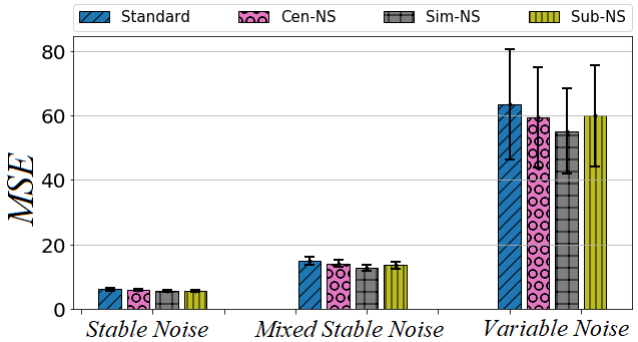

Figure A.12: Experiment 2.2 - corresponding to Fig. 4.20 showing MSE rather than the sMAPE based results.

Appendix B

Appendix

B.1 The created rules, by the neonatologist and his team

In this section, the created 24 rules ,by the neonatologist and his team, are shown in the table below.

Table B.1: The created rules, by doctors, for O_2 support modelling of neonate baby.

Rule Numbers	**Inputs**	**Output**
Rule 1:	IF HR is Low and SpO2 is Low and the current O2 support is Low	THEN O2 support should be moderate
Rule 2:	IF HR is Low and SpO2 is Low and the current O2 support is Moderate	THEN O2 support should be high
Rule 3:	IF HR is Low and SpO2 is Low and the current O2 support is High	THEN O2 support should be high
Rule 4:	IF HR is Low and SpO2 is Moderate and the current O2 support is Low	THEN O2 support should be moderate
Rule 5:	IF HR is Low and SpO2 is Moderate and the current O2 support is Moderate	THEN O2 support should be high
Rule 6:	IF HR is Low and SpO2 is Moderate and the current O2 support is High	THEN O2 support should be high
Rule 7:	IF HR is Moderate and SpO2 is Low and the current O2 support is Low	THEN O2 support should be moderate
Rule 8:	IF HR is Moderate and SpO2 is Low and the current O2 support is Moderate	THEN O2 support should be high
Rule 9:	IF HR is Moderate and SpO2 is Low and the current O2 support is High	THEN O2 support should be high
Rule 10:	IF HR is Moderate and SpO2 is Moderate and the current O2 support is Low	THEN O2 support should be low
Rule 11:	IF HR is Moderate and SpO2 is Moderate and the current O2 support is Moderate	THEN O2 support should be moderate
Rule 12:	IF HR is Moderate and SpO2 is Moderate and the current O2 support is High	THEN O2 support should be high
Rule 13:	IF HR is Moderate and SpO2 is High and the current O2 support is Low	THEN O2 support should be low
Rule 14:	IF HR is Moderate and SpO2 is High and the current O2 support is Moderate	THEN O2 support should be low
Rule 15:	IF HR is Moderate and SpO2 is High and the current O2 support is High	THEN O2 support should be moderate
Rule 16:	IF HR is High and SpO2 is Low and the current O2 support is Low	THEN O2 support should be moderate
Rule 17:	IF HR is High and SpO2 is Low and the current O2 support is Moderate	THEN O2 support should be high
Rule 18:	IF HR is High and SpO2 is Low and the current O2 support is High	THEN O2 support should be high
Rule 19:	IF HR is High and SpO2 is Moderate and the current O2 support is Low	THEN O2 support should be low
Rule 20:	IF HR is High and SpO2 is Moderate and the current O2 support is Moderate	THEN O2 support should be moderate
Rule 21:	IF HR is High and SpO2 is Moderate and the current O2 support is High	THEN O2 support should be high
Rule 22:	IF HR is High and SpO2 is High and the current O2 support is Low	THEN O2 support should be low
Rule 23:	IF HR is High and SpO2 is High and the current O2 support is Moderate	THEN O2 support should be low
Rule 24:	IF HR is High and SpO2 is High and the current O2 support is High	THEN O2 support should be moderate

B.2 The HR and SpO_2 and O_2 inputs visualisation

In this section, a sample visualisation of non-singleton HR, SpO_2 and O_2 over the created antecedent MFs and 24 rules are shown in Fig. B.1.

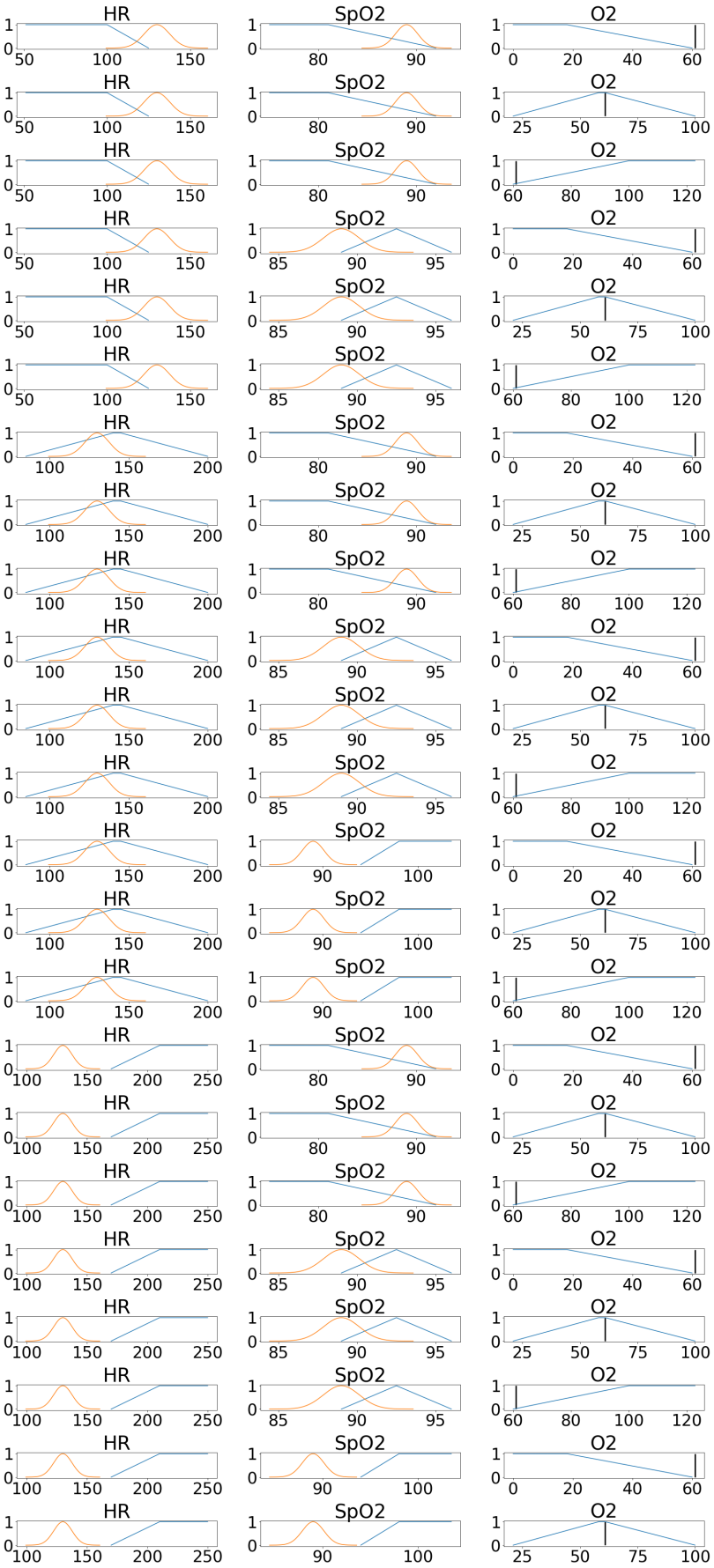

Figure B.1: The HR and SpO_2 and O_2 inputs visualisation over the all 24 rules

B.3 O_2 Suggestion Results of ADONiS and SFLS

Both models (ADONiS and SFLS) O_2 support suggestion behaviours are tested on the given six real-world datasets.

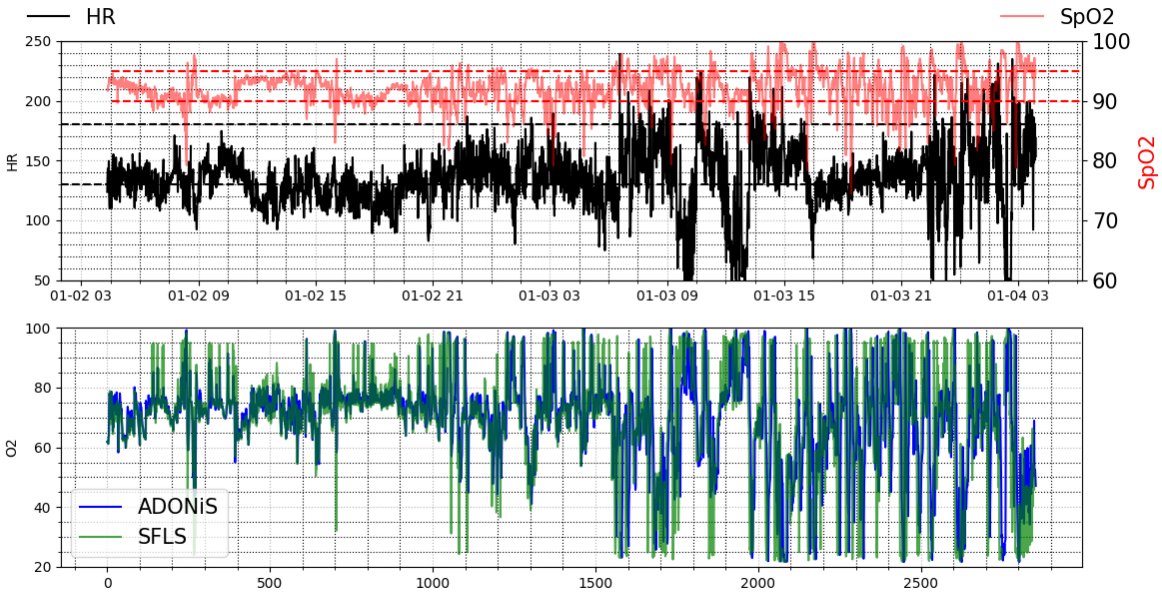

Figure B.2: Dataset 18: HR and SpO_2 levels of the baby '18' and both models suggestions

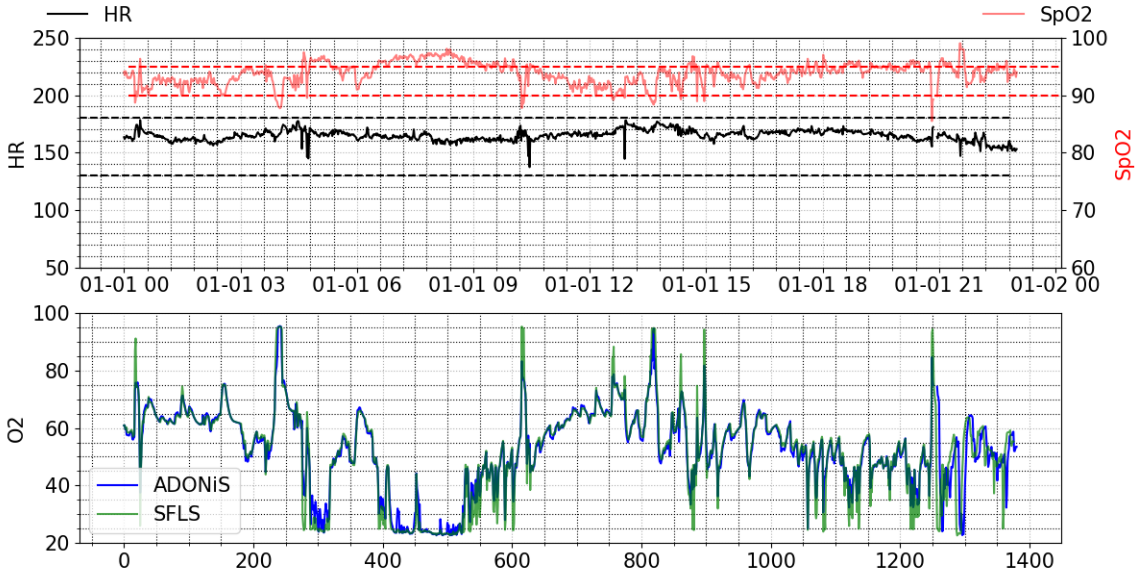

Figure B.3: Dataset 21: HR and SpO_2 levels of the baby '21' and both models suggestions

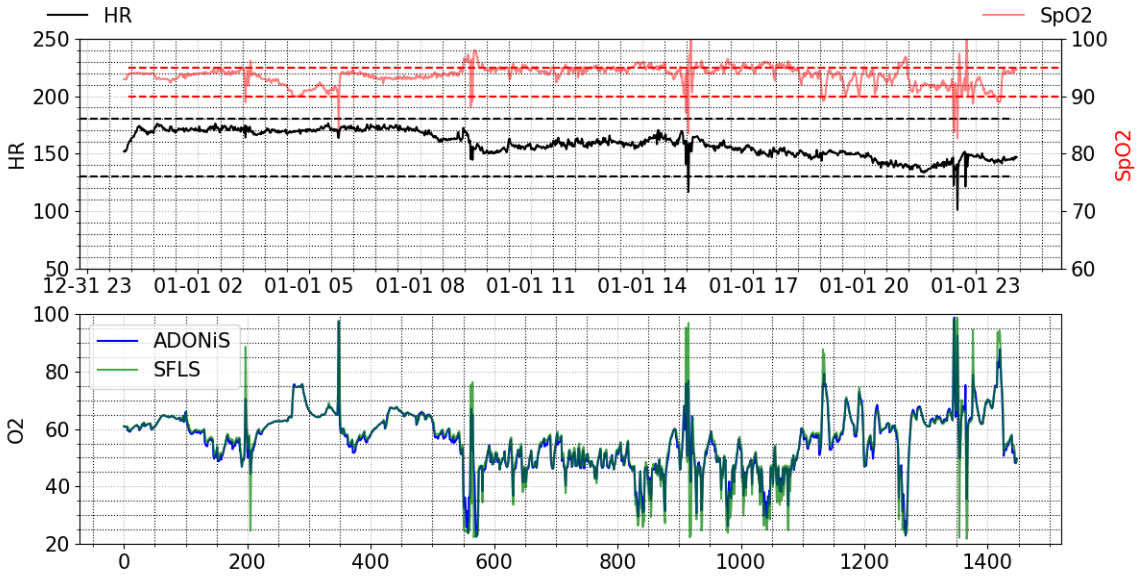

Figure B.4: Dataset 25: HR and SpO_2 levels of the baby '25' and both models suggestions

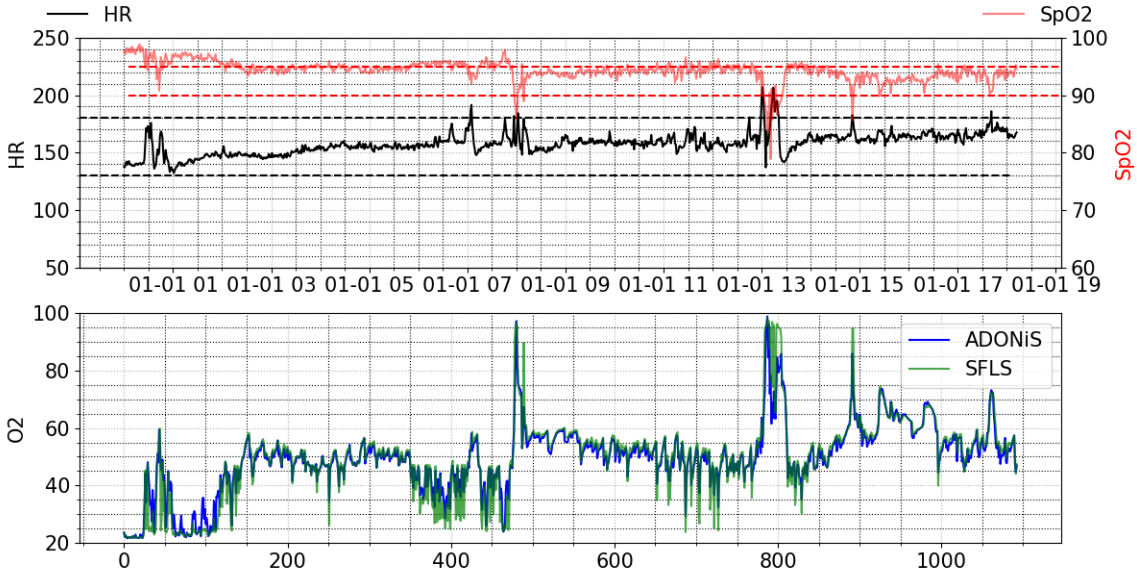

Figure B.5: Dataset 28: HR and SpO_2 levels of the baby '28' and both models suggestions

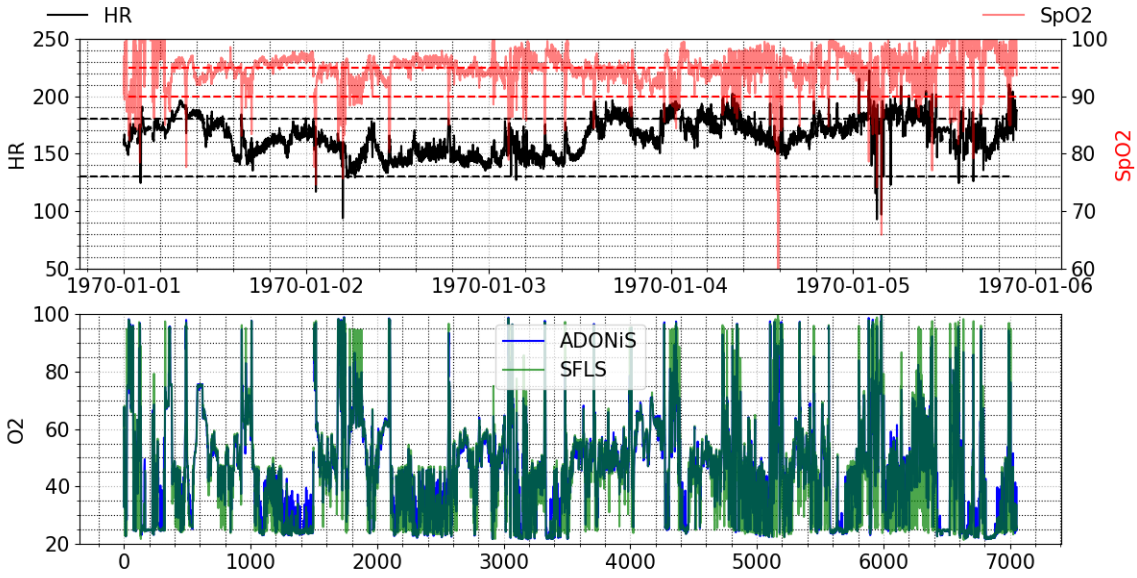

Figure B.6: Dataset 30: HR and SpO_2 levels of the baby '30' and both models suggestions

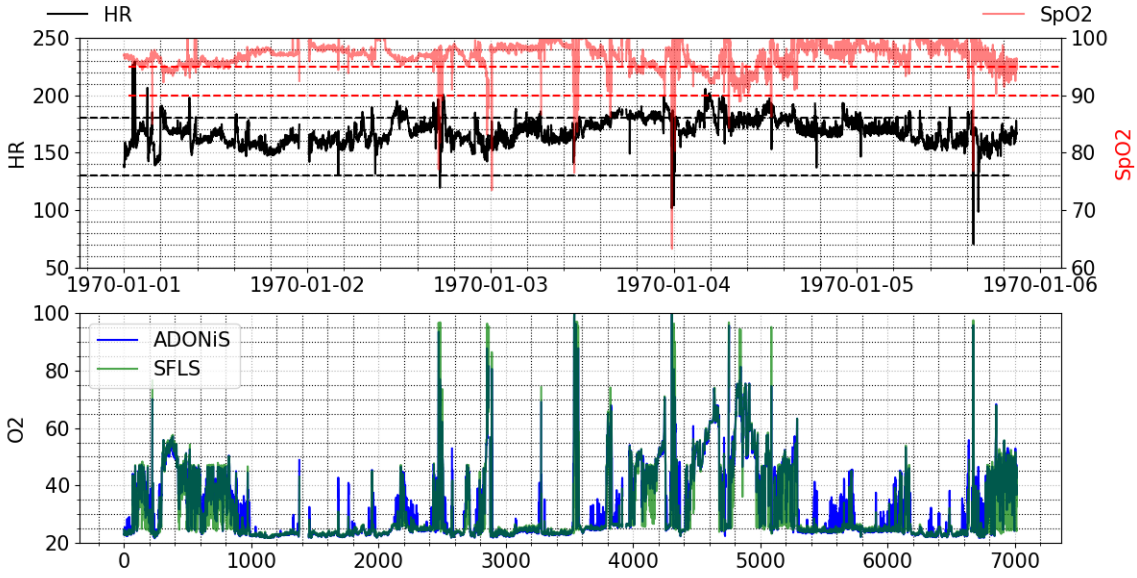

Figure B.7: Dataset 31: HR and SpO_2 levels of the baby '31' and both models suggestions